Bulletin
of
The Geological Society of America

VOLUME 68 May 1957 NUMBER 5

CONTENTS

Pages

Stratigraphy of upper part of sediments of Silver Bay area, Lake Superior. By F. M. Swain and N. Prokopovich 527–542

Flysch sedimentation. By Zb. L. Sujkowski 543–554

Contribution to the geology of the islands Margarita and Cubagua, Venezuela. By H. G. Kugler 555–566

Mechanical analysis of the dike pattern of the Spanish Peaks area, Colorado. By Helmer Odé 567–576

Metamorphism and volume losses in carbonate rocks near Johnson Camp, Cochise County, Arizona. By John R. Cooper 577–610

Nature of faulting in large earthquakes. By John H. Hodgson 611–644

Short Notes

Nature of faulting in large earthquakes. By Donald B. McIntyre and John M. Christie 645–652

Origin of porphyroblasts. By George J. Neuerburg 653–654

Occurrence of 1350 million-year-old granitic rocks in western United States. By L. T. Aldrich, G. W. Wetherill, and G. L. Davis 655–656

Subscription $15.00 per year.

Printing Office: Mt. Royal & Guilford Aves., Baltimore 2, Md.

Communications for publications should be addressed to The Geological Society of America, Dr. H. R. Aldrich, Secretary, 419 West 117 Street, New York, N. Y.

Please give notice of change of address 4 weeks in advance. Claims for nonreceipt of the Bulletin of a given month must be sent to the Secretary of the Society before the end of the second succeeding month.

Entered as second-class matter at the Post Office at Baltimore, Md., under the Act of Congress of July 16, 1894.
Accepted for mailing at special rate of postage provided for in Section 1103 Act of October 3, 1917, authorized on July 8, 1918.

PAPERS IN PRESS FOR FORTHCOMING ISSUES

Taconic Klippe: A Stratigraphic-Structural Problem. By Walter H. Bucher

Stratigraphy and Structure of the Copake Quadrangle, New York. By John D. Weaver

Stratigraphy and Structure of the Kinderhook Quadrangle, New York, and the "Taconic Klippe". By J. Campbell Craddock

Potassium-Argon Method of Geochronometry. By D. R. Carr and J. L. Kulp

Submerged River System of Chesapeake Bay. By J. T. Hack

Devonian-Mississippian Transition in Central Texas. By P. E. Cloud, Jr., V. E. Barnes, and W. H. Hass

Pleistocene Geology of the Door Peninsula, Wisconsin. By F. T. Thwaites and Kenneth Bertrand

BULLETIN OF THE GEOLOGICAL SOCIETY OF AMERICA
VOL. 68, PP. 527–542, 11 FIGS. MAY 1957

STRATIGRAPHY OF UPPER PART OF SEDIMENTS OF SILVER BAY AREA, LAKE SUPERIOR

BY F. M. SWAIN AND N. PROKOPOVICH

ABSTRACT

A study of some of the physical, chemical, and biological properties of the sediments has been made at 29 offshore stations in a 15-square-mile area of Lake Superior, near Silver Bay, Minnesota. Color changes in the sediments are believed to be due to the state of oxidation and reduction of the iron oxides. Textural variations are possibly in part caused by turbidity currents resulting from either sublacustrine mud slides or rivers during flood stages or both. Two biofacies of the sediments occur, based on (1) diatoms in offshore areas and (2) oligochaetes and malacostracans in nearer-shore areas. The bituminous fractions of the sediments are small in total but carry relatively more hydrocarbons and less asphalts than eutrophic lake sediments of central Minnesota.

CONTENTS

TEXT

	Page
Introduction	528
Origin of lake	528
Location	528
General geology	528
Bottom topography	529
Field and laboratory procedures	529
Acknowledgments	531
Results	531
Limnologic summary	531
Physical and chemical properties of sediments	533
General description	533
Color	535
Hydrogen-ion concentration	536
Oxidation-reduction potential	536
Total radioactivity	537
Mechanical analyses	537
Moisture content and shrinkage	537
Chemical and mineralogical composition	537
Lipoid substances	539
Discussion	539
Color changes in sediments	539
Comparision with glacial lake clays near Duluth, Minnesota	539
Textural variations in the sediments	540
Compaction and shrinkage of the sediments	540
Biofacies	540
Interpretation of lipoid substances	541
Conclusions	541
References cited	542

ILLUSTRATIONS

Figure	Page
1. Index map showing location of Silver Bay area	528
2. Location of stations, type of sample, colors of bottom sediments, Silver Bay area	529
3. Location of samples for chemical analyses, pH, and Eh	530
4. Bathythermograph records, Silver Bay area	531
5. Mechanical analyses of medium and coarse particle sizes	534
6. Mechanical analyses of fine particle sizes	535
7. Moisture content and shrinkage of core samples	536
8. Comparison of moisture content and shrinkage at top and bottom of core 26	536
9. Differential thermal analyses of grab samples and cores	538
10. Ultra-violet absorption spectrum of pyridine + methanol eluant of lipoid extract from station 26	540
11. Distribution of bottom fauna and diatoms in the Silver Bay sediments	541

TABLES

Table	Page
1. Chemical analyses of water of Lake Superior, near Silver Bay, Minnesota	530
2. Description of cores, Silver Bay area	532
3. Inorganic analyses of Silver Bay sediments	537
4. Heavy minerals in Silver Bay samples	539
5. Chromatographic analyses of lipoid extracts from Silver Bay cores	539

Introduction

Origin of Lake

Lake Superior, the largest body of fresh water in the world, is 360 miles long, a maximum of 160 miles wide, and has an area of approximately 32,000 square miles. Its normal level is 602 feet above sea level and greatest recorded depth is 1302 feet (397 meters) at a point about 13 miles northwest of Caribou Island (Schwartz, 1949, p. 82). The lake owes its origin (Schwartz, p. 83) to probably three causes: (1) early synclinal development during or after extrusion and intrusion of the late Precambrian Keweenawan rocks; (2) later faulting which modified parts of the syncline; (3) Tertiary and Quaternary fluvial erosion and Quaternary glacial erosion which removed part of sedimentary filling of the syncline but modified resistant Precambrian rocks only slightly.

Location

The area sampled lies in the western part of Lake Superior (Fig. 1), 40 miles northeast of Duluth and covers approximately 15 square miles. The village of Beaver Bay at the mouth of Beaver River lies near the northwest corner of the area and the Great Palisades Cliff lies near the northeast corner. The new town of Silver Bay and the taconite beneficiation plant of Reserve Mining Company are in the north-central part (Fig. 2).

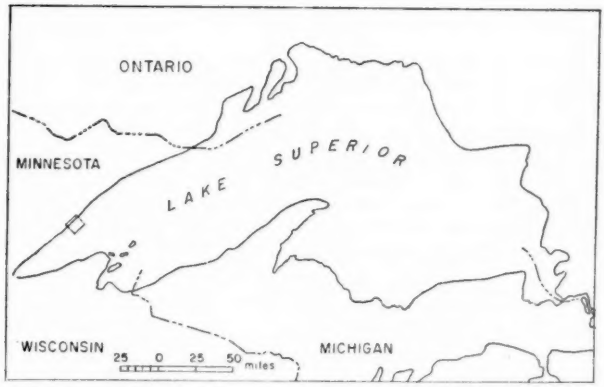

FIGURE 1.—INDEX MAP SHOWING LOCATION OF SILVER BAY AREA

General Geology

The Precambrian bedrock in the vicinity of Beaver Bay and Silver Bay is a complex of diabases, anorthosites, and associated igneous rocks of the Keweenawan Series (Grout and Schwartz, 1939, p. 79). The most prominent feature of the area is the Beaver Bay diabase sill which is a thick southward-dipping stratiform body, having several petrographic facies and inclusions of anorthosite, gabbro, amygdaloid, rhyolite, and other rocks (p. 33).

The small islands lying offshore in Silver Bay are among the few along the Minnesota coast. The rocks on Beaver Island consist of anorthosite and coarsely mottled diabase, whereas Cedar Island is built mainly of rhyolite.

The coast of Silver Bay exposes basalt flows with amygdaloidal tops, and farther northeast "red rock" is prominent in the cliffs. The Great Palisades is formed of rhyolite flows underlain by basalt flows.

Former levels of the lake are represented by wave-cut cliffs, beach ridges, lake terraces, and lake deposits, of which the highest set of features at about 1190 feet above sea level represent the shore line of Lake Duluth. Other, lower features were thoroughly described by Sharp (1953) in Cook County, farther northeast, but have not been studied in detail in the Silver Bay area. The surface rises steeply for the first 1–2 miles inland from the present shore line. The Hudson Bay-Gulf of Mexico divide is not far north of the lake shore, and the drainage areas of the rivers are rather small;

that of Beaver River in which this area lies is only 120 square miles (Grout and Schwartz, 1939, p. 10).

Most of the area northwest of Lake Superior is covered by glacial drift of the Highland terminal moraine and associated morainic belt (Schwartz, 1949, p. 73). The glacial deposits of the Superior lobe are bouldery and gravelly reddish-brown drift. The erosional products of this drift undoubtedly are brought by streams into the Silver Bay area.

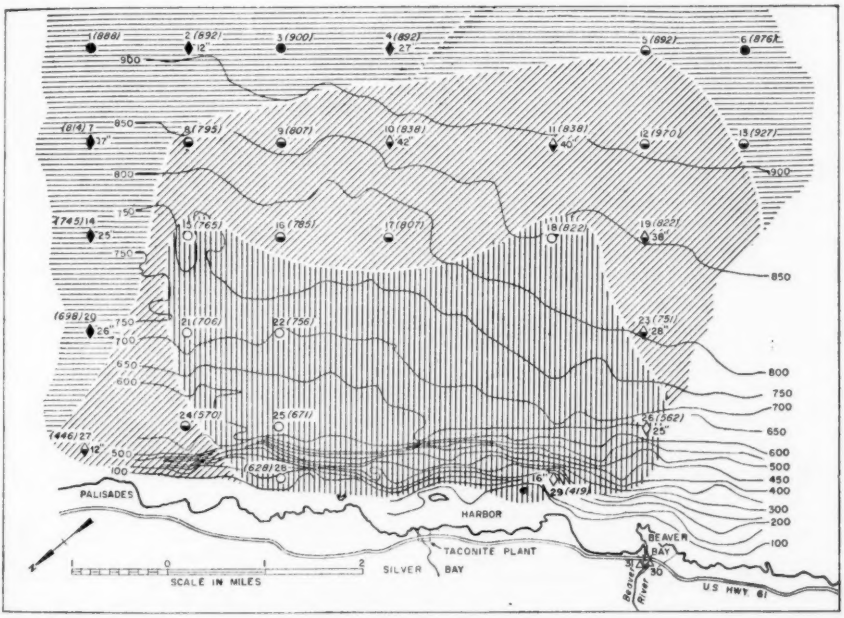

FIGURE 2.—LOCATION OF STATIONS, TYPE OF SAMPLE, COLORS OF BOTTOM SEDIMENTS, SILVER BAY AREA
Circles and discs are core stations in gray and red sediments, respectively. Parallelograms and rhombohedrons are Petersen dredge samples in gray and red sediments, respectively. Triangles are samples collected from Beaver River. Half discs and half rhombohedrons have less than 1 foot of red sediment overlying gray. Depths in parentheses are those determined at time of sampling and more often than not do not conform to echo soundings on which contours are based.

Bottom Topography

Adjacent to the cliffed shore line (Fig. 2) around Silver Bay, there are a sloping shelf 1000–2000 feet wide and great talus blocks of diabase where the gradient is 50–100 feet per 1000 feet. Offshore from this are a steeper slope 1000–3000 feet wide, inclined 200–300 feet per 1000 feet, and beyond, a gentler slope about a mile wide with gradients of 15–20 feet per 1000 feet to depths of 850 feet or more. About 4 miles offshore the bottom shoals southward.

The gentle offshore slope near the mouth of Beaver River is the surface of a submerged delta. There is no positive evidence that the generally steep offshore slope east of Silver Bay is a fault-line scarp (Schwartz, 1949, p. 81), as has been suggested. In general, the steep offshore slopes probably have affected the distribution of clastic sizes in the bottom sediments studied here.

Field and Laboratory Procedures

Twelve Phleger cores, 12–44 inches long, and 17 grab samples were obtained from the area shown in Figure 3. Samples were also obtained in Beaver River near its mouth and from the bank of the river. Duplicate cores were taken for inorganic chemical analyses at 10 stations, and these samples were stored in

bottles with chloroform. Electrometric pH and Eh determinations were made at lakeside. The cores and samples were stored at 40°F. until further studies could be made.

were chosen for determination of moisture content and shrinkage. Differential thermal analyses were run on the clay fractions of samples of the top and bottom of most of the

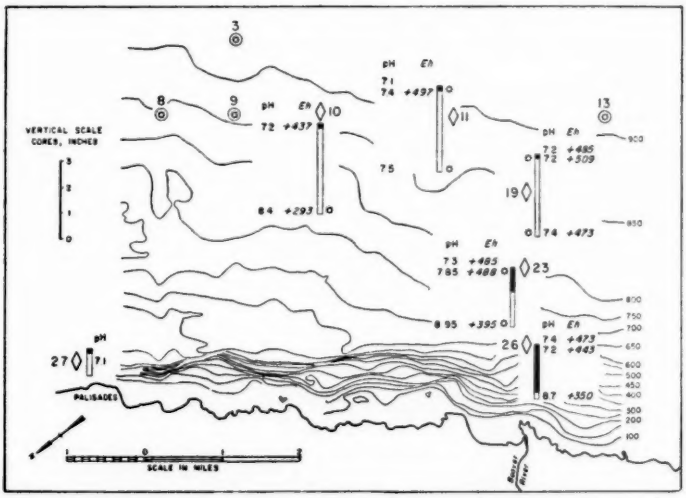

FIGURE 3.—LOCATION OF SAMPLES FOR CHEMICAL ANALYSIS (STARRED CIRCLES, pH, AND Eh) Open column, gray sediment; solid column, red sediment.

TABLE 1.—CHEMICAL ANALYSES OF WATER OF LAKE SUPERIOR NEAR SILVER BAY, MINNESOTA (Courtesy of Minnesota Department of Health)

Station	Year	Depth (Feet)	Turbidity	Color	Total Solids ppm	Fe ppm	Si ppm	Mn ppm	$SO_4^{=}$ ppm	Cl^{-} ppm	Alk ppm	Total alk ppm	pH
15	1953	comp.*	1.0	1.0	73	0.2	3.8	0.02	3.0	nil	48	n.d.	n.d.
16	1953	comp.	1.6	1.0	88	0.2	3.8	0.2	3.0	nil	48	n.d.	n.d.
17	1948	790	1.2	none	59	0.03	3.4	0.03	1.6	nil	40	46	n.d.
18	1953	comp.	1.3	1.0	68	0.2	3.4	0.2	3.0	nil	50	n.d.	n.d.
24	1953	comp.	2.5	1.0	93	0.4	4.6	0.4	3.5	nil	50	n.d.	n.d.
25	1954	comp.	10.0	4.0	57	0.1	4.6	0.1	4.0	nil	47	46	7.8
26	1953	comp.	0.2	1.0	73	0.09	3.4	0.09	3.0	nil	50	n.d.	n.d.

* Composite sample from surface, mid-depth, and full depth.

Analyses made of samples collected previously by the Minnesota Department of Health for turbidity, water chemistry, mud, chemistry, sedimentary particle size, bacteria, plankton, bottom fauna, and water temperatures were kindly turned over to the writers.

The bottom samples collected by Prokopovich for inorganic chemical studies were analyzed by the School of Mines Experiment Station. Portions of the tops and some of the bottoms of the cores and the grab samples were subjected to mechanical analyses by pipette or decantation methods. Selected core samples cores and of the grab samples. Extraction of several of the samples was made with a mixture of 80 per cent benzene and 20 per cent methanol. These bituminous extracts were separated by column chromatography over activated alumina (Smith, 1952; Swain, 1956).

The raw cores and grab samples were examined under the binocular microscope, and size fractions of several cores were studied.

Heavy-mineral separations were made on 7 samples, and total radioactivity was determined on 2 cores.

Acknowledgments

During 1948–1954 the Minnesota Department of Health and the Minnesota Department of Conservation made several surveys of the waters of Lake Superior in connection with the proposed discharge of tailings from a taconite beneficiation plant at Silver Bay, Lake County, Minnesota. During July 1954 through the courtesy of C. A. Johannsen of the Department of Health, Prokopovich collected the samples used in this study. In the laboratory the samples were studied by Prokopovich and Swain, assisted by I. Tkatchenko. Sincere appreciation is expressed to Mr. Johannsen and to J. N. Dornbush, B. B. Barker, J. J. Volkenant of Minnesota Department of Health; E. J. Longdin and R. E. Schumacher of Department of Conservation; D. S. Young of Ogleby Norton Company, Duluth; and H. H. Wade, Acting Director, School of Mines Experiment Station, University of Minnesota, for their assistance. H. E. Wright, Jr., read the manuscript and made helpful suggestions. The illustrations were drafted by B. Mooney and V. Stupnitsky. The work has been supported by a grant-in-aid from the Graduate School and by the Minnesota Geological Survey University of Minnesota. Aid in a study of the lipoid substances was obtained from a grant of the National Science Foundation.

Results

Limnologic Summary

The lake is oligotrophic; the proportion of total dissolved solids is only 50–100 ppm. Chemical analyses of the lake waters near Silver Bay are given in Table 1.

Temperature variations of the lake waters in the Silver Bay area were determined by the Minnesota Department of Health in 1953–1954 with a bathythermograph (Fig. 4). The records show development of thermal stratification; the upper limits of the thermocline are 20 feet and 40 feet and the average is perhaps 30 feet. The lower limits of the thermocline are 60 feet and 100 feet or more, and the average is about 75 feet. Slight variations near shore in the hypolimnion at stations 26 and 27 may be due to influx of denser masses of sediment-laden waters.

The sediments studied here, with the exception of those from Beaver River, accumulated in the hypolimnion zone.

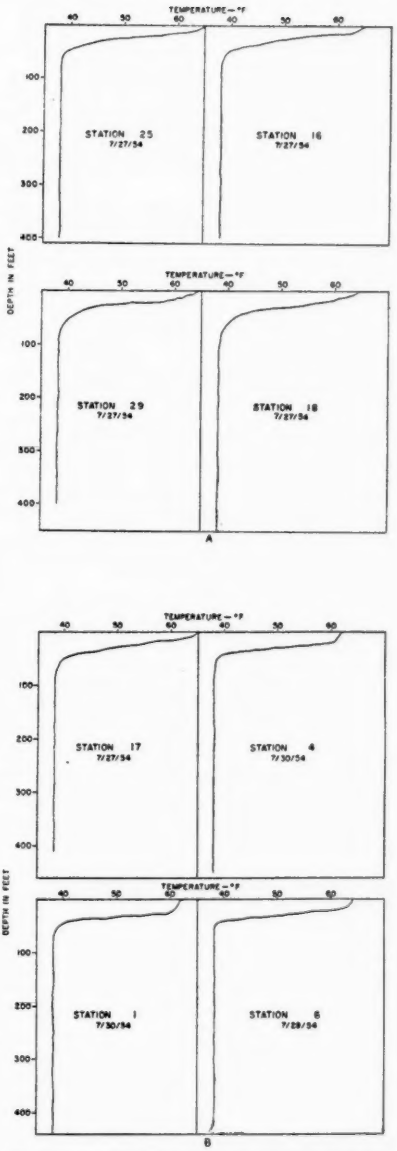

FIGURE 4.—BATHYTHERMOGRAPH RECORDS, SILVER BAY AREA

(*A*) Nearshore and intermediate stations. (*B*) intermediate and offshore stations. Data from Minn. Dept. of Health.

Organic productivity of the water of Lake Superior is low mainly because of lack of nu-

TABLE 2.—DESCRIPTIONS OF CORE SAMPLES, SILVER BAY AREA

Station	Type of sample	Depth of lake (Feet)	Description of core
1	core lost, only few cc recovered	888	10 YR 6/2. Slightly sandy, silty diatomaceous clay; coscinodiscoids, fragilaroids
2	core (27″)	892	5 Y 6/1. Sandy, silty clay
3	grab	900	Near 5 Y 6/1. Slightly sandy, silty diatomaceous clay; coscinodiscoids, few plant fragments, carbonized
4	core (27″)	892	Top. 10 YR 6/2. Slightly sandy, silty, diatomaceous clay; coscinodiscoids. Bottom. 10 YR 6/2 to 5 Y 6/1. Slightly sandy, silty diatomaceous clay, coscinodiscoids
5	grab	892	10 YR 6/2. Silty, slightly sandy diatomaceous clay; coscinodiscoids, plant fragments, patches of vivianite
6	grab	876	10 YR 6/2. Silty diatomaceous clay; coscinodiscoid diatoms; patches blue-green vivianite
7	core (17″)	814	Bottom 10 inches 10 YR 6/2. Slightly sandy, silty diatomaceous clay; fragilaroids, coscinodiscoids, chitinous exoskeletons; trace vivianite
8	grab	795	10 YR 6/2. Only slightly sandy, silty clay; few diatoms, pollen, trace ostracodes, plant fragments, carbonized
9	grab	807	10 YR 6/2. Slightly sandy, silty diatomaceous clay; fragilaroids; coscinodiscoids, chitinous exoskeletons, dark-brown egg case
10	core (42″)	838	Top. Pale-yellowish-brown (10 YR 6/2) slightly sandy silty diatomaceous clay; very abundant coscinodiscoids, few plant fragments, testate Protozoa; cylindrical aggregates organic rich silt, probably coprolites; trace vivianite near edge of core, possibly contamination Middle. 10 YR 6/2. Slightly sandy silty, clay, few diatoms, scattered red-brown feldspar grains and scattered small pebbles and granules of quartz Bottom. Light-olive-gray (5 Y 6/1) slightly silty clay; few carbonized plant fragments chitinous exoskeletons; small patches are pale red
11	core (40″)	838	Top. 10 YR 6/2. Slightly sandy, silty clay; few diatoms, fragilaroids, carbonized plant fragments, pollen, common chitinous exoskeletons, dark-brown egg cases, fish bone fragments Bottom. Light-olive-gray, 5 Y 6/1, slightly sandy, silty clay; testate Protozoa, few plant fragments, chitinous exoskeletons
12	grab	970	10 YR 6/2. Slightly sandy, silty diatomaceous clay; coscinodiscoids, fragilaroids, scattered red-brown feldspar grains
13	grab	927	10 YR 6/2. Slightly sandy, silty clay; few diatoms, fragilaroids; red-brown fish teeth or bone fragments
14	core (25″)	745	Bottom 10 inches 10 YR 6/2. Sandy silty clay; coscinodiscoid diatoms, chitinous exoskeletons; scattered coarse quartz grains
15	grab	765	Lost
16	grab	787	10 YR 6/2. Very fine sandy, silty diatomaceous, slightly carbonaceous clay; coscinodiscoid diatoms
17	grab	807	10 YR 6/2. Slightly sandy, silty clay; coscinodiscoid diatoms, plant fragments, red-brown fish teeth or bones, traces blue-green vivianite
18	grab	822	10 YR 6/2. Slightly sandy, silty clay, plant fragments, coscinodiscoid diatoms, feldspar grains
19	core 38″	822	Top. Pale-yellowish-brown (10 YR 6/2) fine sandy, silty diatomaceous clay; coscinodiscoids; few cladocerans; scattered reddish-brown feldspar grains, chlorite and biotite flakes, authigenic pyrite in small patches Bottom. 10 YR 6/2. Silty, slightly sandy diatomaceous, carbonaceous clay; coscinodiscoids, few cladocerans, sedge fragments

TABLE 2.—*Continued*

Station	Type of sample	Depth of lake (Feet)	Description of core
20	core 26″	698	Top. Near light-olive-gray (5 Y 6/1) pure clay with few pockets, fine to coarse pink feldspathic sand, with grains of dark minerals
21	grab	706	10 YR 6/2. Slightly sandy, silty clay, traces dark grain, very tenaceous
22	grab	756	Pale-brown (5 YR 5/2) slightly sandy, silty clay; traces red-brown fish teeth bones
23	core 28″	751	Top. Near 10 YR 6/2. Slightly silty clay; traces red-brown fish bones. Middle. near 10 YR 6/2. Fine sandy, silty micaceous, feldspathic, diatomaceous clay; coscinodiscoids, red-brown fish bones, plant fragments, red, oxidized worm(?) trails Bottom. Near 5 Y 6/1. Pure clay
24	grab	570	Near 10 YR 6/2. Clayey, silty, very fine to fine, micaceous, feldspathic, angular sand, in parts darker streaks contain diatoms and testate Protozoa
25	grab	671	Near 5 YR 5/2. Fine to coarse sandy, feldspathic clay, mica flakes, dark grains—probably ferromagnesian minerals, few plant fragments
26	core 24 ± 2	562	Top. Near 5 YR 5/2. Very silty, very fine to fine, angular, feldspathic sand or graywacke; ferromagnesian minerals Bottom. Near 10 YR 6/2. Very argillaceous, silty fine sand or sandy clay, feldspathic
27	core 12″	446	Near pale-yellow-brown to medium-yellowish-brown, but contains tinge of red, fine, silty, angular, feldspathic, sand or graywacke; few melosiroid diatoms, abundant dark minerals; few plant fragments
28	grab	628	Near 10 YR 6/2. Clayey, silty, very fine to fine feldspathic angular sand or graywacke, mica flakes, rock fragments, ferromagnesian minerals; plant fragments; red-brown resinous fragments—may be fish bones or teeth
29	core 16″	419	Top. Between 10 YR and 5 YR 5/2. Pale-reddish-brown, fine- to coarse-grained, silty, micaceous, feldspathic, sand or graywacke; melosiroid diatoms, scattered soft brittle red-brown flakes (fish bones or teeth)
30	hand picked	In small pond among boulders and rocks	Beaver River. Pale reddish brown—near 4 YR 5/2. Very fine- to medium-grained, silty feldspathic, micaceous sand or graywacke; twigs, and other plant fragments, aquatic insect parts

trient materials. Diatoms are the most abundant plankters in Silver Bay, and the next most abundant are blue-green algae and protozoans; rotifers, crustaceans, and green algae also occur in small to moderate abundance. Total populations of these organisms as determined by the Minnesota Department of Health in September 1948 and 1949 ranged from 60–600 × 10^3/100 liters of water. There seems to be no consistent relationship between numbers of individuals and depth of water down to 850 feet. Coliform bacteriological populations were negligible at most stations in 1948, at least to depths of 160 feet; total bacterial populations are presumably much higher but have not been determined.

Physical and Chemical Properties of Sediments

General description.—The bottom sediments of the Silver Bay area are principally pale-olive-gray to reddish-brown slightly sandy, silty clay (Table 2). Near the mouth of Beaver River, the sediments become progressively more sandy and at several stations contain lenses of fine- to coarse-grained, angular, micaceous, feldspathic tand and graywacke,

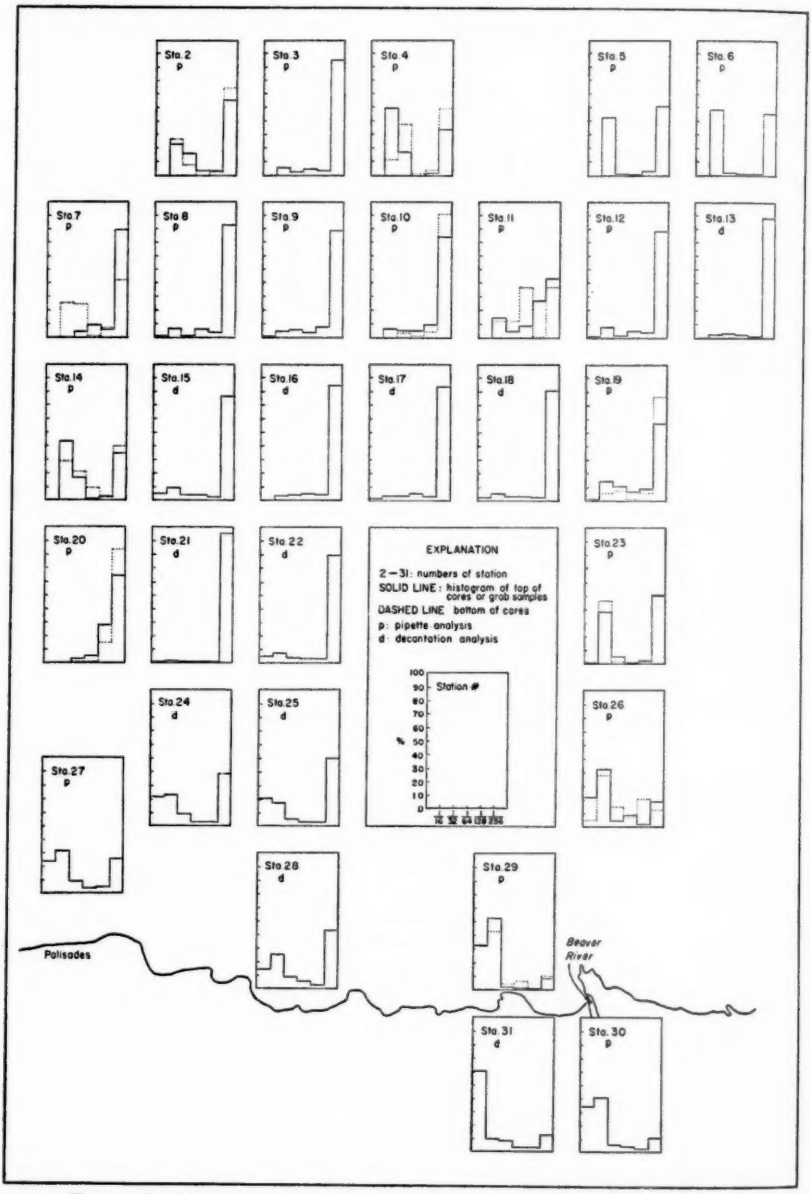

FIGURE 5.—MECHANICAL ANALYSES OF MEDIUM AND COARSE PARTICLE SIZES

Authigenic pyrite (sta. 19) and vivianite (stas. 5, 6, 10, 17) were observed. Organic remains include coscinodiscoid and fragilaroid diatoms, cladocerans, testate protozoans, fragments of fish bones, land plants, questionable worm trails that are oxidized red, brown insect (?) egg cases, and cylindrical aggregates or richly organic silt, probably fecal pellets. The Beaver River sample was very fine- to medium-grained, feldspathic, micaceous sand

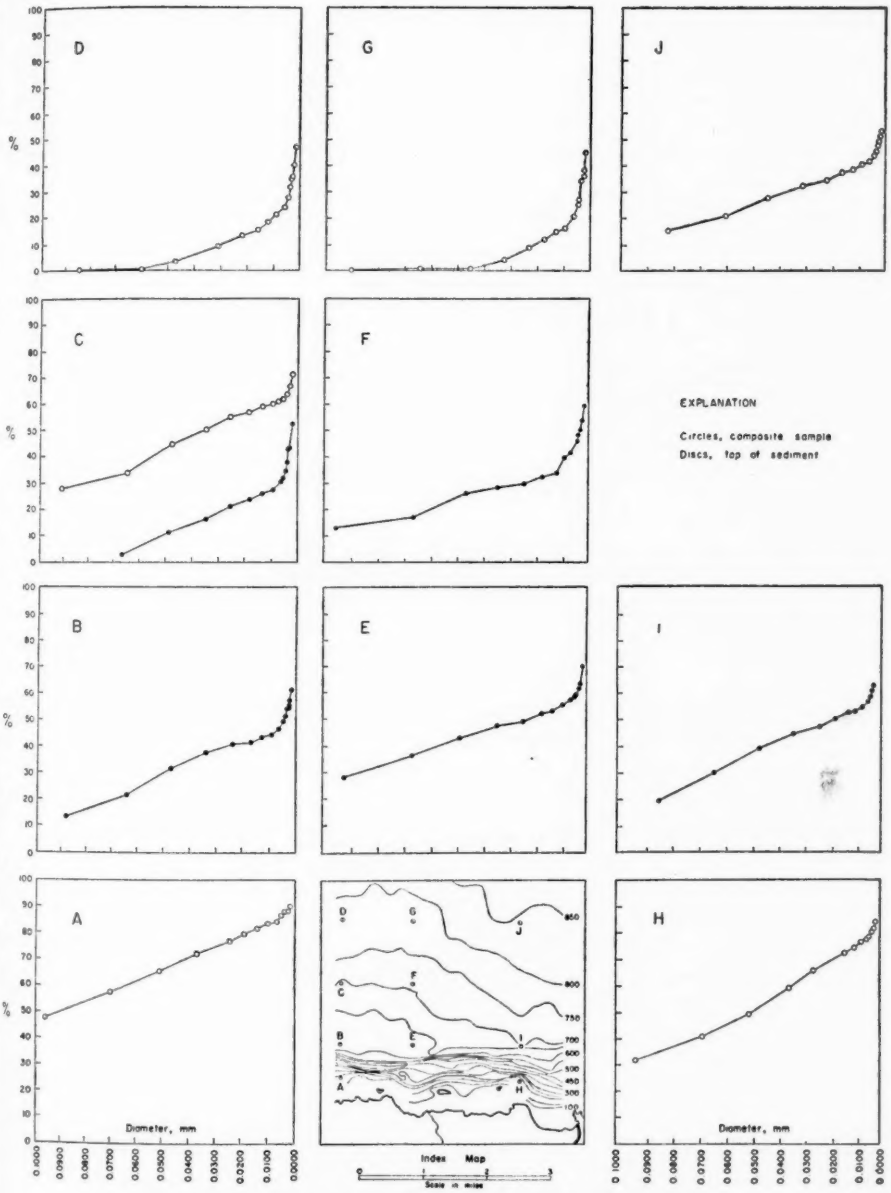

FIGURE 6.—MECHANICAL ANALYSES OF FINE PARTICLE SIZES
Plotted as cumulative curves. Data from Minn. Dept. of Health.

or graywacke with abundant twigs, other plant fragments, and aquatic insect parts.

Color.—The color of the sediments is shown graphically in Figure 2: red (Munsell Color Chart 5 YR 6/2–10 YR 6/2) near shore and near the mouths of incoming rivers or creeks to a depth of 1 foot or more; less than 1 foot of red overlying gray (5Y 6/1) offshore and

near shore away from river and creek mouths; and gray without overlying red at greater distances from shore.

Hydrogen-ion concentration.—The pH of the bottom water (Fig. 3) in July 1954 was only slightly alkaline, 7.1–7.4. The tops of the few cores measured are about the same, but slightly more alkaline at some stations; the pH at the bottom of the cores is typically higher, 7.4–8.95.

Oxidation-reduction potential.—Considering the depth of water the Eh values (Fig. 3) show surprisingly high oxidation intensities, and the

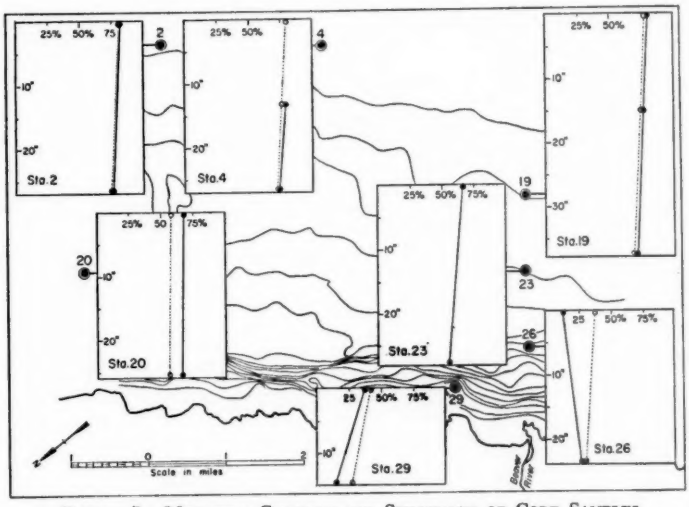

FIGURE 7.—MOISTURE CONTENT AND SHRINKAGE OF CORE SAMPLES
Circles and dashed lines represent percentage of moisture; discs and solid lines represent percentage of shrinkage when sediment is dried.

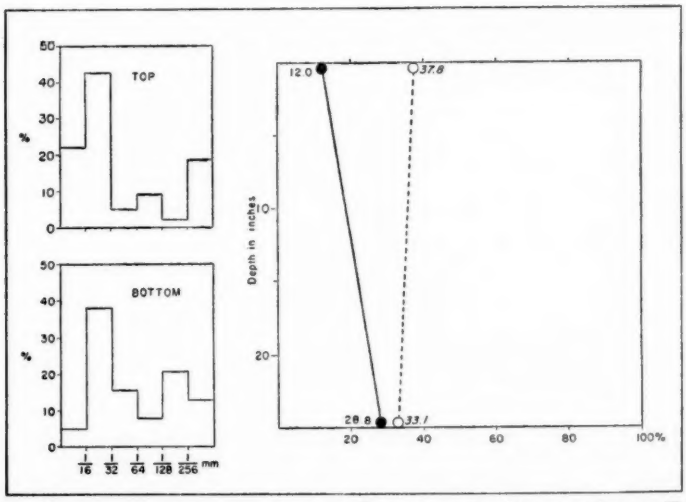

FIGURE 8.—COMPARISON OF MOISTURE CONTENT, SHRINKAGE, AND PARTICLE SIZE AT TOP AND BOTTOM OF CORE 26
Histograms of core samples are on left, percentage of moisture is shown by circles and dashed line; shrinkage is shown by discs and solid line. Lack of parallelism between shrinkage and moisture content results from marked textural difference between top and bottom of core.

high values generally pertain at depths of 1–2 feet, even though other factors such as color suggest that the sediments are held under reducing conditions.

7. At the tops of the cores the moisture ranges from about 38 per cent in sandy near-shore sediments to over 80 per cent in clayey offshore deposits. At depths of 2–3 feet the moisture is

TABLE 3.—INORGANIC ANALYSES OF SILVER BAY SEDIMENTS*

Station	3	8	9	10b	11t	11b	13	19t	19b	23t	23b
SiO_2	54.39	53.94	54.79	50.92	53.82	54.16	54.41	54.53	54.66	55.48	46.60
Al_2O_3	14.33	12.86	15.31	16.01	14.67	14.83	14.90	14.85	14.34	14.73	14.57
Fe_2O_3	9.92	9.46	9.43	10.09	12.20	10.09	10.32	11.89	9.75	13.09	8.94
FeO	2.57	2.78	2.98	3.51	2.14	2.69	2.37	1.63	2.67	1.64	3.40
MgO	4.00	....	1.77	5.08	3.15	3.86	3.63	3.69	4.02	4.10	5.09
CaO	2.39	....	2.74	3.28	2.75	2.65	2.67	3.30	3.04	3.82	7.06
Na_2O	1.55	1.74	1.82	1.61	....	1.72	1.68	1.69	1.76	1.73	1.57
K_2O	2.83	2.06	1.70	3.62	....	3.03	3.17	2.81	2.95	3.16	3.42
TiO_2	0.47	0.41	0.60	0.63	0.67	0.62	0.66	0.63	0.65	0.57	0.52
P_2O_5	0.49	0.33	0.37	0.27	0.33	0.36	0.48	0.23	0.16	0.26	0.30
MnO	0.16	0.10	0.12	0.18	0.33	0.15	0.16	0.77	0.14	0.23	0.15
Ign. loss	6.89	5.65	....	5.07	....	....	....	....	....	....	7.94
CO_2	(0.16)	(0.20)	0.24	(1.24)	....	....	(0.20)	....	(0.14)	0.28	(4.38)
S	(0.02)	(0.08)	0.02	(0.04)	....	....	(0.03)	....	....	....	(0.04)
H_2O^+	....	....	4.89	....	....	4.99	4.79	4.86	4.91	....	....
H_2O^-	....	....	3.50	....	....	....	....	....	....	....	....
Totals	99.99	....	100.28	100.27	....	99.15	99.24	100.88	99.05	99.09	99.56

*Analyses by School of Mines Experiment Station, V. C. Bye, analyst.

Total radioactivity.—Total radioactivity of samples of core no. 10, top, and of core no. 11, top, was 3.6 and 4.67 counts per minute above background, respectively.

Mechanical analyses.—The medium and coarse particle sizes of the Silver Bay sediments based on settling and siphon analyses by Prokopovich and Tkatchenko (Fig. 5) show gradual offshore decrease to positions 2–3 miles out, beyond which a secondary maximum in the fine-sand size appears. This is particularly well illustrated at stations 2, 4–6, and 14. Other stations (23, 26) near Beaver River also show a secondary maximum in the fine sand size.

Cumulative curves (Fig. 6) of the clay and silt sizes recalculated from hydrometer analyses made by the Minnesota Department of Health show a predominantly linear form at near-shore stations; this changes to a typically more definitely hyperbolic form offshore. At station *J* (Fig. 5) the curve is less hyperbolic in agreement with the histograms of particle sizes at stations 5 and 6.

Moisture content and shrinkage.—The moisture content of several cores is shown in Figure

reduced to 33 per cent and 76 per cent in sandy near-shore and clayey offshore sediments respectively. The percentage of shrinkage closely parallels the decreases in moisture from top to bottom of the cores in the clayey sediments, but not in the sandy sediments where total shrinkage is much less (Fig. 8).

Chemical and mineralogical composition.—Partial inorganic analyses of the Silver Bay sediments are given in Table 3, and differential thermograms are shown in Figure 9. The silica content of the sediments is similar to that of diabase of this area (Grout and Schwartz, 1939).

The differential thermograms are very difficult to interpret because of the broad zone of oxidation of organic matter between 100°F. and 600°F. The endothermic shifts around 580–600°F. in the majority of the samples suggest a clay mineral, possibly illite and/or nontronite. This is matched in many of the curves by a slight exothermic shift above 900°F., also suggestive of illite or nontronite. Small endothermal shifts about 725–750°F. in some samples may represent montmorillonite. The absence of distinct quartz endothermal peaks is noteworthy.

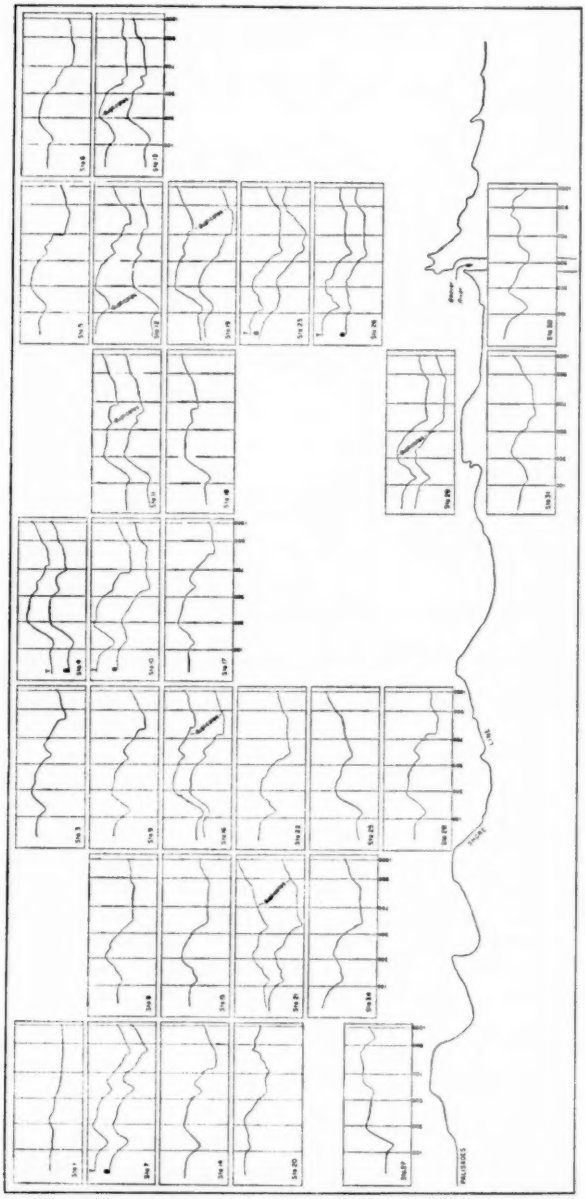

FIGURE 9.—DIFFERENTIAL THERMAL ANALYSES OF GRAB SAMPLES AND CORES

Heavy-mineral fractions of these sediments were particularly rich in epidote (Table 4). The light fractions consist almost entirely of more or less weathered feldspar.

TABLE 4.—HEAVY MINERALS IN SILVER BAY SAMPLES

Station	Total heavy fraction Per cent of sample	Magnetic fraction Per cent of sample	Nonmagnetic Heavies Per cent of heavies
25	18.8	2.83	14.9
26	12.4	1.89	15.2
27	18.3	2.74	15.0
29t	15.2	2.45	16.2
29b	11.6	1.88	16.7
30	4.6	1.07	23.1
31	10.2	1.20	11.7

TABLE 5.—CHROMATOGRAPHIC ANALYSES OF LIPOID EXTRACTS FROM SILVER BAY CORES
In ppm of sample

Lipoid substances	Station 13	Station 22
Total lipoids	290	360
n-Heptane eluant	50	60
Benzene eluant	70	45
Pyridine + methanol eluant	45	45
Polar compounds	125	210

Lipoid substances.—The quantities of lipoids extractable with benzene + methanol and the chromatographic fractions of these extracts of samples from stations 13 and 22 are given in Table 5. The heptane eluants are taken as the saturated hydrocarbon fraction, the benzene eluants as the aromatic hydrocarbons, and the pyridine + methanol eluants as the asphaltene fractions.

The heptane fractions consist of colorless oil droplets; the benzene fractions are colorless to pale-yellow oil; and the pyridine and methanol fractions are colorless to pale-yellow oily wax. Fluorescence was not seen in these samples, but the benzene eluant of an unweighed extract from station 26 had golden fluorescence. An ultra-violet absorption spectrum of the pyridine cut of the extract from station 26 is given in Figure 10 and shows the presence of an unidentified aromatic compound.

DISCUSSION

Color Changes in Sediments

The sediment transported to the Silver Bay trough by Beaver River and other streams and by wave action is pale reddish brown owing to the partly oxidized state of the iron oxides in the sediments. The reddish-brown color is preserved near the stream mouths probably as a result of the oxygenated river water; but offshore at the mud interface and near shore 1–2 feet beneath the surface the ferric oxides are slowly reduced. The reduction apparently goes on in spite of the weak to moderate oxidizing intensities of this environment (Fig. 3). There is evidently enough organic matter to provide at these lowered temperatures a moderately high reducing capacity which overcomes the tendency for the sediments to oxidize. When the gray mud samples are left at room temperatures they rapidly become mottled tan, yellow, and red. There is no evidence of either addition or subtraction of iron in the sediments by halmyrolysis (Hummel, 1922).

Comparison with Glacial Lake Clays near Duluth, Minnesota

In the vicinity of Wrenshall, Minnesota, T. 48N., R. 16W., southwest of Duluth and elsewhere near the southwestern end of Lake Superior are red and gray clays of Glacial Lake Duluth. At Wrenshall is about 30 feet of calcareous gray clay below and about 10 feet of red clay above. In the upper part of the gray clay reddish-brown beds are intercalated. Both the red and gray carry common Ostracoda of the genus *Limnocythere*, a shallow-water genus. Schwartz (1949, p. 120) attributes the red colors of the Wrenshall clays to surface weathering. The writers agree that the more solidly red upper Wrenshall clay probably may be due in part to recent weathering but suggest that the red layers interbedded in the gray clay represent a primary color. The origin of the bedded red layers is probably similar to that which characterizes the Silver Bay red clays—*i.e.*, weathered red sediments deposited rapidly enough to prevent complete reduction of the ferric oxide. In the Wrenshall deposits, fluctu-

ation of rates of deposition, amount of organic matter, climate, or combinations of these factors probably account for the layering.

On the basis of his studies in northeastern Minnesota Wright (1955, p. 410) believes that other offshore barriers in the shallower water possibly aid in catching fines and allow a certain amount of coarser materials to travel farther out by means of bypassing. Ice rafting, if effective, should transport pebbles as well as

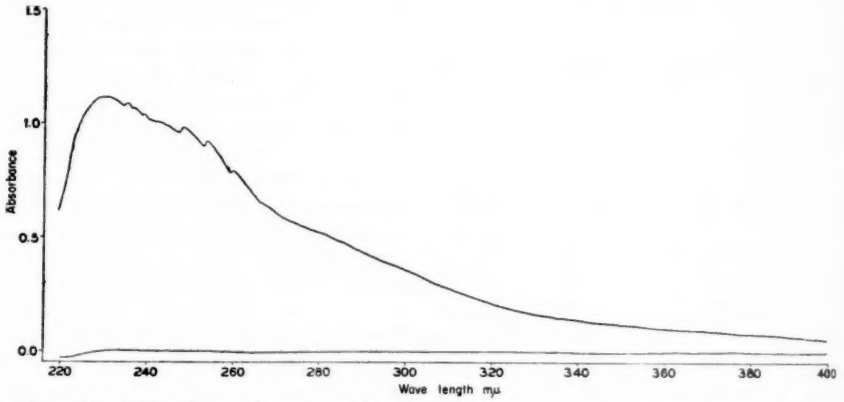

FIGURE 10.—ULTRA-VIOLET ABSORPTION SPECTRUM OF PYRIDINE + METHANOL ELUANT OF LIPOID EXTRACT FROM STATION 26

the color alternations at Wrenshall are all primary and are the result of drainage to Lake Duluth of sediments from two separate ice lobes which carried different till types.

Interlaying of gray and red clays in deep-water cores in Lake Michigan was observed by Hough (1955, p. 957) who attributes the color variations to differences in the state of oxidation of the iron, because little organic matter is present.

Textural Variations in the Sediments

The appearance of larger grains in the sand fractions at stations 2, 4, 5, 6, 14, 23, and 27, offshore from areas that have little such coarser material, has several possible causes: (1) transportation of masses of sediments by turbidity currents, (2) bypassing during storms, (3) ice rafting of coarser particles, (4) different source areas.

The steep offshore slope near Silver Bay probably causes the masses of sediments deposited near shore on the relatively steep slopes to break away and move rapidly downward with momentum sufficient to carry coarser material far offshore. In addition, rock ridges or sand out to deeper waters. The possibility that some of the sediment has been transported along shore by shore currents cannot be evaluated properly from existing data. That such a process has been responsible for the offshore coarsening of some of the other Silver Bay sediments does not seem very likely.

Compaction and Shrinkage of the Sediments

There is an expected slight decrease of moisture downward in similar sediments owing to compacting forces. The shrinkage at most of the stations corresponds very well with the decrease in moisture (Fig. 7), but at station 26 the sediment becomes appreciably more argillaceous downward (Fig. 8) and the shrinkage is much greater in the lower than in the upper part of the core. Similar phenomena were observed in the other Minnesota lake deposits (Swain, 1956, p. 630).

Biofacies

There is very little information on the biofacies of the Silver Bay deposits. In general there seems to be an offshore biofacies having

common diatoms mainly of coscinodiscoid types (Fig. 11) and a biofacies nearer shore and particularly near the river mouth where oligochaetes and malacostracan crustacea are common. In view of the apparent similarity of

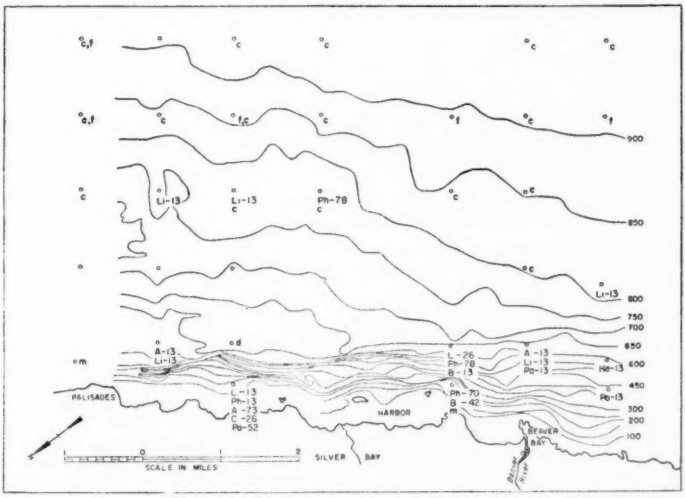

FIGURE 11.—DISTRIBUTION OF BOTTOM FAUNA AND DIATOMS IN SILVER BAY SEDIMENTS

Letter *L*, *Limnodrilus* sp. (oligochaete); *Ph*, *Pontoporeia hoyi* Smith (amphipod); *B*, *Brillia par* (Coq.) (dipteran pupa); *A*, *Aeolosoma* sp. (ologochaete); C, caddis fly cases; *Ha*, *Hyalella azteca* (Saussure) (amphipod); *Li Limnocalanus* sp. (copepod); *Pa*, *Pontoporeia affinis* (Lindström) (amphipod); *f*, fragilaroid diatoms; *c*, coscinodiscoid diatoms; *m*, melosiroid diatoms; *d*, undifferentiated diatoms.

limnologic conditions nearer shore, it is not clear why diatoms are principally restricted to bottom sediments beyond the 750-foot contour. Lack of food supply could reasonably account for scarcity of the bottom fauna at offshore stations.

Interpretations of Lipoid Substances

In eutrophic lake deposits and bog accumulations elsewhere in Minnesota, the "polar" compounds form 50–65 per cent of the lipoid material (Swain, 1956, p. 643; Swain and Prokopovich, 1954, p. 1189), whereas in an oligotrophic lake these polar substances are only about 20 per cent of the lipoids. The cause for this is believed to be the greater production of pond weeds and other higher plants in the eutrophic lakes and bogs, in the deposits of which tars, resins, and other substances would accumulate in greater quantities. The Silver Bay polar compounds average 55 per cent of the lipoids, and the asphaltene, aromatic hydrocarbon, and saturated hydrocarbon fractions, respectively, average 14, 18, and 17 per cent. As compared to eutrophic lakes in Minnesota, the asphaltenes are much lower—about half the value of the other lakes; and the aromatics and saturated hydrocarbons are about twice as high. The reasons for these interesting and probably significant relationships are obscure.

CONCLUSIONS

The offshore clayey sediments in the vicinity of Silver Bay are in two color facies and two principal biofacies. The reddish-brown feldspathic clay deposits near the river mouths, in water several hundred feet deep, are colored by ferric oxides, the source of which is the weathered Keweenawan igneous rocks and associated interbeds of red clastics and reddish glacial drift which is derived from the red Keweenawan clastics and weathered igneous rocks. The clays farther offshore and beneath the thin red layer are gray owing to diagenetic reduction of the ferric oxide. The offshore increase of grain size

in several cores may be principally the result of turbidity currents resulting from submarine slumping of the soft clays on the steep slopes where they are accumulating. The work of Ericson *et al.* (1952) has demonstrated the probable role of turbidity currents in transporting sand and gravel to distances of 100 miles or more offshore from the Hudson River canyon. In Silver Bay it is perhaps surprising, because of the steep offshore slopes, that coarser material was not found in the offshore sediments. The difference in importance of currents originating from the river during high-water stage as compared to currents initiated by sublacustrine mud slides cannot be evaluated at present in the Silver Bay area.

Offshore areas at Silver Bay are generally characterized by a diatomaceous biofacies as contrasted to a nearer-shore oligochaete-malacostracan biofacies or, stated differently, an offshore facies with settled plankton and a nearer-shore benthonic biofacies. Disturbance of the bottom sediments may account for the absence of the nearer-shore biofacies at several stations, but could scarcely account for the absence of pelagic organisms at some of the offshore stations. The original distribution of the organic remains in the sediments is evidently spotty, and internal standing waves may not be so important in distributing settled plankton in such large, deep lakes as they have been suggested to be in smaller lakes (Swain, 1956, p. 637).

The interesting high-hydrocarbon and low-asphaltene content of the Silver Bay sediments is at present unexplainable but may be the result of the scarcity of total organic producers as compared to consumers in this environment. The more eutrophic environments in Minnesota lakes, but not the bogs, produced the larger quantities of asphaltenes (Swain, 1956, p. 643).

References Cited

Ericson, D. B., Ewing, M., and Heezen, B. C., 1952, Turbidity currents and sediments in North Atlantic: Am. Assoc. Petroleum Geologists Bull., v. 36, p. 489–511

Grout, F. F., and Schwartz, G. M., 1939, The geology of the anorthosites of the Minnesota coast of Lake Superior: Minn. Geol. Survey Bull. 28, 119 p.

Hough, J. L., 1955, Lake Chippewa, a low stage of Lake Michigan indicated by bottom sediments: Geol. Soc. America Bull., v. 66, p. 957–988

Hummel, K. 1922, Die Entstehung eisenreicher Gesteine durch Halmrolyse: Geol. Rundschau, v. 13, p. 40–81, 97–136

Schwartz, G. M., 1949, The geology of the Duluth metropolitan area: Minn. Geol. Survey Bull. 33, 136 p.

Sharp, R. P., 1953, Shorelines of the glacial Great Lakes in Cook County, Minn.: Am. Jour. Sci. v. 251, p. 109–139

Smith, P. V., Jr., 1952, The occurrence of hydrocarbons in Recent sediments from the Gulf of Mexico: Science, v. 116, no. 3017, p. 437–439

Swain, F. M., 1956, Stratigraphy of lake deposits in central and northern Minnesota: Am. Assoc. Petroleum Geologists Bull., v. 40, p. 600–653

Swain, F. M., and Prokopovich, N., 1954, Stratigraphic distribution of lipoid substances in Cedar Creek bog, Minnesota: Geol. Soc. America Bull., v. 65, p. 1183–1198

Wright, H. E., Jr., 1955, Valders drift in Minnesota: Jour. Geology, v. 63, p. 403–411

University of Minnesota, Minneapolis, Minnesota

Received by the Secretary of the Society, September 13, 1956

Published with Permission of Director, Minnesota Geological Survey

BULLETIN OF THE GEOLOGICAL SOCIETY OF AMERICA
VOL. 68, PP. 543-554 MAY 1957

FLYSCH SEDIMENTATION

BY ZB. L. SUJKOWSKI[1]

ABSTRACT

The main problem in understanding the origin of the Flysch is the explanation of the innumerable pelitic and psammitic layers, which alternate without transition zones. Characteristics of Flysch series, both in the Carpathians and elsewhere are the contrast in character between the pelitic and psammitic layers, the scarcity of organic remains, and the monotony and lateral persistence of lithology and structure within any one series. Although the general aspect, or "style" of Flysch series persists, individual beds are not persistent, and sedimentary rhythms are not present. Characteristic structures are graded bedding and "hieroglyphs" on the lower surfaces of psammitic strata. The hieroglyphs are explained as moulds of decayed algae, animal tracks, or mechanically produced flowmarkings, or diastrophic scratches and furrows; the latter are not true hieroglyphs. Accessories to Flysch series include bedded cherts, calcareous marl or limestone, conglomerates and exotic blocks. Flysch series are explained as the product of normal pelitic or pelagic sedimentation, interrupted by the periodic deposition of psammitic layers brought in by turbidity currents. Either oxidizing or reducing conditions may prevail in the basin of deposition, and in the Carpathian Flysch the rate of deposition is of the order of 1 inch per 1000 years; the psammitic layers have a mean thickness of 5 inches, and deposition of a layer took place, on the average, once every 4000 years. The turbidity-current theory implies that Flysch series were deposited in deep water.

CONTENTS

TEXT

	Page
Introduction	543
Definition of Flysch	544
Description of deposit	544
Pelitic layers	544
Psammitic layers	544
Contacts of layers	545
Hieroglyphs	545
Organic remains	546
Other features	546
Subfacies of Flysch	547
Transition to non-Flysch facies	548
Flysch facies outside the Alpine zone	548
Origin of Flysch	548
Chemical conditions of sedimentation	548
Rhythm of sedimentation	549
Rate of sedimentation	549
Depth of sedimentation	550
Conclusion	552
References cited	552

INTRODUCTION

The author studied the petrology and origin of Flysch series for about 10 years before World War II. His chief studies were in the Carpathians, in an area 700 miles in length from Silesia across Poland to north Rumania. (For a recent summary of the geology of this area *see* Książkiewicz, 1956). Trips to south Rumania, Slovakia (Czechoslovakia), Bulgaria, the Tyrol, Switzerland, the Apennines, and Spanish Morocco's Riff furnished material for comparison inside the Alpine ranges. St. Cross Mountain in Poland served as a good example of an older Flysch (Cambrian).

The author concluded earlier (Sujkowski, 1938) that Flysch is not an extremely shallow sea deposit but a slope deposit stretching from neritic to fairly great depths. At that time an adequate explanation did not exist for the deposition of sand layers down the slope without interference with clay sedimentation. The

[1] Dr. Sujkowski died in 1954 and left this paper completed but unrevised. Editing and some rewriting has been undertaken by G. V. Middleton of McMaster University.

density-current theory furnished a necessary explanation for transportation of material and stimulated the author to return to the subject of Flysch sedimentation.

This paper is neither a history nor a review of Flysch researches. Hundreds of papers have been written on the Carpathian Flysch in at least seven languages, and almost as many have been written about the Alpine Flysch.

Definition of Flysch

The term Flysch has been in use for over a century in European geological literature. In Swiss-German dialect the word means "gliding rock". It was first applied (Studer, 1827, p. 39) to a local Alpine series of Tertiary age, over 10,000 feet in thickness, poor in fossils, and composed of marl and shale beds with interstratified sandstone layers. Use of the term was restricted at first to a formation name for the lower Tertiary series in north Switzerland. It soon connoted a facies and was applied to all analogous series of Tertiary age within the Alpine ranges and subsequently to similar series of all ages in all the Alpine regions. Outside the Alpine zone the term Flysch is applied sporadically, with slightly different meanings in different countries. There is no generally accepted definition of the term; as used in this paper it is defined as follows:

The name Flysch is a facies denomination for a marine deposit composed of innumerable alternations of sharply divided pelitic and psammitic layers. Other rocks in the deposit are accidental, and in particular pure limestones are rarely present. The series commonly attain thicknesses of thousands of feet and were deposited in geosynclinal areas.[2]

Description of Deposit

Pelitic Layers

The pelitic layers are composed of either calcareous or noncalcareous shale; the psammitic layers are chiefly sandstone, but mudstones, arkoses, conglomerates, and gravel beds are also found.

Most of the shales are laminated or fissile. The layers are commonly regular and are undisturbed except by folding subsequent to deposition. Some of characteristic laminae can be distinguished over distances of scores of miles. Where grading exists it is limited to a particular lamina and does not affect the layer as a whole. The thickness of a layer ranges from an inch to several feet, but it remains fairly constant over considerable stretches; the average thickness of a layer is estimated at 5-6 inches. Some shale layers, in restricted subdivisions of the same series, contain peculiar types of nodules. Inclusion of these nodules may have been contemporaneous with, or subsequent to, sedimentation (Sujkowski, 1938, p. 29); common flint or phosphatic nodules are either absent or exceptional. In some places pelitic layers succeed each other without intervening psammitic layers.

Psammitic Layers

In general, the sandstone layers are well sorted and exhibit grading, with the coarser material at the bottom and the finer on top. Each layer thus has the character of a unit of sedimentation. If lamination is present, it is subordinate to the grading. No nodules have been observed in the sandstone layers, but there is much foreign material—broken detritus, clastic grains, gravel pebbles, and larger blocks (exotics). Perhaps the most characteristic of this foreign material are pellets of shale, or galets of half-indurated shale (but not clay), most of which are flat, with rounded edges. These are incorporated in the basal part of some sandstone layers and in places are so numerous that the bed assumes the appearance of a conglomerate. The material forming the pellets closely resembles, or is identical with, that of the shale layers.

In some subfacies of Flysch, sand beds contain 10–40 per cent of feldspar grains, and the rock grades into an arkose, which in places is coarse-grained. An example is the upper Cretaceous Czarnohora Series.

The sandstone layers range in thickness from half an inch to dozens of feet, but the average is about 8 inches. In a particular part of a Flysch series, however, the thickness of the sandy

[2] This definition is similar to that of Tercier (1947).

layers is fairly constant. The layers are not persistent horizontally; it is almost impossible to identify a sandstone layer in an exposure a few miles away, even though an adjacent pelitic layer is identifiable there. The sandy stratum has either edged out or changed in composition and thickness, so that it is almost or quite unrecognizable. A psammitic layer at any particular part of its length is thus a flat lens and a possible oil trap.

In places, contorted structures are found within a psammitic layer and take the following forms:

(1) A pecular sort of ripple marking, in which each lamina is bent into a wavy pattern, like a sheet of corrugated iron. All the lamellae remain strictly parallel throughout the thickness of the bed. There are no traces of the erosional grading or cutting of one lamina before the deposition of the next; the whole layer has the appearance of a single unit, deposited in one body of moving water.

(2) "Slip" structure, which occurs chiefly in siltstones and is generally confined to the inside of the layer. The top and the base are undisturbed. This structure probably resulted from the flowing of a plastic interior after the whole layer was deposited and was probably induced by tilting, either through subsidence or the beginning of folding. The neighboring shale layers are not involved in the movement. Książkiewicz (1950) described similar phenomena observed in the Carpathians. In some places this internal disturbance has the character of minute folding of unbroken laminae, but in other places the structure is more complicated, and a disrupted and broken pattern appears. Water squeezed from the shale during folding, or by the pressure of the overburden, may account for the half-fluid state of the siltstone, which seems to have come into existence after, not during, deposition (Sujkowski, 1938; Książkiewicz, 1950).

(3) Exceptionally, cross-bedding has been observed in sandy layers (Książkiewicz, 1948).

(4) Normal-wave ripple marks are restricted to parts of some subfacies, but where present are numerous. Current-ripple marks with a wave length of several inches are more common, but such markings never cover large surface areas.

Contacts of Layers

Contacts of the layers are everywhere sharp and clean cut, but there is a difference between the upper and lower contact of each layer. In many places the contact of a sandstone with an underlying shale layer cuts the top of the shale and looks like a plane of discontinuity. The upper contact of the same sandstone layer, however, exhibits no discontinuity; it is not pronouncedly sharp, and in a few places a tendency toward a passage bed is evident.

Hieroglyphs

In some Flysch series the top and bottom surfaces of sandstone layers carry a special pattern of marking known as hieroglyphs or fucoids; definition of the terms is vague. If the markings occur on both surfaces of a layer, they differ widely in character from one surface to the other, but generally they are rare or absent on the upper surface and common on the basal surface.

In some places they are repeated in crowded masses on thousands of successive layers. The basal hieroglyphs are the infillings of impressions which were on the surface of the shale layer at the time of deposition. The sharpness of the markings indicates rapid deposition of the sand grains. Where hieroglyphs are present on the upper surface, they are convex and concave markings, both positive (*i.e.*, not casts), and record what happened in the upper part of the sand layer. The scarcity of hieroglyphs on upper surfaces indicates that there was little movement in the sandy layers, in striking contrast to the activity in the shale strata.

The pattern of the markings varies from one layer to another, but in many places some common characteristic persists through part of a series and aids stratigraphical identification.

The hieroglyphs range from half an inch to many yards in length, but on a single surface they are all about the same size.

The markings are of three genetically different groups. The first group comprises the hollow flattened moulds left by decayed plants (chiefly algae) and filled with sand or mud; some have a thin cover of carbonized coaly substance, the remains of plant tissue. Many

of the forms are branched, and some have moulds of floating air bulbs. The charred stems of land plants are rare in some units, but in others they are numerous, as in the Eocene of the West Carpathians.

The second group comprises the traces of animal life. Most of these are vestiges of animal tracks and trails, but there are also signs of worm activity and burrowing in the mud. Almost no shells are preserved.

The third group consists of the results of mechanical action on the clay bottom. These include bubbles (probably made by gas generated by the decomposition of organic matter), signs of mud creep on inclined slopes, small asymmetrical depressions (all pointing in the same direction on a given surface), and ripple marks, most of which are large and clearly the effect of a strong current; less commonly normal-sized ripple marks occur. The peculiar ripple-mark structure found within the psammitic layers resembles ripple-mark hieroglyphs. Ripple marks are generally found on the upper surface of sandstone layers.

In the mechanical markings, etching and scratching is very characteristic; in places these marks are parallel narrow furrows, now filled with sand and standing out like small ridges on the basal surface of the sandstone. On a given surface the furrows have a single orientation, but the orientation differs from one surface to another. Nevertheless, in a series of about a hundred layers a predominant orientation is found. Care must be taken to determine whether such scratches are true hieroglyphs, since during folding much gliding took place at the contacts of rocks of different hardness and scratched the surfaces. Convex parallel rills of mud flow are also known.

Many of the markings are difficult or impossible to identify, so that the relative proportions of the three types cannot be determined. In some Flysch formations, however, one type clearly predominates (*e.g.*, plant markings in the middle Cretaceous grey sandstone of the upper Szipot Series).

Organic Remains

The hieroglyphs of nonmechanical origin indicate an abundance of organic activity in the shale layers and its scarcity in the sandy layers. Proof of the existence of the organisms is limited to the organic matter found in the rocks, which is present almost everywhere in the shales and in some places is several per cent of the total material; organic matter is rare or absent in the sandstones (though this may be a result of diagenesis), unless they are oil traps.

In striking contrast to these indications of a rich life existing at the time of sedimentation is the extreme rarity or absence of macrofossils. Unbroken macroskeletons, especially of bottom-living organisms, are so rare that in many Flysch series thousands of feet thick not one has been found. However, in some layers broken pieces of Bryozoa or lithothamnian algae, of the same size as sand grains, are incorporated in sand beds but absent in the shale. Shell material, reduced to sand-grain size, and microfossils do exist in Flysch formations, especially in certain units. Detritus of this kind is concentrated in a particular lamina or in part (usually the coarsest part) of a layer; it is almost absent from shaly layers. Foraminifera are about the same size as sand grains in the enclosing sandstone, as are broken benthonic elements. Many Foraminifera show traces of transport, and this probably explains local mixture of Foraminifera from more than one horizon. If remains of micro-organisms exist in a shale layer neighboring a fossil-bearing psammitic layer, the fossils in the shale differ from those in the psammite and in most cases have siliceous instead of calcareous skeletons. The shell detritus and the Foraminifera seem to have been brought with the coarse material from outside the site of deposition. Some shale layers are rich in fish skeletons, but this is exceptional.

Other Features

Although the pelitic and psammitic layers form more than 95 per cent of the total mass of a Flysch series, some other elements appear.

Among siliceous rocks the most common but least important are beds of spongolitic cherts, which in places replace sand beds but more commonly occur in the upper part of sandstone beds (*e.g.*, Szipot Series). Much more remarkable are diatomaceous cherts—for example, the

Menilitic chert formation of early Oligocene (or, according to some authors, latest Eocene) age in the Carpathian Mountains. The well-banded, and generally perfectly laminated beds of chert appear with uniform character along the mountain range from central Rumania to Austria, along a zone nearly 1000 miles long, and everywhere underlie a thick black shale rich in fish remnants.

Another strange element is represented by radiolarian cherts (red jaspers), which are everywhere connected with pure argillaceous shale and with the disappearance (or near disappearance) of sandstone layers. Examples occur in the middle Cretaceous strata of the outer tectonic units of the Carpathians, in some units in the Alps, and in other Alpine regions (*e.g.*, Turkey).

Where a new element appears it is persistent along a very long zone and is commonly connected with the obliteration or temporary disappearance of the main Flysch character. In all these cases sandy beds disappear or become scarce.

Beds of calcareous pelagic marl or, less commonly, limestone are also known; they are also limited to some subzone but where present are persistent. *Globigerina* beds, *Globotruncana* beds, and *Coccolithophoridae* beds (upper Cretaceous-Ptzemysl) are good examples. Such beds do not obliterate the Flysch character as much as the siliceous elements. But in places, such as the Scaglia in the Apennines, they indicate the passage from pure Flysch to other facies.

If limestone beds replace sandstone beds in some particular unit, the Flysch character of such a unit is doubtful, as Tercier (1947) stressed for the Valanginian Flysch (?) near Bucharest. The Pyrennees Flysch described by some French authors—*e.g.*, that containing the limestone of Hendaye region—is further removed from the true Flysch than the Rumanian Valanginian series. (See Eardley and White, 1947).

Another element in a Flysch unit is represented by conglomerate. Conglomerates are an extreme type of psammitic layer and in places form only the lower part of a sandstone bed. In some cases the conglomerates present a new problem in a Flysch. Some of them are characteristic of the "Wild Flysch" of the Alps. If they are unicomponent and range in size from blocks several scores of feet in diameter to small pebbles, all of which are slightly rounded and localized to a narrow and relatively short zone, they probably represent a product of the destruction of some high cliff near by. Examples are the many granitic conglomerates in the Alps and the hard Titonian (Stramberg) limestone, or upper Carboniferous rocks, in the Carpathians near Przemysl, Poland; at Dobromil the latter include blocks of coal up to 20 feet long. These conglomerates are composed characteristically of rocks of the Alpine geosyncline and not of rocks of the foreland. Possibly some blocks are of Carboniferous age and represent islands formed by nappes protruding above the water.

Other conglomerates occur more commonly than the transgressional conglomerates and represent quite different types from them. They are oligomictic and are composed of well-rounded boulders in thin narrow formations up to 100 miles long. The blocks are not closely spaced and in many cases are separated by several feet of matrix. They grade into exotic blocks.

Blocks and lenses of foreign rocks, known as exotics, are fairly common in some parts of the Flysch series. Some are dozens of feet long but more commonly they are 1 or 2 feet long. Some are of granite or of metamorphic rock, but more commonly they are sedimentary. Near Przemysl, in the upper Cretaceous "Inoceramus" Flysch of the Carpathians, blocks of hard upper Jurassic limestone occur in scores of thousands, and in the same region blocks of coal several feet in diameter occur as exotics. Analogous material is characteristic of the Wild Flysch of the Alps (Heim, 1922). Some of these inclusions may be of tectonic origin, but most were deposited with the Flysch series, as is clear from the concordance of the lenses with the stratification and from the rounded edges of the boulders.

Subfacies of Flysch

Disregarding the transition facies which some authors consider a variety of Flysch, it is still possible to subdivide a thick Flysch unit

into several smaller parts, each with its own characteristics. These are subfacies.

The presence of the third element (*e.g.*, pelagic limestone or diatom chert) helps this subdivision, but even a pure typical Flysch mass can be subdivided fairly successfully. Useful criteria are: (1) color of the shale, with or without distinct laminations, (2) abundance of organic matter in the shale, (3) absence or presence of nodules, (4) quartz or arkosic composition of sand layers and coarseness and roundness of grains, (5) kind of cement (calcareous in most Tertiary Flysch deposits), (6) type of hieroglyphs, (7) average thickness of both types of beds, (8) total proportion of sandstones to shale. These criteria combined provide a means of differentiating some subfacies easily: for example, a series with red shale in beds averaging 1 foot thick which alternate with green or greenish sandstone beds 6 inches thick, having siliceous cement, and so recrystallized that the rock is almost a quartzite. Hieroglyphs are small but sharp and numerous. The total proportion of shale to sandstone is 2:1. Such a subfacies is characteristic of most of the lower Eocene in the Carpathian ranges.

Such subfacies extend long distances, and their persistence contrasts with the strong variability of individual sandstone beds within the subfacies.

Transition to Non-Flysch Facies

Where pure limestones occur in the Flysch two questions arise: what is meant by Flysch in different countries, and what should be the proper nomenclature for transitions from the Flysch to other facies. In most cases the questions are of local importance, but a very large formation can be involved. Some passage types to more quiet pelagic sedimentation are cited above, and more cases can be cited from nearly every Flysch region: for example, from all "klippen" zones in the Alps, or Pennine klippen in Poland. Passage types or contact zones with near-shore or shallow-water deposits are also found.

It is easy to distinguish Flysch series from Molasse series. The latter have more definite separation into homogeneous sandy and shaly parts, with cross-bedding and passage zones from sandstone to siltstone or shale, and in many cases have a fresh-water character. It can be more difficult to separate Flysch from nummulitic facies, which may be poor in nummulites and dominantly detrital, but abundant debris of bottom-living organisms and lack of alternation of shale-sandstone beds are the best distinguishing criteria.

Flysch Facies Outside the Alpine Zone

In the Alpine zone in Europe, Flysch facies appear in the Oligocene, Eocene, and throughout the Cretaceous. A few other series—*e.g.*, some Liassic series—resemble Flysch but are not typical.

Many rock series outside the Alps resemble Flysch, and there is no reason why they should not be classified as Flysch. Many authors have applied the term Flysch, however, without defining it, so that many formations very unlike the Swiss Flysch have been called Flysch. Others closely resembling Flysch were never called Flysch. The Cambrian series (dominantly Lower Cambrian) in St. Cross Mountain in Poland differ from Flysch only in that they are Cambrian. They are thick, with alternating shale-sandstone beds of marine origin, deposited in a geosyncline. It is difficult to know which series of older orogeneses can be called Flysch. There is no reason to limit the term to the Alpine zone only, although its application outside that zone varies. In the United States, for example, after several attempts to apply the term, Eardley and White (1947) rejected it as without useful application in the United States.

Origin of Flysch

Chemical Conditions of Sedimentation

Some Flysch series exhibit evidence of oxidizing conditions, though such conditions do not seem to have been typical of Fysch deposition. Some parts of thick Flysch series were deposited in the presence of free oxygen, whereas in other parts free oxygen was absent or rare. In a great series like the Carpathian Flysch, between the basal Cretaceous and the middle Tertiary (middle Oligocene), there are

two important formations of black shale, several less-continuous horizons (the Barremian and lower Oligocene are noteworthy, and both persist with unchanged character for over 1000 miles), and at least two strongly oxidized formations with red and green shales—one middle Cretaceous and one lower Eocene. The latter formations have great lateral distribution, and both are characterized by the same type of hieroglyphs and the same type of interbedding sandstone layers.

In some cases the oxidation potential between shales and their interbedded sandstones differs. The difference can be the result of later oxidation of organic bituminous remains in the sandstone by percolating water which did not penetrate the shale, but in many cases the difference is primary—for example, where an abundance of glauconite occurs in one type of rock and is absent from the other.

Rhythm of Sedimentation

The countless repetition of sandstone and shale beds suggests a rhythmic occurrence. Hundreds of selected profiles (one over a mile long) were measured, and the thickness of successive beds of sandstone and of shale were plotted. Sandstone beds were numbered in order above the Barremian-Aptian contact, which near the Polish-Rumanian border consists of a knife-sharp passage from black shales and porous sandstones (Barremian) to bluish siliceous sandstone with gray shale (Aptian). In several cases where the profiles extended across the contact zone of two subdivisions, it was possible to find the exact correlation point for different profiles. It was never possible to identify layers from different profiles by their thickness or relative thickness: sandstone beds especially could not be compared even in two profiles across the same tectonic unit 1 mile apart. For example, in the first profile sandstones nos. 1, 7, 15, 17, and 29 were thicker than 3 feet, in the second profile sandstones nos. 5, 15, and 19 were thicker than 3 feet, and in a third profile sandstones nos. 7, 9, 11, and 13 were thicker than 3 feet. If the sandstone beds were excluded, the thicknesses of shale beds were correlatable but only over very short distances. From distances over 3 miles, identification of shale layers was impossible, probably because of the disappearance of several sandstone layers so that shale beds came together, and because of the splitting of shale beds by the edging in of a new sandstone bed. In some places an individual layer might be recognized over long distances by its spongolitic composition or by nodules or other characteristics, but the thickness varied greatly.

It was possible to obtain as many different rhythmic curves as the number of profiles measured. Rhythm, as it is known in a varved clay or in tree rings, does not exist in Flysch. The author's opinion (Sujkowski, 1938) concerning the lack of rhythm in Flysch was confirmed by Kuenen and Carozzi (1953, p. 307). A composite curve, summing up the results of many parallel measured profiles, shows more regular curves, but such variations are not rhythm.

In contrast to extreme variability in thickness of particular beds, the general character or pattern of sedimentation is persistent in most subfacies. This persistent character is here called the style of Flysch sedimentation. Some sandstone beds are on the average only a few inches thick and siliceous (*e.g.*, lower Eocene in the Carpathians); some are up to 60 feet thick and porous white sandstone (*e.g.*, lower Oligocene Kliwa sandstone). The total proportion of all psammitic beds to all pelitic is also persistent. If some sandstone beds are arkosic, probably hundreds of others in the same series are also arkosic. These characteristics combined with persistent colors of shales (black, red, gray) and with different sets of hieroglyphs give to some parts of Flysch series a style not existing in other subunits, but it is not rhythm.[3]

Rate of Sedimentation

Assuming that the psammitic layers represent frequent accidental phases of short duration, the true rate of sedimentation is shown only by the shaly bands. For example, the cretaceous part of the Carpathian Flysch comprises all stages from Valanginian at the bottom to

[3] The author (Sujkowski, 1938) tried to recognize triple rhythm for some local series but found it of very restricted value.

Maestrichtian at the top, and its total maximum thickness is estimated at nearly 3 miles. The shale forms about half, or approximately 9200 feet. The shale was deposited over a period of about 60 million years, or at a rate of about 150 feet per million years or 1.8 inches per 1000 years. The Tertiary portion of the series is less than 1 mile thick. The shale is about 3000 feet thick, deposited during Eocene and at least half of Oligocene time; thus, it was deposited in about 30 million years, or 1.2 inches per 1000 years. The rate of deposition is of the same order of magnitude as it is in the Cretaceous Flysch, and the order of magnitude is all that can be considered here. Since thicknesses have been quoted for the thickest part of the series, it is perhaps safer to estimate the average rate of deposition at 0.8–1.0 inches per 1000 years.

The average thickness of the individual layers is about 5 inches. Thus a sandy phase occurred about every 4000 years. In some parts of the Carpathian Flysch, sedimentation was probably much more rapid than the average rate, since in other parts (for example, the red shales of the middle Cretaceous, or the black menilitic shales of the lower Oligocene) it was much slower.

The average rate is not far from the estimate of the rate of deposition of recent Blue Muds and other deposits on the continental slopes of the present oceans. Schott (*in* Sverdrup *et al.*, 1946) gives the average rate for recent Blue Mud as 0.7 inches per 1000 years.

Depth of Sedimentation

The author concludes that the normal type of deposit *in situ* in a Flysch series is represented by the pelitic layers.

The psammitic layers are interlopers in a strange environment. Each psammitic layer represents a local accident which interrupted the normal sedimentation and brought foreign material from outside the area. Since these intrusions of foreign coarse material were repeated with fair regularity thousands of times, there must have been a continuously unstable condition in the source region of the material; the material was abruptly removed periodically and brought to the bottom where clay sedimentation was proceeding.

The abundance of sandstone, the instability of sedimentation, and the hieroglyph markings were considered in the past to be proof that the Flysch was deposited in an unstable very shallow basin. Some authors (*e.g.*, Glangeaud, 1939) considered the Flysch a deposit of coastal plains flooded with sea water. But this assumed shallow-water deposition is inconsistent both with field observation in a Flysch region and with recent oceanographic research of the sea bottom.

The majority of subfacies developed in a Flysch series are very stable and persistent. This is clearly incompatible with conditions on a coastal plain or in an extremely shallow basin, such as the Sea of Azov. In the Carpathians, a Flysch series which is black with organic matter, has fish skeletons in great numbers, and is underlain by diatomaceous chert, preserves this character for 1000 miles.

However, recent submarine observation indicates the presence of sand, ripple marking and even cross-bedding in sediments at great depth on the ocean floor. Sand layers have been obtained in cores from various basins off California at depths up to a mile below sea level. (*See* Emery and Rittenberg, 1952, p. 743.)

Northrop's (1951, Pl. 2, fig. 2) photograph of the Atlantic Ocean bottom at a depth of 2250 feet shows the surface covered with tracks and trails. The markings differ from hieroglyphs only in that they are concave. The convex forms in the Flysch are negatives, not positives. Thus, the presence of sand and bottom markings is not adequate proof of unusually shallow conditions. That each sand layer represents an upward, and each shale a downward movement of the sea bottom is highly improbable in a series in which these two types alternate many thousands of times.

Brongersma-Sanders (1948) showed that in special conditions, on the western slopes of continents where upwelling waters occur, abnormal types of sediment appear. She studied principally conditions on the west coast of Africa, at Walvis Bay. Here, upwelling water brings additional mineral nutrition, which can support an extra-rich planktonic population. These conditions are susceptible to epidemics caused by the outbreak of dinoflagelata. An

epidemic lasts for several weeks and kills all plankton-feeding fish. In a later stage, all, or nearly all, the bottom fauna (if it existed) is destroyed. The sea bottom and shore is covered with a thick layer of dead animal tissue, including both macro- and micro-organisms. The fish fauna returns within a few months after the epidemic, but scores of years are needed to replenish the bottom fauna, and if a new epidemic breaks out within that period (a common occurrence) no bottom fauna exists. The decomposition product of the dead animals helps to destroy part of the foraminiferal skeleton and other calcareous plankton, but (unexpectedly for these geographical latitudes) diatoms congregate so abundantly in some places that they form diatom ooze. The depths of the slopes on which these observations were made ranged from less than 100 to over 1000 m.

The analogy with Flysch sedimentation is not direct, except perhaps for menelitic shale layers with their abundant fish remains and except for the diatom-chert layers, but it offers one explanation of the absence of bottom fauna in Flysch facies.

Heezen, Ewing, and Ericson (1951) and Heezen and Ewing (1952) found many sand layers among typical *Globigerina* oozes and Red Clay in a zone stretching from the Grand Banks to the Bahama Islands. The area they covered is 2000 sea miles long and 100 wide and lies along the foot of the slope of the American continent, at an average of 750 miles from the coast and at a depth of 4370–5100 m. In some places there were as many as 20 sand layers in one core a few feet long; few are on the surface, but they are discovered by drilling and are interstratified with typical deep-sea deposits.

These sand layers show a remarkable resemblance to the sandstone beds found in Flysch series. It may be possible to connect them with the breaks in the submarine cables which occur along the upper edge of the Atlantic slope of the American continent. The breaks seem to be caused by submarine sliding movements. The time each break occurs can be closely determined, so that in some places it is possible to assess the speed of the slide by the interval of time between the breaks in adjoining cables. The sliding movement apparently causes suspension or density currents, the importance of which in sea-bottom structure has been pointed out by Kuenen (1950, p. 366).

The problem of the Flysch can now be reviewed in the light of these observations: each sand layer corresponds to one sedimentological episode, probably the arrival of a turbidity current bringing down slumped material from an ancient shelf edge or shore line. The deposition of the Flysch proceeded along a slope or at the foot of it. In the Carpathian Flysch, the accumulation was probably on a slope, since no tectonic unit is known between the Flysch unit and the outer marginal unit.

Assuming that the slope on which deposition took place was about 100 miles wide, the depth at its lower end must have been considerable to enable the turbidity currents to travel so far. In the Atlantic of today about 600 miles separates the zone of cable breaks, situated along the upper part of the slope (below the lower edge of the shelf), and the region of sand accumulation. The inclination of the slope is therefore about 2250 feet in 100 miles. The limited data available do not permit the assumption of the same inclination in a Flysch series. Nevertheless, contemporary data indicate the probable order of the inclination.

The type of sedimentation envisaged would require a concave slope with an upper part sufficiently steep to initiate the frequent slides of material from the shelf edge (in some cases probably directly from the shore line). The remainder of the slope would have to be sufficiently steep for the density current to flow to the bottom. For this reason shallow water cannot have characterized areas of Flysch deposition.

A submarine slide moving as a subaqueous mass, not under the subaerial conditions of a continent, would behave differently from a landslide. In the water the disintegration of the loose and uncemented material would be much more rapid than on land. As it moved, its consistency would become that of a turbidity current, and with continued spreading and thinning it would reach a sheetlike condition resembling a quicksand.

Such a sheet brought to a standstill would cover the sea bottom suddenly, fill all depressions, cracks, and markings in the mud surface, and preserve as in an enormous natural

mould the pattern of all sea-bottom activity; thus the hieroglyphs would be formed. The scratches and furrows which are found commonly among the hieroglyphs trend in one direction and are repeated on several successive layers; they indicate a dragging movement along the bottom and support the theory of subaqueous slides and consequent turbidity currents. The area of operation of each slide was limited, but slides continually developed along neighboring parts of the shelf edge so that the series was slowly built up.

The permanently unstable condition of the slope, with slides occurring at more or less regular intervals over millions of years, indicates some tectonic movement in the basin itself, or at least some steady subsidence of the lower end of the slope. Subsidence was uniform rather than rhythmic, but a steady steepening of the submarine slope caused breaks of equilibrium and in consequence submarine landslides at rhythmic intervals. As on a cliff recessing by erosion, the accidents shifted along the slope and did not commonly occur twice in the same place. Each landslide of loose soft sediment moving down the slope might become a turbidity current; each spread a layer of psammitic deposit at the bottom of the slope and made a future lens of sandstone. Inclination of the slope, rate of sinking, and amount of detrital material brought to the shelf rim above the slope influenced the frequency of turbidity currents, their size, and the amount of material in suspension. Earthquakes probably released the landslides commonly and influenced the type of turbidity current. Landslides frequently repeated were not loaded with much material in suspension and were probably responsible for thin but widely spread layers. Those which were rare but strong are represented by a thick lens, limited in distribution.

The shaly part of a subfacies was influenced only indirectly by the condition above the slope; the rate of accumulation and the character of the deposit depended more on the amount of solid material in fine suspension brought to the basin of sedimentation. When the amount of fine clay particles decreased, pelagic elements played a more important part, and half-pelagic marl, or even pelagic argillaceous limestone rich in Foraminifera, was formed instead of shale. The pelitic part of a subfacies reflects the general paleogeographical condition at some moment of the existence of a Flysch basin and might have been uniform along long zones. The sandstone beds, however, are in foreign environments, and it is probably impossible to explain their uniform pattern along long zones without understanding the tectonic movement in the region of the Flysch trough.

Conclusion

As a result of the common acceptance of the density-current theory, the author's opinion of 1938 that the Flysch is not necessarily a shallow-water deposit is no longer exceptional. Carozzi (1952) expressed this change of opinion thus: "Flysch is typical of coarse deep-water deposits." Modern oceanographic research has provided a new approach to Flysch problems, and it is now possible to recognize a number of facts fundamental to study of the Flysch.

Flysch is a facies, characterized by both monotony and variability. The pelitic (monotonous) element represents the indigenous deposit; the psammitic (variable) element is exotic. The nature of the pelitic layers and the required mechanism for the introduction of the psammitic layers make it clear that Flysch was deposited in a deep-water environment. The introduction of the psammitic layers is genetically connected with the tectonic instability of an associated geanticline, and the author believes that the next step toward solving the problem of the Flysch will probably be the definite connection of the development of a Flysch basin with contemporary tectonic movements in the geosynclinal area.

References Cited

Brongersma-Sanders, M., 1948, The importance of upwelling water to vertebrate paleontology and oil geology: K. Nederlansch Akad. Wetensch., afd. natuurk., Verh., sec. 2, Deel 45, no. 4, 112 p.

Carozzi, A. I., 1952, Les Phénomènes de courants de turbidité dans la sédimentation alpine: Archives des Sciences (Soc. de Physique et d'Histoire nat. de Genève) v. 5, p. 35–39

Eardley, A. J., and White, M. G., 1947, Flysch and molasse: Geol. Soc. America Bull., v. 58, p. 979–989

Emery, K. O., and Rittenberg, S. C., 1952, Early Diagenesis of California basin sediments in relation to origin of oil: Am. Assoc. Petroleum Geologists Bull., v. 36, no. 5, p. 735–806

Glangeaud, L., 1939, Transport et sédimentation dans l'estuaire et à l'ambouchure de la Gironde; caractères pétrographiques des formations fluviatiles, saumâtres, littorales et néritiques: Soc. Geol. France Bull., ser. 5, tome 8, fasc. 7–8, p. 599–630

Heezen, B. C., and Ewing, M., 1952, Turbidity currents and submarine slumps and the 1929 Grand Banks earthquake: Am. Jour. Sci., v. 250, p. 849–873

Heezen, B. C., Ewing, M., and Ericson, D. B., 1951, Submarine topography in the North Atlantic: Geol. Soc. America Bull., v. 62, p. 1407–1417

Heim, A., 1922, Geologie der Schweiz: Leipzig, Tauchnitz, Band II, p. 350

Książkiewicz, M., 1948, Przekątne uwarstwienie niektórych skał fliszowych (Current bedding in the Carpathian Flysch): Soc. Géol. Pologne, Ann., tome 17, p. 137–152

——1950, Uwarstwienie splywowe we fliszu Karpackim (Slip-bedding in the Carpathian Flysch): Soc. Géol. Pologne, Ann., tome 19, p 493–504

——1956, Geology of the Northern Carpathians: Geol. Rundschau, Band 45, p. 369–411

Kuenen, Ph. H., 1950, Marine Geology: N. Y., John Wiley & Sons, 568 p.

Kuenen, Ph. H., and Carozzi, A., 1953, Turbidity currents and sliding in geosynclinal basins of the Alps: Jour. Geology, v. 61, p. 363–373

Northrop, J., 1951, Ocean-bottom photographs of the neritic and bathyal environment south of Cape Cod, Massachusetts: Geol. Soc. America Bull., v. 62, p. 1381–1384

Studer, B., 1827, Geognostische Bemerkungen über einige Theile der nördlichen Alpenkette: Zeitschr. für Mineralogie, Jahrg. 1827, no. 1, p. 1–52

Sujkowski, Zb., 1938, Serie Szypockie na Huculszczyźnie (Les séries de Szipot dans les Karpates polonaises orientales; étude géologique et pétrographique d'un complexe du Flysch): Serv. Géol. Poland Trans., v. 3 livr. 2, 105 p.

Sverdrup, H. U., Johnson, M. W., and Fleming, R. H., 1946, The Oceans, their physics, chemistry and general biology: N. Y., Prentice-Hall, 1087 p.

Tercier, J., 1947, Le Flysch dans le sédimentation Alpine: Eclogae Geol. Helvetiae, v. 40, no. 2, p. 163–198

McMaster University, Hamilton, Ontario, Canada

Manuscript Received by the Secretary of the Society, August 9, 1954

BULLETIN OF THE GEOLOGICAL SOCIETY OF AMERICA
VOL. 68, PP. 555-566, 1 FIG., 1 PL. MAY 1957

CONTRIBUTION TO THE GEOLOGY OF THE ISLANDS MARGARITA AND CUBAGUA, VENEZUELA

BY H. G. KUGLER

ABSTRACT

The Tertiary formations of the Islands Margarita and Cubagua comprise fossiliferous sedimentary rocks of Eocene, Oligocene, Miocene, and Pliocene age. Remnant blocks of limestone with Midwayan fossils are also reported. The orbitoid-bearing Punta Carnero Formation is about 2000 m thick. The Oligocene Los Vagres limestone contains a coral fauna which is related to that of the San Luis limestone of Falcón. About 300 m of mottled graywacke in Cubagua borehole No. 1 is considered to be Oligocene and is correlated with the San Lorenzo Formation of eastern Falcón. Miocene clays and sands are about 1600 m thick in Cubagua borehole No. 2. On Cubagua and Margarita these rocks are unconformably overlain by the Cubagua Formation with fossils known from the Caujarao, La Vela and Ojo de Agua Formations of Falcón. Pliocene is represented on Cubagua by about 10 m of fossiliferous sandy marl with *Lyropecten arnoldi*, a marker fossil of the Cabo Blanco Formation.

The Eocene and the lower Oligocene rocks are strongly folded. The upper Oligocene Los Vagres limestone appears to rest unconformably on vertical dipping lower Eocene. In the deep structural trough of Cubagua the lower Miocene was found also to be compressed. The middle and upper Miocene was less affected by orogenic movements, of which at least two phases are recognized by unconformities at the base of the Caujarao and of the younger La Vela Formation.

CONTENTS

TEXT

	Page
Introduction and acknowledgments	555
Previous work and literature	556
Areal geology	557
Eocene	557
Punta Carnero Formation	557
Conglomeratic shale member	557
Age and correlation	557
Lower orbitoid beds	557
Intermediate shale member	558
Upper orbitoid beds	558
Upper shale member	559
Cubagua borehole No. 1	559
Oligocene	561
Los Vagres limestone	561
Cubagua borehole No. 1	562
Miocene	562
Pliocene	564
Pleistocene	565
Structure	565
Tertiary history	565
References cited	566

ILLUSTRATIONS

Figure	Page
1. Section through Cubagua wells No. 1 and No. 2	560

Plate	Facing page
1. Geological sketch map of the Punta Carnero area southern Margarita	566

INTRODUCTION AND ACKNOWLEDGMENTS

A report on the first part of the geologic reconnaissance of the Island of Margarita was published in 1949 by H. H. Hess and J. C. Maxwell when the preparation of this contribution was announced. The delay of this paper was mainly due to contradictory information on the age of some of the Tertiary fossils. The most vital discrepancy has been corrected, but there remain sufficient ambiguities to make revisionary field work desirable.

In September 1947 Creole Petroleum Corporation and H. H. Hess offered the author an opportunity to study the Punta Carnero section of the south coast of Margarita in company of

A. N. Dusenbury of Creole Petroleum Corp. He is obliged to Creole Petroleum Corp. and to Dusenbury for assistance, and to K. F. Dallmus of the same company, for field data obtained during an earlier survey. An excellent geologic map and sections by A. Palombo were kindly made available by Ely Mencher of Socony-Vacuum Oil Co.

J. W. Wells of Cornell University undertook the study of the corals of the Los Vagres limestone. W. P. Woodring identified some additional Tertiary mollusks. The foraminiferal assemblages were investigated by H. H. Renz and P. Bronnimann. The last study was carried out by J. P. Beckmann and W. H. Blow of Trinidad Leaseholds Ltd. D. O. Nelson of Socony-Vacuum Oil Co. reported on some samples through recommendation of Ely Mencher. From air photographs, supplied by Victor Lopez, a photogeologic base map was prepared by K. Rohr of Leaseholds.

Sr. Gonzalo Senior and Sr. Carlos Henry of Caracas furnished core samples from boreholes Cubagua No. 1 and No. 2, a copy of a report on a geologic survey of Cubagua by J. A. Bullbrook, a geologic map of Cubagua by P. Andrews, and a paleontologic report by H. L. Tipsword of Socony-Vacuum Oil Co. Sr. Gonzalo Senior granted permission to publish these documents and supplied reports of T. F. Grimsdale and H. Stauffer of Caribbean Petroleum Co. The author is grateful to all contributors.

Previous Work and Literature

The first contribution to the knowledge of the Tertiary strata of Margarita was apparently made by Wall (1860). On the southeast end of the Island he noticed a small basin of sandstones and shales 600–800 feet thick and dipping 38°. The sandstones were sufficiently indurated to serve as building stones, but no fossils are reported.

Dalton (1912, p. 206) introduces the term "Cumaná Series" for Tertiary fossiliferous calcareous sandstones and shales exposed on the mainland opposite Margarita. His "Cubagua Beds" cover the whole of the Island Cubagua and are correlated with those of Cabo Blanco near La Guaira and also with those along the coast east of Coro. Dalton attributes a Pleistocene age to the Cubagua beds.

Maury (1925, p. 412) mentions from Margarita "Beds with *Venericardia planicosta*" belonging to the Midwayan Soldado Formation.

Aguerrevere (1936, Fig. 1) reports sedimentary rocks of possible Eocene age near the Morro of Porlamar. Rutten (1940, p. 839) studied specimens of rocks collected by P. M. Hummelinck from Punta Balena, Pampatar, Guaiquire, Punto Mosquito, and Isla Blanca. Such orbitoids as *Discocyclina georgiana* and *Lepidocyclina trinitatis* induced Rutten to assign the majority of these rocks to the Eocene. Among the clastic components of the conglomeratic members belonging to these Eocene beds he mentions porphyrites, cherts, radiolarites, and schists. Exposures of the first three types are unknown on Margarita. According to H. H. Hess (personal communication) they were probably overlying the metamorphic rocks immediately north of the present exposures of the conglomerates.

Senn (1940, p. 1565) reports that Gonzalez de Juana found orbitoid-bearing sandstones and quotes Hedberg who compares these with similar rocks of the Scotland Formation of Barbados.

Gonzalez de Juana (1947) made the most significant contribution to the knowledge of the Tertiary in his "Cubagua basin". The term "Cubagua Beds" of Dalton is replaced by "Cubagua Formation" which includes the surface rocks of Cubagua and about 4000 feet of Oligo-Miocene sedimentary rocks found in the two exploration holes on Cubagua. His "Araya Formation" is considered Pliocene, and the "Punta Carnero Group" Eocene. To the "Punta Carnero Group" he attributes a thickness of about 7500 feet and, like Rutten, recognizes the significance of the polygenetic nature of the conglomerates at its base.

Woodring (1928, p. 82) reports that "a collection from (U. S. Geological Survey station 6309 entrance to Boca Laguna de Marites, eight miles west of Porlamar) contains a *Turritella* of the group of *T. gatunensis* Conrad, another species that probably is *T. plebeia alowensi* Hodson, and also a species of the group of *T. bifastigata* Nelson. This material is considered middle Miocene. No Miocene

fossils have heretofore been recorded from Margarita." Hess and Maxwell (1949, p. 1862) use the term Punta Carnero Formation, and this is here applied until future surveys justify the term "group" of C. Gonzalez de Juana (1947, p. 696) by establishing well-defined formations.

Areal Geology

Eocene

Punta Carnero Formation.—The type section of this formation is well exposed on either side of the trail leading from the village Los Vagres to Punta Carnero, about 15 km west of Porlamar and near the south coast of Margarita. The section starts about 2 km south-southwest of the houses of Las Bermudez and extends almost uninterruptedly for a distance 2¼ km to the shelter house of Represa on the southernmost scarp near the coastal lagoon (Pl. 1).

A steeply dipping sequence, about 2000 m thick, of Eocene block conglomerates, sandstone, shales, mudstones, and calcareous orbitoidal sandstones constitutes the Punta Carnero Formation. Two prominent scarps formed by the "Lower and Upper Orbitoid beds" allow for a subdivision of the section into members which from top to bottom are:

(5) Upper shale over 150 m thick
(4) Upper orbitoid beds 300 m thick
(3) Intermediate shale 580 m thick
(2) Lower orbitoid beds 260 m thick
(1) Conglomeratic shale 700 m thick

Conglomeratic shale member.—The contact of this shale with the underlying vertical calcareous phyllites of the Upper Cretaceous(?) "Los Robles Group" of Hess and Maxwell (1949) could not be observed on account of a strip about 40 m wide of Oligocene coralligeneous limestone, the "Los Vagres limestone".

The olive-green angular-fracturing silty shale weathers reddish and brown. Layers of "pepper and salt" sandstone, scattered pebbles, and small blocks of limestone and igneous rocks are part of this 700 m-thick member between the Los Robles group and the base of the lower orbitoid beds. E. Mencher (Personal communication), by assuming isoclinal folding, considers the thickness to be less; but there is no positive paleontologic evidence for such assumption. Mencher found some dark algal, coral-bearing dense crystalline limestone lenses in the upper part of the shale where conglomeratic layers are more common. D. O. Nelson identified in these limestones a possible *Eoconuloides* and *Discocyclina* cf. *mesteri*, besides a *Nummulite*, some small Foraminifera, and remains of Echini, algae, and mollusks.

The components of the conglomerates are well rounded. Among them are porphyrites, amygdaloidal basalt, andesites, probably some tuffs, cherts, and vein quartz. Cobbles up to 10 cm in diameter are common, and large blocks occur erratically in the midst of silty shale. Some of these boulders appear to be limestone of Cretaceous age, but unfortunately no samples have been collected for study. The "Wild-Flysch" character of this conglomeratic shale is reminiscent of the upper Eocene San Fernando block conglomerate of Trinidad. It probably represents a block facies of the Pointe-a-Pierre Formation, unknown in Trinidad, however.

FOSSIL CONTENT: The foraminiferal fauna of the shale is poorly preserved, and most of the samples are barren. D. O. Nelson (Report to Socony-Vacuum) listed about 12 genera among which he noticed *Globigerina* cf. *triloculinoides*, *Globorotalia* cf. *acuta*, *Globorotalia* cf. *incrassata*, and *Globorotalia ?velascoensis*.

Age and correlation.—According to P. Bronnimann (Private report) most of the foraminiferal faunas are heterogeneous; middle Eocene forms occur with typical Paleocene ones. He is reminded of conditions from the Pointe-a-Pierre shales of Trinidad, which are placed in the upper Paleocene to middle Eocene. The resemblance of the olive-green shales of this conglomeratic shale to the Pointe-a-Pierre shale is often striking.

The great thickness of monotonous, well-bedded shales, silt, mudstone, and occasional sandstones constituting the typical Flysch facies of the Misoa-Trujillo Formation of western Venezuela is probably related to this lower part of the Punta Carnero Formation.

Lower orbitoid beds.—This member, which is about 50 m thick, forms a conspicuously straight row of hills about 30 m in elevation.

The lower orbitoid beds strike N. 70° E. and are underlain by about 50 m of the top of the conglomeratic shale. Upward they pass into thin-bedded calcareous shale of the intermediate shale member. The yellow-tinged lower orbitoid beds strongly contrast with the reddish-weathering conglomeratic shale.

The lower 5 m of the lower orbitoid beds consists of vertical-dipping siltstones and shales with a layer of 0.5 m dense orbitoidal limestone. Most of the upper part, which is about 45 m thick, is a cubical-fracturing mudstone with finely comminuted mollusks, algae, Echini remains, and a few Foraminifera. The layers of mudstone are interbedded with well-layered silt. The mudstone and silt layers are a few cm to less than 50 cm thick.

FOSSIL CONTENT: P. Bronnimann (Private report) observed the following Foraminifera in the orbitoidal limestone: *Asterocyclina* sp., *Discocyclina* sp., *Proporocyclina tobleri*, *Cymbalopora* cf. *irregularis*, *Gypsina globulus* and also some smaller Foraminifera.

The intercalated silty shale contains a fauna of smaller Foraminifera related to that of the middle Eocene Navet Formation of Trinidad. It also has affinities with the Pointe-a-Pierre Formation. According to P. Bronnimann a middle Eocene age for the lower orbitoid beds is probable, and a correlation with the *Discocyclina*-bearing beds of the Scotland Formation of Barbados is indicated.

Intermediate shale member.—This almost uniformly developed series of shales form a depression between the lower and upper orbitoid beds. They dip steeply southward and gradually change from almost vertical and even overturned to dip about 55° S.-SE. The well-bedded calcareous shale is about 750 m thick. In its lower part and just above the mudstone ledge of the lower orbitoid beds are a yellow-weathering thin-bedded siltstone and gray silt containing interbedded laminated sandstones and variegated shale. The top of the intermediate shale member is at the base of a 2-foot-thick cream-colored mudstone at the base of the upper orbitoid beds.

When fresh the intermediate shale is light gray and is intercalated with darker and commonly variegated clays. Thin calcareous sand layers, silt bands, and limonitic mudstone concretions occur. "Sericitic" coating of the variegated shales is reminiscent of Pointe-a-Pierre shale. The weathered surface is strewn with iron claystones and fibrous calcite slabs.

FOSSIL CONTENT: In addition to Radiolaria, coprolites, and ostracods, P. Bronnimann observed a *Globorotalia* of the Navet type and a number of other smaller Foraminifera of characteristic Pointe-a-Pierre affinities.

D. O. Nelson also observed: *Hastigerinella* cf. *eocenica*, *Asterigerina crassata*, *Cibicides* cf. *grimsdalei*, and *Globigerina dissimilis* from which he deduces a middle Eocene age.

Age and correlation.—According to Bronnimann the faunal assemblage of smaller Foraminifera of the intermediate shale member is typical for Pointe-a-Pierre shale of Trinidad and as such must be considered to be of middle Eocene age.

No corroboration for such identification has been furnished by the shales of the Scotland Formation of Barbados, but it is hoped that a similar assemblage will result from additional search. Synchronous sediments have been found in great thickness in the Misoa-Trujillo Formation of the Serrânia de Agua Negra of Lara. They are also known from an exploitation well at Esperanza, 2 km north of Pozon in the District Acosta of the State of Falcón. The hard dark silty shales below typical upper Eocene orbitoidal limestone are, however, almost barren of fossils and thus defy detailed correlation.

Upper orbitoid beds.—The bottom layer of these beds which are bout 300 m thick and which dip 45° S.-SE., is a polygonal-jointed mudstone about 2 feet thick showing tracks of former marine life and forming the rim of a scarp standing above the depression of the intermediate shale. Above this mudstone lies about 100 m of silts and thin flaggy mudstone containing several silty limestone layers up to 60 cm thick, and in places consisting almost entirely of orbitoids. Regular alternation of layers of silt about 50 cm thick, well-bedded mudstones with tracks and cracks, polygonal-jointed and honey-combed sandstone layers, lie above the orbitoid-bearing beds. The polygonal-jointed mudstones strongly resemble those of the Eocene orbitoid-bearing Cerro Campana Formation of the Esperanza uplift, north of Pozon, in the lower Tocuyo area of eastern Falcón. Laminated sandstones and

shales grade upward into shales. The top sandstone layer of the upper orbitoid beds marks the top of these beds just a few meters north of a shelter house west of La Represa.

FOSSIL CONTENT: The oldest zone from which fossils were collected is exposed at locality K. 7551; P. Bronnimann identified the following larger Foraminifera:

Lepidocyclina pustulosa	*?Eoannularia eocenica*
Lepidocyclina sp.	*Amphistegina* sp.
Asterocyclina sp.	*Operculinoides* sp.
Discocyclina sp.	*Gypsina globulus*
Eodictyoconus cubensis	*Gypsina vesicularis*
Fabiana cubensis	

Among the smaller Foraminifera, Bronnimann and Renz mention a number of species of the genera *Bolivinopsis*, *Cibicides*, *Eponides*, *Gaudryina*, *Globigerina*, *Globorotalia*, *Glomospira*, *Nodosinella*, and *Guembelina*, which indicate a middle to upper Eocene age. W. H. Blow (Private report) correlates this bed with the *Globigerinatheka barri* zone of the upper middle Eocene part of the Navet Formation of Trinidad.

Locality K. 7549 is stratigraphically about 200 m higher than K. 7551 and, according to Bronnimann (Private report) carries the already mentioned larger Foraminifera and *Lepidocyclina* cf. *yurnagunensis*, *Pliolepidina tobleri*, and *Schlumbergerina*. To this Bronnimann remarks:

"The co-existence of *Lepidocyclina pustulosa*, *Pliolepidina tobleri*, *Lepidocyclina* cf. *yurnagunensis* with *Discocyclina* sp. and *Asterocyclina* sp. indicates upper Eocene. The most interesting fossil in this assemblage is *Eodictyoconus cubensis* first described by Cole and Bermudez (New foraminiferal genera from the Cuban middle Eocene, 1944, p. 6) from Cuba. Cole reports this species from the middle Eocene Lisbon formation of Florida. Keijzer (Outline of the geology of the eastern part of the Province of Oriente, Cuba, 1945, p. 213–214) mentions *E. cubensis* also from the Eocene of Cuba, where its occurrence is widespread and where it is generally found associated with Discocyclinae, Lepidocyclinae and species of *Coskinolina* and *Dictyoconus*. These species are common in the upper Eocene San Luis formation of Cuba. Furthermore, *E. cubensis* has been found in the upper Eocene Pauji formation (Rio San Pedro, Venezuela) and in the upper Eocene of Central and Southern Europe. The vertical range of this species, based on above data appear to embrace middle Eocene and upper Eocene with maximum development in the upper Eocene".

Bronnimann later considered *Eodictyoconus* and also *Tschoppina* (Keijzer, 1945, p. 213) to be synonyms of *Fabiana*. Bronnimann also observed *Schlumbergerina* in the upper Eocene of the Pauji Formation of Venezuela. *Lepidocyclina* cf. *yurnagunensis* has previously been noticed by C. M. B. Caudri (Private report) in the upper Eocene San Fernando Formation of Trinidad, and Keijzer (1945, p. 216) reports it from the San Luis Formation of Cuba.[1]

Of particular interest is the discovery by Anisgard (1956, p. 49) of *Eorupertia* in the upper Eocene orbitoidal limestone of the Punta Carnero section. This larger Foraminifera has so far been found only in Europe and Asia.

The larger Foraminifera indicate essentially a late Eocene age, but the smaller ones are strongly reminiscent of the middle Eocene Navet Formation of Trinidad. Even the youngest sample, from locality K. 7548, shows such a Navet assemblage, according to Bronnimann. Possbly these Navet Foraminifera were reworked.

Upper shale member.—Not more than 150 m of upper shale is exposed in the section studied. This gray well-bedded silty shale with sandstone layers is little different from the upper part of the upper orbitoid beds. No samples have been collected.

OTHER OCCURRENCES OF THE PUNTA CARNERO FORMATION: Aguerrevere (1936, Fig. 1) and Hess and Maxwell (1949, Pl. 1) show additional occurrences of the formation along the southeastern coast of Margarita. A synclinal position of the beds is indicated but, as no samples are at our disposal for study, little information can be added.

Cubagua borehole No. 1 (Fig. 1).—In Cubagua borehole No. 1 the formation between 4220 feet and 4670 feet (total depth) has to be assigned to the Eocene. According to H. L. Tipsword (Private report) the beds are "shale,

[1] The name San Luis Serie of Falcón was established by F. Hodson in 1926 (p. 174). R. A. Liddle (1928, p. 252) introduced the name San Luis Formation. Its age is middle and upper Oligocene. C. Schuchert (1935, p. 492) introduced the name San Luis Formation for late Eocene sedimentary rocks in Cuba. Schuchert's homonym should be suppressed.

dull gray, medium hard, slightly calcareous, silty, thin bedded in places. Dips 50°–90°. Extremely fractured with subconchoidal surfaces. Carbonate veins scattered irregularly".

FOSSIL CONTENT: Tipsword observed about 50 foraminiferal species. *Globigerina* is predominant. Among the larger Foraminifera he identified *Lepidocyclina hubbardi* Hodson. The

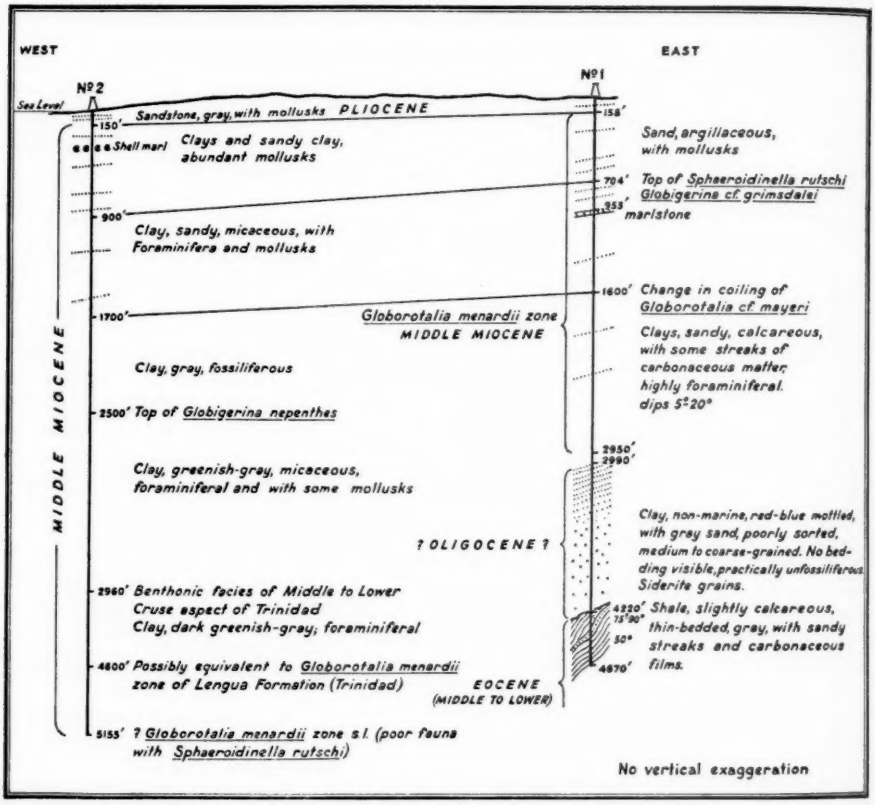
WEST
EAST
No 2
No 1
Sea Level
150'
Sandstone, gray, with mollusks PLIOCENE
Shell marl
Clays and sandy clay, abundant mollusks
900'
Clay, sandy, micaceous, with Foraminifera and mollusks
1700'
Globorotalia menardii zone
MIDDLE MIOCENE
Clay, gray, fossiliferous
2500' Top of Globigerina nepenthes
Clay, greenish-gray, micaceous, foraminiferal and with some mollusks
2960' Benthonic facies of Middle to Lower Cruse aspect of Trinidad
Clay, dark greenish-gray, foraminiferal
4600' Possibly equivalent to Globorotalia menardii zone of Lenga Formation (Trinidad)
EOCENE (MIDDLE TO LOWER)
5155' ? Globorotalia menardii zone s.l. (poor fauna with Sphaeroidinella rutschi)
MIDDLE MIOCENE
158'
Sand, argillaceous, with mollusks
794'
Top of Sphaeroidinella rutschi
Globigerina cf. grimsdalei
953'
marlstone
1600' Change in coiling of Globorotalia cf. mayeri
Clays, sandy, calcareous, with some streaks of carbonaceous matter, highly foraminiferal. dips 5°-20°
2950'
2990'
? OLIGOCENE ?
Clay, non-marine, red-blue mottled, with gray sand, poorly sorted, medium to coarse-grained. No bedding visible, practically unfossiliferous. Siderite grains.
4220' Shale, slightly calcareous, thin-bedded, gray, with sandy streaks and carbonaceous films.
75°-90°
50°
4670'
No vertical exaggeration

FIGURE 1.—SECTION THROUGH CUBAGUA WELLS NO. 1 AND NO. 2

Six cores were recovered from this part of the borehole:

Feet	
4255–4267	12 feet recovered, no information
4346–4366	20 feet recovered, almost vertical, dark gray calcareous shale streaked with sandstone and lignite; core extremely shattered
4450–4470	20 feet recovered, gray shale
4512–4518	3 feet recovered, gray shale
4564–4584	20 feet recovered, gray compact calcareous silty shale; dip 45°
4665–4670	4 feet recovered, dark-gray slickensided calcareous shale containing quartz grains and clay concretions.

presence of *Lepidocyclina*, *Camerina*, and some stratigraphically restricted forms of smaller Foraminifera caused Tipsword to assume a possible upper Eocene age for the fauna.

From the last core (4665–4670 feet) T. F. Grimsdale (Private report of May 1941) lists among others the following species:

Anomalina dorri Cole var. *aragonensis* Nuttall
Spiroplectoides clotho Grzybowski
Cibicides cushmani Nuttall
Cibicides grimsdalei Nuttall
Cibicides luxpanensis Cole
Eponides trumpyi Nuttall
Globorotalia eocenica Nuttall

Nodosarella subnodosa (Guppy)
Nonion micrus Cole
Textularia eocaena Gümbel *teste* Nuttall

The different orbitoids found are not specifically mentioned, but Grimsdale states "The above fauna is strongly in favour of a Middle Eocene (Claiborne) age". H. H. Renz (Private report) who studied parts of the cores 4346 feet, 4584 feet and 4670 feet reports a poor upper Eocene fauna and one specimen of *Helicolepidina paucispira* Barker and Grimsdale (identified by C. M. B. Caudri).

J. P. Beckmann (Private report) studied the fauna of core 4670 feet and found it to be middle or lower Eocene mixed with younger forms, a heterogeneous assemblage. Contamination with drilling mud, however, has to be considered.

Oligocene

The only sedimentary rock of Oligocene age known from Margarita is the Los Vargres limestone. It is at the northern end of the Punta Carnero section and seemingly rests on the contact of the middle Eocene beds with the slightly metamorphosed Los Robles group. This rubbly limestone was originally considered to be at the base of the Punta Carnero Formation (Hess and Maxwell, 1949, p. 1862) but paleontologic evidence disputes this. Blocks of this limestone are also found at the base of the transgressive Miocene limestone.

Los Vagres limestone.—This irregular lenticular mass of limestone appears to be about 30 m wide and 200 m long. Like the adjacent Eocene it appears to be vertical. This statement requires a careful investigation especially as the attitude of the limestone is difficult to recognize on account of the formation of scree and caliche. It apparently rests unconformably on vertical and steeply southward-dipping fine-bedded chloritic, calcareous phyllites of the Los Robles group. No basal conglomerate can be seen, but pebbles and small blocks of older rocks appear to form part of the limestone. The coral reef seems to have grown directly on the phyllites. Thin, flat layers of seemingly mud-resisting corals 50 cm above the contact are surrounded by silt which is derived from the phyllites. Above the thin-bedded corals lies dark rubbly nodular coral limestone of irregular layers 30–50 cm thick and intercalated with calcareous silt and calcareous rubble. Some of the limestone, which is very fine-grained and dense, indicates quiet back-reef conditions; other parts are coarsely crystalline.

FOSSIL CONTENT: No larger Foraminifera were observed in the samples collected by the writer. Three samples of typical Los Vagres limestone collected by E. Mencher were also barren of larger Foraminifera. The grayish-tan very fine-grained dense limestone carries only Radiolaria and some *Globigerina*. From one sample of limestone collected by Mencher at the type locality of the Los Vagres limestone, however, D. O. Nelson mentions (Private report):

Discocyclina cf. *barkeri* Vaughan and Cole
Athecocyclina cf. *cookei* (Vaughan)
Amphistegina cf. *senni* or *lopeztrigoi*
Valvulineria cf. *extensa* Cushman and Bermudez
Globorotalia aff. *velascoensis*

as well as a number of genera of smaller Foraminifera. From this fauna he concludes a possible lower Eocene age and remarks "the presence of *Athecocyclina* would indicate Paleocene to lower Eocene while the other forms indicate lower to middle Eocene".

Nelson describes three other samples of limestone containing an almost identical fauna of possible Paleocene or lower Eocene age. The matrix of these limestone specimens consists of a fine- to coarse-grained debris of corals, Algae, mollusks, and Echini.

Amphistegina senni Cushman, now *Tremastegina senni* (Cushman) Bronnimann (1950), is a typical middle Eocene form from the Scotland beds of Barbados and from similar beds of Trinidad.

The presence of Paleocene sedimentary rocks on Margarita is indicated by Maury (1925, p. 412), who mentions the finding of *Venericardia planicosta* known from the Soldado Formation of Trinidad.

It is suggested that this *Venericardia planicosta*-bearing rock, as well as the lower Eocene *Discocyclina* limestone, represents blocks and pebbles in the conglomeratic shale.

H. H. Hess visited the outcrop of the Los Vagres limestone in August 1956 and confirmed the presence of a vertical limestone which possibly contains the above-mentioned Paleo-

cene to lower Eocene Foraminifera. The position of the coral-bearing limestone appears to Hess to be identical with this Paleocene limestone. The possibility that this coral-bearing limestone rests unconformably on the vertical limestone must be considered in view of the Oligocene age of the coral fauna, however. Due to an earlier cursory examination a Cretaceous age was ascribed to this fauna. Bucher (1952, p. 68), relying on this erroneous information, attributed a Cretaceous age to the Los Vagres limestone.

As already pointed out, no larger Foraminifera were found in the numerous thin sections of coral-bearing Los Vagres limestone prepared from samples collected by the writer.

The corals collected were forwarded to J. W. Wells of Cornell University who in January 1953 reports (Personal communication) from the type locality of the Los Vagres limestone K. 7561:

Stylophora imperatoris Vaughan
N. gen., n. sp. (*astrocoeniid*)
Acropora n. sp. (*A. echinata* group)
Leptoseris n. sp. (same as form from San Luis Formation of Venezuela)
Actinacis sp. indet.
Agathiphyllia (?)*tenuis* (Duncan)

Of this coral fauna Wells remarks: "the Margarita corals from K. 7561 are definitely Oligocene." They suggest an extension of the San Luis Formation of Falcón, but the fossils from Margarita have a slightly deeper water facies.

AGE: Unfortunately no larger Foraminifera are associated with these corals as is the case with the San Luis limestone of Falcón, Antigua limestone of Antigua, or the Kapur limestone of Trinidad. Nevertheless, if the Los Vagres limestone can be correlated with the San Luis limestone, an upper, rather than a middle Oligocene age has to be attributed to it.

Cubagua borehole No. 1.—In this well a series of sedimentary rocks was penetrated between the 2990 and 4220 feet assigned to possible Oligocene. H. L. Tipsword (Private report, July 1940) describes them as "non-marine, arenaceous clay, mottled red, brown and bluish grey, with interbedded sand, loosely consolidated, poorly sorted, medium to coarse grained. Sand in clay is mostly medium, subangular to angular quartz . . . possible equivalent to El Fausto and Icotea formations of the Maracaibo Basin".

The writer studied eight cores between 3267 and 4200 feet and made the same observations as Tipsword. The greenish-gray micaceous sandstone appears to be a typical graywacke. Fossils are absent, but occasional siderite grains indicate possible swamp conditions. Sandstones predominate in the upper part (2990–3200 feet) and in places contain pebbles and layers of mudstone. Below lie mottled clays and silts.

In the search for contemporaneous sedimentary rocks of similar stratigraphic position one would consider the Oligocene San Lorenzo Formation of Acosta in the State of Falcón (Renz, 1948 p. 9). This formation contains a middle Oligocene (Rupelian) foraminiferal fauna and remains of fishes and plants indicating shallow water conditions.

This formation, as well as the deeper Eocene of Cubagua No. 1, has not been found in the 5155-foot borehole, Cubagua No. 2, which is only 2500 m west of No. 1. The explanation for this is the assumption of a normal fault with a downthrow to the west and a strike through the gap between Margarita and Macanao. The oil seeps at the west end of Cubagua, and out at sea (J. A. Bullbrook, Private report), may be connected with this fault.

Miocene

The oldest Miocene rocks are to be found in Cubagua well No. 1 between 158 and 2990 feet, and in Cubagua well No. 2 between 150 and 5155 feet (total depth). An almost horizontal correlation is possible between these two wells to approximately 2000 feet. T. F. Grimsdale (Private report, April 1941) gives the following description of the formation including the ?Oligocene beds from 2990 to 4220 feet and the Eocene beds from 4255 to 4670 feet.

Cubagua No. 1

Feet	
218–800	Sandstone, somewhat argillaceous, containing micaceous beds in some places. Mollusca locally common; Foraminifera rare
953	Marlstone, hard, sandy, containing Foraminifera

1100–2900	Clays, sandy, calcareous, often micaceous; in some places streaked with carbonaceous matter, commonly crowded with Foraminifera, and in some places containing Mollusca, fish scales, otoliths; dip 5°–20° (1100 feet—5°, 1500 feet—10°, 2400 feet—40°?, 2900 feet—5°)
3096–3900	Clays, sandy clay, and sandstones, mottled and variegated, often micaceous; no bedding visible; practically unfossiliferous
4584–4670	Shales, hard, gray, calcareous containing sandy streaks and partings, and carbonaceous seams; calcite veins; dips 50° and higher

Cubagua No. 2

Feet	
80	Hard gray sandstone, containing Mollusca and crab remains
150–600	Clays and sandy clays, gray, fossiliferous, locally forming a shell marl (300 feet); abundant Mollusca
700–1000	Sandy clays and argillaceous sandstones, containing fossils; Mollusca in some places common; Foraminifera everywhere present
1330	Clay, micaceous sandy, containing Foraminifera and Mollusca
2000	Clay, gray, fossiliferous
2800–4600	Clay, dark greenish gray compact micaceous, sandy containing plentiful Foraminifera and a few Mollusca
5000–5155	Clay, gray compact micaceous, sandy, containing fish scales and scarce Foraminifera; at 5155 feet dip approximately 45°

J. P. Beckmann (Private report), who again studied the samples we received from Sr. Gonzalo Senior, reports the following:

Cubagua No. 1

Feet	
158–2950	*Globorotalia menardii* zone s.l.
704	Top of occurrence of *Sphaeroidinella rutschi*, *Globigerina* cf. *grimsdalei*
1600	Change in direction of coiling of *Globorotalia* cf. *mayeri*

Cubagua No. 2

Feet	
150–4600	*Globorotalia menardii* zone s.l.
900	Top of occurrence of *Sphaeroidinella rutschi*, *Globigerina* cf. *grimsdalei*
1700	Change in direction of coiling of *Globorotalia* cf. *mayeri*
2500	Top of occurrence of *Globigerina nepenthes* Todd
2960	Benthonic facies fauna of Middle to Lower Cruse aspect (Cruse Formation of Trinidad)
4600	Possibly equivalent of *Globorotalia menardii* zone, Lengua Formation of Trinidad
5155	*?Globorotalia menardii* zone s.l. (poor fauna with *Sphaeroidinella rutschi*)

To this he adds: "*Globorotalia menardii* zone s.l. includes the time interval base of Lengua formation and Recent. The greater part of the Miocene of Cubagua seems to be younger than the Lengua formation. In contrast to beds of corresponding age in Trinidad (Cruse, Forest, Morne l'Enfer formations) the faunas of Cabagua are predominantly planktonic. An exact correlation with Trinidad is therefore not possible. A more detailed comparison will be possible with the Pozon section of East Falcón, where a similar sequence occurs."

Contrary to González de Juana (1947) and more in agreement with Dalton (1912), the writer suggests that only the beds from the surface to 194 feet of Cubagua No. 1 be included in this formation and that the highly fossiliferous beds exposed over most of the Island be added. According to P. Andrews (Private report) the beds from the surface to 194 feet are mainly bluish-gray massive calcareous clays alternating with siltstones, thin limestones, and in the upper part with sandstone layers. Beds of white quartz gravel, and oysters, (probably *Crassostrea*) occur in at least four levels

These oyster-bearing beds probably correspond to those of the Ojo de Agua Formation of Eastern Falcón and are probably the same as those immediately north of the outcrop of the Los Vagres limestone. At this locality (K. 7541), about 6 m of almost horizontal cavernous-weathering irregularly bedded limestone rests on steeply dipping calcareous phyllites of the Los Robles group. The lower part of the limestone is very knobbly and contains large oysters and a nodose pecten. The pecten is reminiscent of a form found in the Mataruco limestone at the base of the La Vela Formation near Cumarebo, East Falcón.

West of the Eocene section of Punta Carnero the same type of limestone dipping 15°–20° SW. forms a scarp striking westward to Agua

Verde where it resembles the Cumarebo limestone.

Westward, and along the coast, are large Crassostreas, a few Arcas, and Turritellas which are seemingly the same as those in the Ojo de Agua Formation, which is probably synchronous with the La Vela Formation of Falcón.

At K. 7572 about 4 m of hard sandy limestone is exposed. It carries Pectens reminiscent of those in the Corocorote beds of the La Vela Formation at Cumarebo. Above this sandy limestone lie the beds exposed at K. 7571 which contain 5 m of thickly layered hard silty limestone and a few corals. Westward this silty limestone is covered by at least 100 m of silts and clays belonging to the Tucupido Formation of the Cumarebo area in East Falcón.

The fossiliferous beds of Las Tejitas and El Yaque west of Laguna Las Marites were considered by Woodring (1928, p. 82) to be of middle Miocene age. The fauna of U. S. Geological Survey locality 6309 at the entrance to Boca de Laguna de Marites occurs, according to Ralph Arnold, the collector, in a white-streaked limestone dipping with 75° toward N. 25° W. Recently W. P. Woodring restudied this fauna and supplied the following list:

Natica (*Naticarius*) *canrena* (Linne)?
Turritella matarucana F. Hodson
Turritella gatunensis Conrad, subsp.
Turritella bifastigata Nelson
Unidentified *muricid*
Cymatophos paraguanensis (F. Hodson)?
Xancus falconensis H. K. Hodson

Woodring attributes a late middle Miocene age to this fauna and considers it to be equivalent to part of the Urumaco and Caujarao Formations of the State of Falcón. The *Turritella* listed by Woodring as *T. matarucana* is the species listed by him in 1928 as *T. plebeia alowensi* Hodson. He now considers *T. "plebeia" alowensi* a synonym of *T. matarucana*. When Woodring examined these fossils in 1927 the collection consisted of only three species of *Turritella*. Later additional specimens in Arnold's collection were found.

Aerial photographs show the steeply dipping beds of Laguna Las Marites to be clearly different from the more gently inclined limestones at K. 7541, 7551, and 7552. This implies orogenic movements at the end of middle Miocene time. The same unconformity is known between the Agua Salada group and the Ojo de Agua Formation of eastern Falcón. It is also found between the Caujarao and younger La Vela Formation of Central Falcón. For this reason the beds of Laguna Las Marites should be separated from the Cubagua Formation but field observations are inadequate.

On Macanao (western half of Margarita Island) Miocene beds crop out at Laguna Boca Chica, the site of an oilseep.

The postulation that the "Cumaná Series" of Dalton (1912, p. 206) is below the Cubagua Formation requires confirmation.

From the Island of Coche, Aguerrevere (1936, p. 400) reports "upper Tertiary" dipping 65° N.-NW. and extending between Zulica and El Guamache. These beds may well belong to the Cumaná beds of late Miocene or Pliocene age (Liddle, 1946, p. 530).

Pliocene

P. Andrews (Private report) shows on his geologic map of Cubagua a columnar section of the Cubagua Formation. In this formation he shows a layer 10 m thick of blue-gray sandy marl containing giant Pectens and other shells. This bed is possibly represented in the lowest sedimentary rocks of Cabo Blanco which contain the giant Pecten *Lyropecten* (*Modipecten*) *arnoldi* Aguerrevere, according to W. P. Woodring (Personal communication).

Gonzalez de Juana (1947, p. 693) mentions the deposition of the Araya Formation in the Cubagua basin during Pliocene time. He states: "In the Cubagua basin a quartz gravel bed exposed on the north side of the Island of Cubagua, in the locality called Las Calderas, probably represents the Miocene-Pliocene break, but for the rest both formations appear to be conformable. . . . In the Cubagua area, the Pliocene deposits consist of brown, calcareous, friable, fossiliferous sands and brown sandy, fossiliferous clays of shallow marine origin". It is this section of Las Calderas to which the description refers, to judge from the map of P. Andrews. This probably was also the section Dalton studied for he compares the

large mollusks of his Cubagua beds with those of Cabo Blanco. He does not, however, state that the beds below belong to his "Cumaná Series" which, according to Liddle (1946, p. 531), might be correlated with the Cabo Blanco beds.

Pleistocene

H. G. Richards (1943, p. 120) describes a deposit of unconsolidated calcareous clay 4–5 m thick which is from Juan Griego on the north coast of Margarita and contains a molluscan fauna of which he describes 18 species. The formation extends several miles along the coast west of Juan Griego and is considered to be Pleistocene.

Structure

The Eocene Punta Carnero Formation, about 2000 m thick, appears to strike directly toward the Cretaceous calcareous phyllites and limestones exposed north of Porlamar. This suggests a northwestward-trending cross-fault which is probably situated along the northeast rim of the Laguna Las Marites. The northward-directed, westward-dipping Miocene beds between Laguna Las Marites and the east-northeastward-striking Eocene outcrops of the Punta Carnero section suggest another cross-fault between the two areas.

The northwestward-striking scarps of Miocene beds between Punta Carnero and the area south of Cerro Maria Guevara are repeated at the west end of Macanao and thus indicate faults separating Macanao from Margarita on the east.

It is not, therefore, surprising to find at least one major fault of pre–late upper Miocene age between the bore-holes Cubagua No. 1 and No. 2.

The surface of Cubagua Island shows a symmetrical anticline with a south flank dipping about 5° and a slightly steeper north flank. The structure lies in a trough filled with at least 4000 m of Tertiary sedimentary rocks. Inside this trough one has to expect the Eocene, Oligocene, and lower Miocene sediments to be compressed into steeply dipping synclinal folds. The fault system affected the youngest beds also. High-angle displacement is indicated by the proximity of the metamorphosed sedimentary rocks of Coche Island.

At least two orogenic movements are revealed by the attitude of the Miocene beds which in Laguna Las Marites strike almost at right angles to that of the Eocene sedimentary rocks.

Tertiary History

The oldest Tertiary remnant of Margarita is apparently equivalent to the Soldado Formation of Trinidad or the Guasare Formation of the Maracaibo area, and is of Midwayan age. To judge from the occurrences at Toas Island in Maracaibo Lake, or from Trinidad, one would expect a glauconitic shell bed indicating shallow seas above the eroded metamorphic rocks of Margarita. Early Eocene is represented by limestone blocks carrying *Discocyclina* cf. *barkeri*, *Athecocyclina* cf. *cookei*, and *Tremastegina senni*. The Paleocene and lower Eocene sedimentary rocks were removed during the transgression of the middle Eocene sea that gave rise to the formation of the "Conglomeratic Shale". The blocks and conglomerate components of this shale point to a source north of Margarita, for the parent rock of many of these components is known neither on Margarita nor on the Mainland.

The "Conglomeratic Shale" is a typical Flysch deposit and as such can be correlated with the "Midden-Curaçao lagen" of Curaçao (Molengraaff, 1929, p. 23) and the great thickness of Misoa-Trujillo Formation in Falcón, Lara, and Trujillo.

During the deposition of the rest of the Punta Carnero Formation shallow seas must have prevailed, to judge from the nature of the orbitoidal sandstones and limestones accompanied by silty shales. The "Seroe di Cueba serie" of Curacao, the Pauji Formation in Maracaibo, and the Cerro Campana Formation of eastern Falcón are contemporaneous.

The paralic sediments in borehole No. 1 of Cubagua apparently indicate brackish-water swampland during part of Oligocene time. These beds may be related to the more marine, but leaf-bearing San Lorenzo Formation of District Acosta in Eastern Falcón.

Diastrophism was renewed after the deposition of the Oligocene sediments. The Miocene

clays of Cubagua No. 1 and No. 2 can be correlated with the Lengua Formation of Trinidad which is transgressive. Deposits synchronous with the Cruse Formation of Trinidad seem to follow in normal sequence above the Lengua Formation. The highly fossiliferous Cubagua Formation is closely related to the shallow-water deposits of the Springvale Formation of Trinidad and with the late Miocene infill of the Cubagua trough this sedimentary cycle was brought to an end. The equivalent of the Cubagua Formation occurs along the coast of Falcón, from Cumarebo over Paraguaná into Western Falcón from where it is known as the Cumarebo, La Vela, and Urumaco Formations. In Eastern Falcón the Ojo de Agua Formation and Capadare limestone are closely related to the Cubagua Formation. The Capadare limestone is the mountain-forming element of the Cerro Misión in Eastern Falcón. With the Ojo de Agua and other Miocene formations it extends from the lower Tocuyo Valley far west into the basin of Carora. This great Miocene syncline is superimposed on thick Paleocene, Eocene, and Oligocene Flysch and must be considered the western extension of the Cubagua trough.

Pliocene appears to be represented on Cubagua by a cover about 10 m thick of a shallow offshore deposit with large Pecten and is probably the same as the Cabo Blanco beds west of La Guaira.

References Cited

Aguerrevere, P. I., 1936, Notas geológicas sobre Margarita y Coche: Soc. Venezolana de Cienc. Nat. Bol., v. 3, no. 28, p. 397–403

Anisgard, H. W., 1956, *Eorupertia* in the Eocene of Venezuela: Contr. Cushman Found. Foram. Res., v. 7, pt. 2, p. 48–59

Bronnimann, P., 1950, *Tremastegina*, ein neues Genus der Familie Asterigerinidae d'Orbigny: Eclog. geol. Helv., v. 43, p. 255–265

Bucher, W. H., 1952, Geologic structure and orogenic history of Venezuela: Geol. Soc. America Mem. 49, 113 p.

Dalton, L. V., 1912, On the geology of Venezuela: Geol. Mag., v. 9, no. 575, p. 203–210

González de Juana, C., 1947, Elements of diastrophic history of Northeastern Venezuela: Geol. Soc. America Bull., v. 58, p. 689–702

Hess, H. H. and Maxwell, J. C., 1949, Geological reconnaissance of the Island of Margarita, Pt. 1: Geol. Soc. America Bull., v. 60, p. 1857–1868

Hodson, F., 1926, Venezuelan and Caribbean Turritellas: Bull. Am. Paleontology, v. 11, p. 171–220

Keijzer, F. G., 1945, Outline of the geology of the eastern part of the Province of Oriente, Cuba: Thesis. University Utrecht, 238 p.

Liddle, R. A., 1928, The geology of Venezuela and Trinidad: Fort Worth, Texas, J. P. MacGowan, 552 p.

——1946, The geology of Venezuela and Trinidad: Pal. Res. Inst. Ithaca, 890 p.

Maury, C. J., 1925, Venezuelan stratigraphy: Am. Jour. Sci., 5th ser., v. 9, p. 411–414

Molengraaff, G. J. H., 1929, Geologie en Hydrologie van het eiland Curaçao: Acad. Thesis Delft., 126p.

Renz, H. H., 1948, Stratigraphy and fauna of the Agua Salada group, State of Falcón, Venezuela: Geol. Soc. America Mem. 32, 219 p.

Richards, H. G., 1943, Pleistocene mollusks from Margarita Island. Jour. Paleontology, v. 17, p. 120–123

Rutten, L., 1940, On the geology of Margarita, Cubagua, and Coche (Venezuela): Konink. Akad. v. Wetensch. Amsterdam, v. 43, p. 828–841

Schuchert, C., 1935, Historical geology of the Antillean-Caribbean Region, N. Y., John Wiley and Co., 811 p.

Senn, A., 1940, Paleogene of Barbados and its bearing on history and structure of Antillean-Caribbean region: Am. Assoc. Petroleum Geologists Bull., v. 24, p. 1548–1610

Wall, G. P., 1860, On the geology of a part of Venezuela and Trinidad: Geol. Soc. London Quarterly Jour., v. 16, p. 460–470

Woodring, W. P., 1928, Miocene mollusks from Bowden, Jamaica: Carnegie Inst. Washington Pub. 385, 564 p.

Pointe-a-Pierre, Trinidad, B.W.I.

Manuscript Received by the Secretary of the Society, August 30, 1956

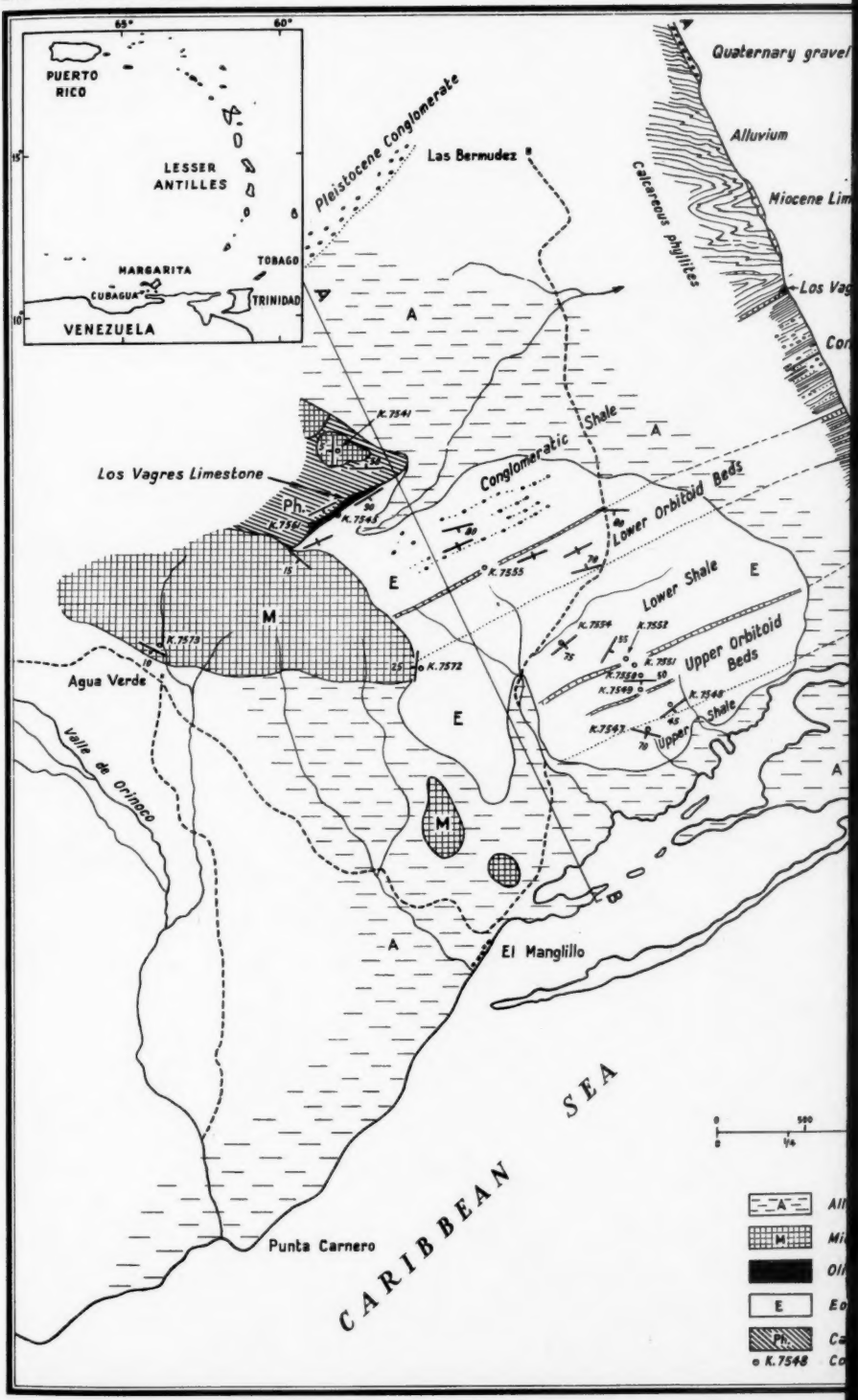

GEOLOGICAL SKETCH MAP OF THE PUNTA CA
SOUTHERN MARGARITA

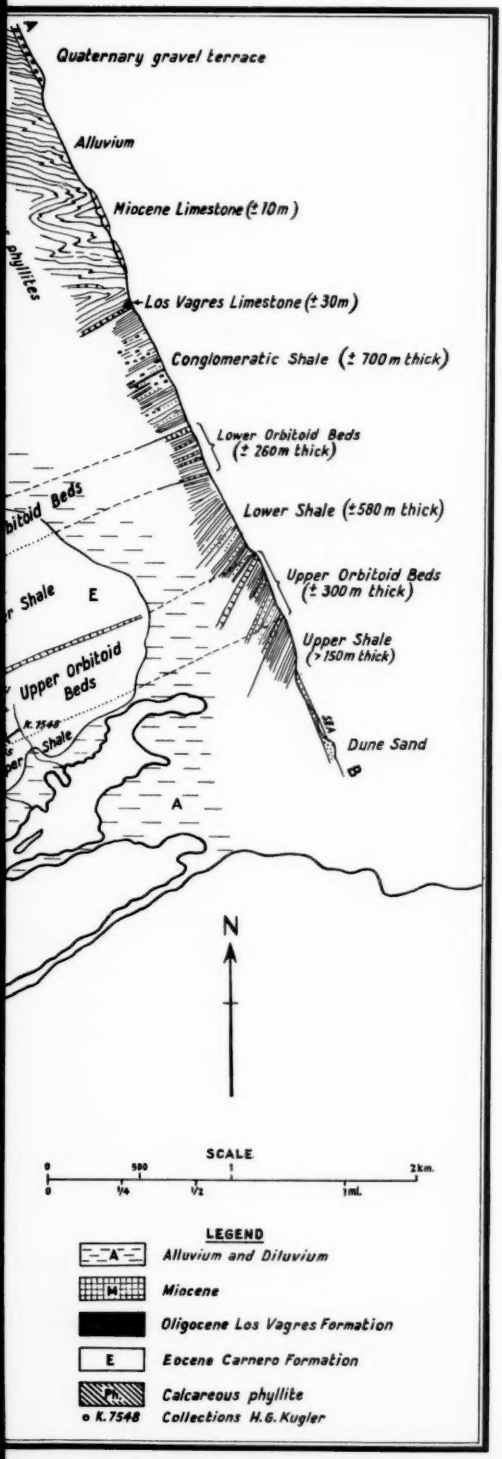

PUNTA CARNERO AREA,
RITA

BULLETIN OF THE GEOLOGICAL SOCIETY OF AMERICA
VOL. 68, PP. 567–576, 9 FIGS. MAY 1957

MECHANICAL ANALYSIS OF THE DIKE PATTERN OF THE SPANISH PEAKS AREA, COLORADO

BY HELMER ODÉ

ABSTRACT

It is possible to explain the shape of the remarkable dike pattern surrounding the Spanish Peaks, Colorado, by an analysis of stresses if a regional-stress system in which the direction of greatest principal pressure was parallel to the line of symmetry exhibited by the dike pattern superposed on a local-stress system is assumed. This local-stress system is caused by hydrostatic pressure exerted by the intrusive mass of the Spanish Peaks. For simplification of the computations a circular hole is assumed at the position of West Spanish Peak.

The mountain front west of the Spanish Peaks provides an unknown boundary condition, which however can be described with satisfactory results by the assumption of an image source. On the basis of the assumption that the relation between stress field and dike pattern is the one proposed by Anderson (1951, Chap. 3) it is then possible to compute the dike pattern. This computed dike pattern agrees in many respects with the observed dike pattern.

CONTENTS

TEXT

	Page
Introduction	567
Local-stress field	569
Superposition of the regional-stress field	573
Displacements	574
References cited	575

ILLUSTRATIONS

Figure	Page
1. System of dikes surrounding the Spanish Peaks	568
2. Displacements at the mountain front	570
3. Stresses acting on a small element of volume	571
4. Co-ordinate notation used in stress analysis	571
5. Definition of the angle α	572
6. Pattern of principal-stress trajectories caused by two sources of equal sign	572
7. Pattern of principal-stress trajectories caused by two sources of opposite sign	572
8. Pattern of principal-stress trajectories caused by two sources of equal sign and superposed regional-stress system	574
9. Pattern of principal-stress trajectories caused by two sources of opposite sign and superposed regional-stress system	574

INTRODUCTION

Just east of the Culebra Range in Colorado a double mountain, the Spanish Peaks, rises from the surrounding plain to an elevation of 13,633 feet. The locality, well known for its system of radial dikes and accompanying sills, was first described by Hills (1900; 1901).

Intrusive bodies surrounded by an aureole of dikes are not rare in the western United States. Weed and Pirsson (1894) had already described such radial patterns in the Highwood Mountains of Montana. Later Pirsson (1905) published his classical study of the Highwood Mountains. In a petrological study of the dike rocks of the Spanish Peaks area, Knopf (1936, p. 1784) drew attention to the great similarity in chemical composition of the rocks of both regions. Other systems of radiating dikes along the eastern border of the Rocky Mountains are in the Sunlight area of Wyoming (Parsons, 1939) and in the Big Belt Range of Montana (Lyons, 1944). Mention of a radiating system of dikes in the Mitre Peak area of Texas is also made by Ives (1941, p. 347).

The dike pattern of the Spanish Peaks area is made unique by its peculiar shape (Fig. 1). Whereas the other patterns described are

regularly radial or are confused because of several superposed systems, the geometrical pattern of dikes surrounding the Spanish Peaks shows the following three significant characteristics:

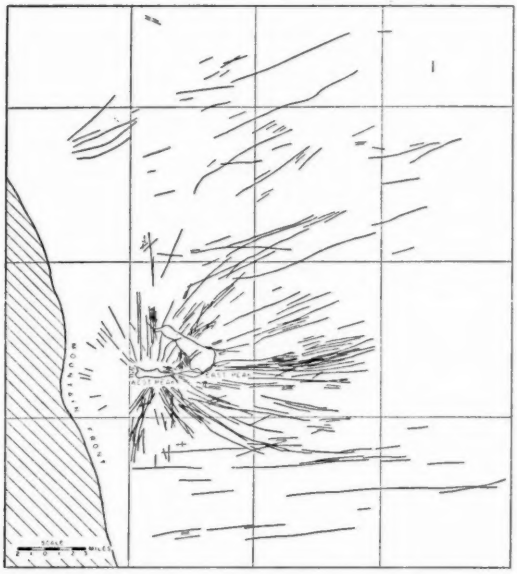

FIGURE 1.—SYSTEM OF DIKES SURROUNDING THE SPANISH PEAKS
After Knopf, 1936

(1) The pattern of dikes is clearly symmetrical about a line running N. (75°) E. through West Spanish Peak.

(2) Originating for the most part in West Spanish Peak, the dikes tend to curve eastward.

(3) The westward-trending dikes are much shorter than those trending eastward, which can be followed for distances of more than 25 miles.

Most of the dikes of the Spanish Peaks area which, according to Knopf, number probably not less than 500, are vertical; a few dip less than 80°. Their thickness ranges from 2 to 60 feet; 10 feet is the most common. Most of the dikes appear to have originated after the formation of West Peak. A few shorter dikes, originating from East Peak, were probably intruded earlier.

Knopf's explanation for the origin of the remarkable dike system at Spanish Peaks is as follows (Knopf, 1936, p. 1739):

"Possibly, the cause for this swinging around to an east-west direction is that the forces that, near the stocks, produced the radial fissuring, opened up, at a greater distance from the stocks, the latent tension fissures produced during the compression that had folded the sedimentary beds into a broad syncline before the stocks were injected, *i.e.*, the dikes availed themselves of latent tension breaks across the axis of the fold."

From a mechanical viewpoint a more satisfactory explanation can be given by an analysis of the dike pattern in terms of stress. Such an explanation is based on the assumption that an intimate relation exists between stress field and dike pattern. Anderson (1951, Chap. 3) postulated that the formation of dikes is due to a wedging effect of the intruding magma. According to his theory dikes form along planes lying normal to the direction of least principal stress or in other words along planes of greatest and intermediate principal stress.

Anderson's assumptions are derived directly from the work of Griffith (1921; 1924). From

determinations of the tensile strength of brittle materials it was noted that the observed values of the tensile strength were one or two orders of magnitude lower than values expected from theoretical considerations (Orowan, 1949, p. 192). To explain this discrepancy Griffith assumed that the tested brittle material contained numerous small cracks of random orientation. These small cracks he envisaged as small ellipsoids of large eccentricity. Stresses applied to the material cause large stress concentrations at points near the ends of the ellipsoids. The sudden and rapid propagation of the crack occurs then as follows. If the crack is given a small virtual increase in length some energy is required to break the bonds between particles in the material. There is also a small increase in strain energy of the plate. Griffith postulated that, as soon as the total work done by the external forces exceeds the sum of the increases in surface energy and strain energy of the material, the crack will spread. In this manner the observed tensile strength can be related to the length of the crack. Also the orientation of the cracks first to become unstable under various systems of applied loadings can be investigated. In general the orientation of those cracks does not coincide with that of the principal stresses in the plate. Therefore Griffith suggested that his theory could explain the inclined fractures often observed in specimens of brittle material deformed under various states of triaxial stress. In view of the basic assumption made by Griffith that the stress-strain relation satisfies Hooke's law exactly up to the moment of rupture this suggestion seems doubtful. His analysis probably can be applied to the wedging effect of a fluid under pressure, however, because little energy will be dissipated in permanent deformation. It is then assumed that the dike is an ellipse of large eccentricity on the walls of which a hydrostatic pressure p is exerted by the intruding magma. This leads to large but very localized tensile stresses at the tip of the crack (Griffith, 1921; 1924). The largest tensile stresses occur for a crack whose long axis is oriented in the direction of the largest principal stress. Because the dike will originate in this orientation it will during its growth remain along such a maximum stress trajectory. The problem therefore is to determine the maximum stress trajectories of the stress field.

The stress field in the material of the crust is obtained by superposition of two simpler fields. The first, which we shall call the local field, is caused by the fluid pressure in the central hole, and the second is a regional field which is assumed to vary little over large distances. This is the field in the crust at the moment the dikes were injected.

The symmetry of the dike pattern indicates that the total-stress field must be symmetric in the same manner. The absence of dikes west of the mountain front suggests that this mountain front acted as a more or less rigid boundary, and the divergence of dikes from one central area indicates that the stress in this area can be described by the formulas used to compute the stress around a hole—which for convenience shall be considered circular—in an infinite plate caused by an internal pressure p.

The dike pattern derived on the assumptions that there is no regional-stress field does not resemble the dike pattern around the Spanish Peaks. Thus the existence of a regional field at the time of dike injection is very probable. It seems plausible then to assume a regional-stress field in which the greatest principal stress had the direction of the line of symmetry exhibited by the Spanish Peaks dike system. This agrees with the intuitive notion that the mountain ranges west of the Spanish Peak are related to such a stress field. The superposition of this regional-stress field over the local-stress field created by the dike injection yields a stress pattern which is in striking agreement with the pattern of dikes surrounding the Spanish Peaks.

Local-Stress Field

To simplify the problem of finding the local-stress field, it is necessary to make the following assumptions:

(1) The "fluid" igneous mass rose through a vertical circular hole to the surface.
(2) The focal point of the curvilinear dike pattern is at West Spanish Peak.
(3) The mountain front was straight and acted as an almost rigid boundary.

Treating the problem in two dimensions reduces it to the problem of finding the stresses in a

semi-infinite plate pierced near its boundary by a circular hole, in which a hydrostatic pressure is exerted. The boundary condition imposed by the mountain front is attained by assuming an "image" source, as is commonly done in potential theory. By "image" source here is meant another circular hole in which either the same or a different hydrostatic pressure is exerted, and which is placed somewhere at the other side of the mountain front. The usefulness of the concept of image sources lies in the fact that the stresses, which act along the mountain front, and which must be given to obtain a solution, are determined by superposition of the stresses caused by the real hole and its images. The stresses along the mountain front are unknown, and, therefore, it is impossible to decide where the image sources must be placed and what their respective pressures are. However, the symmetry of the dike pattern suggests that an "image source" can be placed at a point which is the mirror image of the real hole with respect to the mountain front. This image source, which will be assumed to be of the same magnitude as the real source, may be positive or negative. When the image is positive, *i.e.*, if the fluid within it exerts a hydrostatic pressure, there is a displacement along the front (Fig. 2A). If the source is negative, *i.e.*, the hole tends to close, the mountain front is displaced normal to itself (Fig. 2B). These displacements are relatively small.

The preference to treat the problem in this manner, rather than to solve the analogous problem for an exactly rigid boundary, has a simple reason. Although the "exact" problem can be solved with the appropriate mathematical tools, its greater complexity in no way guarantees greater accuracy, since the exact boundary conditions along the mountain front are unknown. Moreover the "exact" solution leads essentially to the same results.

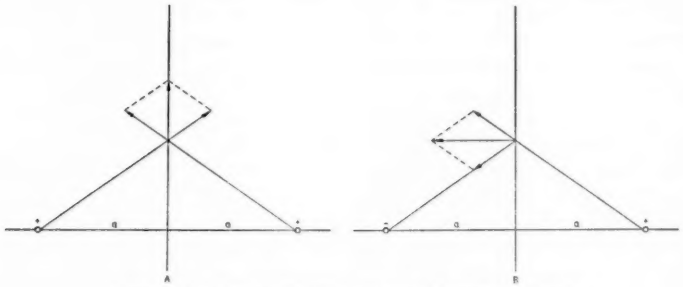

FIGURE 2.—DISPLACEMENTS AT THE MOUNTAIN FRONT
A. For a positive image source
B. For a negative image source

For a single hole in an infinite plane, the stresses at a point P, which result from hydrostatic pressure in the hole, are functions only of R, the distance from the center of the hole to the point P. The easiest way of solving the problem is to use Airy's stress function ϕ, which satisfies the equation $\nabla^2\nabla^2\phi = 0$. From this function ϕ the stress components are derived from the following equations (Timoshenko, 1934, Chap. 3):

$$\sigma_R = \frac{1}{R}\frac{\partial\phi}{\partial R} + \frac{1}{R^2}\frac{\partial^2\phi}{\partial\theta^2};$$

$$\sigma_\theta = \frac{\partial^2\phi}{\partial R^2}; \qquad (1)$$

$$\tau = -\frac{\partial}{\partial R}\left(\frac{1}{R}\frac{\partial\phi}{\partial\theta}\right),$$

where σ_R, σ_θ and τ are the normal radial, normal tangential, and shear stress respectively. The stresses which act on a small element of volume are shown in Figure. 3. The stress function ϕ for a hole in an infiite plane is obtained from $\nabla^2\nabla^2\phi = 0$ with the condition that the stresses are independent of θ and vanish at infinity; then $\phi = A \ln R$, where A is a constant. If in two holes the same hydrostatic pressure is exerted, and the origin of the co-ordinate

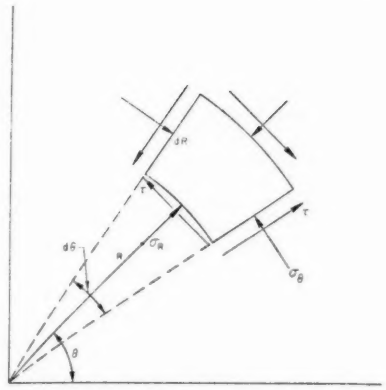

FIGURE 3.—STRESSES ACTING ON A SMALL ELEMENT OF VOLUME

where for simplification of the formulae the following substitution is made:

$$R^2 + a^2 = 2\xi^2.$$

In case $\phi = A_2 \ln (r_1/r_2)$, which applies if the pressure in both holes is equal but opposite in sign, the stress components are given by

$$\sigma_R = -\sigma_\theta = \frac{A_2 aR \cos\theta}{(\xi^4 - a^2R^2\cos^2\theta)^2} [\xi^4 - 2a^2\xi^2 + a^4\cos^2\theta], \quad (4)$$

$$\tau = A_2 \frac{aR \sin\theta}{(\xi^4 - a^2R^2\cos^2\theta)^2} [\xi^4 - a^4\cos^2\theta].$$

To draw the stress pattern, the angle α, which the direction of one of the principal stresses makes with the radial direction, must be known

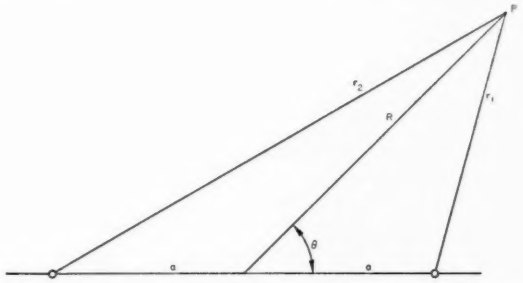

FIGURE 4.—CO-ORDINATE NOTATION USED IN STRESS ANALYSIS

system is taken halfway between the two holes (Fig. 4), the function ϕ is given by

$$\phi = A_1 \ln (r_1 r_2);$$
$$r_1^2 = R^2 + a^2 - 2aR\cos\theta; \quad (2)$$
$$r_2^2 = R^2 + a^2 + 2aR\cos\theta.$$

Since $\phi = A_1 \ln r$ satisfies $\nabla^2\phi = 0$ and $\sigma_R + \sigma_\theta = \nabla^2\phi$, then

$$\sigma_R + \sigma_\theta = 0.$$

Performing the differentiations indicated by (1), the stress components in a point (R, θ) are given by

$$\sigma_R = -\sigma_\theta = \frac{A_1}{(\xi^4 - a^2R^2\cos^2\theta)^2} [\xi^6 - \xi^4 a^2\sin^2\theta - \xi^2 a^2R^2\cos^2\theta - a^4R^2\cos^2\theta\sin^2\theta],$$

$$\tau = -\frac{A_1 a^2 \sin\theta\cos\theta}{(\xi^4 - a^2R^2\cos^2\theta)^2} [\xi^4 - 2\xi^2R^2 + a^2R^2\cos^2\theta], \quad (3)$$

as a function of the variables. This angle α (Fig. 5) is given by

$$\tan 2\alpha = \frac{2\tau}{\sigma_R - \sigma_\theta} = \frac{\tau}{\sigma_R}. \quad (5)$$

Substituting (3) into (5):

$$\tan 2\alpha = -\frac{a^2 \sin\theta\cos\theta[\xi^4 - 2\xi^2R^2 + a^2R^2\cos^2\theta]}{[\xi^6 - \xi^4 a^2\sin^2\theta - a^2R^2\xi^2\cos^2\theta - a^4R^2\cos^2\theta\sin^2\theta]}.$$

It is obvious that as R goes to infinity $\tan 2\alpha$ goes to zero. Hence, the stress trajectories at infinity are parallel to a pencil of rays through the origin, *i.e.*, these rays are asymptotic to the stress trajectories. This is quite as should be expected, for at infinity the two holes act as one.

Singular points in the stress pattern are obtained from indeterminate values of $\tan 2\alpha$

or in other words for values of R and θ which make both σ_R and τ zero. There are only four such points

$$\begin{matrix} R = a \\ \theta = 0, \pi \end{matrix} \quad \text{and} \quad \begin{matrix} R = a \\ \theta = \pm\pi/2. \end{matrix}$$

The first two correspond with both sources and are, therefore, of little interest.

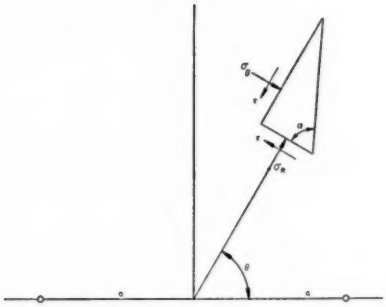

FIGURE 5.—DEFINITION OF THE ANGLE α

The stress pattern can now be drawn by computing values of α for different values of R and θ. In points of the circle $R = a$, the directions of the two principal stresses point toward both sources.

The resulting stress pattern is shown in Figure 6. The magnitude of the two principal stresses σ_p at any point is given by

$$\sigma_p = \pm\sqrt{\sigma_R^2 + \tau^2} = A_1 \frac{\sqrt{\xi^4 - a^2R^2\sin^2\theta}}{\xi^4 - a^2R^2\cos^2\theta}. \quad (7)$$

In case of an "image" source of negative sign $\tan 2\alpha$ is given by

$$\tan 2\alpha = \frac{\tan\theta \times (\xi^4 - a^4\cos^2\theta)}{\xi^4 - 2\xi^2a^2 + a^4\cos^2\theta}. \quad (8)$$

This pattern also possesses the property that the directions of the principal stresses in the circle $R = a$ point toward both sources. It can be shown that the point $R = 0$ is, apart from both sources, the only singular point in the stress pattern. The resulting stress pattern is shown in Figure 7. The magnitude of the principal stress is given by

$$\sigma_p = \pm\frac{A_2aR}{\xi^4 - a^2R^2\cos^2\theta}. \quad (9)$$

In both cases the value of σ_p at singular points is zero, which is immediately apparent from the fact that σ_R and τ are zero. This means that the material in these points is in an unstressed state. But it can be verified that the

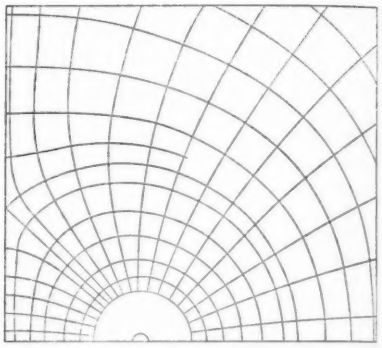

FIGURE 6.—PATTERN OF PRINCIPAL-STRESS TRAJECTORIES CAUSED BY TWO SOURCES OF EQUAL SIGN

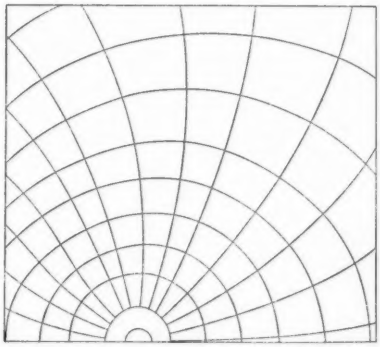

FIGURE 7.— PATTERN OF PRINCIPAL-STRESS TRAJECTORIES CAUSED BY TWO SOURCES OF OPPOSITE SIGN

displacements reach a maximal value in those points. Figures 6 and 7 show that the sign of σ_p changes along a trajectory passing through a singular point.

If the stress components of both cases multiplied by different factors are added, the stress pattern resulting from the case of two sources of different "strength," situated symmetrically with respect to the mountain front, is obtained. However, stress patterns obtained in this manner do not resemble the dike pattern of the Spanish Peaks area.

Superposition of the Regional-Stress Field

As pointed out in the Introduction, the most probable reason for this discrepancy is that at the time the dikes were injected a regional-stress field existed. The symmetry of the pattern immediately suggests that this regional-stress field was also symmetrical; in particular the eastward curving of the dikes suggests that its direction of greatest principal stress was parallel to the line of symmetry of the pattern. It is not unlikely that this pattern was related to the northward-trending mountain range west of the Peaks. Therefore, it is assumed that this regional-stress pattern can be described by

$$\phi = \frac{B}{2}x^2 + \frac{C}{2}y^2,$$

where

$$\sigma_x = \frac{\partial^2\phi}{\partial y^2} = C, \qquad \sigma_y = \frac{\partial^2\phi}{\partial x^2} = B,$$

$$\tau_{xy} = -\frac{\partial^2\phi}{\partial_x \partial y} = 0,$$

or expressed in polar co-ordinates:

$$\begin{aligned} \phi &= \frac{B}{2}R^2\cos^2\theta + \frac{C}{2}R^2\sin^2\theta, \\ \sigma_R &= B\sin^2\theta + C\cos^2\theta, \\ \sigma_\theta &= B\cos^2\theta + C\sin^2\theta, \\ \tau &= \frac{B-C}{2}\sin 2\theta. \end{aligned} \tag{10}$$

If expressions (3) and (10) are added the stress pattern caused by the two superposed stress patterns can be determined in the same manner as before. A stress pattern closely resembling the stress pattern of the dikes radiating from the Spanish Peaks will result.

Computations were carried out for the positive case $C = 2B$; $B = A_1/a^2$. In the superposed system the principal stress in the x direction (normal to the mountain front) is twice as great as the stress in the y direction, and its magnitude is equal to the magnitude of the principal local stress in the origin in the case of two symmetric holes with equal hydrostatic pressure, as may be seen when $R = 0$ is substituted in (7).

The stress components and tan 2α are then given by

$$\sigma_R = \frac{A}{(\xi^4 - a^2R^2\cos^2\theta)^2}$$

$$[\xi^6 - \xi^4a^2\sin^2\theta - \xi^2a^2R^2\cos^2\theta - a^4R^2\cos^2\theta\sin^2\theta]$$

$$+ \frac{A}{a^2}\sin^2\theta + \frac{2A}{a^2}\cos^2\theta.$$

$$\sigma_\theta = \frac{-A}{(\xi^4\ a^2R^2\cos^2\theta)^2}$$

$$[\xi^6 - \xi^4a^2\sin^2\theta - \xi^2a^2R^2\cos^2\theta - a^4R^2\cos^2\theta\sin^2\theta]$$

$$+ \frac{A}{a^2}\cos^2\theta + \frac{2A}{a^2}\sin^2\theta.$$

$$\tau = -\frac{Aa^2\cos\theta\sin\theta}{(\xi^4 - a^2R^2\cos^2\theta)}[\xi^4 + a^2R^2\cos^2\theta - 2\xi^2R^2]$$

$$- \frac{A}{2a^2}\sin 2\theta.$$

$$\tan 2\alpha = \frac{\begin{array}{r}-2a^4\cos\theta\sin\theta[\xi^4 + a^2R^2\cos^2\theta \\ - 2\xi^2R^2] - \sin 2\theta[\xi^4 - a^2R^2\cos^2\theta]^2\end{array}}{\begin{array}{r}2a^2[\xi^6 - \xi^4a^2\sin^2\theta - \xi^2a^2R^2\cos^2\theta \\ - a^4R^2\cos^2\theta\sin^2\theta] + \cos 2\theta \\ [\xi^4 - a^2R^2\cos^2\theta]^2\end{array}}.$$

As R approaches infinity tan $2\alpha = -\tan 2\theta$, or the stress trajectories coincide at infinity with the stress trajectories of the superposed system. The resulting stress pattern is shown in Figure 8. In all of its important aspects, this pattern resembles that of the dikes radiating from the Spanish Peaks.

If the holes have opposite signs, expressions for the stresses are obtained in the same manner as above by addition of (4) and (10). For tan 2α we obtain

$$\tan 2\alpha = \frac{\begin{array}{r}2a^3R\sin\theta\,[\xi^4 - a^4\cos^2\theta] \\ - \sin 2\theta[\xi^4 - a^2R^2\cos^2\theta]^2\end{array}}{\begin{array}{r}2a^3R\cos\theta[\xi^4 - 2a^2\xi^2 + a^4\cos^2\theta] \\ + \cos 2\theta[\xi^4 - a^2R^2\cos^2\theta]^2\end{array}}.$$

The corresponding stress pattern is shown in Figure 9. Figures 8 and 9 show a remarkable resemblance. That the difference between the patterns is greatest near the mountain front is not surprising, as the boundary conditions along that front are different, whereas at infinity they are the same. The question of which case provides the best fit to the Spanish Peaks dike system is not very important.

As already pointed out, the boundary conditions along the mountain front are uncertain, and, therefore, neither of the two cases will be quite correct. The map published by Knopf (1936, Fig. 1) shows that most of the westward-trending dikes end at an acute angle to the mountain front, which is slightly bent inward. This may indicate that the assumption of an image of opposite sign is the better one. It is important to note that if the ratio of the constants A_1, A_2, B, C is changed a better fit between computed and observed pattern may be obtained. So a large value of B with respect to A_1, A_2, and C gives a stress pattern in which the stress trajectories diverging from the Spanish Peaks and asymptotic to eastward-trending trajectories of the regional stress system are compressed into a narrow band. If the value of B is decreased, this band can be broadened. If the values of A_1 and A_2 are increased and B and C are kept constant, the influence of the local stress system is emphasized. Therefore, if the right ratios of A_1, A_2, B, and C are selected, it is possible to obtain a better fit between computed and observed pattern than is shown in Figures 6, 7, 8, and 9.

Of much interest are the dikes which are normal to the mountain front and do not originate in the center of West Spanish Peak. Some of these dikes are crossed by, and some cross, dikes converging to the Spanish Peaks. Thus not all dikes are formed contemporaneously. It seems probable, however, that both are the result of the same igneous mechanism.

Inspection of the other dike systems mentioned in the Introduction shows that most are regularly radial. Only the map of dikes surrounding Sunlight Volcano (Parsons, 1939, p. 14) shows a pattern with very slight curvature. This indicates that, in these cases, the boundary condition imposed by the mountain front was absent.

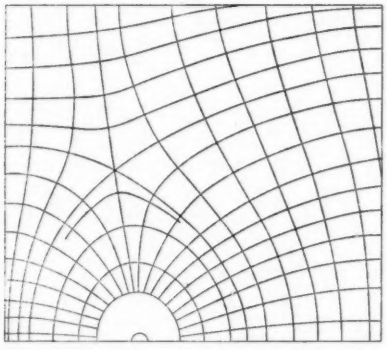

FIGURE 8.—PATTERN OF PRINCIPAL-STRESS TRAJECTORIES CAUSED BY TWO SOURCES OF EQUAL SIGN AND SUPERPOSED REGIONAL-STRESS SYSTEM

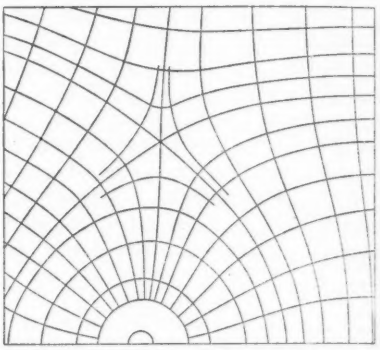

FIGURE 9.—PATTERN OF PRINCIPAL-STRESS TRAJECTORIES CAUSED BY TWO SOURCES OF OPPOSITE SIGN AND SUPERPOSED REGIONAL-STRESS SYSTEM

DISPLACEMENTS

The order of magnitude of the elastic displacements is easily found if no regional stress is present. If U_R is the radial displacement, E Young's modulus, and ν Poisson's ratio we have:

$$\frac{\partial U_R}{\partial_R} = -\frac{1}{E}(\sigma_R - \nu\sigma_\theta) = \frac{1+\nu}{E}\frac{\partial^2\phi}{\partial R^2};$$

or

$$U_R = \frac{1+\nu}{E}\frac{\partial\phi}{\partial R} + f(\theta); \qquad (11)$$

or

$$U_R = \frac{2(1+\nu)}{E} A_1 R \left\{\frac{R^2 + a^2 - 2a^2\cos^2\theta}{(R^2+a^2)^2 - 4a^2R^2\cos^2\theta}\right\} + f(\theta).$$

Quantity U_R must be zero, for $R = 0$, hence $f(\theta) \equiv 0$. The value of U_R along the mountain

front is obtained if $\theta = \pi/2$ is substituted in (11):

$$U_R = \frac{2(1+\nu)}{E} \cdot \frac{A_1 R}{a^2 + R^2}$$

which reaches its greatest absolute value if $R = a$. Therefore:

$$U_R(\max) = \frac{A_1}{2\mu a};$$

where μ is the coefficient of rigidity for surface rocks. To obtain an estimate of this maximal displacement, probable values of the quantities involved must be substituted. The value of μ for rocks under surface conditions is about 3.5×10^{11} dynes/cm^2. Hence if A/a^2 represents a stress of about 10^9 dynes/cm^2, which is undoubtedly high, and as a, the distance from West Spanish Peak to the mountain range is about 1.4×10^6 cm, A is approximately 2×10^{21} dynes. Thus the magnitude of U_R is found to be

$$\frac{2 \times 10^{21}}{7 \times 10^{11} \times 1.4 \times 10^6} = 2 \times 10^3 \text{cm}.$$

However, it is not very likely that A had this very great order of magnitude. Stresses of the order of 10^5 dynes/cm^2 are more likely to produce overthrusting and rupturing. Even if the value of μ was taken too large, then still the fact that the value of A is rather high makes the value of 2×10^3 cm a likely one. However, when an additional stress is present, all the displacements are different. The displacements caused by the superposed stress system alone are given by

$$U_x = \frac{1}{E}(2 - \nu)Bx,$$

$$U_y = \frac{1}{E}(1 - 2\nu)By.$$

(A surface element in the origin of the coordinate system is considered fixed.) These displacements are greater with increase in distance from the origin. Therefore, the total displacements far from the sources are due only to the superposed stress field. To what extent the elastic shortening of the area is compensated by the dilation caused by the injected matter of the dikes is a matter of conjecture. The data, on which such a calculation must be based, are too inaccurately known.

References Cited

Anderson, E. M., 1951, The dynamics of faulting and dike formation: 2d ed., London, Oliver and Boyd, 206 p.

Griffith, A. A., 1921, The phenomena of rupture and flow in solids: Philos. Trans. Royal Soc., ser. A, v. 221, p. 163–198

——1924, The theory of rupture: Delft, Proc. 1st Internat. Cong. Applied Mech., p. 55–63

Hills, R. C., 1900, Description of the Walsenburg quadrangle, Colo.: U. S. Geol. Survey Atlas, folio 68, 6 p.

——1901, Description of the Spanish Peaks quadrangle, Colo.: U. S. Geol. Survey Atlas, folio 71, 7 p.

Ives, R. L., 1941, The Mitre Peak area, Trans Pecos, Texas: Am. Jour. Sci., v. 239, p. 339–353

Knopf, A., 1936, Igneous geology of the Spanish Peaks region, Colorado: Geol. Soc. America Bull., v. 47, p. 1727–1784.

Lyons, J. B., 1944, Igneous rocks of the northern Big Belt Range, Montana: Geol. Soc. America Bull., v. 55, p. 445–472

Orowan, E., 1949, Fracture and strength of solids: Rept. on Progress in Physics, v. XII, p. 185–232

Parsons, W. H., 1939, Volcanic centers of the Sunlight area, Park County, Wyoming: Jour. Geology, v. 47, p. 1–26

Pirsson, L. V., 1905, Petrography and geology of the igeneous rocks of the Highwood Mountains, Montana: U. S. Geol. Survey Bull. 237, 146 p.

Timoshenko, S., 1934, Theory of elasticity: N. Y., McGraw-Hill, 506 p.

Weed, W. H., and Pirsson, L. V., 1894, Highwood Mountains of Montana: Geol. Soc. America Bull. v. 6, p. 389–422

Shell Development Co., 3737 Bellaire Boulevard, Houston 25, Texas

Received by the Secretary of the Society, December 15, 1956

Publication No. 92, Exploration and Production Research Division, Shell Development Co., Houston, Texas

BULLETIN OF THE GEOLOGICAL SOCIETY OF AMERICA
VOL. 68, PP. 577-610, 2 FIGS., 3 PLS. MAY 1957

METAMORPHISM AND VOLUME LOSSES IN CARBONATE ROCKS NEAR JOHNSON CAMP, COCHISE COUNTY, ARIZONA

BY JOHN R. COOPER

ABSTRACT

Contact-metamorphosed carbonate rocks occur near a stock of quartz monzonite at Johnson Camp, in Chochise County, Arizona. The metamorphosed carbonate rocks show successive zones characterized by (1) chlorite (locally talc), (2) tremolite, (3) forsterite and diopside, and (4) garnet (with local wollastonite and idocrase), as the stock is approached. The mineralogical and textural changes indicate an origin of the silicate minerals by a fixed sequence of chemical reactions between original constituents of the sedimentary rock, with a negligible amount of material added from an outside source but with considerable interchange of material between beds. Silicate minerals generally did not form in pure carbonate rocks in any zone. The distinctive silicates of the outer three zones formed in abundance only in impure dolomites. Garnet, wollastonite, and idocrase of zone 4 formed only in impure limestones; the mineral assemblages in the once dolomitic rocks remained the same in zone 4 as in zone 3.

The chemical reactions that can reasonably be inferred release carbon dioxide and result in the formation of denser minerals, suggesting a decrease in volume, which is confirmed by stratigraphic measurements showing that the silicated facies is as much as 30 per cent thinner than the unsilicated facies. Structural features resulting from the loss in volume are very obscure because of greater deformation not due to the metamorphism and because of recrystallization during the metamorphic process. The losses in volume must be taken into account in comparing chemical analyses of the unmetamorphosed and metamorphosed facies to determine the gains and losses of constituents.

Metasomatism, which included the formation of copper and zinc replacement deposits that have yielded about $20,000,000 to date, started near the temperature maximum and increased as the temperature fell.

CONTENTS

TEXT

	Page
Introduction and acknowledgments	578
Geologic setting	579
Zones of metamorphism	581
General features	581
Metamorphism of dolomitic rocks	582
Metamorphism of calcareous rocks	588
Metamorphism of quartzite	590
Metamorphism of shale	591
Metasomatic effects	592
Johnson area	592
Gunnison Hills	594
Volume relations	595
Chemical and spectrographic data	597
Sample collection, preparation and analysis	597
Unit 7 of the Martin Formation	598
Lithology and calculated mineral composition	598
Gains and losses of constituents	601
Units 5 and 6 of the Abrigo Formation	603
Lithology and calculated mineral composition	603
Gains and losses of constituents	605
Summary of chemical changes	607
General conclusions and speculations	608
References cited	609

ILLUSTRATIONS

Figure	Page
1. Generalized sketch map of Johnson Camp area, Arizona	579
2. Cross section through Republic mine showing thinning of middle member of Abrigo Formation with garnetization	591

Plate	Facing page
1. Lower serpentine marker and bed from which derived	584
2. Upper serpentine marker and bed from which derived	584
3. Hand specimens of metamorphosed rocks	585

TABLES

Table		Page
1.	Distribution of metamorphic minerals	581
2.	Chemical and semiquantitative spectrographic analyses of sedimentary rocks and their metamorphosed equivalents	599
3.	Calculated mineral composition of unit 7 of the Martin	601
4.	Gains and losses of constituents on metamorphism of unit 7 of the Martin	602
5.	Calculated mineral composition (weight per cent) of units 5 and 6 of the Abrigo	603
6.	Gains and losses of constituents on metamorphism of units 5 and 6 of the Abrigo	606
7.	Summary of gains and losses of constituents	607

Introduction and Acknowledgments

The contact metamorphic or pyrometasomatic mineral deposits constitute a distinctive group of deposits that have yielded important amounts of iron, copper, zinc, tungsten, and other metals. They occur where igneous bodies have intruded limestone or other calcium-rich wall rocks. The invaded rocks, and in some cases the marginal part of the intrusive body as well, have been altered to silicate minerals, among which the garnets, pyroxenes, amphiboles, and epidotes are conspicuous. The zone of metamorphism is generally much more extensive than the ore bodies, which occur as sheets, pipes, lenses, or irregular masses in the altered rocks. Detailed study commonly shows that the valuable minerals were introduced late in the metamorphic process and have replaced previously altered rock. In some districts, like Morenci, Arizona, observers (Lindgren, 1905, p. 163) have concluded that silication and metalization were contemporaneous.

Contact metamorphism of carbonate rocks has been known and studied by geologists for 100 years or more. In the early days the metamorphism was regarded as essentially a recrystallization process due to heat from the magma with little change in composition other than loss of carbon dioxide. Detailed studies in several mining districts about 1900, notably Lindgren's study (1905) at Morenci, showed that much material was removed and much added in the conversion of limestone to lime-silicate rock. In classic studies at Marysville, Montana (Barrell, 1907), and Kristiania (Oslo), Norway (Goldschmidt, 1911), a distinction was made between an earlier metamorphic or normal stage with little or no addition of material and a later metasomatic or pneumatolytic stage during which ore minerals and some of the silicates were introduced.

During the first several decades of this century there was a lively controversy between the additive and nonadditive schools, though almost all the latter group granted that the ore was brought in from a distant source. Most of the argument centered about the volume relations. The formation of silicates by nonadditive metamorphism of impure carbonate rocks involves a large loss in volume because carbon dioxide is expelled and because most of the metamorphic minerals are denser than the original minerals of the sedimentary rock. Very little convincing field evidence for the required loss in volume appeared in the geologic literature, but evidence for little or no volume change was pointed out in many areas. After reviewing the literature on the subject Lindgren (1933, p. 709) concluded, "On the whole, it may be asserted that contact metamorphism takes place without change in bulk volume, though in places some vuggy or drusy structures may appear."

For many years economic geologists have generally adopted Lindgren's theory of constant volume in interpreting field facts and making petrologic calculations. This theory is incompatible with pure thermal metamorphism of impure carbonate rocks, for the large losses in volume in the silicate-forming reactions are not compensated by an increase in porosity of the metamorphosed rock. Continuing critical analysis is needed in every area of contact-metamorphosed limestone. This paper presents the results of such an analysis at Johnson Camp, in the Cochise mining district of Cochise County, in southeastern Arizona. The paper is one aspect of a comprehensive study of the geology of the area started in 1944. Other aspects already published include a brief description of the ore deposits (Cooper, 1950), a geochemical prospecting experiment (Cooper and Huff, 1951), and a description of the late Paleozoic stratigraphy (Gilluly, Cooper, and Williams, 1954). A com-

prehensive report is planned for later publication by the U. S. Geological Survey.

Grateful acknowledgment is made to mine operators in the area, particularly to officers and employees of the Coronado Copper and Zinc Company, who have co-operated in many ways. Acknowledgment is also made to the writer's geological assistants, particularly T. W. Amsden, F. W. Farwell, A. E. Disbrow, F. G. Bonorino, and L. T. Silver who participated most actively in the work on metamorphism of the carbonate rocks. The author accepts full responsibility for the interpretations presented.

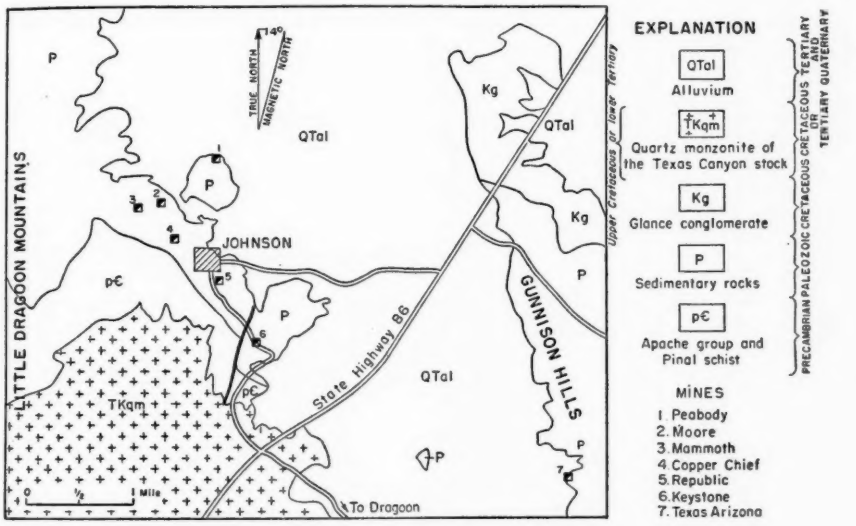

FIGURE 1.—GENERALIZED SKETCH MAP OF JOHNSON CAMP AREA, ARIZONA

GEOLOGIC SETTING

The Johnson Camp area is in the Basin and Range province about 55 miles east of Tucson and 50 miles north of Bisbee, Arizona. The region is one of isolated mountain ranges composed of middle Tertiary and older rocks separated by desert basins filled with late Tertiary and Quaternary alluvial and lacustrine deposits. The specific area includes parts of the Little Dragoon Mountains and the Gunnison Hills, a smaller range about 2 miles to the east (Fig. 1).

In the Little Dragoon Mountains a large stock of quartz monzonite, called the quartz monzonite of the Texas Canyon Stock, intrudes rocks ranging in age from the lower Precambrian Pinal schist to the Lower Cretaceous Bisbee group. The quartz monzonite is probably of Late Cretaceous or early Tertiary (Laramide) age, but it could be younger, for the Cretaceous and older rocks were folded and thrust-faulted before intrusion. The carbonate rocks in the Paleozoic and Mesozoic formations are metamorphosed in the vicinity of the intrusive body, particularly on the northeastern side.

Generalized section of formations in Little Dragoon Mountains and Gunnison Hills

	Feet
Quaternary and Tertiary: alluvium	500+
Uncomformity	
Lower Cretaceous: Bisbee group	
Morita-Cintura Formation	2500
Glance conglomerate	500
Uncomformity	
Jurassic or Triassic: Andesitic and rhyolitic tuff breccia and conglomerate (of local occurrence)	400
Uncomformity	
Permian and Pennsylvanian: Naco group	
Concha limestone	130
Scherrer Formation	690

Colina limestone	440+
Earp Formation	1100
Horquilla limestone	1600
Pennsylvanian (?) or Mississippian: Black Prince limestone	125
Mississippian: Escabrosa limestone	650
Devonian: Martin Formation	250
Cambrian:	
Abrigo Formation	700
Bolsa quartzite	20–335
Uncomformity	
Upper Precambrian: Apache group	
Dripping Spring quartzite	300
Barnes conglomerate	5
Pioneer shale	300
Scanlan conglomerate	2
Unconformity	
Lower Precambrian: Pinal schist	5000+

The Apache group and overlying Paleozoic formations up to the Horquilla limestone form the northeastern side of the Little Dragoon Mountains and have dips averaging about 30° N. or NE. The structure is complicated by many faults that are not shown on the sketch map. In the vicinity of Johnson the Paleozoic formations dip 20°–45° NE. They are here intensely metamorphosed and contain pyrometasomatic deposits that have yielded about $20,000,000 in copper and zinc.

The Gunnison Hills are part of a tilted fault block in which formations from the upper part of the Abrigo to the Glance conglomerate are exposed, dipping 20°–40° NE. Numerous transverse faults have been omitted from the sketch map. Low-grade metamorphic effects are evident at the north end of the hills but disappear toward the south. Small lead-silver veins and replacement deposits in the metamorphosed area have yielded about $40,000 in metal.

The metamorphism of the Abrigo and Martin formations has been studied in greatest detail. The following are typical sections of these formations in their unmetamorphosed condition.

Section of Abrigo Formation in Little Dragoon Mountains 2 miles west of Johnson

	Feet
Martin Formation	
Fine-grained dolomite	
Abrigo Formation	
Upper member:	
10. White quartzite, coarse-grained at base, fine-grained at top	20
9. Gray dolomitic sandstone weathering brown. Laminated and in part cross-laminated. Top 10 feet dolomite with disseminated granules of quartz	41
8. Interbedded sandy dolomite and dolomitic sandstone in beds up to 2 feet thick	54
7. White quartzite	9
6. Cross-bedded dolomitic sandstone weathering brown	37
Middle member:	
5. Coarsely crystalline gray limestone with many fossil fragments, interbedded with siltstone, fine-grained sandstone, and intraformational conglomerate. Beds 2–12 inches thick	45
4. Reddish-brown calcareous sandstone in beds 1 inch to 3 feet thick	46
3. Gray fine- to medium-grained limestone in 1-inch beds separated by irregular silty and sandy partings up to 2 inches thick that weather in relief	70
2. Gray coarse-grained limestone in 1- to 6-inch beds separated by thin irregular partings that weather in relief. A little intraformational conglomerate. Many thin sandstone beds in lower part	70
Lower member:	
1. Shale, brownish and slightly fissile near base, olive and more fissile near top. Intercalated thin beds of quartzite and tan-weathering dolomite near base. Thin quartzite beds and beds of gray limestone with intraformational conglomerate in upper part	297
Total thickness	689
Bolsa quartzite	
Light-gray to reddish-gray quartzite	

Section of Martin Formation in Little Dragoon Mountains 1½ miles west of Johnson

	Feet
Escabrosa limestone	
Fine-grained dolomite, weathering to smooth surface	
Martin Formation	
7. Red and brown shale and siltstone	32
6. Cream to gray medium-grained dolomite in 1- to 2-foot beds. Many stylolite seams. Top 20 feet darker and probably silty (unit 6A)	98
5. Fine-grained silty dolomite with quartz geodes. *Atrypa* horizon 3 feet thick at base	30
4. Sandy and silty dolomite. Sandy and silty layers and lenses weather reddish and in relief	40

3. Sandstone, reddish brown and "case-hardened" to quartzite on weathered surfaces 16
2. Thin-bedded dolomitic siltstone. Dark gray, weathering reddish brown 20
1. Fine-grained gray dolomite except for basal 6 feet, which is tan and aphanitic. Weathered surface irregular like elephant hide. Three-foot lamprophyre sill near middle 39

Total thickness (excluding lamprophyre) 272

Abrigo Formation

White quartzite 8

TABLE 1.—DISTRIBUTION OF METAMORPHIC MINERALS

Original rock	Metamorphic minerals			
	Zone 1	Zone 2	Zone 3	Zone 4
Dolomite:				
Pure	None	None	None	None
Impure	Chlorite or talc + calcite	Tremolite and calcite	Forsterite, diopside, tremolite, ± calcite	Same as zone 3
Limestone:				
Pure	None	None	None	None
Impure	None?	None?	Tremolite, epidote*	Garnet, diopside, epidote wollastonite, idocrase

*These minerals occur in very minute amounts and are not evident in hand specimen. It is possible that they occur in zones 1 and 2 also.

ZONES OF METAMORPHISM

General Features

The aureole of contact metamorphic rocks is widest and best developed on the northeast side of the quartz monzonite stock (Fig. 1). Wollastonite, garnet, and other relatively high-temperature silicates were formed in the carbonate rocks as far north and east as exposures and underground exploration extend near Johnson. In the northern part of the Gunnison Hills the rocks were locally recrystallized and silicified; the low-temperature minerals—talc and tremolite—have been formed in the Glance conglomerate near State Highway 86.

Northwest of Johnson it is possible to subdivide the metamorphic aureole into zones, each containing one or more metamorphic minerals not found farther from the quartz monzonite. Arranged according to increasing grade, the zones are characterized by: (1) chlorite, (2) tremolite, (3) forsterite and diopside, (4) garnet with local idocrase and wollastonite. Talc, found in the Gunnison Hills but not northwest of Johnson, probably belongs in zone 1 or in a zone between 1 and 2, as it was found farther from exposed quartz monzonite than tremolite; chlorite was not noted in the metamorphosed carbonate rocks of the Gunnison Hills. Important bodies of copper-zinc ore are in zone 4. Small concentrations of lead-silver ore occur in and beyond the limits of zone 1. The distinctive minerals of each zone did not form in every bed but only in those beds having appropriate composition. The general relations are given in Table 1.

The zones cannot be accurately shown on a map without more field and laboratory work than was feasible during this investigation, because they have irregular boundaries and locally contain islands of lower or higher grade. The metalized area near Johnson and the isolated outcrop of rock of Paleozoic age 2⅔ miles southeast of Johnson are almost wholly in zone 4. The northwestern edge of zone 4 is exposed several hundred feet northwest of the Mammoth mine. The other three zones each average about 900 feet in width; the outer boundary of zone 1 is about 3000 feet northwest of the Mammoth mine. The western edge of the outcrop of Glance conglomerate in the Gunnison Hills is in zone 2, and the eastern part is in zone 1.

Excluding ore and certain small-scale phenomena, the succession of metamorphic silicates bordering the stock is best explained by nonad-

ditive thermal metamorphism—that is, by a fixed succession of chemical reactions between original constituents of the rock under the influence of heat supplied from the stock. The reactions that can reasonably be inferred differ in several respects from those postulated for similar rocks in other areas. A brief review of pertinent geological literature is therefore desirable before the metamorphism of different rock types is considered in detail.

Teall (1903) pointed out that silica has a greater chemical affinity for magnesia than for lime, and that therefore magnesium-rich silicates formed first during metamorphism of carbonate rocks and continued to form as long as magnesia and silica were available. This reaction results in dedolomitization.

Harker (1932, p. 17, 79) emphasized that the metamorphic reactions in carbonate rocks release carbon dioxide, and once this kind of reaction starts the carbon dioxide acts as a solvent which causes the reaction to go rapidly to completion if an adequate amount of heat is available (the reactions are endothermic). Thus, advancing metamorphism of carbonate rocks is generally expressed by a series of abrupt changes in the mineral assemblage without gradations like those characteristic of most other kinds of rocks.

Based in part on field data then available, and in part on the concept that metamorphism of carbonate rocks is a progressive decarbonation process, Bowen (1940) deduced that the metamorphism of siliceous limestones and dolomites might exhibit 13 successive reactions or steps resulting in the formation of 10 minerals in the following order: tremolite, forsterite, diopside, periclase, wollastonite, monticellite, akermanite, spurrite, merwinite, and larnite. Later, Tilley (1948) showed that talc precedes tremolite in the metamorphism of siliceous dolomite. Only the quartz-carbonate rocks were considered in these studies. The presence of aluminum, water, iron, and other material commonly present in natural rocks complicates the phase relations by adding components to the system. According to field observations by Eskola (1922, p. 283), magnesium-rich biotite and in places epidote appear in a lower-grade zone than tremolite; and garnet, idocrase, scapolite, and other silicates commonly occur in the diopside zone.

There is no evidence that metamorphism near the Texas Canyon stock went beyond the wollastonite stage (Bowen's step 6), which is generally the highest grade encountered in contact aureoles around intrusives of granitic to granodioritic composition. No field evidence was found to indicate that forsterite (step 2) formed at a lower grade than diopside (step 3), to indicate that the calcite-tremolite assemblage was converted to diopside and forsterite (step 4), or to indicate that periclase (step 5) ever formed in these rocks. Garnet was not strictly isofacial with diopside but followed it at a higher grade.

Metamorphism of Dolomitic Rocks

The dolomitic rocks yielded a variety of products depending on their initial composition and the degree of metamorphism. Pure dolomite merely recrystallized to marble; impure dolomites were transformed to mixtures of silicate and carbonate minerals.

Examples of essentially pure dolomite beds are found in the upper part of the Martin Formation (unit 6 in the section measured 1½ miles west of Johnson) and in several units in the Escabrosa limestone. These beds are recrystallized to dolomite marble in all the metamorphic zones but generally are not otherwise altered. Locally in the higher-grade zones, irregular masses a few feet to a few tens of feet across have been dedolomitized, but these masses are invariably in fractured areas where elements presumably migrated. Some of these rocks contain calcite and the magnesium-rich silicates, tremolite, and forsterite (or serpentine), which probably formed by reaction between the dolomite and silica brought into the rocks by fluids migrating along fractures. Others consist only of calcite; the magnesia of the dolomite has been leached out, perhaps by solutions rich in carbon dioxide, as suggested by Faust and Callaghan (1948, p. 58–60), leaving a residue of calcite. The local and very small-scale alteration of pure dolomite in areas where all the impure dolomite is much silicated is evidence that introduced material played a very minor role in the metamorphic process.

No evidence was found in the Johnson dis-

trict for the partial dissociation of dolomite according to the equation:

$$\underset{\text{dolomite}}{CaMg(CO_3)_2} = \underset{\text{periclase}}{MgO} + \underset{\text{calcite}}{CaCO_3} + \underset{\text{carbon dioxide}}{CO_2}$$

This reaction has taken place in many metamorphic areas (Faust, 1949, p. 795–797). Bowen (1940, p. 246–248) places the reaction fifth in his 13 steps of progressive metamorphism, preceding the reaction of quartz and calcite to form wollastonite—a reaction that probably did take place locally in the Johnson district. Recent experiments by Harker and Tuttle (1956) have shown that, with CO_2 pressures between 5,000 and 40,000 pounds per square inch, calcite and quartz become unstable together and react to form wollastonite and CO_2 at temperatures at least 100° C. and generally about 150° C. below those at which dolomite dissociates to form calcite, periclase, and CO_2. As pressures of 5,000 to 40,000 pounds per square inch are equivalent to the weight of about 4,500 to 36,000 feet of rock, the CO_2 pressure conditions at Johnson were probably within the limits of the experiments.

Impure dolomites are as abundant as pure varieties among the rocks subjected to metamorphism near Johnson. The impurities take several forms. Chert nodules occur in some of the dolomite beds in the Escabrosa, and all ratios of dolomite to detrital quartz or other siliceous matter are found in the Martin Formation and the upper member of the Abrigo Formation. A little sericitic and chloritic material is generally present, and feldspar (most of which is probably authigenic) is abundant in dolomites of the Abrigo Formation.

The essential feature of the metamorphism of all varieties of the impure dolomites is the development of silicates of magnesium, or of magnesium and calcium, such as chlorite, talc, tremolite, forsterite, and diopside. Silicates of calcium are scarce; andesine, epidote, and zoisite were detected at a few places and garnet at one place; sphene, the titanosilicate of calcium, is widespread but sparse; wollastonite and idocrase were not found. The absence or scarcity of these calcium silicates probably reflects the high content of magnesium and relatively low content of aluminum in the unmetamorphosed rock.

The outermost metamorphic zone near Johnson is characterized by chlorite. This mineral is conspicuous in only one stratigraphic unit—the dolomite (unit 1) at the base of the Martin Formation—but traces of chlorite are present in other dolomite beds in the same zone. In unit 1 of the Martin Formation, chlorite is found for roughly 1000 feet northwest from the point where the next silicate, tremolite, was detected. The chlorite occurs in scattered flakes up to 1 mm in diameter, commonly intergrown with quartz. The chlorite is optically positive with very small optic angle, β near 1.584, and birefringence about 0.008. These properties indicate clinochlore, an aluminous variety of chlorite.

The extension of the chlorite zone in one bed suggests that this bed was particularly susceptible to the formation of chlorite. This susceptibility probably was not to the introduction of material, because this is one of the densest and most impermeable beds in the section, but it probably reflects a particularly favorable composition. Possibly the chlorite is not a metamorphic mineral but is recrystallized chlorite from the original rock, but its intergrowth with quartz suggests that it was formed, at least in part, by reaction between dolomite, quartz, and aluminnous matter.

In the Gunnison Hills, talc formed locally in a zone peripheral to the tremolite zone. The occurrences observed are near State Highway 86 near small quartz-galena veins cutting the Glance conglomerate, a formation made up of fragments of sedimentary rocks of Paleozoic age in a sandy matrix, tightly cemented by calcite. Alteration extended as much as 20 feet from the veins but affected only certain pebbles. These pebbles have been altered to a soft white porous material that is conspicuously different from any pebbles in the unaltered rock. Several of the altered pebbles were studied in detail, and all consist of fine-grained calcite and talc in almost equal proportions. X-ray and differential thermal analysis of the talc in the Geological Survey laboratory shows it to be a remarkably pure form of the mineral (G. T. Faust, personal communication).

Most of the pebbles that have been altered are completely replaced, but one cobble was found that had an altered rim and an unaltered core. The core is a limy and siliceous dolomite with an estimated composition of 85 per cent dolomite, 7 per cent calcite, 6 per cent quartz,

and 2 per cent feldspar and unidentified heavy minerals. The rim, like the completely altered pebbles, consists of almost equal amounts of calcite and talc. The alteration evidently involved dedolomitization and partial decarbonation, in accordance with the equation given by Tilley (1948, p. 275):

dolomite *silica* *water* *talc*
$3CaMg(CO_3)_2 + 4SiO_2 + H_2O = H_2Mg_3(SiO_3)_4$

calcite *carbon dioxide*
$+ 3CaCO_3 + 3CO_2$

As the quartz originally present in the cobble is below the stoichiometric proportions in the equation, silica had to be introduced either from the quartzose matrix of the conglomerate or from the solutions that formed the near-by quartz-galena veins. As the talc is associated in space with metalliferous veins, it may have formed at a different time and under different conditions from the metamorphic silicates northwest of Johnson. The assignment to the metamorphic sequence is therefore tentative.

Changes that took place along the outer edge of the tremolite zone (zone 2) near Johnson are well illustrated by a siliceous dolomite bed in the upper member of the Abrigo Formation. Several hundred feet outside the tremolite zone, the bed consists of polygonal grains of dolomite averaging about 1 mm in diameter with 2–10 per cent of quartz in disseminated grains 0.1–0.3 mm in diameter. There are traces of chlorite (optically positive clinochlore) and sericite between the dolomite polygons and a little limonite in disseminated granules and along microscopic seams. About 2200 feet northwest of the Moore mine, quartz is absent, and practically pure tremolite occurs (colorless, α near 1.601, γ near 1.628, Z ∧ C = 19°). The tremolite is more abundant (about 15 per cent in the thin section studied) than the quartz had been. Much of it occurs in scattered aggregates 0.2–0.6 mm in diameter which evidently mark the positions previously occupied by quartz grains. The carbonate has essentially the same texture as in the chlorite zone, but it is more lucid. Its indices of refraction indicate that most of it is dolomite (ω near 1.68), but some is calcite (ω near 1.66). Thus the metamorphism involved partial dedolomitization.

The above facts suggest the following reaction between original constituents of the rock:

dolomite *quartz* *water*
$5CaMg(CO_3)_2 + 8SiO_2 + H_2O$

tremolite *calcite* *carbon dioxide*[1]
$= Ca_2Mg_5(OH)_2(Si_4O_{11})_2 + 3CaCO_3 + 7CO_2$

The field and petrographic evidence shows that the dolomite and silica needed in this reaction

[1] The same result would be obtained indirectly if talc had formed previously, as shown by Tilley (1948, p. 275) by the following equations:

talc *calcite* *tremolite*
$2H_2Mg_3(SiO_3)_4 + 3CaCO_3 = Ca_2Mg_5(OH)_2(Si_4O_{11})_2$

dolomite *water* *carbon dioxide*
$+ CaMg(CO_3)_2 + H_2O + CO_2$

and/or:

talc *calcite* *quartz*
$5H_2Mg_3(SiO_3)_4 + 6CaCO_3 + 4SiO_2$

tremolite *water* *carbon dioxide*
$= 3Ca_2Mg_5(OH)_2(Si_4O_{11})_2 + 2H_2O + 6CO_2$

PLATE 1.—LOWER SERPENTINE MARKER AND BED FROM WHICH DERIVED

FIGURE 1.—Sugary dolomite with granules of quartz, about 20 feet below the top of the Abrigo Formation; 3500 feet west of the Moore mine

FIGURE 2.—Unserpentinized facies of the lower serpentine marker formed by metamorphism of the bed (Pl. 1, fig. 1); natural size. Each original quartz granule is represented by an aggregate of forsterite surrounded by a narrow halo of calcite that has weathered to form a depression. Matrix is dolomite except in upper part of specimen where no dolomite remains.

PLATE 2.—UPPER SERPENTINE MARKER AND BED FROM WHICH DERIVED

FIGURE 1.—Unit 5 of the Martin Formation showing geodes of quartz; 4000 feet west of Moore mine

FIGURE 2.—Upper serpentine marker derived from unit 5 of the Martin Formation, showing metageodes of tremolite; near Mammoth mine. Part of the surface is dark because of a growth of lichens.

FIGURE 1

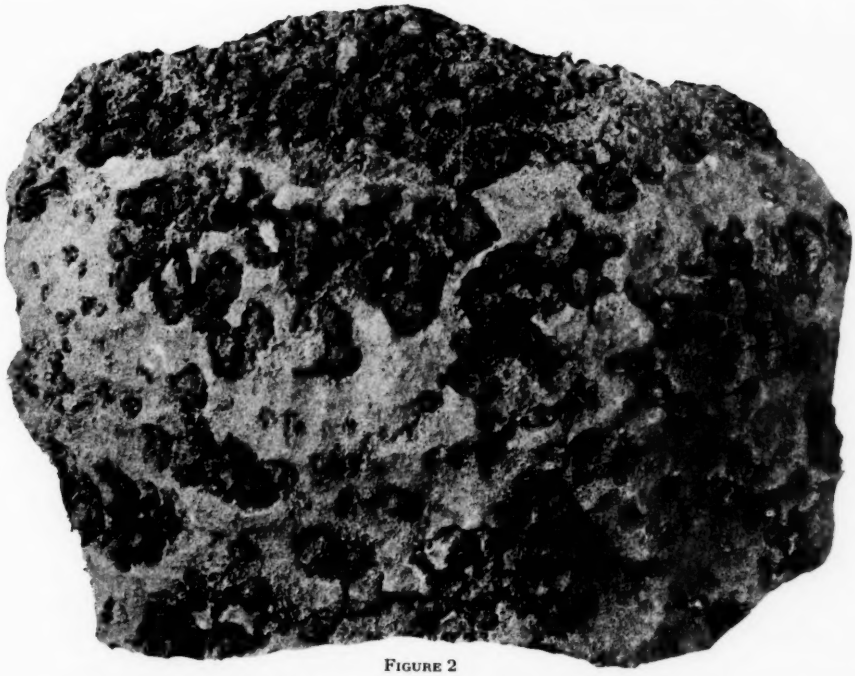

FIGURE 2

LOWER SERPENTINE MARKER AND BED FROM WHICH DERIVED

FIGURE 1

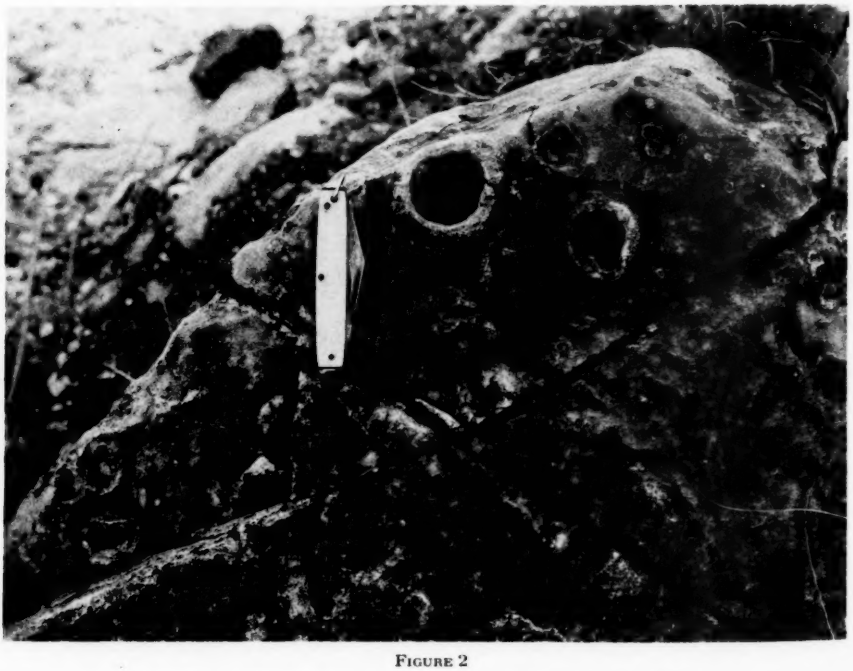

FIGURE 2

UPPER SERPENTINE MARKER AND BED FROM WHICH DERIVED

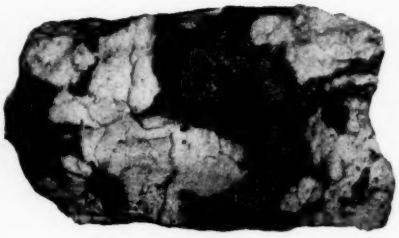

FIGURE 1

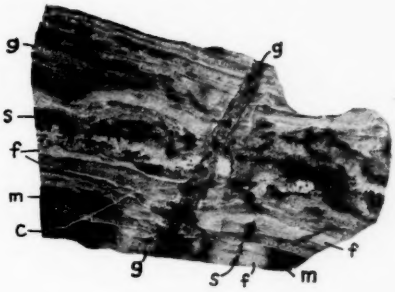

FIGURE 2

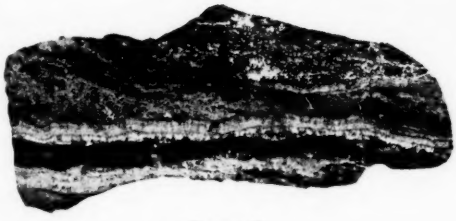

FIGURE 3

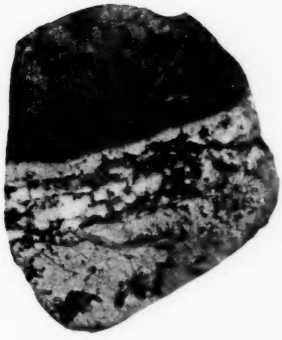

FIGURE 4

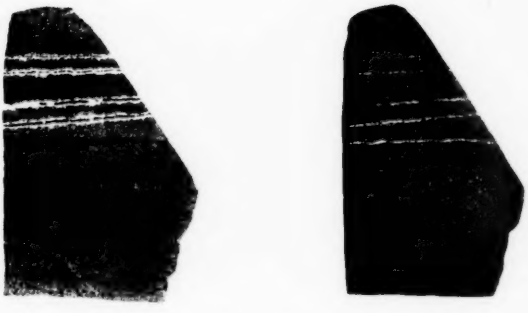

A FIGURE 5 B

HAND SPECIMENS OF METAMORPHOSED ROCKS. X 2/3

were present in the original rock in the approximate proportions required, though rigorous stoichiometric equivalence cannot be demonstrated. The necessary water may have been present as a pore filling or may have come from fluids that were migrating through the rock during the metamorphism. The carbon dioxide was expelled from the rock.

The bed selected to illustrate the reaction characteristic of the tremolite zone was low in quartz and therefore represents a special case. In a rock consisting of dolomite and quartz only, 34.2 per cent of quartz by weight is required to dedolomitize the rock completely in forming tremolite by the equation given. If the metamorphism is nonadditive except for water, the mineral assemblages will be tremolite-calcite-dolomite, tremolite-calcite, or tremolite-calcite-quartz, depending on whether the quartz-dolomite ratio in the original rock is below, at, or above the critical amount of 34.2/65.8. Other beds of the Abrigo and Martin within the tremolite zone provide examples of the other two mineral assemblages if minor and nonreactive constituents are disregarded. The tremolite in each assemblage has optical properties near those of the pure mineral.

The course of metamorphism beyond the tremolite stage is determined by the mineral assemblage in the tremolite zone. It is necessary therefore to consider each of the three tremolite-zone assemblages separately.

The tremolite-calcite-dolomite assemblage, formed from beds low in silica, is modified at a higher grade (zone 3) by reaction of tremolite with the remaining dolomite as follows:

tremolite		*dolomite*		*forsterite*		*calcite*		*carbon dioxide*		*water*
$Ca_2Mg_5(OH)_2(Si_4O_{11})_2$	+	$11CaMg(CO_3)_2$	=	$8Mg_2SiO_4$	+	$13CaCO_3$	+	$9CO_2$	+	H_2O

To complete dedolomitization of a pure quartz-dolomite rock at this stage requires 14.0 per cent quartz by weight in the original rock; the three mineral assemblages determined by this critical ratio are forsterite-calcite-dolomite, forsterite-calcite, and forsterite-tremolite-calcite. The first two assemblages are found near Johnson, but the third has not been recognized.

An excellent example to illustrate the forsterite reaction is provided by a conspicuous bed near Johnson known as the lower serpentine marker. This bed is near the top of the Abrigo Formation and is about 10 feet thick. In its unmetamorphosed condition it consists of sugary dolomite that is laminated, in part cross-laminated, and contains sparsely disseminated granules of quartz (Pl. 1, fig. 1). In zones 3 and 4 the quartz granules are represented by small knots of forsterite or more commonly its alteration product serpentine; each knot is surrounded by a narrow rim of calcite (Pl. 1, fig.2). Where the knots are close together, as in the upper part of the specimen, the rock is dedolo-

PLATE 3.—HAND SPECIMENS OF METAMORPHOSED ROCKS. ×⅔

FIGURE 1.—Grossularite with rims of wollastonite (darker in photograph) in calcite marble of the Horquilla Formation southwest of Peabody mine

FIGURE 2.—Partly garnetized shale from dump of Mammoth mine. Bedding planes dip gently to right. Two parallel veinlets dip steeply to left. Aphanitic dark-gray areas are micaceous hornfels (m). Aphanitic white rims surrounding these areas are almost pure potassium feldspar (f). Granular gray material is an aggregate (g) of garnet, diopside, epidote, and some potassium feldspar. Black grains are chalcopyrite and sphalerite (s). White transecting seam is crack filled with supergene calcite (c).

FIGURE 3.—Banded vein cutting garnetite from dump of Republic mine. Vein consists, from walls inward, of quartz with comb structure (light gray), potassium feldspar (white), and central quartz containing pyrite (light gray), limonite, chalcopyrite, and chalcocite (all black).

FIGURE 4.—Vein cutting garnetite near 700 station ore body, 650 level of Republic mine. Vein consists of microcline (light gray) veined and replaced by quartz (gray), calcite (white,) sulfides (black), and fluorite (not distinguishable). Garnetite near vein has been replaced by a dark aggregate of potassium feldspar, quartz, calcite, sulfides, green mica, and chlorite.

FIGURE 5.—Polished surface of mineralized lamprophyre from dump of Peabody mine. A.—Chalcopyrite seams (black) cut upper part of specimen. White alteration product next to four upper seams is diopside. B.—Same surface under direct reflection to show dissemination of chalcopyrite (white). Small black spots are depressions in polished surface; many are caused by concentrations of chlorite.

mitized and consists of forsterite and calcite only. In the outcrop the knots are strung out in lines that reveal the original lamination and cross-lamination, as the quartz granules do in the unmetamorphosed rock. The forsterite has α near 1.635 and γ near 1.671 and is therefore practically pure magnesium silicate.

It is assumed above that the original quartz and dolomite first reacted to form tremolite, which was then converted to forsterite by further reaction. This sequence would be expected in the ideal case of advancing metamorphism and is in accord with the gross field relationships; but it cannot be proved by the petrographic features of the final product. Some of the forsterite bodies are single crystals, but most are aggregates of several roughly equidimensional anhedrons. Irregular inclusions of calcite are common. The forsterite is partly serpentinized in every thin section examined and is completely serpentinized in most specimens. Other late minerals present in small amounts are tremolite and an almost isotropic chlorite that has replaced an acicular mineral in the groundmass. These retrogressive minerals probably formed during the metasomatic stage.

The quantitative relations of the forsterite reaction have been explored mathematically on the assumption that there was no change in composition except loss of carbon dioxide. A sphere of quartz 1 cm in diameter embedded in dolomite should yield a sphere of forsterite 1.24 cm in diameter surrounded by a halo of calcite and empty space 0.32 cm thick. If the empty space were destroyed by recrystallization of the carbonates, as would be expected under the temperature and pressure conditions of metamorphism, the calcite halo would be 0.25 cm thick. Thus the hypothesis of simple thermal metamorphism leads to the prediction that a rock like that shown in Figure 1 of Plate 1 will yield a rock like that shown in Figure 2 of Plate 1, that the diameter of each forsterite knot in the latter rock will be a quarter larger than the original quartz granule, and that the thickness of each calcite halo will be a fifth of the diameter of the forsterite knot that it surrounds. The facts agree with this prediction within the limits of measurement. The quantitative relations will be the same whether tremolite was formed as an intermediate product, as here assumed, or whether forsterite formed directly according to the reaction:

dolomite *quartz* *forsterite* *calcite*

$$2MgCa(CO_3)_2 + SiO_2 = Mg_2SiO_4 + 2CaCO_3$$

carbon dioxide

$$+ 2CO_2$$

It requires 34.2 per cent silica by weight to dedolomitize a pure quartz-dolomite rock at the tremolite stage, with neither dolomite nor quartz left over. Natural rocks with this composition are very rare, but the bed in unit 5 of the Martin Formation shown in Figure 1 of Plate 2 almost fulfills the requirement. This rock is fine-grained dolomite containing about 35 per cent quartz in the form of geodes and disseminated silt-sized particles. It was first converted to a calcite-tremolite rock containing no dolomite or quartz (zone 2). The reaction of tremolite and dolomite to form forsterite could not take place, and the bed remained in perfect equilibrium (zones 3 and 4), while near-by beds low in silica became unstable and had their tremolite converted to forsterite. In the vicinity of the mines the bed is known as the upper serpentine marker (Pl. 2, fig. 2), and in its least altered form consists of metageodes of tremolite fibers in a groundmass of fine-grained calcite with disseminated tremolite. The groundmass tremolite is generally altered to light-green serpentine, and in some specimens all the tremolite has been serpentinized.

According to Bowen (1940, p. 245) the tremolite-calcite assemblage becomes unstable at a higher temperature (his step 4), and the following reaction takes place:

tremolite *calcite*

$$3Ca_2Mg_5(OH)_2(Si_4O_{11})_2 + 5CaCO_3$$

diopside *forsterite*

$$= 11CaMg(SiO_3)_2 + 2Mg_2SiO_4$$

carbon dioxide *water*

$$+ 5CO_2 + 3H_2O$$

No evidence for this reaction was recognized near Johnson.

The tremolite-calcite-quartz assemblage, formed from rocks containing more than enough quartz to dedolomitize the rock in the tremolite zone (that is, more than 34.2 per cent by weight in a pure quartz-dolomite rock), was unstable

n the higher-temperature zones (zones 3 and 4), here the following reaction took place:

$$\underset{\text{tremolite}}{Ca_2Mg_5(OH)_2(Si_4O_{11})_2} + \underset{\text{calcite}}{3CaCO_3} + \underset{\text{quartz}}{2SiO_2} = \underset{\text{diopside}}{5CaMg(SiO_3)_2} + \underset{\text{carbon dioxide}}{3CO_2} + \underset{\text{water}}{H_2O}$$

t requires 39.4 per cent of quartz by weight to convert a pure quartz-dolomite rock to a pure liopside rock at this stage. If there is more than 9.4 per cent quartz some will remain with the liopside in the final rock. If there is between 4.2 and 39.4 per cent the assemblage will be liopside-tremolite-calcite.

These mineral assemblages (disregarding ninor and nonreactive constitutents) character- ze almost all the upper member of the Abrigo Formation and much of the middle part of the Martin Formation, from the alluvium contact outheast of Johnson to a point about 1500 feet orthwest of the Moore mine, where the tremo- ite zone starts. The rocks are known locally as white tactite, a granular rock which is generally greenish white on fresh fracture and light rusty brown on weathered surfaces. The diopside in these rocks ranges in optical properties from pure diopside to diopside$_{85}$ hedenbergite$_{15}$; the pure variety occurs in siliceous dolomite, and the impure occurs in hornstones derived from dolomitic shale. A little sphene, apatite, and pyrite and variable quantities of potassium feldspar are common. The principal constituents are generally slightly replaced by calcite, tremolite, chlorite, and sulfides, assigned to the metasomatic stage.

The reaction producing diopside from calcite, tremolite, and quartz involves replacement of tremolite by diopside. Petrographic evidence of this replacement was detected near the boundary of the tremolite zone, where part of the diopside is in typical stubby crystals, and part is in slender needles which are probably pseudomorphous after tremolite. This texture is not evident near Johnson, presumably because it was destroyed by recrystallization. A common rock type in this area consists of euhedral to subhedral crystals of diopside about 0.25 mm in diameter in a groundmass of quartz and potassium feldspar. The quartz is wholly lacking in crystal form and is commonly in relatively large grains that include several diopside crystals. In many specimens from the Abrigo Formation, potassium feldspar makes up 20 to 25 per cent and in a few specimens as much as 50 per cent of the rock by volume. The feldspar grains have the same size and textural relations as the quartz grains but have developed crystal faces against the quartz.

The high potassium feldspar content of the white tactites of the Abrigo Formation was first taken as an indication of significant potassium metasomatism. Later it was discovered that the formation contains large amounts of this mineral in all parts of the Little Dragoon Mountains and near-by ranges; some is detrital, but apparently most is authigenic. Most of the feldspar in the metamorphosed facies probably is this feldspar that recrystallized without participating in the metamorphic reactions; some was probably formed by reaction of sericitic material and quartz with potassium leached from garnetized limestones below.

Sedimentary textures and structures disappear gradually in the white tactites. For example, sandstones with only a small quantity of dolomite cement tend to retain the sandy texture, even though the rock is recrystallized and small crystals of tremolite (zone 2) or even diopside (zones 3 and 4) occur in place of the interstitial dolomite. The larger sedimentary features, like peculiarities of bedding and distribution of sand, are retained to an even greater extent. Where metamorphism was particularly intense, all but the largest sedimentary characteristics are lost, and there was a vigorous interchange of material between beds, so that a general uniformity in texture and mineral composition results. In this way carbonate beds as much as 10 feet thick intercalated between siliceous beds (like the lower serpentine marker) were obliterated locally by incorporation into the white tactite.

If all the facts connected with the metamorphism of the dolomitic rocks are considered, the only reasonable conclusion is that essentially nonadditive metamorphism took place. Pure dolomite generally lacks new minerals even near fissures, but reactions to form silicates took place around chert nodules in otherwise pure dolomite. Impure dolomites are invariably and extensively silicated above the chlorite zone. Some relatively thin beds may be traced for long distances in their metamorphosed state by dis-

tinctive lithology. If ore and late-stage retrogressive minerals are disregarded, the mineral assemblages predicted for any composition by means of a series of nonadditive reactions generally occur in beds of that composition. Certain peculiar facts of mineral association, like the occurrence in zones 3 and 4 of calcite-tremolite, calcite-forsterite, and diopside rocks close to one another are explained by nonadditive metamorphism and do not require local lack of equilibrium or any other special conditions.

Metamorphism of Calcareous Rocks

Rocks in which the carbonate constituent is calcite are relatively inert compared with the dolomitic rocks. In the outer three zones near Johnson, the only metamorphic effects noted in the calcareous rocks are simple recrystallization and the appearance of traces of tremolite and epidote. In the highest-grade zone, much garnet, diopside, epidote, wollastonite, and idocrase were formed locally, but silication was erratic, and some migration of material commonly took place. Although the metamorphic products are generally very different from those described above, a moderately large block of impure calcareous rock in the Republic mine has been altered to white tactite that is indistinguishable from that derived from siliceous dolomite.

Pure limestone beds in the Escabrosa, Black Prince, and Horquilla formations are recrystallized to calcite marble but otherwise unaltered except very locally. In the highest-grade zone (zone 4), traces of garnet have been detected along fault zones; at a few places southwest of the Peabody mine calcite marble has been replaced on a small scale by wollastonite and grossularite (Pl. 3, fig. 1). Grossularite forms the center of the silicate masses, and wollastonite forms the rims. Most of the silicate masses are localized along cracks, and therefore they are evidently the product of reactions of the limestone with silicon and aluminum introduced in solution. The distribution of the silicates indicates that silicon was more mobile than aluminum and ran ahead of it to greater distances from the feeding fissure. Specks of chalcopyrite partly replaced by chalcocite are distributed sparsely in the grossularite, more abundantly in the wollastonite, and at a few places in the adjacent marble.

Numerous chert nodules in the calcite marbles of the Escabrosa were examined to determine whether quartz and calcite in juxtaposition had become unstable and had reacted to form wollastonite according to the familiar reaction (Bowen's step 6):

calcite		*quartz*		*wollastonite*		*carbon dioxide*
$CaCO_3$	+	SiO_2	=	$CaSiO_3$	+	CO_2

Most of the chert nodules examined display no reaction rim of any kind, but some in zone 4 have fibrous rims several inches wide. All the rims studied microscopically consist of fine-grained quartz and calcite that appear to have replaced a fibrous mineral. As rims of this kind were not noted around chert nodules in other areas, wollastonite was probably formed by the reaction given and was altered later to quartz and calcite, the original minerals.

The most profoundly altered of the calcareous rocks are in the middle or ore-bearing member of the Abrigo Formation. The unmetamorphosed facies of this member contains calcite, quartz, potassium feldspar, sericite, chlorite, and clay minerals in various proportions. Most of the calcite is segregated from the other minerals in the form of thin limestone beds and lenses that alternate with layers of shale and calcareous sandstone. On metamorphism, these beds yield pale-yellowish-brown garnet as the most abundant and widespread mineral. The garnet is believed to be grossularite because of its color, index of refraction (1.74 to 1.78), and mode of occurrence. A little iron, manganese, and perhaps other elements are present in the mineral, at least locally.

The main ore-bearing beds (unit 5) and the generally similar beds (units 2 and 3) at the base of the middle member consist of thin beds and lenses of almost pure limestone alternating with thin layers of shale and siltstone. The argillaceous layers were sensitive to metamorphism and have been converted to grayish-olive hornfels even beyond the limits of the chlorite zone (zone 1) in the carbonate beds. In zones 3 and 4 the hornfels consists of very fine-grained dark mica (which gives the color to the rock) and feldspar, with variable and generally small

amounts of quartz, sphene, epidote, and apatite. The associated limestone beds are recrystallized and contain scarce epidote and tremolite for some distance from zone 4.

At many places within zone 4 the limestone and hornfels pass into garnetite. Garnet formed first in the limestone portion and at the same time mica disappeared from the immediately adjacent hornfels; its place was taken by fine-grained orthoclase (Pl. 3, fig. 2). The resulting rock consists of a granular portion containing garnet separated from an aphanitic dark portion by a light-colored band of aphanitic orthoclase. The rock, which is remarkably similar to the main variety of hornfels at the Ophir Hill Consolidated mine in the Ophir district, Utah, as described and pictured by Gilluly (1932, p. 105, Pl. 21A), probably formed by a reaction between the limestone and hornfels that can be expressed in simplified form as follows:

muscovite + *calcite* + *quartz*
$H_2KAl_3(SiO_4)_3 + 3CaCO_3 + 3SiO_2$

= *grossularite* + *orthoclase* + *carbon dioxide*
$Ca_3Al_2(SiO_4)_3 + KAlSi_3O_8 + 3CO_2$

+ *water*
H_2O[2]

The hornfels has lost aluminum, silicon, and ferromagnesian elements; these constituents have been added to the limestone portion to make lime silicates. The specimen photographed (Pl. 3, fig. 2) is somewhat unusual in two respects: (1) copper and zinc sulfides occurring in the lime-silicate portions are not in all rocks of this type and thus are not an essential part of the alteration; (2) transecting veins of lime silicates are very rare.

With increasing alteration, the garnetite and orthoclase zones expand at the expense of the dark hornfels until the latter is destroyed. The garnetite continues to expand at the expense of the orthoclase zone until that also is destroyed and the rock becomes nearly uniform garnetite. Some orthoclase remains as an interstitial mineral in the garnetite but in much smaller amounts. The relations suggest that, with rising temperature, a point was reached at which orthoclase and calcite, or orthoclase, calcite, and epidote became unstable when together and reacted to form garnet, as illustrated by the following equations:

orthoclase + *calcite* = *grossularite*
$2KAlSi_3O_8 + 3CaCO_3 = Ca_3Al_2(SiO_4)_3$

+ *quartz* + *carbon dioxide* + *potassium oxide*
$+ 3SiO_2 + 3CO_2 + K_2O$

orthoclase + *epidote* + *calcite*
$2KAlSi_3O_8 + 2HCa_2(Al,Fe)_3Si_3O_{13} + 8CaCO_3$

= *grossularite* + *potassium oxide* + *water*
$4Ca_3(Al,Fe)_2(SiO_4)_3 + K_2O + H_2O$

+ *carbon dioxide*
$+ 8CO_2$

Both these inferred reactions release potassium. The relative scarcity of potassium-bearing minerals in the garnetite indicates that potassium was leached and removed from the rock with carbon dioxide. Some potassium probably was added to the overlying white tactites and hornstones to form orthoclase. Whether potassium was transported as carbonate, hydroxide, or in some other form is not known.

Defeldspathization by garnetization is illustrated in the lower part of Figure 2 of Plate 3, where garnet has replaced orthoclase for a width of a quarter of an inch adjacent to the larger vein. Evidently fluids moving along the vein fissure added calcium and removed potassium from the adjacent rock. The calcium may not have been carried more than a few inches from the adjacent limestone bed; the same process took place with no introduction of calcium, where the rock contained the proper proportion of material.

The main ore-bearing beds are underlain by relatively siliceous beds (unit 4) that outside the aureole of metamorphic rocks consist of fine-grained (about 0.1 mm) feldspathic sandstone with almost as much feldspar as quartz. Most of the interstitial matter, which is variable in quantity but averages about 25 per cent, is calcite but includes chloritic and sericitic material and opaque minerals. After moderate metamorphism, such as that which has taken place southwest of the Mammoth mine (outer edge of zone 4), the rock retains a sandy texture and original structures like lamination and cross-lamination; but notable changes are evident in

[2] The mica is assumed to be muscovite. As both "sericite" and "biotite" seem to be present in the rock, some magnesium and iron are involved in the natural reaction.

thin section. The quartz and feldspar have been recrystallized, although the increase in grain size is slight. Most of the interstitial calcite has disappeared and has been replaced by diopside and epidote. These new silicates, which probably represent reactions between calcite, quartz, sericite, and chlorite, are interstitial like the original carbonate but are slightly aggregated in tiny nests. Apatite and sphene are conspicuous accessory minerals.

After more intense metamorphism such as that which has affected most of the mining area, the sandy texture, lamination, and cross-lamination are no longer evident, and garnet appears. Most garnetite of this origin is indistinguishable in hand specimens or outcrops from that derived from less siliceous beds. Thin sections reveal fine- to medium-grained euhedral garnet, diopside, sphene, and apatite in a groundmass of large (1–4 mm) poikiloblastic anhedra of quartz. Traces of potassium feldspar occur in the quartz, but most of the feldspar has disappeared. Thus garnetization and defeldspathization occurred together, as indicated by reactions previously suggested.

Locally on the 700 level of the Republic mine and at other places where metamorphism was intense, much wollastonite and idocrase appear in the garnetites derived from both high-silica and low-silica beds. Occurrences are probably most common in the high-silica beds. The wollastonite-idocrase rocks probably represent a higher-temperature facies than the garnetite. The way some occurrences are related to fissures suggests that local metasomatism was involved; calcium was introduced into the siliceous beds, and silicon into the calcareous beds.

Almost every thin section of the garnetite (and the local wollastonite-idocrase facies) shows some late-stage effects, including partial replacement by calcite, chlorite, tremolite, quartz, and ore minerals.

Local metasomatism that appears to have been contemporaneous with the general metamorphism is evident in the Republic mine, where impure limestones of units 3, 4, and 5 of the Abrigo Formation were altered to white tactite instead of garnetite in a chimneylike mass 100–200 feet in diameter beneath the Republic fault (Fig. 2). The rock is indistinguishable in hand specimen and in thin section from siliceous and feldspathic white tactites derived from the upper dolomitic member. A calcium-magnesium ratio near 1:1 is indicated by the abundance of diopside and the absence of calcite and calcium silicates. Thus there was a relative gain in magnesium and probably silicon. The Republic fault probably influenced the abnormal alteration. The lower shale member of the formation is garnetized in a similar position with respect to the same fault. As the abnormally metamorphosed rock is in each case the same as that characteristic of the overlying member, leaching and downward transportation of material might be postulated; however, magnesium could have been leached during garnetization of the lower member and carried upward beneath the fault, which acted as an impervious barrier.

Metamorphism of Quartzite

Quartzite, as distinguished from dolomitic and calcareous sandstones discussed above, makes up the Bolsa quartzite and two units in the overlying Abrigo Formation—unit 10 at the top of the formation and unit 7 about 100 feet below the top. The bolsa, which is the thickest of these three units, is not appreciably affected by metamorphism. The others, thinner and intercalated between dolomitic rocks, have been much altered.

Unit 10 of the Abrigo as exposed about 1500 feet southeast of the Republic mine is essentially unaltered quartzite about 20 feet thick, near the maximum for the unit. Diamond drilling near by by the U.S. Bureau of Mines has revealed that the quartzite is partly replaced at depth by diopside and that the diopside penetrates irregularly inward from both contacts. The alteration seems to be due to reaction between the quartzite and adjacent beds of dolomite, calcium and magnesium having moved in one direction and silicon in the other. The unit is rarely recognized in the Republic-Mammoth mine area, presumably because this kind of alteration has affected the entire unit and has made it indistinguishable from the white tactites below.

Unit 7 of the Abrigo, which is commonly 2–4 feet thick and nowhere more than 9 feet thick, disappears as a distinguishable bed in most parts of zones 3 and 4, probably because of alteration like that of unit 10. The bed is distinguishable at a few places, notably in a conspic-

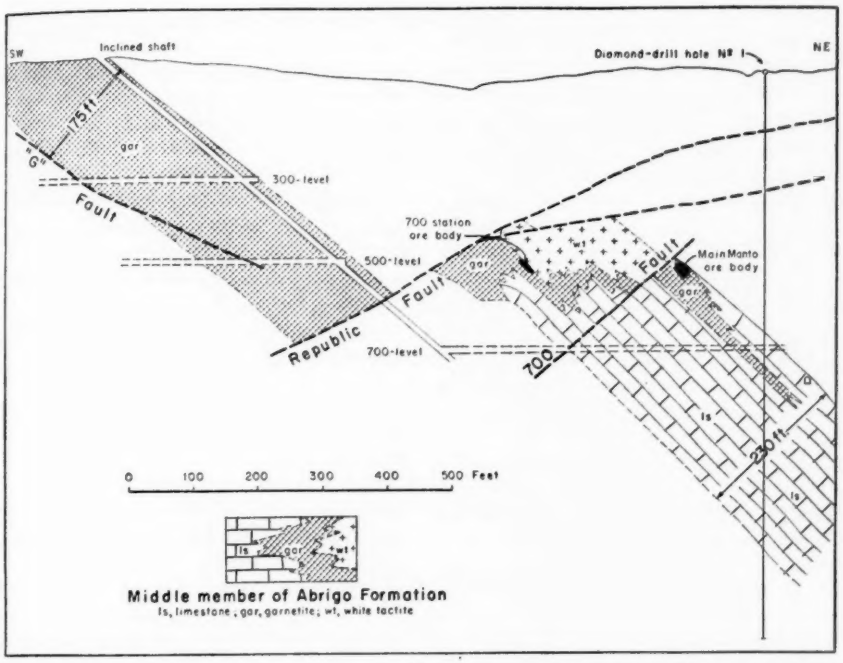

FIGURE 2.—CROSS SECTION THROUGH REPUBLIC MINE SHOWING THINNING OF MIDDLE MEMBER OF ABRIGO FORMATION WITH GARNETIZATION

uous outcrop near the Dragoon Road 1150 feet southeast of the Keystone mine.

Metamorphism of Shale

The shales that were metamorphosed near Johnson are of two general types. Those of the Martin Formation contain much dolomite. Those of the lower and middle members of the Abrigo Formation are essentially carbonate free but do contain intercalated beds and lenses of limestone. The metamorphism of these two types is very different.

The dolomitic shale beds of the Martin Formation (units 2 and 7) have yielded hard, light-gray porcellanite characterized by conchoidal fracture and a little disseminated pyrite. An aphanitic to very fine-granular texture is remarkably persistent, even though the minerals in the rock are not notably different from those of the white tactites. The distinctive mineral is tremolite in a medium grade of metamorphism (zone 2) and diopside (with tremolite) at a higher grade (zones 3 and 4). There is much interstitial potassium feldspar and some quartz. All thin sections show a little sphene, and some contain minor amounts of epidote, andesine, and chlorite.

The carbonate-free shales of the middle and lower members of the Abrigo Formation are hardened and darkened far from the quartz monzonite. The low-grade modifications have not been studied in detail. In zones 3 and 4 the typical rock is dark-greenish-gray or brown hornfels consisting of much dark mica (which gives the color to the rock) and potassium feldspar, with small amounts of quartz, sphene, epidote, and apatite. The modifications of this type of rock where limestone interbeds are abundant have been discussed in connection with the calcareous rocks. Where limestone interbeds are scarce, they have localized bands of essentially pure epidote (instead of garnet) at places in the garnet zone. This seems to be an expression of the aluminum-rich and iron-rich environment. Epidote contains a higher ratio of Al_2O_3 (or Fe_2O_3) to lime and silica than other calcium-aluminum silicates of the district.

	Al_2O_3:CaO	Al_2O_3:SiO_2
Epidote	3:4	2:3
Grossularite	1:3	1:3
Idocrase	1:4	1:4

The formation of epidote is favored by the shale environment, and the formation of garnet and idocrase is limited by the scarcity of available calcium and silicon.

Shales of the lower member of the Abrigo Formation have been converted to garnetite at one place near the Republic mine. The area affected is several hundred feet in diameter and is located 1200 feet northwest of the shaft collar immediately north of and structurally below the Republic fault. The garnet rock, like the white tactite in limestone stratigraphically above it, is close to the Republic fault; fluids moving along the fault probably were responsible for the abnormal alterations. The shale gained calcium and lost other bases; the limestone had a relative gain in magnesium. This local metasomatism was probably contemporaneous with the widespread thermal metamorphism.

Metasomatic Effects

Johnson Area

Most of the data presented above indicate reactions between original constituents of the rock, with migration of material (except carbon dioxide) limited to a few feet. The principal exceptions to this generalization are evident loss of potassium from some of the impure calcareous rocks, local development of small quantities of silicate and sulfide minerals in pure carbonate beds, and local abnormal alteration of impure calcareous and argillaceous units near the Republic fault. These metasomatic effects are most evident near fractures that provided channels for the movement of solutions. There is evidence, moreover, that metasomatism increased near the close of the metamorphic stage. The early-formed pale-yellowish-brown grossularite crystals commonly have thin reddish-brown rims where in contact with interstitial quartz or calcite. These late rims have a higher index of refraction and according to Baker (1953, p. 1274) contain a relatively high proportion of manganese. Thus late manganese metasomatism is indicated. Late metasomatism may be indicated by the diopside also, but this is less clear. Most of the diopside is almost colorless and has optical properties near those of the pure calcium-magnesium silicate. In several ore specimens the diopside is pale gray or brownish green and has indices of refraction equivalent to those of diopside containing 12 to 22 per cent of hedenbergite by weight.

The most obvious and important metasomatic effect is, of course, the copper-zinc ore bodies near Johnson. The sulfur and ore metals in these bodies had a distant source, presumably in the magma that was responsible for the entire igneous metamorphism. Some ore minerals were introduced during formation of the high-temperature metamorphic silicates, but most of the metalization took place later and at lower temperatures than the general metamorphism of the host rock. The ore minerals—which include chalcopyrite, sphalerite, pyrite, scheelite, locally bornite and a little magnetite and molybdenite—are intimately associated with small amounts of calcite, ferroan tremolite, chlorite, and in places quartz and traces of fluorite and biotite. These minerals are generally interstitial to the garnet, diopside, wollastonite, and other high-temperature minerals of the metamorphic stage but they have also veined and replaced these older minerals. Some thin and polished sections show that the early metamorphic minerals were bent and broken before replacement occurred. Further fracturing during metalization is indicated by complex intersection relationships of microscopic veins containing ore and late gangue minerals.

The ore bodies, which to the end of 1954 had yielded about $20,000,000 in copper and zinc, are lenses and pipes formed by replacement of certain beds along faults or other channelways. The known ore is in metamorphic zone 4, and most of it is in garnetized beds at the top of the middle member of the Abrigo Formation (unit 5 and in places unit 4).[3] Some, but not all, of the ore bodies are at or near the limestone side of garnetite masses—that is, where garnetite passes laterally into ungarnetized rock. The ore is generally banded parallel to the beds, for sulfides and associated minerals are generally con-

[3] Small ore bodies have been mined from other stratigraphic units, notably at the Peabody mine, where an unknown but important amount of copper ore was taken from the Horquilla limestone many years ago.

centrated in layers 2–12 inches thick separated by almost barren garnetite layers of about the same thickness. The barren layers are the metamorphosed equivalent of clastic beds, for they pass locally into hornfels of the kind formed from these beds. Baker (1953, p. 1275) has noted that ". . . at the edges of ore bodies sulphide bands often grade out into ungarnetized limestone, while the intervening garnetite bands continue several feet or yards beyond the ends of the sulphide bands." This distribution confirms that the sulfide-rich layers represent original beds of limestone and suggested to Baker that these beds were not thoroughly garnetized. Interstitial calcite remaining in the garnet rock probably localized the ore.

The gangue minerals formed during metalization seem to be richer in iron than those formed during the progressive metamorphism but otherwise suggest reversal of reactions that took place during metamorphism. All the reactions of the metamorphic stage are reversible. They proceed in one direction when the temperature rises into the stability field of the high-temperature mineral assemblage. When the temperature falls into the stability field of the lower-temperature assemblage, the reaction must be reversed, provided carbon dioxide is available under sufficient vapor pressure for the temperature (Bowen, 1940, p. 265–266). Lack of carbon dioxide at the requisite pressure is the main reason why the reactions are seldom reversed in igneous contact zones.

Late-stage retrogressive effects are not confined to the immediate vicinity of ore bodies but are found in small amounts in almost every thin section of the silicated rocks. The most common alteration products are calcite, quartz, ferroan tremolite, and a pale-green slightly pleochroic chlorite. These minerals commonly are accompanied by small amounts of copper and zinc sulfides. Alteration either pervaded the rock along grain boundaries and cracks or was concentrated in tiny spots. The latter habit is particularly characteristic of the white tactites, which are marked in many drill cores by scattered gray spots several millimeters in diameter consisting of calcite, tremolite, sulfides, and in some cases quartz, chlorite, and fluorite.

Northeastward-trending faults and fissures cutting the metamorphic rock are commonly marked by quartz veins generally less than 1 foot thick but rarely as much as 2 or 3 feet thick. Almost all these veins were formed by filling of open fissures rather than by replacement of the host rock, for they have smooth matching walls and display symmetrical banding and comb structure (Pl. 3, fig. 3). Quartz of several generations is generally the most abundant mineral. Potassium feldspar is very common, as are small amounts of fluorite, calcite, pyrite, chalcopyrite, and bornite. Sphalerite, galena, argentiferous tetrahedrite, and scheelite were found at several places; near the surface supergene limonite, copper carbonates, chalcocite, and wulfenite occur. The veins contain abundant hypogene sulfides only where they cut bedded replacement ore bodies and near such intersections. As they contain galena and tetrahedrite, which are not present in the replacement bodies, they are presumably younger and therefore not feeders.

A vein that cuts garnetite near an ore body in the Republic mine is shown in Figure 4 of Plate 3. The vein shows early microcline veined and replaced by quartz and calcite containing fluorite, chalcopyrite, bornite, and traces of pyrite and galena. The garnetite immediately adjacent to the vein has been replaced by potassium feldspar (approximately 50 per cent), quartz, calcite, and sulfides. Green mica and chlorite are concentrated in a band between the potassium feldspar and the garnet. Except for the introduction of abundant sulfides, the reactions suggest reversal of the reactions that formed garnet.

Hornfels derived from shales of the lower member of the Abrigo Formation have been argillized on the 300 and 500 levels of the Republic mine, south of and structurally above the Republic fault. The argillized rock is soft and either white or stained brown by iron oxides. It contains numerous thin seams of quartz and limonite parallel to the beds. Some copper sulfates occur in or near the seams. The intimate association of argillized rock with the seams, which evidently were once quartz-sulfide veinlets, suggests origin during the ore-forming period. Possibly the argillization was later than the metalization and was due to leaching by acid waters formed by supergene oxidation of the sulfides.

Evidence bearing on the age of the metalization in the district is provided by specimens of metalized lamprophyre from the dump of the

Peabody mine. No lamprophyre dikes are now to be seen in the Johnson mining area, but Scott (1916, p. 141) states that one of the main ore bodies at the Peabody mine was "in a contact vein between lime and diabase." The mine workings that show the "diabase" are not now accessible, but fragments from the dump indicate that it is lamprophyre, showing remnants of brown hornblende and lath-shaped plagioclase with the same properties and textural relationships as in dikes that cut the quartz monzonite of the Texas Canyon stock and have chilled borders against it.

Some features of the altered lamprophyre are shown in Figure 5 of Plate 3. The lamprophyre contains several per cent by volume of chalcopyrite, which is interstitial to and corrodes the silicates. Calcite, which is present in all other specimens of the lamprophyre studied, has been replaced by clinozoisite, fluorite, and tremolite. The rock is cut by seams of chalcopyrite, associated with sphalerite, potassium feldspar, oligoclase, diopside, and fluorite. These seams are bordered by bands of intensely altered lamprophyre, about a millimeter wide, in which the hornblende and feldspar of the lamprophyre have been converted to diopside. In the specimen photographed, the diopside next to the four upper seams is white. The other seam is also bordered by diopside which looks the same in thin section but is inconspicuous in the hand specimen. The alteration of the lamprophyre at the Peabody mine is of the pyrometasomatic type, like that in the adjacent limestone. The association of metallic sulfides with diopside unaffected by retrogressive minerals suggests an origin at relatively high temperature, presumably early in the metalization process.

If the lamprophyre at the Peabody mine is the same age as the dikes in the quartz monzonite—which seems probable—then the metalization at Johnson took place after the quartz monzonite now exposed had solidified, cooled, and been fractured and injected by lamprophyre.

Gunnison Hills

The north end of the Gunnison Hills is regarded as an exposure of the outermost zones of the Johnson aureole of metamorphic rocks. The tremolite zone is the highest metamorphic grade represented and is confined as far as known to the west side of the outcrop of Glance conglomerate north of State Highway 86. The talc-calcite alteration took place in the Glance conglomerate farther east. No metamorphic silicates were noted in the formations of Paleozoic age, though some simple recrystallization has taken place as much as a mile south of the Glance conglomerate contact.

Metasomatism in the area includes local silicification and lead-silver mineralization. Silicification was the more widespread and quantitatively important of these processes but took place on a very small scale except at one locality, about 1000 feet southeast of Highway 86, where the Concha limestone has been converted to silica breccia in an oval area 400 feet long and 300 feet wide. Although it is along a fault contact with the Scherrer Formation, the breccia seems to represent a pipelike rather than a tabular mass. The breccia is a compact rock consisting of angular to subrounded white fragments 1 or 2 inches in diameter in a gray to brown matrix. The white fragments are almost pure chalcedonic quartz. The darker matrix is predominantly quartz but contains abundant dustlike inclusions and sparsely distributed hexagonal crystals of jarosite. Fine-grained green chlorite has impregnated the rock near some fractures. At places there are sparsely disseminated limonite grains and tiny prisms of a colorless mineral probably belonging in the apatite group. Some of the limonite is in pseudomorphs after pyrite cubes. No ore minerals were found.

Minor silicification has also taken place locally along faults and in shear zones in the Gunnison Hills area. Small amounts of oxidized iron and copper minerals are common in the silicified rock, and concentrations of silver and gold are reported by local prospectors. Small quartz veins of the filled-fissure type contain streaks and pockets of galena and oxidized lead minerals. Small shipments have been made, but the deposits have proved too small for profitable mining.

About $40,000 in oxidized ore averaging 38.5 per cent lead and 49 ounces of silver to the ton has been taken from the Texas Arizona mine. The ore contained 1.6 per cent copper and 0.05 ounce of gold per ton. Zinc appears to have been

fairly abundant in the primary ore, for oxidized zinc minerals (willemite, hemimorphite, and hydrozincite) are now more abundant in the mine workings than other ore minerals. Most of the ore was in small tabular bodies that had replaced favorable beds in the Escabrosa limestone. Where it is clear that ore metals have not been moved by supergene processes, the way the ore minerals are associated with small amounts of quartz and dolomite indicates that these minerals were introduced with the primary sulfides.

Volume Relations

Reactions of the type that probably took place during the progressive metamorphism involve a substantial loss in volume, because carbon dioxide is expelled and because the silicate minerals formed are for the most part denser than the sedimentary minerals from which they were derived. The volume losses (in per cent) for some of the reactions are as follows, according to calculations similar to those of Van Hise (1904, p. 209–211):

(1) 3 dolomite + 4 quartz + H_2O (added) → talc + 3 calcite + $3CO_2$ (lost) 12.6

(2) 5 dolomite + 8 quartz + H_2O (added) → tremolite + 3 calcite + $7CO_2$ (lost) 22.5

(3) 2 dolomite + quartz → forsterite + 2 calcite + $2CO_2$ (lost) 22.6

(4) dolomite + 2 quartz → diopside + $2CO_2$ (lost) 39.9

(5) muscovite + 3 calcite + 3 quartz → grossularite + orthoclase + $3CO_2$ (lost) + H_2O (lost) .. 26.8

(6) 2 orthoclase + 3 calcite → grossularite + 3 quartz + $3CO_2$ (lost) + K_2O (lost) 40.8

(7) 2 orthoclase + 2 clinozoisite + 8 calcite → 4 grossularite + $8CO_2$ (lost) + H_2O (lost) + K_2O (lost) 35.5

(8) calcite + quartz → wollastonite + CO_2 (lost) ..... 31.4.

As these computations are intended to illustrate volume changes to be expected in particular rock types in the various metamorphic zones, some steps in the process have been eliminated. The left side of each equation gives the original sedimentary minerals in so far as possible. Although dolomite and quartz did not react to form forsterite or diopside directly (tremolite formed as an intermediate product), the net volume reduction at any stage is the same as by the direct reaction. Thus the volume losses in the dolomitic rocks given in the first four examples are not cumulative. The situation for the calcareous rocks is more complex. Orthoclase formed in reaction 5 has reacted with remaining calcite at a later stage, according to reactions like (6) or (7); these reactions involve a cumulative loss in volume. Presumably some additional volume loss is indicated by the clinozoisite (epidote) on the left side of equation (7). Field evidence shows that a little epidote was formed in the calcareous rocks at an early stage of metamorphism, but data indicating the manner of origin are not available.

If no material is added during metamorphism, the indicated volume losses must result in increased porosity, decreased bulk volume, or both. A decrease in bulk volume without increase in porosity appears to have taken place near Johnson.

Before the mineral transformations were determined and the volume implications appreciated, it was noted in constructing cross sections through the mines at Johnson that silicated members of the Abrigo and Martin formations plotted out thinner than the same beds in near-by unsilicated areas. Stratigraphic thicknesses in unmetamorphosed and metamorphosed states are as follows:

	Little Dragoon Mountains, northwest, west, and southwest of Johnson	*Johnson district (metamorphic zone 4)*	*Gunnison Hills southeast of Johnson*
Martin Formation	220 233 241* 254 272 — 245	195–225	219 257 — 245 258
Abrigo Formation			
Upper member (units 6–10)	95 128 141 143* 156 — 133	100–120	150
Middle member (units 2–5)	223 231 233 257 — 236	175–230	(121 feet exposed, lower part concealed)

* This measurement was made about 3500 feet northwest of the Moore mine, considerably nearer the aureole of metamorphic rocks than the others in this group.

The error in measurements outside the Johnson district may be as high as 10 per cent, owing to the difficulty of accurate measurement of dip. The accuracy within the metamorphic area is considerably greater, because mine workings and diamond-drill cores give information on the location of beds in depth.

The measurements show that the section in the Little Dragoons has essentially the same thickness as that in the Gunnison Hills, whereas the thicknesses in the Johnson district are of a lower order. As the Johnson district is between the other areas, a regional variation in original thickness does not explain the thinning in the Johnson district.

The thinning is almost certainly due to metamorphism. The indicated losses in volume based on reasonable assumptions of original thickness are as follows:

		Original thickness (feet)	*Loss (in volume) on metamorphism (per cent)*
Martin Formation		241 (nearest unmetamorphosed section)	7–19
Abrigo Formation	upper member	143 (nearest unmetamorphosed section)	16–30
	middle member	236 (average)	2½–26

The volume losses are essentially those required by the metamorphic reactions. The Martin Formation contains much almost pure dolomite (units 1 and 6) that is only slightly silicated or not at all. The upper member of the Abrigo Formation lacks pure carbonate units and is invariably much-silicated. The middle member shows all degrees of silication from very slight to almost complete, and the thickness variations correlate with the amount of silication, as shown by cross sections through the Republic mine (Fig. 2). On the 300 level, where silication is almost complete, the thickness is 175 feet. Near diamond-drill hole no. 1, where silication is very slight, the thickness is 230 feet.

No increase in porosity accompanied the decrease in volume, as shown by measurements of bulk and powder densities given in Table 2. The metamorphosed facies of each rock pair is less porous than the unmetamorphosed facies, which indicates that voids were destroyed, presumably by compaction. The density data indicate that the metamorphosed facies of unit 5 of the Abrigo Formation has a small negative porosity, which must be due to a small error in the density measurements or more probably to a slight concentration of less dense constituents during preparation of the sample.

Some who grant that the variations in thickness are post-depositional might contend that they are due to rock flowage or other form of deformation. This interpretation, which has been advanced in other areas, has nothing to recommend it for the Johnson district. The rocks at Johnson lack cleavage or other evidence of dynamic thinning. Neither the regional pattern of the formations nor the attitude of the beds suggest that the area was under greater stress than the adjacent unmetamorphosed areas. Where stratigraphic units display the same degree of silication, the thicknesses remain remarkably constant, as shown by fences of closely spaced diamond-drill holes. Where the units have different degrees of silication the thicknesses vary markedly and correlate with the degree of silication, as they would if controlled by metamorphism.

The shrinkage must have resulted in structural adjustments in and above the affected beds, but structural features formed in this way are so obscure that not one can be identified positively. Large-scale effects, such as downwarping or downfaulting of beds above a silicated (shrunken) area, would be easy to detect in an undeformed terrain but are here masked by much greater regional deformation not related to the metamorphism. Small-scale deformation, such as that which must have taken place around an isolated chert nodule or quartz granule that was reacting to form silicates, yielded no perceptible structure because of general recrystallization that accompanied metamorphism. (*See* Figure 2 of Plate 1 and related discussion.)

Some of the faulting and fracturing in the silicated area could be due to shrinkage during metamorphism. The silicated rocks are cut by many northeastward-trending fractures that were once open, for they are filled with quartz, potassium feldspar, fluorite, calcite, and ore minerals. Some low-dipping unmineralized

faults of eastward trend are found near the boundary between silicated (shrunken) and unsilicated rock and thus might represent slump structures. Stresses must have been greatest at such boundaries, and the fracturing that might result could be a factor in the localization of ore bodies near the limestone side of silicated zones—a relationship that was pointed out by Umpleby (1916) and applies to some of the ore bodies at Johnson. These possibilities are speculative, for the fracture pattern at Johnson conforms to a broader regional pattern formed before the metamorphism.

One reason that field evidence of shrinkage like that at Johnson Camp has not been found in other areas is that contact metamorphism is different at different places. Iron-rich skarns that have replaced pure limestone formations in many mining districts must have had a different origin from the silicate rocks at Johnson. Less obviously different are certain relatively low-iron types such as those at Bingham, Utah, described by Lindgren (1924). The metamorphism at that locality was an essentially volume-for-volume replacement process in which losses of carbon dioxide and other constituents were made up by gains in silica, iron, magnesium, and other elements. The metamorphic process was fundamentally different from that at Johnson, however, as shown by petrographic evidence. Winchell (1924, p. 890), who made a microscopic study of the Bingham rocks, found that ". . . original quartz is not used (at least in all cases) in the formation of lime silicates, for in some thin sections the calcite matrix has been converted completely to lime-silicate minerals with no encroachment on the rounded outlines of the detrital quartz grains." At Johnson Camp the original quartz apparently invariably participated in the silicate-forming reactions.

So great is Lindgren's influence that many geologists have taken for granted the volume-for-volume process that he espoused. Under the most favorable circumstances, much detailed work must be done to reach a reliable conclusion with respect to volume relations. In many districts the data necessary to come to a valid conclusion are unobtainable.

Metamorphic aureoles of the type found at Johnson have certain characteristics that give the impression of volume-for-volume metasomatism. Indeed such metasomatism did take place on a small scale, as shown by the specimen in Figure 2 of Plate 3. Although the dark micaceous hornfels has been altered to potassium feldspar and then to lime silicates and sulfides next to the transecting veins, the bedding planes pass through the three zones without the sagging or bulging that would be required if volume changes had taken place. If only this relation were considered, it would be inferred that there had been no change in volume in the aureole.

The lack of evident deformation around silicate masses of the kind shown in Figure 2 of Plate 1 might be taken as an indication that the masses were formed by volume-for-volume metasomatism, although geologic evidence shows an origin by thermal metamorphism. Under certain circumstances, losses in volume result in an apparent increase in thickness of a given bed, because portions of the adjacent beds have been incorporated in the silicate facies. According to equations given above, a 1-inch bed of pure quartzite on reacting with adjacent limestone would yield a wollastonite layer 1.8 inches thick. A similar quartzite bed reacting with adjacent dolomite would yield 1.6 inches of tremolite, 1.9 inches of forsterite, or 1.5 inches of diopside. If attention were centered on the quartzite bed alone, volume-for-volume replacement or even an increase in volume might be deduced, even though there had been an actual loss in over-all volume. The apparent expansion of the quartzite would be far less than the contraction of the adjacent carbonate rock, and the reacting constituents together would shrink 22.5–39.9 per cent, depending on the reaction.

Relatively small-scale phenomena may be misleading in regard to the over-all volume relations of the metamorphic process, but at Johnson large masses of metamorphosed rock occupy less space than the unmetamorphosed rock from which they were derived.

Chemical and Spectrographic Data

Sample Collection, Preparation, and Analysis

Geologic evidence presented above indicates that most of the metamorphic reactions were nonadditive and resulted in a loss in volume. A comparison of the chemical composition of the

unmetamorphosed and metamorphosed facies is required for quantitative measurement of constituents that may have been added and removed during the process. This involves a difficult sampling problem. The stratigraphic units that were silicated not only show lateral variation but are heterogeneous in detail, and geologic evidence shows that material was interchanged between adjacent beds of different compositions during silication. The silicated rock is also heterogeneous, though much less so than the parent material. Large samples are required for reliable results, but even these results must be approximations, because it is impossible to obtain large samples of metamorphosed rock that are free from late-stage metasomatic effects, or any large samples free of calcite seams of supergene origin.

Pairs of samples were collected from unit 7 of the Martin, and units 5 and 6 of the Abrigo. One sample of each pair was collected from the unmetamorphosed unit and consisted of a continuous channel sample roughly 1½ inches wide and 1 inch deep cut with hammer and moil at the surface across a minimum thickness of 20 feet of beds. The other sample of each pair was taken from the same unit in its intensely metamorphosed condition and consisted of split diamond-drill core from a vertical hole 550 feet southeast of the Moore shaft. This hole is about 100 feet from the "A" ore body of the Moore mine in an area of intense metamorphism but little metallic mineralization. The split drill-core samples weighed approximately 10 pounds each, and the channel samples approximately 35 pounds each.

M. K. Carron and Leonard Shapiro in the Geological Survey laboratory prepared the samples for analysis. They determined the bulk specific gravity of each sample by dividing the weight of the entire sample by the weight of water displaced. To prevent penetration of water into pores and cracks they encased the entire sample in a single cake of paraffin before immersion in water and made a correction for the amount of paraffin used. Preliminary experiments with a smaller amount of material indicated that the paraffin-cake method gave specific gravities 1–2 per cent below the weighted-average specific gravity of the individual fragments, which had very thin coats of paraffin. A discrepancy of this order of magnitude is of no significance in view of inevitable errors from other sources.

After determining the bulk specific gravity, they removed most of the paraffin by melting and decanting, and dissolved out the remainder with carbon tetrachloride. They repeated treatment with carbon tetrachloride until the weight of the sample was the same as it was originally. They then ground and quartered the samples to a size suitable for analysis and determined the specific gravity of the powder. Portions of the powder were then analyzed chemically and spectrographically (Table 2).

Unit 7 of the Martin Formation

Lithology and calculated mineral composition.—The shale unit at the top of the Martin Formation, referred to here as unit 7, was selected to represent the dolomitic shales. The unit is well suited for study because it is very different from the adjacent beds and is uniform in thickness and general lithologic characteristics over broad areas. On metamorphism it passes from a soft reddish shaly rock to a conspicuous hard gray unit called the hornstone marker.

Where the unmetamorphosed sample was cut the unit is about 25 feet thick and lies, with sharp contacts, between dark-gray fossiliferous dolomite below (Martin unit 6A) and smooth-weathering gray dolomite above (Escabrosa). The thickness determination is not precise because the beds are almost parallel to the hill slope, and therefore a very small error in measurement of the dip results in a large error in the thickness calculated. The unit consists of pale-reddish-brown (10R 5/4)[4] to pale-yellowish-brown (10YR 6/4) siltstone. Most of the silt is in the fine part of the silt range, but its particle size is variable and approaches very fine sand (Wentworth scale) in one 7-foot interval in the lower part. The finer-grained portions are thinly but weakly laminated and are shaly; the coarser are unlaminated and massive. Scarce grains of limonite about 1 mm in diameter are scattered through some por-

[4] Color designation according to Rock-Color Chart of National Research Council (1948). Hand specimens were compared with the chart several years after collection. The red in some specimens has probably faded, but it is not restored on soaking in water.

TABLE 2.—CHEMICAL AND SEMIQUANTITATIVE SPECTROGRAPHIC ANALYSES OF SEDIMENTARY ROCKS AND THEIR METAMORPHOSED EQUIVALENTS

Chemical analyses by R. T. Telfer, U. S. Geological Survey Denver laboratory; specific-gravity measurements by M. K. Carron and Leonard Shapiro, U. S. Geological Survey Washington laboratory; spectrographic analyses by A. T. Myers, U. S. Geological Survey Washington laboratory

	(1) Martin 7	(2) Martin 7 (metamorphosed)	(3) Abrigo 6	(4) Abrigo 6 (metamorphosed)	(5) Abrigo 5	(6) Abrigo 5 (metamorphosed)
Chemical analyses (in weight per cent)						
SiO_2	50.68	53.74	39.75	55.03	32.78	39.20
Al_2O_3	9.17	10.10	3.37	5.44	7.51	7.85
Fe_2O_3	1.93	.78	.91	.35	1.82	4.11
FeO	.53	1.64	.90	1.99	1.14	1.69
MgO	6.40	8.79	9.33	10.64	1.97	3.04
CaO	10.82	13.48	18.04	17.83	26.55	30.09
Na_2O	.06	.39	.01	.15	.06	.10
K_2O	3.48	5.46	2.14	3.21	4.64	.67
H_2O-	.21	.63	.02	.14	.06	.18
H_2O+	1.53	1.34	.29	.71	.97	.61
TiO_2	.45	.49	.22	.32	.38	.40
CO_2	14.13	2.47	23.38	2.36	21.08	9.39
P_2O_5	.18	.25	1.02	1.06	.74	.63
Cl	.03	.03	.03	.08	.03	.03
F	.14	.16	.12	.09	.10	.31
S	.03	.01	.03	.13	.04	.55
MnO	.07	.20	.23	.45	.23	1.27
	99.84	99.96	99.79	99.98	100.10	100.12
Less O for Cl, F, and S	.09	.08	.07	.12	.07	.42
Total	99.75	99.88	99.72	99.86	100.03	99.70
Specific-Gravity Measurements						
Specific gravity (bulk)	2.54	2.57	2.28	2.79	2.41	3.00
Specific gravity (powder)	2.70	2.64	2.71	2.99	2.62	2.96
Porosity (calc.)	5.93%	2.65%	15.87%	6.69%	8.02%	−1.35%
Spectrographic Analyses*						
BeO	—	0.000X	—	0.000X	—	0.000X
Cu	0.00X	.0X	0.00X	.0X	0.00X	.00X
Mo	—	—	—	.00X	—	.0X
Zn	—	—	—	.0X	—	.0X
Mn	.0X	.X	.X	.X	.0X	.X
Ni	.00X	.00X	—	.000X	.000X	.000X
Fe_2O_3	.X	.X	.X	.X	.X	.X
Ga	.00X	.00X	—	Tr.	Tr.	.00X
Cr	.00X	.00X	.000X	.00X	.00X	.00X
V	.0X	.0X	.00X	.00X	.00X	.00X
Y	.00X	—	—	—	.00X	—
Ti	.X	.X	.X	.X	.X	.X
Zr	.0X	.0X	.0X	.0X	.0X	.0X
CaO	X.0	X.0	X.0	X.0	X.0	X.0

TABLE 2—*Continued.*

	(1) Martin 7	(2) Martin 7 (metamorphosed)	(3) Abrigo 3	(4) Abrigo 6 (metamorphosed)	(5) Abrigo 5	(6) Abrigo 5 (metamorphosed)
Spectrographic Analyses*—continued						
Sr	.0X	.0X	.0X	.0X	.0X	.0X
Ba	.00X	.0X	.00X	.0X	.00X	—
MgO	X.0	X.0	X.0	X.0	.X	.X
B	.00X	—	—	—	.00X	.00X

* Looked for but not found: Ag, As, Bi, Cd, Cb, Co, Ge, In, La, Pb, Sb, Sn, Tl, and W

(1) Unit 7 of Martin Formation, unmetamorphosed. Channel sample across unit at head of draw 5200 feet northwest of Moore shaft. The unit is here 25 feet thick and consists of reddish dominantly shaly siltstone with scarce small knots of limonite.

(2) Unit 7 of Martin Formation, metamorphosed. Split core, depth 56–91 feet (80 per cent recovery), from Coronado Copper and Zinc Company diamond-drill hole no. 71, 550 feet southeast of Moore shaft. Sample equivalent to about 26 feet of beds consisting of aphanitic to fine-grained gray porcellanite with scarce disseminated pseudomorphs of limonite after pyrite.

(3) Unit 6 of Abrigo Formation, unmetamorphosed. Channel sample across 21.7 feet of beds at base of unit on southwest slope of hill 3700 feet northwest of Moore shaft. The sample interval consists of interbedded sandy dolomite and dolomitic sandstone with a few thin beds of shale.

(4) Unit 6 of Abrigo Formation, metamorphosed. Split drill core, depth 420.00 to 450.5 feet (98 per cent recovery), from Coronado Copper and Zinc Company diamond-drill hole no. 71, 550 feet southeast of Moore shaft. The sample interval is equivalent to 23 feet of beds and consists of granular white tactite with thin bands of gray porcellanite in lower part.

(5) Unit of Abrigo Formation, unmetamorphosed. Channel sample across 23.1 feet of beds at top of unit on south slope of hill 4000 feet west of Moore shaft. The sample interval consists of interbedded limestone, sandstone, and shale.

(6) Unit 5 of Abrigo Formation, metamorphosed. Split drill core, depth 450.5 to 481.0 feet (95 per cent recovery), from Coronado Copper and Zinc Company diamond-drill hole no. 71, 550 feet southeast of Moore shaft. The sample is equivalent to 23 feet of beds consisting of garnet-rich tactite with some bands of brown to white porcellanite and residual limestone; it contains scarce small pockets of chalcopyrite, sphalerite, pyrite, and molybdenite.

tions. All parts are dolomitic, but some contain considerably more dolomite than others. The chief insoluble constituents are quartz and dusty sericitic and chloritic material. Traces of detrital feldspar were detected. Thin seams of calcite (caliche) are common along bedding planes and joints but make up less than 2 per cent by weight of the sample collected. No correction for this contaminant has been made in the analysis or in calculations based thereon.

The mineral composition of unit 7 calculated from the chemical analysis in terms of simple and partly hypothetical mineral molecules is given in the first column of Table 3.[5] There are no deficiencies in the calculation, but 0.7 per cent of alkalies and 0.1 per cent of total water are in excess and are unaccounted for. The calculated specific gravity of the mixture checks well with the specific gravity of the powder analyzed, as shown in Table 3.

The analyzed sample of the metamorphosed facies was split drill core from a vertical interval of about 35 feet according to depth markers in the core box; the interval was represented by 28 feet of core. The corresponding stratigraphic thicknesses are 29 feet and 23 feet respectively. The unit is underlain and overlain by limy dolomite containing small amounts of silicate minerals, formed from the original dolomite. In contrast with the granular carbonate rocks above and below, the unit sampled is a porcelaneous to fine-grained rock so hard that it is difficult to scratch with a knife blade. It is light gray (N6 to N7) with abundant greenish

[5] The procedure was to calculate P_2O_5 as apatite, remaining F as fluorite, S as pyrite, TiO_2 as rutile, Fe_2O_3 as goethite, Al_2O_3 as sericite; remaining CaO was distributed between calcite and dolomite as required by the CO_2 content; remaining (Mg, Fe, Mn)O was calculated as antigorite, and remaining SiO_2 as quartz.

(5GY 7/2) and yellowish (5Y 7/2) streaks and mottlings generally parallel to the bedding. The color markings correspond with textural changes from aphanitic (less than 0.1 mm) to fine granular (0.5 mm). The upper and thicker part of the unit is largely aphanitic and does not effervesce with acid except along minute cracks and seams. Near the base most of the rock is fine granular and gives some general effervescence in addition to that from veinlets. Throughout the unit there are dendritic manganese stains, traces of blue-green copper stain, and sparse 1-mm spots of limonite, which are commonly cubic and are pseudomorphs after pyrite.

TABLE 3.—CALCULATED MINERAL COMPOSITION (WEIGHT PER CENT) OF UNIT 7 OF THE MARTIN

(*See* Table 2 for description of units)

Mineral	Unmetamorphosed (1)	Metamorphosed (2)	Specific gravity (assumed)
Dolomite	25.2	—	2.85
Calcite	4.9	5.6	2.71
Quartz	38.7	2.3	2.66
Sericite	23.9	4.9	2.76
Antigorite	3.1	—	2.55
Apatite	.5	.6	3.18
Fluorite	.3	.3	3.18
Rutile	.4	—	4.23
Pyrite	.1	.2	5.02
Goethite	2.1	.9	4.17
Tremolite	—	27.5	2.9
Diopside	—	16.2	3.2
Orthoclase	—	28.9	2.56
Plagioclase (An_{50})	—	6.8	2.69
Zoisite	—	3.0	3.25
Sphene	—	1.2	3.5
Total	99.2	98.4	....
Specific gravity calculated from above	2.75	2.80	....
Powder specific gravity (measured)	2.70	2.64	....

Microscopic study of the analyzed material and other specimens from the same area shows that potassium feldspar generally makes up 20–40 per cent of the rock and that tremolite and diopside in highly variable proportions make up most of the remainder. Tremolite is most abundant in the upper, finer-grained part of the unit as sheafs and radiating aggregates of slender needles 0.05–0.5 mm long with a slight preferred orientation parallel to the bedding. Diopside is most abundant in the coarser-grained portions and has two crystalline habits: roughly equidimensional subhedral grains that are locally as much as 0.5 mm in diameter and in places are molded on tremolite, and acicular crystals that are probably a replacement of tremolite. Potassium feldspar is a groundmass constituent either as a very fine-grained aggregate (0.01 mm or less) or as irregular poikiloblastic grains as much as 1 mm in diameter. It contains fine sericitic and chloritic alteration products at places. Quartz is rare, but calcite is fairly abundant as large poikiloblastic grains in the lower portion. Some specimens contain a few grains of recognizable epidote, and most specimens contain a few per cent of very fine grains (0.005 mm), with high index of refraction and birefringence, which are also regarded as epidote. The fine grains are commonly aggregated in tiny lenses parallel to the bedding. Andesine, in 1-mm grains that show albite twinning at places, is fairly abundant in one specimen. Apatite and sphene are constant as accessories. A recalculation of the chemical analysis in terms of minerals is given in Table 3.[6] There are no deficiencies, and the only excess is 1.0 per cent of total water. The calculated specific gravity is greater than the specific gravity of the powder analyzed.

Gains and losses of constituents.—To determine the gains and losses of constituents during metamorphism, the chemical analyses were recalculated to 100 per cent, and each oxide was multiplied by the bulk specific gravity to obtain the grams in each cubic centimeter of the rock. The results and indicated gains and losses on two different hypotheses are presented in Table 4. The two hypotheses lead to different conclusions concerning the chemical changes involved.

The calculations on the constant-volume

[6] The first step was to calculate P_2O_5 as apatite, remaining F as fluorite, S as pyrite, TiO_2 as sphene, Fe_2O_3 as goethite, CO_2 as calcite, and Na_2O as plagioclase (An_{50}). Ten per cent of the remaining Al_2O_3 was then arbitrarily assigned to zoisite, and the rest was distributed between orthoclase and sericite. The (Mg, Fe, Mn)O and remaining CaO were distributed between diopside and tremolite; the balance of SiO_2 was calculated as quartz.

basis imply a large loss in CO_2 and gains in all other constituents, if total iron and total water are considered and trace constituents ignored.[7] It is difficult to account for most of these additions. There is no geologic evidence for widespread introduction of material from outside the system. The adjacent beds could provide CaO and MgO but almost nothing else, because they are dolomites.

The computations on the volume-loss basis imply significant losses of SiO_2 and Al_2O_3, moderate gains in MgO and K_2O, and small gains in CaO and Na_2O. These changes are essentially what would be expected from interchange of constituents between beds, as indicated by geologic evidence. The Martin 7 unit is underlain and overlain by dolomite beds, which are partly silicated and dedolomitized near their contacts with unit 7 of the Martin, and the latter is the probable source of the silica. The dolomites might be expected to furnish MgO and CaO to the silicious and aluminous beds of unit 7, and such an increase is shown by the analytical data and calculations; the greater increase in MgO than in CaO is consistent with the partial dedolomitization of the adjacent carbonate rock.

TABLE 4.—GAINS AND LOSSES OF CONSTITUENTS ON METAMORPHISM OF UNIT 7 OF THE MARTIN

	Grams per cm³		Grams gained (+) or lost(−) per cm³ of original rock	
	(1) (unmetamorphosed)	(2) (metamorphosed)	No volume change (col. 2 − col. 1)	20 per cent decrease in volume (80 per cent col. 2 − col. 1)
SiO_2	1.291	1.383	+.092	−.185
Al_2O_3	.233	.260	+.027	−.025
Fe_2O_3	.049	.020	−.029 Total Fe	−.033 Total Fe
FeO	.013	.042	+.029 +0.002	+.021 −0.007
MgO	.163	.226	+.063	+.018
CaO	.276	.347	+.071	+.002
Na_2O	.002	.010	+.008	+.006
K_2O	.089	.141	+.052	+.024
H_2O-	.005	.016	+.011 Total H_2O	+.008 Total H_2O
H_2O+	.039	.034	−.005 +.006	−.012 −.004
TiO_2	.011	.013	+.002	−.001
CO_2	.360	.063	−.297	−.310
P_2O_5	.005	.006	+.001	.000
Cl	.001	.001	.000	.000
F	.004	.004	.000	−.001
S	.001	Trace	−.001	−.001
MnO	.002	.005	+.003	+.002
Total	2.544	2.571	+.359 −.332	+.081 −.568
Less O for Cl, F, S	.002	.002	0	0
Net	2.542	2.569	+.027	−.487

(1) Unit 7 of Martin Formation, unmetamorphosed. Channel sample across unit at head of draw 5200 feet northwest of Moore shaft. The unit is here 25 feet thick and consists of reddish dominantly shaly siltstone with scarce small knots of limonite.

(2) Unit 7 of Martin Formation, metamorphosed. Split core, depth 56–91 feet (80 per cent recovery), from Coronado Copper and Zinc Company diamond-drill hole no. 71, 550 feet southeast of Moore shaft. Sample equivalent to about 26 feet of beds consisting of aphanitic to fine-grained gray porcellanite with scarce disseminated pseudomorphs of limonite after pyrite.

[7] The trivial loss in sulfur has no significance, as the analyzed sample of the metamorphosed facies contains limonite pseudomorphs after pyrite and thus has lost sulfur by weathering or other post-metamorphism process.

The source of the alkalies gained was not in the adjacent beds but possibly in the Abrigo Formation several hundred feet below. Several units of the Abrigo Formation lost much K_2O when they were garnetized, as shown by petrographic and chemical data; this K_2O may have been carried upward until it encountered materials to form a stable mineral phase. The increase in soda is so small that it could have been due to the entry of soda from connate water into a silicate phase. Flushing by recent groundwater circulation would explain why the soda is not present in the unmetamorphosed facies. Only constituents fixed in a mineral phase would remain.

A loss in volume of 20 per cent is consistent with the nature and abundance of silicates in the metamorphosed facies and with the geologic evidence of nonadditive metamorphism. The gains and losses of constituents calculated on this basis check with field evidence and theory. Computations on the constant-volume basis give different results that are difficult to explain.

TABLE 5.—CALCULATED MINERAL COMPOSITION (WEIGHT PER CENT) OF UNITS 5 AND 6 OF THE ABRIGO

(*See* Table 2 for description of units)

Mineral	Unit 6		Unit 5		Specific gravity (assumed)
	Unmetamorphosed facies (3)	Metamorphosed facies (4)	Unmetamorphosed facies (5)	Metamorphosed facies (6)	
Dolomite	43.7	—	4.4	—	2.85
Calcite	6.1	5.4	43.2	21.4	2.71
Quartz	31.2	8.7	13.3	12.2	2.66
Orthoclase	9.9	15.3	21.5	4.3	2.56
Sericite	4.1	6.8	9.3	.7	2.76
Antigorite	.6	—	3.3	—	2.55
Magnetite	1.3	.3	2.6	5.0	5.20
Apatite	2.5	2.6	1.8	1.5	3.18
Fluorite	.1	.1	.1	.6	3.18
Rutile	.2	—	.4	—	4.23
Pyrite	.1	.2	.1	1.0	5.02
Diopside	—	41.7	—	21.3	3.20
Tremolite	—	17.8	—	—	2.90
Grossularite	—	—	—	30.0	3.42
Wollastonite	—	—	—	.2	2.80
Sphene	—	.8	—	1.0	3.50
Total	99.8	99.7	100.0	99.2	..
Specific gravity (calculated)	2.78	2.95	2.76	3.12	..
Specific gravity (powder)	2.71	2.99	2.62	2.96	..
H_2O excess	Trace	.1	.2	.8	..

Units 5 and 6 of the Abrigo Formation

Lithology and calculated mineral composition.—The two other stratigraphic units analyzed chemically are from the Abrigo Formation and are contiguous: unit 5 is at the top of the middle (calcareous) member, and unit 6 is at the base of the upper (dolomitic) member. Unit 5 is an impure limestone that alters to garnetite and contains most of the known ore in the Johnson district. Unit 6 is siliceous dolomite that alters to white tactite. Chemical analyses of the unmetamorphosed and metamorphosed facies of each unit are given in Table 2 and the mineral compositions calculated from these analyses are given in Table 5. There are no deficiencies in any of the calculations, and total water is the only constituent in excess. The amount of excess water in each case is indicated in the table, as are the calculated and measured specific gravities of the mineral mixtures.

The chemical and mineralogical compositions shown in the tables are overall or average compositions for stratigraphic units tens of feet in thickness. Individual beds depart widely from the average, particularly in the unmetamorphosed facies, as shown in the following detailed sections measured where the samples representing the unmetamorphosed facies were obtained.

Section of unit 6 of the Abrigo Formation NW¼SE¼ sec. 22, T. 15 S., R. 22 E.

	Feet
Unit 7	
Quartzite	2.0
Unit 6	
23. Like beds below, but partly covered and not sampled	7.3
22. Irregular-bedded sandy dolomite	1.0
21. Sandy shale	0.2
20. Irregular-banded dolomitic sandstone and sandy dolomite	2.6
19. Intraformational dolomite conglomerate grading upward to cross-bedded quartzitic sandstone	1.0
18. Like bed no. 16 below	2.3
17. Thin-bedded sandstone and shaly material	0.6

16. Irregular-bedded to cross-bedded sandy dolomite and dolomitic sandstone with four or five shale partings up to 1 inch thick 4.2
15. Laminated siltstone and sandy dolomite 0.7
14. Dolomite with very little sand 0.4
13. Irregular-bedded sandy dolomite with one shale seam; top irregular and not a splitting plane 1.3
12. Thin-bedded shale and sandy dolomite. 0.6
11. Coarse-grained dolomite with very little sand, light bluish gray weathering pale yellowish brown 0.5
10. Dolomitic sandstone, knobby-bedded, with irregular top 0.9
9. Thin-bedded shale and sandstone 0.9
8. Fine-grained sandy dolomite 0.5
7. Dolomitic sandstone, thinly laminated in lower part, knobby-bedded in upper part, shale parting at top 0.9
6. Shale, pale olive 0.2
5. Laminated dolomitic sandstone with traces of cross-bedding 0.5
4. Knobby-bedded dolomitic sandstone with shale 0.2
3. Laminated sandy dolomite with some cross-bedding 0.8
2. Knobby-bedded dolomitic sandstone ... 0.9
1. Fine-grained sandy dolomite, thinly laminated, light bluish gray weathering light brown 0.5

Total 29.0
Total sampled (beds 1–22) 21.7

Unit 5
Thin-bedded sandy and shaly material (could be assigned to either unit 5 or unit 6). 0.4
Coarse-grained limestone with some irregular patches of dolomite 0.5

Section of unit 5 of the Abrigo Formation Southwest slope of hill 4000 feet west of Moore shaft

Feet

Unit 6
Interbedded sandy dolomite and dolomitic sandstone
Unit 5
44. Limestone with shaly partings 0.8
43. Dolomitic sandstone, fine-grained, light olive gray weathering grayish brown; upper part thinly laminated, lower part unlaminated but with ½-inch pockets of coarse dolomite that form pits on the weathered surface; forms ledge 1.2
42. Limestone, very thin-bedded with shaly partings 2.0
41. Limestone, sugary textured, light olive gray, weathering light brown 0.8
40. Calcareous sandstone, laminated 0.2
39. Limestone, very thin-bedded, with a few limestone pebbles 0.5
38. Intraformational limestone conglomerate, medium bluish gray, weathering pale yellowish brown, in two beds separated by several inches of shale 1.1
37. Calcareous shale 0.9
36. Intraformational limestone conglomerate 0.3
35. Calcareous sandstone and shale 0.2
34. Intraformational limestone conglomerate 0.1
33. Limestone, very thin-bedded, with shaly partings 0.8
32. Intraformational limestone conglomerate with median shaly parting 1¼ inches thick 0.6
31. Interbedded shale and intraformational limestone conglomerate in 1- to 4-inch beds 4.0
30. Shale, olive gray, with small limestone lenses 0.4
29. Limestone, coarse-grained, with pebbles at base 0.5
28. Shale 0.5
27. Intraformational limestone conglomerate 0.5
26. Shale 0.3
25. Coarse limestone with scattered limestone pebbles 0.5
24. Shale with recurrent 1-inch beds of intraformational conglomerate 1.4
23. Limestone, coarse-grained, with pebbles at base 0.4
22. Shale, partly sandy, with recurrent 1- to 3-inch beds of limestone conglomerate. 3.0
21. Intraformational limestone conglomerate 0.6
20. Shale, partly sandy with several ½- to 2-inch beds of limestone 1.5
19. Limestone, coarse-grained with a few shale seams 1.4
18. Shale with several 1- to 2-inch beds of limestone and intraformational conglomerate 1.1
17. Limestone, coarse-grained 0.6
16. Shale, olive gray, in part sandy and calcareous 0.7
15. Limestone, coarse-grained with shale partings 2.6
14. Calcareous sandstone and shale 1.2
13. Limestone, coarse-grained 1.1
12. Interbedded limestone and shaly sandstone in 1- to 5-inch beds 5.7
11. Dolomite, fine-grained, weathering tan. 0.1
10. Sandstone, very calcareous 0.5

9. Limestone, coarse-grained, with sandstone lenses	1.1
8. Interbedded limestone and sandstone	1.0
7. Limestone, coarse-grained, intraformational conglomerate at base	1.2
6. Sandstone	0.2
5. Limestone	0.3
4. Sandstone	0.6
3. Intraformational limestone conglomerate with a few sandstone seams	2.0
2. Sandstone	0.4
1. Intraformational limestone conglomerate	0.3
Total	45.2
Total sampled (beds 20–44)	23.1
Unit 4	
Sandstone with a few thin beds of limestone	4.5

The preponderant minerals in the unmetamorphosed facies of units 5 and 6 are the carbonates, quartz, and potassium feldspar. Flakes of sericite 0.1–0.2 mm in diameter are disseminated in some of the beds, and small grains of magnetite and pyrite can be detected in places with a hand lens. At least two unidentified clay minerals and chloritic material are conspicuous in the shale beds. In making the calculations of Table 5, constituents of the argillic and chloritic material were computed as sericite and antigorite.[8] Perhaps 1 or 2 per cent of the calcite in Table 5 represents seams of caliche that could not be avoided. There are no deficiencies, and the only excess is in total water, as given in the table.

The metamorphosed facies are much more uniform rocks than the unmetamorphosed. The sample representing the metamorphosed facies of unit 6, obtained from a drill core, is typical white tactite—a medium-grained light-greenish-gray (5GY 7/1) rock with sparsely disseminated sulfides of copper, iron, and zinc associated with calcite, chlorite, and tremolite in scattered spots several millimeters in diameter. There are a few thin aphanitic light-olive-gray (5Y 6/1) bands that represent shale beds and one thin band of medium-gray feldspathic quartzite. The principal minerals are shown in Table 5, but the proportions vary from bed to bed. For example, sericite is abundant only in the metamorphosed shale beds, and most of the quartz is concentrated in portions that are slightly darker than the rest. The analyzed sample represents the entire thickness (23 feet) of the stratigraphic unit, which is underlain by the garnetite of unit 5 and overlain by partly silicated quartzite of unit 7. The calculated mineral composition is given in Table 5.[9] There are no deficiencies, and the only excess is 0.1 per cent of total water.

The sample of the metamorphosed facies of unit 5 was taken from the upper part of the unit, immediately below the sample for unit 6 in the drill core. The top 4 feet resembles the diopsidic white tactite above, except that it contains bands and pockets of yellowish-brown garnet. Below this transition zone the proportion of garnet is much greater, and most of the rock is yellowish brown (10YR 5/2) and medium-grained. Bands and lenses of brownish-gray (5YR 3/1) to greenish-gray (GY 6/1) hornfels represent the remains of shale beds; remnants of unreplaced limestone are abundant in the lower 6½ feet of the 23 feet of beds sampled. Thin bands of medium- to coarse-grained almost white wollastonite occur in the garnet at several places. A little sphalerite, chalcopyrite, pyrite, scheelite, and molybdenite were detected in places. In recalculating the chemical analysis,[10] small amounts of epidote and retrogressive amphibole and chlorite were eliminated from the computation. Part of the iron calculated as magnetite occurs in these minerals and in other silicates like garnet and pyroxene. Probably less than 1 per cent of magnetite is present. There are no deficiencies, and the only excess is 0.8 per cent of total water.

Gains and losses of constituents.—Computed gains and losses of constituents on metamorphism of units 5 and 6 are given in Table 6. The procedure in computation was the same as explained in the discussion of unit 7 of the

[8] The procedure was the same as outlined in footnote 5, except that Fe_2O_3 was calculated as magnetite instead of goethite, and Al_2O_3 was distributed between orthoclase and sericite as required by the alkali content.

[9] After computing calcite and accessory minerals, Al_2O_3 was distributed between orthoclase and sericite as required by the alkali content, and the remaining CaO and (Mg, Fe, Mn)O were distributed between diopside and tremolite.

[10] After computing calcite and accessory minerals, the alkalies were assigned to orthoclase and sericite in the arbitrary ratio of 9:1; the remaining Al_2O_3 was calculated as grossularite, the remaining (Mg, Fe, Mn)O as diopside, and the remaining CaO as wollastonite.

Martin, except that the loss in volume on the shrinkage hypothesis was taken at 30 per cent instead of 20 per cent to agree better with the shrinkages indicated by stratigraphic measurements that include these units.

and lost CaO, but the quantities involved are much less than on the constant-volume basis. At least SiO_2 and CaO would tend to balance out if larger masses of rock are considered, for units 5 and 6 are underlain and overlain by

TABLE 6.—GAINS AND LOSSES OF CONSTITUENTS ON METAMORPHISM OF UNITS 5 AND 6 OF THE ABRIGO
(In grams gained (+) or lost (−) per cm³ of original rock)

	Unit 6		Unit 5	
	No volume change	30 per cent decrease in volume	No volume change	30 per cent decrease in volume
SiO_2	+0.629	+0.167	+0.390	+0.036
Al_2O_3	+.075	+.029	+.055	−.016
Fe_2O_3	−.011 Fe=	−.014 Fe=	+.080 Fe=	+.043 Fe=
FeO	+.035 +.020	+.018 +.004	+.023 +.074	+.008 +.036
MgO	+.084	−.005	+.044	+.017
CaO	+.086	−.064	+.266	−.006
Na_2O	+.004	+.003	+.002	+.001
K_2O	+.041	+.014	−.092	−.098
H_2O-	+.003 +.016	+.002 +.009	+.004 −.001	+.002 −.009
H_2O+	+.013	+.007	−.005	−.011
TiO_2	+.004	+.001	+.003	−.001
CO_2	−.470	−.489	−.225	−.310
P_2O_5	+.006	−.003	+.001	−.005
Cl	+.002	+.001	.000	.000
F	.000	−.001	+.007	+.004
S	+.003	+.002	+.015	+.011
MnO	+.007	+.004	+.033	+.021
Total	+.992 −.481	+.248 −.576	+.923 −.322	+.143 −.447
Less O for Cl, F, S	.002	.001	.011	.007
Net	+.509	−.329	+.590	−.311

Calculations on the constant-volume basis imply large losses in CO_2, in K_2O from unit 5, and gains in all other constituents (ignoring oxidation state of iron). Loss of K_2O from unit 5 and gain in unit 6 could be due to interchange between beds, but the other additions are difficult to explain. Geologic evidence, particularly the general lack of silication of pure carbonate units in the district, precludes the widespread introduction of material from outside the system.

Calculations on the volume-loss basis suggest interchange of material between beds, as inferred from the geologic evidence. Unit 5 lost Al_2O_3, and K_2O and gained MgO, whereas unit 6 shows the reverse relationship for these constituents. Both units gained SiO_2 and Fe

siliceous beds that gained CaO and lost SiO_2 during metamorphism.

However the chemical analyses are interpreted, potassium was removed from unit 5 in large quantities. Petrographic evidence shows that this phenomenon and probably the lack of evident reduction in iron are related to the development of garnet in the metamorphosed facies. The crystal structure of garnet requires aluminum or ferric iron or both. Under the temperature and pressure conditions of metamorphism, aluminum had a greater affinity for the garnet structure than for orthoclase and sericite, the other two aluminous phases present. As a result aluminum entered garnet preferentially, and potassium was purged from the rock

by diffusion or transportation in migrating fluids.

Summary of Chemical Changes

If the metamorphism was a volume-for-volume replacement process, as most contemporary students of rock alteration assume for aureoles of this type, tremendous changes in composition must have taken place. For example, unit 7 of the Martin is about 25 feet thick and in its metamorphosed form is exposed for a strike length of more than 10,000 feet in the Johnson district. A rough calculation, based on these figures and the data for no volume change given in Table 4, shows that about 2500 tons of material would have to be added for every foot down the dip. The additions to the other units analyzed would be almost three times larger per volume unit. (Compare Tables 4 and 6.) If these figures are extrapolated to the entire exposed areas of silicated rocks in the district, the additions would probably exceed 100,000 tons per foot of dip depth. Essentially the only loss would be in carbon dioxide, which in unit 7 of the Martin would amount to about 2250 tons per foot down the dip. Most of the gains indicated are in ordinary rock-forming constituents.

By modifying the computations to make them consistent with geologic evidence of loss in volume, the indicated changes in composition (Tables 4, 6) compare as shown in Table 7 in grams per cubic centimeter of original rock.

Table 7 shows that CO_2 was lost in immense amounts from each unit, but the only other constituents consistently gained or consistently lost are present in very minor amounts (Na_2O, MnO). The principal rock-forming constituents other than K_2O tend to be lost or gained depending on whether they occur in relatively large or relatively small amounts compared with the immediately adjacent beds. An active interchange of constituents across contacts evidently took place, as inferred from geologic evidence. Most of the material involved in the interchange probably moved only a few inches or a few feet, but some constituents like K_2O, SiO_2, and CaO appear to have moved tens and even hundreds of feet.

The carbon dioxide that was expelled from the rocks in huge quantities must have carried heat and contributed to the solution, transportation, and intergranular diffusion of material. Atoms released by the breakdown of minerals of sedimentary origin moved or were carried until they encountered other atoms with which they could form a stable mineral phase. In theory there is no limit to the distance constituents might be carried, but in fact there was a definite and restricted limit for all constituents except carbon dioxide, which presumably moved out of the aureole of metamorphic rocks.

TABLE 7.—SUMMARY OF GAINS AND LOSSES OF CONSTITUENTS

	Martin 7	Abrigo 6	Abrigo 5
SiO_2	−0.185	+0.167	+0.036
Al_2O_3	−.025	+.029	−.016
Fe (total)	−.007	+.004	+.036
MgO	+.018	−.005	+.017
CaO	+.002	−.064	−.006
Na_2O	+.006	+.003	+.001
K_2O	+.024	+.014	−.098
H_2O (total)	−.004	+.009	−.009
TiO_2	−.001	+.001	−.001
CO_2	−.310	−.489	−.310
P_2O_5	.000	−.003	−.005
Cl	.000	+.001	.000
F	−.001	−.001	+.004
S	−.001	+.002	+.011
MnO	+.002	+.004	+.021

Some small changes in composition are not easily explained by the processes outlined. Any way the chemical analyses are interpreted, small but consistent gains in Na_2O, MnO, and probably S are indicated, for the tiny apparent loss in sulfur from unit 7 of the Martin is misleading. Among the minor constituents, beryllium, copper, zinc, molybdenum, and tungsten were added, judging from examination and spectrographic analyses of the samples. The additions of sulfur, ore metals, and some manganese are almost certainly metasomatic, as they are in the ore bodies. The trivial additions of Na_2O may be due to metamorphic reactions involving connate water, rather than to metasomatism. Some metasomatic additions of iron and fluorine probably occurred in unit 5 of the Abrigo which was particularly susceptible to metasomatism, as shown by a relatively

large increase in sulfur and manganese and particularly by the outstanding favorability of the unit as a locus for replacement ore bodies. Material from outside the system was added in large quantities to form the ore but apparently in very small quantities to unmetalized ground. The small additions are the same constituents concentrated in the ore bodies, and some, like the ore, are products of metasomatism that followed the essentially nonadditive metamorphism.

General Conclusions and Speculations

The temperature rose and then fell during the alteration process near Johnson Camp. While the temperature was rising, large masses of rock underwent progressive and essentially nonadditive metamorphism, which resulted in substantial loss in volume. Metalization started near the temperature maximum, but most metalization, related weak but pervasive metasomatism, and vein filling took place during the time of falling temperature.

The original source of heat energy and later of substance was the quartz monzonite stock. Heat was transferred by fluids rather than conduction because (1) the metamorphism and metalization probably took place after the upper part of the quartz monzonite mass had cooled, and (2) beds at Johnson at least 1000 feet from the stock and 2000–8000 feet from the nearest known contact were more intensely altered than the same beds in actual contact with the stock in other parts of its periphery. Regardless of the composition or state of these fluids, they were capable, during the progressive metamorphism, of reducing Fe_2O_3 to FeO (Tables 4 and 6) and of transporting potassium and some silicon, iron, aluminum, and other rock-forming elements. At the same time they probably deposited very small amounts of manganese, sulfur, ore metals, and perhaps other elements that appear to be of exotic source.

What sort of hot fluid would do these things without altering the over-all composition of the rocks more drastically? Was the fluid different in composition or only in state from the fluids that caused profound metasomatism in other contact metamorphic aureoles? Could the fluid have contained chemically active ingredients that because of physical conditions left little or no evidence of their presence?

It may be assumed that heat was transported from the quartz monzonite mass by emanations that boiled off the residual magma at an advanced stage of crystallization. Much evidence has been presented in the geologic literature to show that such emanations are largely gaseous water but contain other volatile substances; though acidic, their solvent power is limited until they condense to a liquid phase (Bowen, 1933, p. 119–125). Burbank (1936, p. 246) emphasized the dissociated state of the gas molecules and the relative enrichment in hydrogen with respect to oxygen in the early emanations, and he says: "Not until these gases reached rock of temperature so low that undissociated water-vapor could exist in quantity would they be capable of producing recognizable alteration." The alteration to which Burbank refers is metasomatism, and the emanations, while still dissociated, would be a potent agent of metamorphism because of heat alone. The excess hydrogen would eventually give the emanations the capacity to reduce Fe_2O_3 to FeO. Burbank (1936) stressed that the selective emanation of hydrogen would increase the concentration of oxygen in the residual magma, and the resulting oxidation of iron, an exothermic reaction, would be a potent source of heat. Burbank's mechanism explains the metamorphism at Johnson Camp, if the emanations remained dissociated so far from their source.

The CO_2 expelled from the rocks in immense quantities during metamorphism undoubtedly was of great importance in the over-all process. Though magmatic emanations provide heat for the endothermic reactions, the CO_2 expelled at high temperature transported and distributed heat and probably caused reactions at higher levels. Faust (1949) has considered the thermal relationships involved in such a mechanism. Under the physical conditions of metamorphism, the CO_2 was probably a dense gas with practically unknown solvent properties (Garrels and Richter, 1955). As soon as it was formed it was probably reduced in part to CO by hypogene emanations enriched in hydrogen and thus would have a reducing effect on Fe_2O_3 (Hawley and Robinson, 1948, p. 606). The CO_2 and CO that went into solution in the

magmatic emanations may have increased their power to hold ore metals in solution, for ore minerals were not deposited in quantity until the temperature started to fall and expulsion of CO_2 ceased.

During essentially nonadditive metamorphism there was a vigorous interchange of material between beds, and the scale of this interchange increased with the intensity of metamorphism. Two-way diffusion of material seems clear, as in the diopsidization of quartzite inward from both its contacts with dolomite and a corresponding silication of the dolomite. Two-way diffusion gives some indication of the rate or direction of flow of the heat-transporting fluids. Either the rate of flow was slower than the rate of diffusion, or the flow was parallel to the beds so that composition gradients perpendicular to the beds would be maintained regardless of the rate of flow, and constituents would move obliquely to the beds, *i.e.*, along the resultant of the diffusion and flowage directions. Where structural features channelized solution flow, some substances were carried considerable distances, and local metasomatism took place, as in the areas of anamolous alteration near the Republic fault.

By ore-forming time less heat was supplied from below than was being dissipated toward the surface. Carbon dioxide ceased to form locally, and the regimen was changed. Hypogene solutions probably continued to arise, and these solutions may have been richer in sulfur and base metals than they had been previously. In any event they were able to attack the previously metamorphosed rock and replace it with ore and retrogressive gangue minerals. The factors that localized ore bodies of importance were stratigraphic (certain favorable beds, of which unit 5 of the Abrigo Formation is the outstanding example), metamorphic (garnetite facies), and structural (fissures or other structural features that channelized metalizing solutions).

The metamorphism at Johnson Camp is different from that in many mining districts, but it gives cause to question the constant-volume interpretation now generally made by economic geologists. In comparing chemical analyses to obtain the gains and losses of constituents, the volume relations must be appraised correctly and used in the comparison. Account must be taken also of material that was diffused locally. Comparison of chemical analyses of a few small samples may lead to serious error if used as a basis for generalization regarding the process. Ideally many small samples should be studied in their true quantitative proportion, but the gross picture is obtained by comparing samples commensurate in size with the scale of diffusion of material.

References Cited

Baker, Arthur, III, 1953, Localization of pyrometasomatic ore deposits at Johnson Camp, Arizona: Am. Inst. Min. Metall. Eng. Trans., Tech. Paper 36841, Min. Engineering, v. 5, p. 1272–1277

Barrell, Joseph, 1907, Geology of the Marysville mining district, Montana; a study of igneous intrusion and contact metamorphism: U. S. Geol. Survey Prof. Paper 57, 178 p.

Bowen, N. L., 1933, The broader story of magmatic differentiation briefly told, p. 106–128 *in* Ore deposits of the Western States (Lindgren volume): Am. Inst. Min. Metall. Eng. 797 p.

—— 1940, Progressive metamorphism of siliceous limestone and dolomite: Jour. Geology, v. 48, p. 225–274

Burbank, W. S., 1936, A source of heat-energy in crystallization of granodiorite magma, and some related problems of volcanism: Am. Geophys. Union Trans., pt. 1, p. 236–255

Cooper, J. R., 1950, Johnson Camp area, Cochise County, Arizona, p. 30–39 *in* Arizona zinc and lead deposits, Part I: Ariz. Bur. Mines, Geol. ser. 18, Bull. 156, 144 p.

Cooper, J. R., and Huff, L. C., 1951, Geological investigations and geochemical prospecting experiment at Johnson, Arizona: Econ. Geology, v. 46, p. 731–756

Eskola, Pentti, 1922, On contact phenomena between gneiss and limestone in western Massachusetts: Jour. Geology, v. 30, p. 265–294

Faust, G. T., 1949, Dedolomitization, and its relation to a possible derivation of a magnesium-rich hydrothermal solution: Am. Mineral., v. 34, p. 789–823

Faust, G. T., and Callaghan, Eugene, 1948, Mineralogy and petrology of the Currant Creek magnesite deposits and associated rocks of Nevada: Geol. Soc. America Bull., v. 59, p. 11–74

Garrels, R. M., and Richter, D. H., 1955, Is carbon dioxide an ore-forming fluid under shallow-earth conditions?: Econ. Geology, v. 50, p. 447–458

Gilluly, James, 1932, Geology and ore deposits of the Stockton and Fairfield quadrangles, Utah: U. S. Geol. Survey Prof. Paper 173, 171 p.

Gilluly, James, Cooper, J. R., and Williams, J. S., 1954, Late Paleozoic stratigraphy of central Cochise County, Arizona: U. S. Geol. Survey Prof. Paper 266, 49 p.

Goldschmidt, V. M., 1911, Die Contactmetamorphose im Kristianiagebiet: Vidensk. Skr., I, Mat.-Naturv. Kl., No. 1, p. 1–483

Harker, Alfred, 1932, Metamorphism, a study of the transformation of rock-masses: London, Methuen and Co., 360 p.

Harker, R. I., and Tuttle, O. F., 1956, Experimental data on the P_{CO_2}-T curve for the reaction: calcite + quartz $\rightleftarrows$ wollastonite + carbon dioxide: Am. Jour. Sci., v. 254, p. 239–256

Hawley, J. E., and Robinson, S. C., 1948, The supposed oxidation of Fe_3O_4 by carbon dioxide: Econ. Geology, v. 43, p. 603–609

Lindgren, Waldemar, 1905, The copper deposits of the Clifton-Morenci district, Arizona: U. S. Geol. Survey Prof. Paper 43, 375 p.

—— 1924, Contact metamorphism at Bingham, Utah: Geol. Soc. America Bull., v. 35, p. 507–534

—— 1933, Mineral deposits: 4th ed., N. Y., McGraw-Hill Book Co., 930 p.

National Research Council, 1948, Rock-color chart: Washington, D. C.

Scott, W. A., 1916, Mining operations at Johnson, Arizona: Mining and Engineering World, v. 45, p. 141–143

Teall, J. J. H., 1903, On dedolomitization: Geol. Mag., new ser., decade 14, v. 10, p. 513–514

Tilley, C. E., 1948, Earlier stages in the metamorphism of siliceous dolomites: Mineralog. Mag., v. 28, p. 272–276

Umpleby, J. B., 1916, The occurrence of ore on the limestone side of garnet zones: Calif. Univ., Dept. Geol. Bull. 10, p. 25–37

Van Hise, C. R., 1904, A treatise of metamorphism: U. S. Geol. Survey Mon. 47, 1286 p.

Winchell, A. N., 1924, Petrographic studies of limestone alterations at Bingham: Am. Inst. Min. Metall. Eng. Trans., v. 70, p. 884–899

U. S. GEOLOGICAL SURVEY, DENVER, COLORADO

MANUSCRIPT RECEIVED BY THE SECRETARY OF THE SOCIETY, FEBRUARY 20, 1956

PUBLICATION AUTHORIZED BY THE DIRECTOR, U. S. GEOLOGICAL SURVEY

BULLETIN OF THE GEOLOGICAL SOCIETY OF AMERICA
VOL. 68, PP. 611-644, 22 FIGS. MAY 1957

NATURE OF FAULTING IN LARGE EARTHQUAKES

By JOHN H. HODGSON

ABSTRACT

The Dominion Observatory, Ottawa, Canada, has applied Byerly's method to determine the direction of faulting in 65 earthquakes, which makes a total of 75 earthquakes so analyzed. To date 10 solutions have received some confirmation by comparison with observed faulting.

The method is ambiguous in that two planes, neither of which is indicated as the fault, are defined for each solution. This does not obscure the fact that of the 75 earthquakes all but 8 resulted from strike-slip faulting. Of these 8, 5 are on the Pacific coast of North America, 2 in the Hindu Kush, and 1 was an anomalously deep-focus earthquake off the coast of Spain. Otherwise, for all circum-Pacific areas and for the Mediterranean, and for focal depths ranging from 12 to 650 km, strike-slip faulting appears to be the rule. Within any area the strike directions of the faults appear to be random. The dip direction on the other hand may have some consistent orientation. This apparent inconsistency could be explained by supposing that planes whose strikes deviate from a favored direction tend to develop very steep dips.

In any solution the intersection of the two planes defines a unique line, here called the null vector. Whichever plane represents the true solution, this vector is perpendicular to the displacement couple and so undergoes no displacement; hence its name. In the southwest Pacific the null vectors lie parallel to vertical planes striking in the direction of the associated geographical features. In other circum-Pacific areas the correlation is less certain, but it is still definite enough to suggest a considerable measure of confidence in the validity of the fault-plane techniques.

CONTENTS

TEXT

	Page
Introduction	612
Acknowledgments	612
Theory	613
Discussion of some particular solutions	621
Presentation of the solutions	621
Earthquake of July 6, 1934	621
Montana earthquake of June 28, 1925	621
Kern County earthquake of July 21, 1952	621
Tango, Japan, earthquake of March 7, 1927	621
Ancash, Peru, earthquake of Nov. 10, 1946	622
Ecuador earthquake of August 5, 1949	622
Ionian Islands earthquakes of Aug. 9–13, 1953	622
Nevada earthquakes of 1954	623
Spanish earthquake of March 29, 1954	623
Discussion	624
Summary and discussion of available solutions	625
Summary of the solutions	625
Nature of the faulting	625
Direction of faulting	629
Direction of dip	630
Direction of the null vectors	632
Areas of anomalous mechanism	639
Discussion and conclusion	640
References cited	642

ILLUSTRATIONS

Figure		Page
1.	Distribution of compressions and dilatations about vertical fault which undergoes strike-slip displacement	613
2.	Mechanisms which give quadrant distributions of initial compressions and dilatations (After Nakano)	614
3.	Shear-wave distributions resulting from the mechanisms of Figure 2 (After Nakano)	614
4.	Curvature of the seismic ray and the concept of extended position	615
5.	Stereographic projection and the concept of extended distance	616
6.	Type solution, demonstrating the orthogonality criterion	616
7.	Various ray paths and the corresponding extended distances	617
8.	Fault-plane solution for the deep-focus Spanish earthquake of March 29, 1954	617
9.	Fault-plane solution for the New Hebrides earthquake of May 17, 1950	619
10.	Perspective projection of the fault-plane solution for the New Hebrides earthquake of May 17, 1950	620
11.	Mean directions of nodal planes for Greek earthquakes of August 1953	622
12.	Two possible fault mechanisms in the deep-focus Spanish earthquake of March 29, 1954	624

Figure Page
13. Diagram illustrating definition of fault types 629
14. Diagrams showing strike directions of the faults determined by the seismic method . 631
15. Projection used in drawing dip vectors 632
16. Diagrams showing points of emergence of the dip vectors for Pacific earthquakes ... 633
17. Diagrams showing points of emergence of the null vectors for Pacific earthquakes .. 634
18. Map of the southwest Pacific, showing earthquake epicenters 635
19. Map of the northwest Pacific, showing earthquake epicenters 637
20. Map of the Aleutians, showing earthquake epicenters 638
21. Map of the northeast Pacific, showing earthquake epicenters 639
22. Null-vector directions in South American earthquakes 640

TABLES

Table Page
1. Summary of fault-plane solutions carried out by Byerly's method 626
2. Relationship of thrust (+) and gravity (−) dip components to focal depth and geographic feature 630

Introduction

About 30 years ago Perry Byerly, of the University of California, began to develop a technique whereby the direction of faulting in an earthquake may be determined from the records which it writes at seismograph stations throughout the world. From time to time Byerly or his students have collected records from the seismograph stations of the world and have carried out detailed studies of particular earthquakes. As part of these studies they have attempted to produce fault-plane solutions. Many valuable solutions were obtained in this way (Byerly, 1926; 1928; 1930; 1934; 1938; 1955; Adkins, 1940; Tocher, 1955 Ph.D. thesis, Univ. Calif.; Romney, 1956). These solutions, based on the careful study of so many records, were very accurate; but solutions did not accumulate very rapidly by this method.

A program to produce solutions at a much greater rate, as a tool of tectonophysical research, was begun at the Dominion Observatory in 1949. If satisfactory progress were to be made the time could not be taken to collect the seismograph records from all over the world for each earthquake under study. Instead it was necessary to depend on data supplied by seismologists through questionnaires. It was recognized that such data would be less accurate than those obtained from collected records since a uniform reading policy could not be assured, but it was felt that the increased speed at which the data could be obtained would probably justify the method. The program has resulted in the publication of solutions for 65 earthquakes. Combining these 65 solutions with 10 carried out by other investigators using Byerly's method, 75 solutions are available for analysis.

Of these 75 solutions, 67 have indicated that the associated earthquake was the result of strike-slip faulting. This conclusion is not at all in accord with modern tectonophysical thought. It is the purpose of this paper to review the project and to bring its rather unexpected findings to the attention of geologists.

There are four schools of fault plane studies; this paper summarizes the findings of only one. Comparable studies have been carried out in Japan, in Russia, and in Holland. The Japanese method depends on the existence of a large number of stations in the vicinity of the epicenter, and the method is therefore not generally applicable. Scheidegger (In press) has recently compared the methods used by the Russians and the Dutch with the methods described in this paper and has shown that they are equivalent both in the assumptions and in the amount of labor involved. Scheidegger has also summarized (1955; In press) all fault plane studies and has reduced the findings of each of the groups to a common notation.

Acknowledgments

The author is indebted to the colleagues and students who have assisted in the work, as indicated by the joint authorship of the papers listed in the bibliography. Two of the students, R. S. Storey and J. F. J. Allen, have made important contributions to the theory. A special note of thanks is due P. L. Willmore for the many helpful discussions we have had; the discovery of the null-vector pattern is due to a suggestion of his.

I am much indebted to B. Gutenberg, C. F. Richter, and the Princeton University Press for permission to adapt Figures 18–22 from the equivalent maps in *Seismicity of the earth*, and to J. D. Moody and M. J. Hill who sent me a copy of their paper *Wrench-fault tectonics* in advance of publication.

The manuscript has been read by a number of distinguished geologists and geophysicists, including C. S. Beals, P. P. Bijlaard, P. Byerly, Mason L. Hill, D. B. McIntyre, and H. W. Wellman. I am very grateful for the suggestions they have made, both with respect to this paper and to the future course of the research.

Theory

An introduction to the theory can best be given by a simple example. In Figure 1 FF′ represents, in plan, a vertical fault which undergoes a purely transverse motion, in the sense shown, at the instant of an earthquake. It is intuitively evident that points ahead of an arrow are pushed, whereas points behind an arrow are pulled, so that the area surrounding the earthquake epicenter is divided into quadrants, alternately compressional and dilatational with respect to first motion. These quadrants are defined by the traces of the fault plane and a plane drawn perpendicular to the displacement vector. This second plane is called the auxiliary plane.

A second simple example is provided by a vertical fault undergoing purely vertical displacement. If the focus is on the surface the auxiliary plane, being horizontal, provides no trace on the paper. The area surrounding the earthquake is divided into only two zones, one compressional, the other dilatational, by the trace of the fault plane.

These simple cases are of course exceptional in nature. Faulting is not ordinarily vertical, and displacement in most cases has both a strike and a dip component. Thus, whereas the fault plane and the auxiliary plane are always mutually perpendicular, they may be oriented with respect to the surface of the earth in any way, so that the traces of the planes may have any angle between them.

The inverse problem is the interesting one. If there are sufficient stations in the vicinity of an epicenter it is possible to separate those receiving an initial compression from those receiving an initial dilatation by a pair of lines, not necessarily at right angles. One of these lines represents the fault.

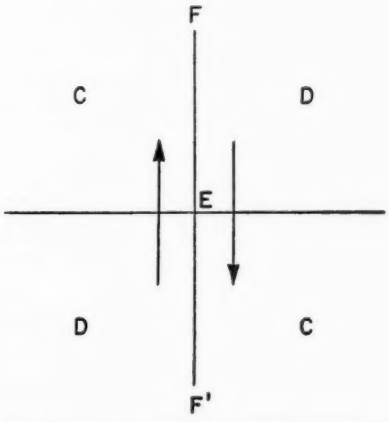

Figure 1.—Distribution of Compressions and Dilatations About Vertical Fault Which Undergoes Strike-Slip Displacement

The above reasoning has been intuitive, but the conclusions reached are in accordance with theoretical studies by Nakano (1923). He showed that two mechanisms give the quadrant distribution here discussed. The first was failure under a couple, as in Figure 2a, the second was failure under two pairs of equal and opposite forces, one pair directed inward at a point, the other pair directed outward from the same point (Fig. 2b).

The Ottawa program has assumed that failure under a couple, the mechanism shown in Figure 2a, is responsible for earthquakes. Under this assumption the plane along which the couple acts becomes a fault plane, and the earthquake is caused by movement along this fault. Most Japanese seismologists have assumed that the mechanism shown in Figure 2b is the appropriate one. Here the planes separating zones of compression from zones of dilatation do not represent planes of failure but are simply planes of no motion—nodal planes.

Insofar as the problem of obtaining solutions is concerned, it does not matter which assump-

tion is made, for in either case one obtains a pair of orthogonal planes. The results of the Japanese and the Ottawa studies can thus be combined. It is only in interpreting the results

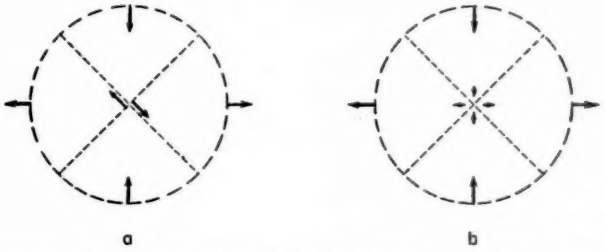

FIGURE 2.—MECHANISMS WHICH GIVE QUADRANT DISTRIBUTIONS OF INITIAL COMPRESSIONS AND DILATATIONS (AFTER NAKANO)

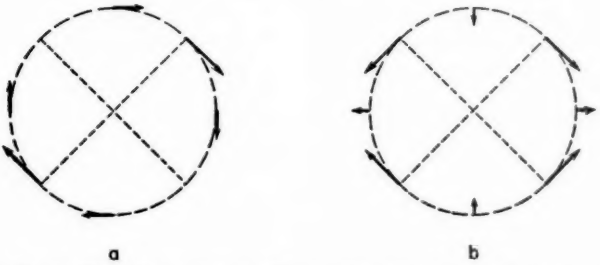

FIGURE 3.—SHEAR-WAVE DISTRIBUTIONS RESULTING FROM THE MECHANISMS OF FIGURE 2 (AFTER NAKANO)

that a difference arises. Do the planes represent a fault and an auxiliary plane, or do they represent a pair of nodal planes?

In theory this matter can be decided through a study of shear waves. Figure 3, taken from Nakano, shows that the direction of shear displacement differs in the two cases. The findings of investigators are not consistent in this matter, however Honda and Masatuka (1952) have shown that the distribution of shear displacements in Japanese earthquakes favors the mechanism of Figure 2b. On the other hand (Scheidegger, In press) the Russians have found many examples in which the "fault" mechanism of Figure 2a is clearly the cause.

This disagreement may be due to the difficulty of identifying S at short distances. For earthquakes originating in the crust some assumption must be made about the number of crustal layers, their thickness, and physical properties. Recent detailed studies as summarized by Gutenberg (1955b) have raised serious doubts about the validity of the multilayered crust previously accepted. Aside from this the identification of S at short distances is never easy. The difficulty of recognizing S at distances of less than 30° has long been recognized (Gutenberg and Richter, 1934, p. 99). Lehmann (1955, p. 366) has recently shown that, in North America at least, S_n has two branches. Hodgson (1953, p. 146) has shown that S_1 and L_g are confused at distances near 10°.

On grounds of geological plausibility the idealized mathematical model of Figure 2b is inacceptable. Even if it is possible for a pressure in one direction and a tension in another to exist at any appreciable depth, the nature of the collapse is difficult to visualize. Faulting, the mechanism of Figure 2a, is, however, commonplace. The San Francisco earthquake was clearly shown (Reid, 1933, p. 87) to be the result of displacement on a visible fault under the action of a couple. Most earthquakes occur at some depth so that the faulting is not visible at the surface, but a majority of seismologists

believe that all large earthquakes are the result of faulting. In a later section of this paper examples will be given in which the direction of faulting obtained from seismological studies has been substantiated by field observations. Thus, on grounds of geological logic, the fault mechanism is preferred. It will be assumed, without further discussion, throughout the remainder of this paper. Figure 3a shows that the use of S would allow the fault plane to be distinguished from the auxiliary plane. The difficulties of using S have already been pointed out. It seems clear that S should be used only after the most careful study of original records. This did not fit in with the concept of the project—to produce a large number of solutions through questionnaires. For that reason S has not been used in the Ottawa project.

It has already been stated that, if there are a large number of stations in the vicinity of an epicenter, the position of the fault plane and of the auxiliary plane can be determined. The only seismic area in the world having a network of seismograph stations adequate for this purpose is Japan. For earthquakes in other areas one must depend on the records from distant stations. This raises two problems.

The first problem is illustrated in Figure 4. Because the velocity of wave propagation increases with depth, seismic impulses travel along curved paths. A ray starting on one side of a fault may curve around to emerge on the other side. Under these circumstances the fault and auxiliary planes cannot accomplish the separation of compressions from dilatations. This difficulty is overcome by a device due to Byerly. Instead of being plotted in its true position S, a station is plotted at a position S', the point where the tangent drawn to the ray at the epicenter meets the surface of the earth. Point S' is known as the extended position of the station. If all stations are plotted on a globe in their extended positions, areas of compression may be separated from areas of dilatation by a pair of orthogonal planes. One of these planes represents the fault.

In practice it is not convenient to work on a globe. Therefore, the second problem is mapping and, primarily, finding the best projection to use. On the globe, areas of dilatation and compression are separated by the intersections of the sphere with the fault and with the auxiliary planes. These intersections are circles. This suggests the stereographic projection, for it is a property of the stereographic projection that circles on the globe project into circles on the map. The problem will be reduced to separating compressions from dilatations by a pair of circles drawn on a map.

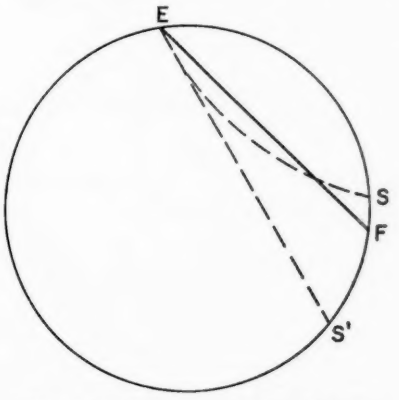

FIGURE 4.—CURVATURE OF THE SEISMIC RAY AND THE CONCEPT OF EXTENDED POSITION

The projection is illustrated in Figure 5. The point on the earth opposite the earthquake epicenter E is used as the pole of projection, and the mapped position of any point, as S', is obtained by joining the pole of the projection to the point, and producing the line to intersect the diametral plane, as at B. Point B is the projected position of S'.

There are two steps in mapping the position of a station: (1) The tangent is drawn to the seismic ray, and the station S is transformed to the point S'; (2) the point S' is projected to B. It is clear from the figure that the two steps can be accomplished simultaneously by mapping the station at its appropriate azimuth with respect to the epicenter and at a distance $OB = R\tan e$ from the center of the map. The length OB is called the extended distance of the station. The radius of the sphere, R, is normally taken as unity, so that the extended distance of any point is the tangent of the angle which the ray, reaching the point, makes with the horizontal.

Figure 5 may be used to illustrate another point. Suppose that a circle is drawn on the sphere to pass through E and S', so that ES' represents the horizontal projection of the circle. It is a property of the stereographic

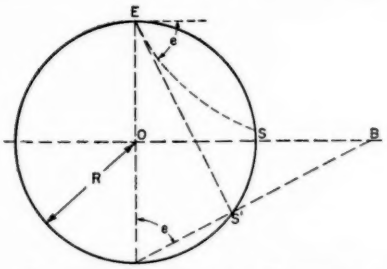

FIGURE 5.—STEREOGRAPHIC PROJECTION AND THE CONCEPT OF EXTENDED DISTANCE

projection that this circle on the sphere projects into a circle on the map. Since the points E and S', at opposite ends of a diameter, plot at distances of zero and *tan e* respectively, the diameter of the circle on the map equals *tan e* that is, the tangent of the angle of dip.

Figure 6 illustrates the sort of map obtained. E represents the projection of the epicenter, and the circles passing through E are the projections of the circles in which the fault plane and the auxiliary plane meet the earth. These circles separate zones of compression from zones of dilatation. The diameters of these circles are proportional to the tangents of the dips of the corresponding planes, and since the tangent of an angle approaches infinity as the angle approaches 90° the diameter of a circle corresponding to a steeply dipping plane becomes very large.

The auxiliary plane was defined as a plane perpendicular to the direction of displacement —that is, perpendicular to a particular line in the fault plane. There must be an equivalent restriction, which has been called the orthogonality criterion, on the circles on the map. This was first realized by Adkins (1940, p. 361) and later by Hodgson and Milne (1951, p. 226) but was never stated in a convenient way. The restriction is stated quite simply. If one circle of radius r is defined, the second circle has its center on a line drawn parallel to the tangent to the first circle, and at a distance $1/4r$ from it. This condition has been illustrated in Figure 6.

This simple approach to the orthogonality condition was discovered by R. S. Storey and has been used since 1952 but was never pub-

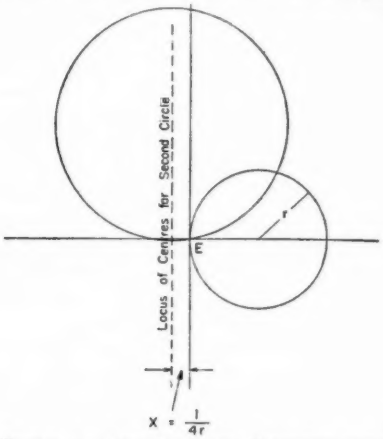

FIGURE 6.—TYPE SOLUTION, DEMONSTRATING THE ORTHOGONALITY CRITERION

lished. It was independently discovered by Ingram (Personal communication), by Baker (Personal communication), and, more recently, by De Bremaecker (1956).

It was demonstrated in Figure 5 that the extended distance of a point is proportional to the tangent of the angle e measured between the horizontal and the ray reaching that particular point. In computing extended distances it is necessary to take into account the fact that this angle varies with the focal depth of the earthquake. Furthermore, energy may reach a particular point by several different pulses: the direct one—P, one reflected off the core—PcP, one reflected off the surface of the earth at a point about half way between the epicenter and the station—PP, and one reflected off the surface of the earth at a point near the focus—pP. The corresponding rays, as shown in Figure 7, leave the focus at different angles; consequently their extended distances are different. If in Figure 7 the point S had been chosen more nearly opposite F, so that the core of the earth interfered with wave propagation, other phases—PKP and $pPKP$—and other angles of emergence would have entered. It is clear that to make a complete study of any earthquake it is necessary to have tables of extended

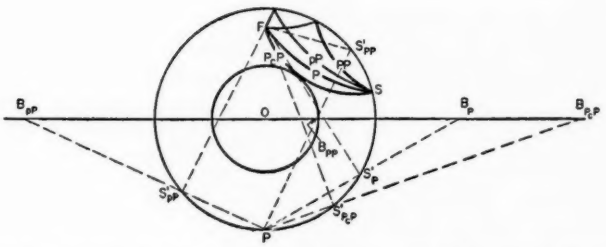

FIGURE 7.—VARIOUS RAY PATHS AND THE CORRESPONDING EXTENDED DISTANCES

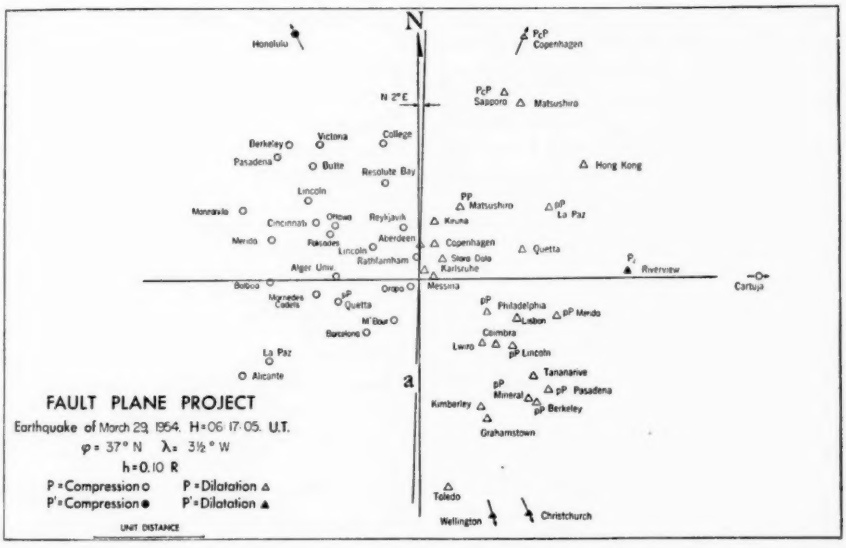

FIGURE 8.—FAULT-PLANE SOLUTION FOR THE DEEP-FOCUS SPANISH EARTHQUAKE OF MARCH 29, 1954

distances for all these phases and for various focal depths. These have been provided (Hodgson and Storey, 1953; Hodgson and Allen, 1954a, b; Hodgson *et al.*, 1956a, b).

In Figure 7 the extended distance corresponding to the phase *pP* is measured in the direction opposite to the extended distances for the other phases. This has come about naturally because the tangent, FS'_{pP}, drawn to the upward-rising ray, is inclined to the opposite side of center. This happens for any phase in which the initial ray rises above the horizontal, for *pP*, for *pPKP*, and for *P* itself if the focus is deep and the station is close to the epicenter. In the table the extended distances for these phases are given with a negative sign; this indicates that in plotting the station an azimuth 180° away from the true one should be used. It is as if the stations had "passed through" the center of the map into their mirror positions.

A recently published solution (Hodgson and Cock, 1956b, p. 325) provides a very good illustration of this "passing through". Figure 8 is reproduced from that paper. The earthquake had its epicenter off the south coast of Spain so that Africa and Australia lie to the south and southeast, Europe to the north and northeast, North America to the northwest, and South America to the southwest. The solution is such that a line striking N. 2° E. separates compressions on the west from dilatations on the east.

Because this earthquake had a focal depth of more than 600 km, the Spanish and Portugese stations received their initial impulse from rays which rose above the horizontal. For this reason Cartuja is plotted off scale to the right, and Lisbon and Coimbra are plotted in the southeastern quadrant with the African stations. Similarly Alicante and Barcelona have passed through center and are found in the southwest quadrant. The impulse recorded on these phases agrees with that recorded directly.

The phase *pP* also provides many examples of this "passing through." The *pP* from many California stations are plotted near the South African stations of Kimberley and Grahamstown and agree with them in phase. Similarly the *pP* for the South American station of La Paz is plotted between Copenhagen and Hong Kong and agrees in phase with those stations. To obtain this agreement it has been necessary to plot *pP* with a phase change due to its reflection.

This matter of phase change on reflection has caused some confusion in fault-plane studies. For example, a very well-known solution by Koning (1941, p. 161) is vitiated by the fact that no allowance has been made for the change of phase on reflection. The question is not a simple one. It has recently been investigated for *PcP* by Båth (1954) and for *pP* and *PP* by Ingram and Hodgson (1956).

By way of example a solution will now be carried out to illustrate the method and its limitations. Figure 9 gives a solution, already published elsewhere (Hodgson, 1956a, p. 186), for a normal-focus earthquake in the New Hebrides. For this earthquake data were available for 28 observations of *P*, for 30 observations of PKP_1, for two observations of PKP_2, and for 11 observations of *PP*. This makes 71 observations. Most of these are plotted on the diagram; a triangle is used to indicate a dilatation, a circle to indicate a compression. The observations are plotted at the calculated azimuth from the epicenter and at an extended distance appropriate to the depth of focus of the earthquake, the distance of the station from the epicenter, and the nature of the phase. In the case of the *PKP* phases (called *P′* in the diagram), which penetrate the core of the earth, the extended distances are so large that they lie far off the diagram. Only their azimuths have been indicated.

After the stations have been plotted, circles are drawn to separate compressions from dilatations. Most of the observations of PKP_1 are compressional. There were six dilatational observations, only two of which are shown, but in each case they were surrounded by a preponderant number of compressional observations so that it is necessary to conclude that the dilatational observations are incorrect. Therefore the field, the area at remote distance from the epicenter, is taken to be compressional, so that the circles must be drawn to contain dilatations.

The Japanese stations are unanimously compressional, but they are surrounded to the east, west, and south by dilatational observations. Therefore, the Japanese stations are placed in the overlap of the two circles, circle *a* being drawn to separate Sendai from the *PP* observation of De Bilt and to include the P_2' observation of Alger University within its compass. This same circle provides a separation between the Australian stations of Brisbane and Riverview and the New Zealand stations, Auckland to Christchurch. Circle *a* has a radius, as drawn, of 2.62 units.

A tangent to this circle is then drawn at the origin and a line is drawn parallel to this tangent and at a distance

$$1/(4 \times 2.62) = 0.095 \text{ units}$$

from it. The center of the second circle must be on this line. By the appropriate choice of the center the *PP* observations at Cartuja, Weston, and State College are included, the compressions at College and at the California stations are excluded. This second circle has a radius of 1.46 units. A line parallel to the tangent drawn to this circle at the origin and at a distance

$$1/(4 \times 1.46) = 0.17 \text{ units}$$

from it, passes through the center of circle *a*. This provides a check on the work, and assures that the orthogonality criterion has been satisfied.

As the circles are drawn there are four inconsistent observations of *P*. One of these, Honolulu, was described as a doubtful reading by officers of the United States Coast and

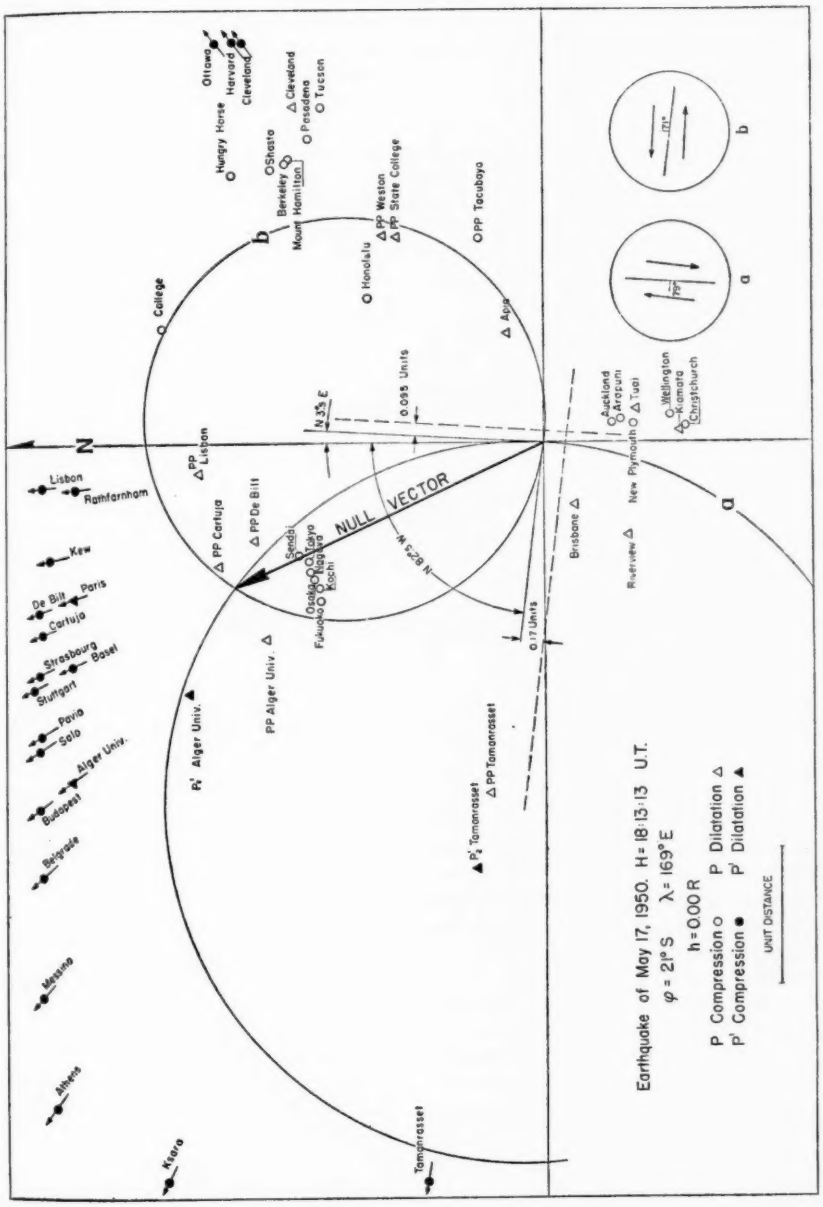

FIGURE 9.—FAULT-PLANE SOLUTION FOR THE NEW HEBRIDES EARTHQUAKE OF MAY 17, 1950

Geodetic Survey who completed our questionnaire. The dilatation reported at Cleveland is inconsistent with compressions both closer to the origin and farther from it. Clearly there is no way of bringing it into the solution. There are two inconsistent observations in New Zealand, but these could be made consistent only at the expense of three other New Zealand stations and by swinging the center of the circle off the line on which it must lie. The four inconsistent observations of P are not too disturbing.

Two cases are distinguished. In the insert diagram a circle a is taken to represent the fault, and circle b to represent the auxiliary plane. The strike of the fault is then parallel to the tangent of circle a, and the tangent of the angle of dip is equal to the diameter of circle a. The arrows in the insert diagram indicate the direction of displacement and show in this case that the faulting is strike-slip with a very slight thrust component. These arrows are drawn parallel to a line joining the center of circle b to the origin.

Insert diagram b gives the other possibility, in which circle b is taken to represent the fault.

Figure 10 is a perspective diagram illustrating the solution of Figure 9. The two planes a and b are shown, and in each plane a vector has been drawn, perpendicular to the other plane. These vectors are labeled the possible positions of the motion vectors; only one of them can, of course, be the motion vector.

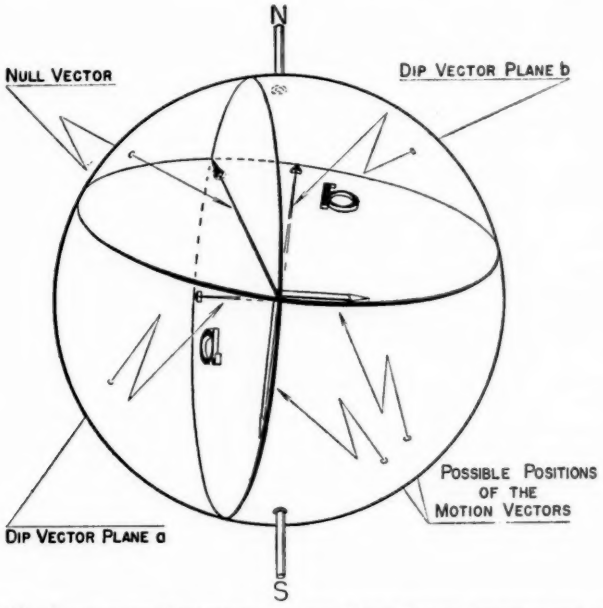

FIGURE 10.—PERSPECTIVE PROJECTION OF THE FAULT-PLANE SOLUTION FOR THE NEW HEBRIDES EARTHQUAKE OF MAY 17, 1950
$\varphi = 21°S.$ $\lambda = 169°E.$

In a later section of this paper much use will be made of the terms dip vectors and null vector. These vectors are defined in Figure 10. The dip vector of a plane is drawn in the direction of the maximum dip of that plane, from the epicenter to the other point of emergence; its length is equal to the separation of the two points of emergence. The null vector is a vector drawn along the line of intersection of the two planes, from the epicenter to the other point of emergence; its length is equal to the separation of these two points of emergence. The null vector is also shown in Figure 9 as the line joining the two points of intersection of the circles.

In the solution shown in Figure 9 there are 13 inconsistent observations out of 71 observations. This is about the usual percentage except in those cases in which the records can be personally examined. If this is possible the number of inconsistencies becomes very small; this may of course be an indication of bias. A statistical study is now under way to investigate these inconsistent observations.

One final observation may be made from Figure 9. In this case where the circles were drawn to contain dilatations the dip component was up-dip, indicative of thrust. Had the circles been drawn to contain compressions the dip component would have been down-dip, indicating tension. Thus, even when the displacement is almost pure strike-slip, the solutions allow a distinction as to whether the dip component was indicative of pressure or of tension.

Discussion of Some Particular Solutions

Presentation of the Solutions

General statement.—In order to gain acceptance for the fault-plane techniques it is desirable whenever possible to obtain solutions for earthquakes in which faulting has been observed. This is difficult because only a very small percentage of earthquakes are accompanied by surface faulting. It is impractical to go far into the past in search of examples. The records for those old earthquakes are usually in dead storage and difficult to obtain, and frequently the seismograph has been too insensitive to give a clear reading of first motion.

Despite these difficulties, several solutions which show agreement either with observed faults or with an inferred direction of faulting have been made by various investigators.

Earthquake of July 6, 1934.—This earthquake, off the coast of northern California, was studied by Byerly (1938). He located the epicenter at 41°26′ N., 124°30′ W., a point which is in line with the San Andreas fault. There was a slight ambiguity in the fault-plane solution, but the mean strike of the plane selected by Byerly as the fault was determined as N. 43° ± 3° W. This plane had an almost vertical dip, and the movement on it was strike-slip so that the oceanic side moved north relative to the continental side. This strike direction, dip, and direction of motion are expected from an earthquake having its epicenter on the San Andreas fault. Although the actual fault cannot be seen, the example may be regarded as a confimation.

Montana earthquake of June 28, 1925.—A fault-plane solution has recently been given for this earthquake by Byerly (1955, p. 81). He again finds strike-slip faulting along a plane striking N. 26° E. and dipping about 87° SE. There was no surface displacement, but Byerly gives evidence that the earthquake occurred at depth on an existing fault. This fault had a strike of between N. 10° E. and N. 20° E., dipped to the northwest, and was regarded as a thrust fault. The fault-plane solution gives a reasonably good agreement with the strike direction but disagrees with the direction of dip and with the sense of movement.

Kern County earthquake of July 21, 1952.—Gutenberg has applied the tables of extended distances (Hodgson and Storey, 1953) to determine the fault mechanism in the earthquake which did so much damage to Tehachapi and Arvin in July 1952.

The published solution (Gutenberg, 1955a, p. 166) shows a fault plane striking N. 50° E. and dipping 63° SE. The auxiliary plane is not so well defined, but in its mean position it indicates that the faulting was principally thrust, and that the hanging wall moved approximately north. Gutenberg has made detailed studies of *S* amplitudes which agree with the conventional solution.

Buwalda and St. Amand (1955, p. 43) report that the observed fault is indeed a thrust, striking N. 50°E. on the average and dipping 45°–60° SE. The strike and dip obtained in the fault-plane solution are thus sustained. Buwalda and St. Amand report that the relative motion along the fault was variable but on an average agrees with a northward motion of the hanging block. Field observations thus confirm the seismic solution.

Tango, Japan, earthquake of March 7, 1927.—The direction of faulting in this earthquake was very well observed, and Prof. H. Honda suggested that it might provide an excellent opportunity to check the fault-plane techniques. The difficulties of working with old records have already been mentioned, but a study of this

earthquake had been made much earlier by E. A. Hodgson (1932, Ph.D. thesis, Saint Louis Univ.), and copies of many of the seismograms have been preserved. The data from these records were not sufficient to permit an independent solution, but it was found (Hodgson, 1955a, p. 40) that the observations which were available were consistent with the observed direction of faulting.

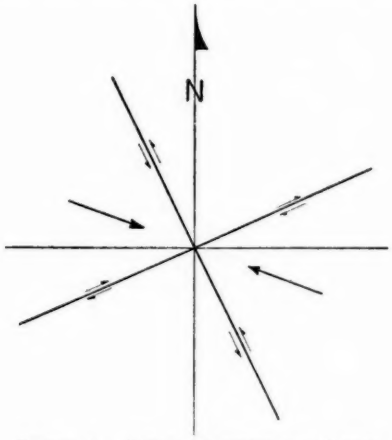

FIGURE 11.—MEAN DIRECTIONS OF NODAL PLANES FOR GREEK EARTHQUAKES OF AUGUST 1953

Ancash, Peru, earthquake of November 10, 1946.—When a paper by Silgado (1951) described the surface faulting which accompanied this earthquake, an excellent opportunity seemed to be afforded for a check on the fault-plane techniques. The faulting consists of a pair of parallel faults, striking N. 42° W. on the average, and dipping toward each other. Motion was almost vertical, so that the ground between the faults had subsided.

The fault-plane solution (Hodgson and Bremner, 1953, p. 122) obtained a satisfactory value for the strike of N. 45° W., but the plane dips northeast instead of southwest as observed, and the motion was almost purely strike-slip instead of normal. This is another example, like that of the Montana earthquake discussed earlier, where the seismic solution confirmed the strike direction but did not agree either with the dip or direction of movement.

In this case there is abundant evidence that the first motion did not arise at the surface, but at a depth of 30 or 40 km, so that the earthquake did not provide the definitive test which had been hoped for.

Ecuador earthquake of August 5, 1949.—The fault-plane solution for this earthquake (Hodgson and Storey, 1954, p. 68) shows one circle corresponding to a plane striking N. 2° W. Ramirez and Semanate (1951, p. 16) mention surface faulting striking northward, show that the isoseismal lines have a northward-trending major axis, and find four separate "seismic focuses" which are aligned "in a direction north to south". This seems to provide another confirmation of the strike direction obtained by the fault-plane analysis.

Ionian Islands earthquakes of August 9–13, 1953.—Solutions have recently been published (Hodgson and Cock, 1956a) for eight earthquakes of the series which did so much damage to the islands of Cephalonia, Ithaca, and Zante in August 1953. This is the first time in which solutions have been obtained for a major earthquake and for its principal foreshocks and aftershocks.

As usual, each solution defined a pair of planes without indicating which plane represented the fault. The solutions were so much alike that it was possible to fix mean directions for the planes. These are shown in Figure 11. The mean directions for the planes are:

for plane *a* N. 67° ± 7° E.,

for plane *b* N. 26° ± 7° W.;

the uncertainties are standard deviations of the means. In seven of the shocks the displacements are as shown in Figure 11; in one of the foreshocks the direction of displacement is reversed.

Galanopoulos, who studied the earthquakes in the field, found that there are two directions of faulting, SSE-NNW and ENE-WSW which form a conjugate system. In the earthquakes of the sequence faulting occurred first on one set, then on the other. Because the two directions of faulting agree very closely with the directions of the two planes found in the seismic solution it is impossible to select a particular plane in any one case. Nevertheless the agreement is

very satisfactory, even though the ambiguity cannot be resolved.

Nevada earthquakes of 1954.—At the Reno meetings of the Cordilleran Section of The Geological Society of America (March 29–31, 1956) a field trip was arranged to Fairview Peak and to Dixie Valley to view faulting associated with the earthquakes of December 16, 1954. At the same meetings Romney (1956) read a paper giving the seismic solution for the fault plane of this earthquake. The faulting was so spectacular, and the agreement between the seismic solution and the faulting is so satisfactory, that it seems desirable to mention the solution here, even though it became available too late to be included in the summary which appears later in this paper.

The Fairview Peak earthquake was one of four which took place in the area during the last half of 1954. The first pair occurred on July 6 and August 24, at 39.5° N, 118.5° W., just east of Fallon. These earthquakes were studied by Tocher (1955, Ph.D. thesis, Univ. Calif.), both in the field and from the seismograph records. Surface faulting, trending slightly east of north, was found in the epicentral area. The seismic solutions suggested a fault strike of N. 24° W. for the earthquake of July 6, and of N. 5° W. for the earthquake of August 24. Thus the seismic solution in each case gave a strike direction with a more westerly trend than that actually observed.

The second pair of earthquakes took place on December 16, about 20 miles east of the first set. They were studied, both in the field and from the seismograph records by Romney (1956, p. 1782). These earthquakes resulted in surface faulting on Fairview Peak and in Dixie Valley. In both areas the faults trend slightly east of north. The displacement on the Dixie Valley fault is principally vertical, but the Fairview Peak fault, which dips 55°–70°E., has a large transverse component. In many places the transverse component is about twice as large as the vertical component, although there was a good deal of graben collapse in the fault zone which tended to accentuate the vertical component.

The two earthquakes occurred within 4 minutes of each other, and because of the resulting confusion of the records a seismic solution for the direction of faulting could be made for the first, or Fairview Peak, shock only. This indicated a fault striking N. 11°W., dipping about 60° to the east, and undergoing right lateral displacement such that the horizontal movement was about twice the vertical. The seismic solution thus agreed very well with the observed fault plane except that, once again, the seismic solution gave a strike with a more westerly trend than that actually observed.

Fortunately in this case the United States Coast and Geodetic Survey had a very close geodetic network set up in the area before the earthquake. A resurvey begun immediately after the earthquake showed that the relative displacement of points on opposite sides of the fault is in a direction slightly west of north, so that the relative horizontal displacement is about 8½ feet, the relative vertical displacement about 4 feet. The geodetic measurements agree with the seismic solution almost exactly. It is clear that in this instance the displacement observed in the surface rocks is a secondary effect and does not give an exact indication of the regional displacement. The seismic solution appears to have given the true picture of regional adjustment.

Spanish earthquake of March 29, 1954.—A description of this earthquake is included, not because it provides any confirmation of the method, but because the solution is interesting in itself. This earthquake occurred near Granada at a depth in excess of 600 km. No earthquake with greater than normal focal depth is known to have occurred in this area previously, and indeed the occurrence of a deep-focus earthquake away from the borders of the Pacific Ocean is remarkable. The fault-plane solution (Hodgson and Cock, 1956b, p. 326) suggests that the mechanism is also unusual.

Part of the solution is shown, in another connection, in Figure 8. That figure suggests a solution in terms of a straight line. In fact the line is not straight but is the arc of a very large circle, and a second circle exists, too small to appear in a diagram of the scale of Figure 8. Within the limits of error, however, the solution may be given in terms of two planes, one striking northward and lying vertical, the other lying horizontal.

The situation is illustrated in Figure 12, which distinguishes two possible cases. In case *a* the fault strikes northward and is vertical, and the motion is such that the eastern side rose vertically with respect to the western side. In the alternative solution, *b*, the fault is horizontal, and the material above the fault moved due eastward, that is, in the direction of the earth's rotation. This suggests that the earthquake may indicate a failure connected in some way with the rotation of the earth.

FIGURE 12.—TWO POSSIBLE FAULT MECHANISMS IN THE DEEP-FOCUS SPANISH EARTHQUAKE OF MARCH 29, 1954

Discussion

The Spanish earthquake cannot be said to have provided any check with inferred direction of faulting, but aside from it 10 examples have been presented in which fault-plane solutions have obtained some measure of geological confirmation. Perhaps the most significant of these is the Kern county earthquake in which a single group of investigators, able to control and compare all aspects of the study, found satisfactory confirmation of the method. Good confirmation also was obtained in the case of the Tango earthquake and in the series of Greek earthquakes. In two other cases, the California earthquake of July 6, 1934, and the Ecuador earthquake of August 5, 1949, a good check was obtained with fault directions determined by reasonable inference.

There remain two cases, the Montana earthquake of 1925 and the Peru earthquake of 1946, in which the fault-plane solutions were confirmed insofar as strike direction is concerned, but were in error in dip direction and in the direction of displacement. In the case of the Montana earthquake of June 28, 1925, Byerly obtained strike-slip faulting on a plane dipping southeastward, whereas the faults observed in the vicinity dip northwestward and have been regarded as thrust faults. No displacements were observed on these faults at the time of the earthquake, which had its focus at some depth within the earth.

There are several possible explanations of the discrepancy. Since no displacement was observed on the surface faults at the time of the earthquake there may be no connection between the earthquake and the visible faults. Alternatively adjustments may be taking place along faults established under an earlier and different system of forces. Or, more significantly, faulting at depth may differ from that at the surface.

This last explanation seems to apply in the case of the Ancash earthquake. Here surface motion was very clearly observed; there is no questioning the fact that, on the surface, a rift fault occurred. The seismic solution make it equally clear that at a depth of 35 or 40 km the faulting was almost purely strike-slip. Is it possible that a strike-slip fault at depth would be accompanied by rift faulting at the surface?

J. Tuzo Wilson (1953, p. 350) quotes E. M. Anderson (1942, p. 154) in support of a theory that rift valleys may be surface manifestations of strike-slip faulting at depth. The argument is based on the very straight strike of rift valleys and on the fact that strike-slip faults in nature frequently have a hinging action, the vertical displacements being in opposite directions on opposite sides of the hinge. There seems to be good agreement between this theory and the seismic solution of the Ancash earthquake.

Finally, the seismic solution of Nevada earthquakes gave strike directions which did not agree exactly with observed surface faulting but which did agree exactly with geodetic evidence in the one case where such evidence was available. In this one instance at least, the

seismic solution, in defining displacement at depth, gave a true picture of the regional displacement. When the fault-plane techniques have been accepted by geologists, their findings can probably be used to cast light on details of fault mechanism which are not well understood.

Summary and Discussion of Available Solutions

Summary of the Solutions

A total of 75 geometrically consistent solutions have been made by Byerly's method by various investigators. The results of these analyses have been arranged, geographically, in Table 1. Numbers have been assigned to the earthquakes as much as possible in a clockwise direction around the Pacific basin. In the western Pacific the numbers run from south to north, in the Aleutians from west to east, and in the eastern Pacific from north to south. For earthquakes in Asia and Europe the numbers have been assigned from east to west, that is from the Hindu Kush through the Mediterranean.

There are seven principal columns in Table 1. The first describes the earthquakes, assigns numbers to them, and gives date, location, and focal depth for each. The second principal column gives the strike and dip of plane *a* and, supposing it to represent the fault, projects a unit displacement vector in the direction of strike and in the direction of dip. The third principal column gives equivalent information for plane *b*, supposing it to represent the fault. Where possible the designation *a* is applied to that plane striking into the northeast quadrant, the designation *b* to that plane striking into the northwest quadrant. In several instances this has resulted in a change from the designation applied in the original paper. It should be stressed that calling a particular plane *a* or *b* is only a matter of convenience. There is no reason to suppose that planes with similar designation form any kind of related system. The fourth principal column lists the trend and plunge of the "null vectors". The term null vector was defined in connection with Figure 10. The fifth and sixth columns indicate which of solutions *a* or *b* has a dextral transverse motion and which a sinistral. The final column gives reference to the publication in which the particular earthquake was originally discussed.

Nature of the Faulting

In the analysis of the nature of the faulting shown in Table 1 a classification similar to that outlined by Billings (1947, p. 152) is used. The fault plane is divided into four quadrants (Fig. 13) by two lines intersecting at *O* and making an angle of 45° with a horizontal line in the fault plane. If the relative movement of the hanging wall is such that the net slip can be indicated by a vector beginning at *O* and lying in the upper quadrant the fault is a thrust fault. If the vector lies in the lower quadrant the fault is a gravity fault. In those cases where the vector lies in the right or left quadrants we shall say that the faulting was strike-slip. An equivalent British term, which has been used in earlier publications, is transcurrent. The term wrench has also been used.

The notation of Table 1 lends itself to the analysis very readily. The 45-degree lines of Figure 13 correspond to faulting in which the strike and dip components were equal. If the strike component of Table 1 is greater than the dip component the faulting is strike-slip; if the strike component is less than the dip component the faulting is either thrust or gravity, depending on the direction of the dip slip. This direction has been defined by signs, + or −, attached to the dip component. A + sign indicates a thrust-dip component, a − sign indicates a gravity-dip component. The equivalent information for the transverse motion, as to which solution represents dextral faulting and which sinistral, has been given in separate columns.

In every earthquake analyzed in New Zealand, the Kermadecs, the Tongas, the New Hebrides, the Solomons, Japan, the Sakhalins, the Kuriles, Kamchatka, and in South America, strike-slip faulting is indicated. The fact that we do not know whether plane *a* or plane *b* represents the fault does not vitiate the conclusion that strike-slip faulting is the rule in most circum-Pacific earthquakes, regardless of focal depth.

In one section of the circum-Pacific this rule about strike-slip faulting does not apply;

TABLE 1.—SUMMARY OF FAULT-PLANE SOLUTIONS CARRIED OUT BY BYERLY'S METHOD

EARTHQUAKE					PLANE a					PLANE b					Null Vector		DEXTRAL Solution	SINISTRAL Solution	REFERENCE
Number	Date	φ	λ	Focal Depth-km.	Strike Direction	Dip Direction	Dip	Strike Component	Dip Component	Strike Direction	Dip Direction	Dip	Strike Component	Dip Component	Trend	Plunge			
	New Zealand																		
1	January 13, 1954	49° S	165° E	Normal	N 43.5° E	S 46.5° E	86°	0.988	+0.156	N 45.5° W	S 44.5° W	81°	0.998	+0.070	S 21° W	80.3°	a	b	Hodgson, 1956 a.
2	September 29, 1953	36.5° S	177° E	300	N 54° E	S 36° E	87°	1.000	+0.017	N 36° W	S 54° W	89°	0.999	+0.052	S 19° E	86.5°	a	b	Hodgson, 1956 a.
	Kermadec Islands																		
3	March 23, 1951	31° S	180°	300	N 33° E	N 57° W	86°	0.906	−0.423	N 59° W	S 31° W	66°	0.998	−0.070	S 41° W	65°	a	b	Hodgson, 1956 a.
4	November 22, 1949	29° S	178° W	Normal	N 49.5° E	N 40.5° W	86°	0.999	+0.035	N 40.5° W	N 49.5° E	88°	0.999	+0.070	N 6° W	85.2°	a	b	Hodgson and Storey, 1954.
5	September 11, 1952	29° S	177° W	Normal	N 33° E	—	90°	0.995	0.104	N 57° W	N 33° E	84°	1.000	0.000	N 33° E	84°	b	a	Hodgson, 1956 a.
6	August 28, 1951	27° S	178° E	600	N 47.5° E	N 42.5 W	87°	0.999	−0.053	N 42.5° W	N 47.5° E	87°	0.999	−0.053	N 6° E	86°	b	a	Hodgson, 1956 a.
	Tonga Islands																		
7	September 8, 1948	21° S	174.2° W	Normal	N 28° E	S 62° E	87°	0.743	+0.670	N 59° W	S 31° W	48°	0.998	+0.070	S 23.5° W	47.8°	a	b	Webb, 1954.
8	July 27, 1952	20.5° S	179° W	500	N 17° E	N 73° W	88°	0.883	+0.470	N 73° W	N 17° E	62°	0.999	+0.040	N 14° E	61.5°	a	b	Hodgson, 1956 a.
9	August 6, 1949	19.2° S	174.7° W	100	N 45° E	N 45° W	80°	0.903	+0.429	N 52° W	S 38° W	65°	0.982	+0.192	S 65° W	62.8°	b	a	Webb, 1954.
10	February 25, 1952	17° S	173.5° W	Normal	N 37.5° E	N 52.5° W	87°	0.951	−0.309	N 52.5° W	N 37.5° E	72°	0.999	−0.052	N 28° E	71.8°	b	a	Hodgson, 1956 a.
11	June 29, 1948	16° S	173° W	100	N 47° E	N 43° W	86°	0.996	+0.087	N 42° W	N 48° E	85°	0.998	+0.070	N 7° E	82.9°	a	b	Webb, 1954.
12	February 13, 1951	15° S	175° W	200	N 58° E	N 32° W	86°	0.999	+0.035	N 32° W	S 58° W	88°	0.998	+0.070	N 66° W	85.5°	b	a	Hodgson, 1956 a.
	Fiji Islands																		
13	September 14, 1953	18.5° S	178.5° E	Normal	N 61° E	N 29° W	83°	0.999	−0.035	N 29° W	N 61° E	88°	0.993	−0.122	N 9° W	82.9°	b	a	Hodgson, 1956 a.
	New Hebrides Islands																		
14	May 17, 1950	21° S	169° E	Normal	N 3.5° E	N 86.5° W	79°	0.944	+0.331	N 82.5 W	N 7.5° E	71°	0.979	+0.202	N 25° W	67.9°	a	b	Hodgson, 1956 a.
15	May 19 A, 1950	20.5° S	169° E	Normal	N 31.5° E	N 58.5° W	84°	0.944	+0.329	N 56.5° W	N 33.5° E	71°	0.994	+0.111	N 14.5° E	69.7°	a	b	Hodgson, 1956 a.
16	May 19 B, 1950	20.5° S	169° E	Normal	N 2° E	N 88° W	84°	0.970	+0.243	N 86.5° W	N 3.5° E	76°	0.994	+0.108	N 20° W	74.3°	a	b	Hodgson, 1956 a.
17	June 24, 1950	20.5° S	169.5° E	Normal	N 88.5 E	N 1.5° W	72°	0.950	+0.313	N 3.5° W	S 86.5° W	81°	0.986	+0.164	N 29° W	69.5°	a	b	Hodgson, 1956 a.
18	July 17, 1950	20.5° S	171° E	100	N 60° E	N 30° W	78°	0.999	+0.053	N 30° W	S 60° W	67°	0.978	+0.208	N 44° W	77.8°	b	a	Hodgson, 1956 a.
19	May 26, 1950	20.2° S	169.2° E	Normal	N 10° E	N 80° W	73°	0.952	+0.306	N 74.5° W	N 15.5° E	73°	0.952	+0.306	N 32° W	65.5°	a	b	Hodgson, 1956 a.
20	June 21, 1950	20.2° S	169.2° E	Normal	N 10.5° E	N 79.5° W	77°	0.936	+0.351	N 75.5° W	N 14.5° E	70°	0.971	+0.239	N 21° W	66.2°	a	b	Hodgson, 1956 a.
21	May 27, 1950	20° S	168° E	200	N 72° E	N 18° W	87°	0.999	−0.054	N 18° W	S 72° W	87°	0.999	−0.051	N 65° W	87°	a	b	Hodgson, 1956 a.
22	May 28, 1950	20° S	169° E	Normal	N 47° E	N 43° W	68°	1.000	0.000	N 43° W	—	90°	0.927	0.375	N 43° W	68°	a	b	Hodgson, 1956 a.
23	July 23, 1949	18.5° S	169° E	200	N 49° E	S 41° E	67°	0.995	+0.095	N 40° W	S 50° W	85°	0.919	+0.393	S 28.5° E	66.4°	a	b	Hodgson and Storey, 1954.
24	July 13, 1952	18.5° S	169.5° E	350	N 16.5° E	S 73.5° E	70°	0.924	+0.381	N 81° W	N 9° E	69°	0.930	+0.367	N 56.5° E	60.6°	b	a	Hodgson, 1956 a.
25	July 2, 1953	18.5° S	169° E	200	← Not defined →				+ →	N 66.5° W	S 23.5° W	87°	←	+ — Not defined —		→	-	+	Hodgson, 1956 a.
26	December 2, 1950	18.2° S	167° E	Normal	N 48° E	S 45° E	86°	0.999	+0.034	N 44° W	S 46° W	88°	0.998	+0.069	S 20° E	85.2°	a	b	Webb, 1954.
27	July 21, 1950	15.5° S	168.5° E	Normal	N 47° E	S 43° E	35°	0.842	+0.539	N 71° W	N 19° E	72°	0.508	+0.861	← Not defined →		b	a	Hodgson, 1956 a.
28	March 10, 1951	15.2 S	167.5° E	150	N 41° E	N 49° W	84°	0.988	−0.157	N 48° W	N 42° E	81°	0.994	−0.105	N 8° E	79.3°	b	a	Webb, 1954.
29	July 22, 1950	14° S	167° E	Normal	N 57° E	N 33° W	76°	1.000	+0.018	N 33° W	N 57° E	89°	0.970	+0.242	N 27.5° W	75.8°	a	b	Hodgson, 1956 a.

Number	Date	φ	λ	Focal Depth-km.	PLANE a: Strike Direction	PLANE a: Dip Direction	PLANE a: Dip	PLANE a: Strike Component	PLANE a: Dip Component	PLANE b: Strike Direction	PLANE b: Dip Direction	PLANE b: Dip	PLANE b: Strike Component	PLANE b: Dip Component	Null Vector: Trend	Null Vector: Plunge	DEXTRAL Solution	SINISTRAL Solution	REFERENCE
	Solomon Islands																		
30	May 9, 1952	6.5° S	155° E	100	N 38.5° E	S 51.5° E	56°	0.928	+0.373	N 63.5° W	N 26.5° E	72°	0.809	+0.588	S 87° E	58°	b	a	Hodgson, 1956 a.
	Japan																		
31	March 7, 1927	35.6° N	135° E	12	N 55° E	S 35° E	79°	0.895	+0.446	N 29° W	S 61° W	64°	0.977	+0.212	S 34° W	61.6°	a	b	Hodgson, 1955 a.
	Vladivostok Area																		
32	April 5, 1949	43° N	131° E	550	N 67° E	N 23° W	64°	0.831	+0.556	N 6° W	N 84° E	60°	0.863	+0.506	N 34.5° E	46.1°	a	b	Hodgson and Storey, 1954.
	Sakhalin Islands																		
33	June 27, 1950	46.5° N	140° E	Normal	N 0.5° W	S 89.5° W	71°	0.957	-0.291	N 85° W	N 5° E	74°	0.941	-0.339	N 47° W	64.4°	b	a	Hodgson, 1956 b.
34	February 26, 1950	46° N	143.5° E	360	N 14.5° E	N 75.5° W	55°	0.955	-0.295	N 66.5° W	N 23.5° E	76°	0.807	-0.591	N 48° W	51.6°	b	a	Hodgson, 1956 b.
	Kurile Islands																		
35	June 22, 1952	46° N	153.5° E	Normal	N 21° E	S 69° E	82°	0.974	-0.227	N 71° W	N 19° E	71°	0.990	-0.143	N 53° E	74.3°	a	b	Hodgson, 1956 b.
36	November 3, 1949	45° N	154° E	200	N 25° E	S 65° E	79°	0.973	-0.229	N 67° W	N 23° E	77°	0.981	-0.196	N 62.5° E	73°	a	b	Hodgson and Storey, 1954.
37	May 3, 1949	49° N	153° E	100	N 89° E	N 1° W	71°	0.962	+0.274	N 6° W	S 84° W	75°	0.941	+0.337	N 42° W	65.3°	b	a	Hodgson and Storey, 1954.
38	January 12, 1953	49.5° N	156° E	Normal	N 24° E	S 66° E	77°	0.850	+0.528	N 58° W	S 32° W	59°	0.968	+0.253	S 5° W	55.9°	a	b	Hodgson, 1956 b.
	Kamchatka																		
39	March 5, 1953	51° N	158° E	Normal	N 47° E	—	90°	0.914	0.407	N 43° W	N 47° E	66°	1.000	0.000	N 47° E	65.7°	b	a	Hodgson, 1956 b.
40	November 4 A, 1952	52.5° N	159° E	Normal	N 10° E	S 80° E	79°	0.937	-0.349	N 84.5° W	N 5.5° E	70°	0.979	-0.203	N 36° E	67.5°	a	b	Hodgson, 1956 b.
41	November 4 B, 1952	52.5° N	159° E	Normal	N 82° E	N 8° W	89°	1.000	-0.017	N 8.5° W	S 81.5° W	89°	1.000	-0.017	N 41° W	83.6°	a	b	Hodgson, 1956 b.
42	November 29, 1952	53° N	160° E	Normal	N 30.5° E	N 59.5° W	76°	0.908	-0.419	N 53.5° W	N 36.5° E	66°	0.964	-0.265	N 2° E	62.2°	b	a	Hodgson, 1956 b.
43	October 5, 1953	53.5° N	160.5° E	Normal	N 16.5° E	N 73.5° W	72°	0.957	-0.290	N 69.5° W	N 20.5° E	74°	0.947	-0.322	N 30° W	65°	b	a	Hodgson, 1956 b.
	Aleutian Islands																		
44	March 27, 1950	53.5° N	173° E	Normal	N 60.5° E	N 29.5° W	80°	0.960	+0.280	N 32.5° W	S 57.5° W	74°	0.984	+0.181	W	71°	b	a	Hodgson, 1956 b.
45	August 28, 1949	52.5° N	178° W	Normal	N 9° E	N 81° W	83°	◄	+	Not defined				+	►		-	-	Hodgson and Storey, 1954.
46	April 1, 1946	53.5° N	163° W	Normal	N 22.5° E	N 67.5° W	85°	0.906	-0.424	N 65° W	N 25° E	65°	0.995	-0.096	N 17° E	64.8°	b	a	Hodgson and Milne, 1951.
47	February 25, 1953	56° N	156.5° W	Normal	N 63° E	N 27° W	71°	0.932	-0.362	N 35° W	S 55° W	70°	0.838	-0.546	N 75° W	61.3°	a	b	Hodgson, 1956 b.
48	November 29, 1952	56° N	155° W	Normal	N 75° E	S 15° E	81°	0.987	-0.158	N 14° W	N 74° E	81°	0.987	-0.158	S 57.5° E	77.2	a	b	Hodgson, 1956 b.
	Alaska																		
49	July 22, 1937	64.7° N	147.0° W	Normal	N 35° E	S 55° E	68°	0.985	-0.261	N 54° W	S 36° W	76°	0.922	-0.386	S 22° E	64.5°	b	a	Adkins, 1940.
50	October 16, 1947	64° N	148° W	Normal	N 30° W	N 60° E	78°	0.000	-1.000	N 30° W	S 60° W	12°	0.000	-1.000	N 30° W	0°	-	-	Hodgson and Milne, 1951.
51	September 27, 1949	60° N	149° W	Normal	◄	Not defined	►	-		N 70° W	N 20° E	72°	◄	-	Not defined	►	-	-	Hodgson and Storey, 1954.

TABLE 1—*Continued*

Number	Date	φ	λ	Focal Depth–km.	PLANE a: Strike Direction	PLANE a: Dip Direction	PLANE a: Dip	PLANE a: Strike Component	PLANE a: Dip Component	PLANE b: Strike Direction	PLANE b: Dip Direction	PLANE b: Dip	PLANE b: Strike Component	PLANE b: Dip Component	Null Vector: Trend	Null Vector: Plunge	DEXTRAL Solution	SINISTRAL Solution	REFERENCE
	Pacific Coast of North America																		
52	August 22, 1949	54.1° N	132.6° W	Normal	N 64° E	S 26° E	72°	0.972	+0.237	N 29° W	N 61° E	77°	0.948	+0.317	S 63.5° E	67.8°	b	a	Hodgson and Milne, 1951.
53	December 30, 1948	51° N	131° W	Normal	N 56° E	S 34° E	67°	0.536	−0.844	N 65° W	N 25° E	39°	0.784	−0.621	N 69° E	29.6°	a	b	Hodgson and Storey, 1954.
54	June 23, 1946	49.9° N	124.9° W	Normal	N 1° E	N 89° W	33°	0.424	−0.906	N 23° W	N 67° E	60°	0.270	−0.963	N 17° W	11.9°	b	a	Hodgson and Milne, 1951.
55	April 13, 1949	47° N	122.6° W	Normal	N 49° E	N 41° W	83°	0.170	+0.985	N 76° W	S 14° W	12°	0.810	+0.586	S 47.5° W	9.7°	b	a	Hodgson and Storey, 1954.
56	July 6, 1934	41.4° N	125.4° W	Normal	N 50° E	S 40 E	64°	0.993	+0.117	N 40° W	N 50° E	84°	0.897	+0.442	S 60° E	62.5°	b	a	Byerly, 1938.
57	July 21, 1952	35.0 N	119.0° W	Normal	N 50° E	S 40 E	63°	0.419	+0.908	E W	N	36°	0.635	+0.772	N 59° E	19°	b	a	Benioff, Gutenberg and Richter, 1954.
	Continental North America																		
58	June 28, 1925	46.4° N	111.2° W	Normal	N 26° E	S 64° E	87°	0.990	−0.140	N 65° W	N 25° E	82°	0.999	−0.053	N 51° E	81.8°	a	b	Byerly, 1955.
59	August 16, 1931	30.9° N	104.2° W	Normal	N 35° E	S 55° E	68°	0.929	+0.369	N 62° W	N 28° E	70°	0.916	+0.402	N 79° E	59.9°	b	a	Byerly, 1934. Scheidegger, 1955.
	South America																		
60	August 5, 1949	1° S	78° W	Normal	N 82.5° E	N 7.5° W	66°	0.969	−0.246	N 2° W	N 88° E	77°	0.909	−0.417	N 24° E	62.3°	b	a	Hodgson and Storey, 1954.
61	November 10, 1946	8° S	78° W	Normal	N 35° E	N 55° W	62°	0.930	+0.387	N 45° W	N 45° E	71°	0.868	+0.496	N 15° W	55.4°	a	b	Hodgson and Bremner, 1953.
62	May 8, 1949	20° S	71° W	100	← Not defined →					N 68° W	N 22° E	78°	← Not defined →				-	-	Hodgson and Storey, 1954.
63	June 12, 1949	27° S	64° W	600	N 2° W	S 88° W	67°	0.921	+0.390	N 82° W	N 8° E	69°	0.908	+0.419	N 44° W	57.8°	a	b	Hodgson and Storey, 1954.
64	April 20, 1949	38° S	72.5° W	100	N 53° E	—	90°	1.000	0.000	N 37° W	—	90°	1.000	0.000	—	90.0°	b	a	Hodgson and Storey, 1954.
	Hindu Kush																		
65	July 10, 1949	39° N	71° E	Normal	N 71° E	N 19° W	76°	← Not defined →									-	-	Hodgson and Storey, 1954.
66	March 4, 1949	37° N	70° E	200	N 86.5° E	N 3.5° W	87°	← Not defined →									-	-	Hodgson and Storey, 1954.
	Mediterranean																		
67	August 9, 1953	38.5° N	21° E	Normal	N 89° E	N 1° W	76°	0.954	−0.301	N 5° W	S 85° W	73°	0.967	−0.253	N 55° W	67.7°	a	b	Hodgson and Cock, 1956 a.
68	August 12 A, 1953	38.5° N	21° E	Normal	N 32.5° E	N 57.5° W	69°	0.994	−0.112	N 56° W	N 34° E	84°	0.932	−0.361	N 42° W	67.9°	b	a	Hodgson and Cock, 1956 a.
69	August 12 B, 1953	38.5° N	21° E	Normal	N 62.5° E	N 27.5° W	71°	0.976	−0.220	N 31° W	S 59° W	78°	0.943	−0.333	N 62° W	67.8°	a	b	Hodgson and Cock, 1956 a.
70	August 12 C, 1953	38.5° N	21° E	Normal	N 46.5° E	N 43.5° W	72°	0.904	−0.428	N 51° W	S 39° W	66°	0.941	−0.331	S 80° W	59.9°	a	b	Hodgson and Cock, 1956 a.
71	August 12 D, 1953	38.5° N	21° E	Normal	N	W	75°	0.662	−0.750	N 88° W	N 2° E	84°	0.336	−0.942	N 67° W	73.3°	b	a	Hodgson and Cock, 1956 a.
72	August 12 E, 1953	38.5° N	21° E	Normal	N 68.5° E	N 21.5° W	72°	0.983	−0.183	N 24.5° W	S 65.5° W	80°	0.949	−0.314	N 52° W	69.6°	a	b	Hodgson and Cock, 1956 a.
73	August 12 F, 1953	38.5° N	21° E	Normal	N 84° E	N 6° W	71°	1.000	0.000	N 6° W	—	90°	0.945	0.326	N 6° W	71°	a	b	Hodgson and Cock, 1956 a.
74	August 13, 1953	38.5° N	21° E	Normal	N 58.5° E	N 31.5° W	70°	1.000	0.000	N 31.5° W	—	90°	0.940	0.342	N 31.5 W	70°	a	b	Hodgson and Cock, 1956 a.
75	March 29, 1954	37° N	3.5° W	650	N 2° E	S 88° E	89°	0.057	+0.998	N 78.5° W	S 11.5° W	3.4°	0.956	+0.294	S 2° W	3.3°	-	-	Hodgson and Cock, 1956 b.

this is the zone from Alaska to California. Here there are three earthquakes (numbers 49, 52, and 56) that resulted from strike-slip faulting, three others (numbers 50, 53, and 54) that indicate gravity faulting, and two (numbers 55 and 57) that were the result of thrust faulting. Within the limits of the studies to date, this particular area is unique in the circum-Pacific in that all types of faulting occur.

Only three other earthquakes indicate non-strike-slip faulting. Two of these (numbers 65 and 66) lie in the Hindu Kush. The solutions for these particular earthquakes were not very well defined but seemed to indicate gravity faulting. A recent statistical study by Ritsema (1955) casts some doubt on these solutions and suggests that the faulting should be thrust; at least the two studies agree that the faulting is not strike-slip. The other exception is the deep-focus earthquake off the coast of Spain (number 75). This solution has already been discussed.

The finding that strike-slip faulting appears to be general in the failure of the earth from depths less than normal to depths as great as 600 km is most surprising. It had not been anticipated either in theories based on the contraction hypothesis or on those based on convection-current hypothesis. The pattern of this faulting must be examined as carefully as possible. First, however, it will be instructive to examine the nature of the dip component.

Table 2 shows the numbers of earthquakes, in each geographic area and for each focal depth, which have a thrust-dip component (+) or a gravity-dip component (−). The table lists only 69 earthquakes. Six of the earthquakes given in Table 1 had solutions in terms of a vertical plane; in such cases it is not possible to define the sign of the dip component.

Most of the earthquakes contributing to Table 2 have resulted from strike-slip faulting. Anderson has pointed out (1942, p. 177) that the direction of vertical movement accompanying a strike-slip fault may be accidental; Table 2 confirms this. Totals for various focal depths and for all the earthquakes are about evenly divided. Certainly there is no suggestion that thrusts predominate near the surface and tensions at depths as would be demanded by the contraction hypothesis. Thrust or tension may be related to the geographical area. For example, in the southwest Pacific 22 earthquakes show a thrust-dip component, whereas only 6 show a tension component. In the north Pacific, on the other hand, 14 show a tension component while only 6 show a thrust component. Many more earthquakes must be analyzed, however, before such conclusions can be accepted as valid.

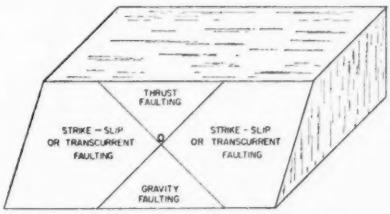

FIGURE 13.—DIAGRAM ILLUSTRATING DEFINITION OF FAULT TYPES

Direction of Faulting

The strikes of the faults are next examined to ascertain whether they show a consistent direction or systematic variation in direction. The diagrams of Figure 14, one corresponding to each geographic zone, have been prepared to facilitate this study. As an example we shall discuss the diagram for the New Hebrides area in some detail.

In this diagram a number of lines radiate from the center, and each is identified by a number with the corresponding earthquake. These lines indicate by their azimuth the strike direction of the planes *a* and *b*, and by their length the focal depth, according to the given scale. Since plane *a* is by definition that plane striking east of north, and plane *b* is that striking west of north, it is clear that there is no favored direction either for the earthquakes taken as a whole or for any particular focal depth. The earthquake numbers in this area are assigned from south to north; if there were any systematic variation to the strike of the planes along the arc there should be some corresponding systematic variation to the numbers in the diagram. It is evident that this does not occur. Therefore, the strike direction of the faults in this area is random.

TABLE 2.—RELATIONSHIP OF THRUST (+) AND GRAVITY (−) DIP COMPONENTS TO FOCAL DEPTH AND GEOGRAPHIC FEATURE

Area	Focal Depth, km.														Total	
	Normal		100		200		300		400		500		600			
	+	−	+	−	+	−	+	−	+	−	+	−	+	−	+	−
New Zealand	1	−	−	−	−	−	1	−	−	−	−	−	−	−	2	0
Kermadecs	1	−	−	−	−	−	−	1	−	−	−	−	−	1	1	2
Tongas	1	1	2	−	1	−	−	−	−	−	1	−	−	−	5	1
Fiji	−	1	−	−	−	−	−	−	−	−	−	−	−	−	0	1
New Hebrides	9	0	1	1	2	1	1	−	−	−	−	−	−	−	13	2
Solomon Islands	−	−	1	−	−	−	−	−	−	−	−	−	−	−	1	0
Japan	1	−	−	−	−	−	−	−	−	−	−	−	−	−	1	0
Vladivostok Area	−	−	−	−	−	−	−	−	−	−	1	−	−	−	1	0
Sakhalin Islands	−	1	−	−	−	−	−	1	−	−	−	−	−	−	0	2
Kurile Islands	1	1	1	−	−	1	−	−	−	−	−	−	−	−	2	2
Kamchatka	−	4	−	−	−	−	−	−	−	−	−	−	−	−	0	4
Aleutian Islands	2	3	−	−	−	−	−	−	−	−	−	−	−	−	2	3
Alaska	−	3	−	−	−	−	−	−	−	−	−	−	−	−	0	3
Pacific Coast of N.A.	4	2	−	−	−	−	−	−	−	−	−	−	−	−	4	2
Continental N.A.	1	1	−	−	−	−	−	−	−	−	−	−	−	−	1	1
South America	1	1	1	−	−	−	−	−	−	−	−	−	1	−	3	1
Hindu Kush	−	1	−	−	−	1	−	−	−	−	−	−	−	−	0	2
Mediterranean	−	6	−	−	−	−	−	−	−	−	−	−	1	−	1	6
Totals	22	25	6	1	3	3	2	2	−	−	2	−	2	1	37	32

From the other diagrams of Figure 14, it is evident that nowhere can a favored direction of faulting be selected. Not only is the faulting strike-slip, but the orientation of the faults is random.

Direction of Dip

The dip of a plane has both a direction and an amount, and may therefore be regarded as a vector quantity. The vector property of the dip might be represented in various ways. For example a unit vector might be drawn in the direction of dip and its horizontal projection plotted. The method used here is that described in Figure 10, in which the dip vector is drawn from the epicenter, in the direction of maximum dip, to meet the surface of the sphere again. The length of the vector is the distance between the two points in which it meets the sphere.

For purposes of mapping these dip vectors the projection defined in Figure 15 is used. The upper section of the figure represents a cross section of the earth; the epicenter is at *E*. A plane is drawn through the epicenter, perpendicular to the plane of the paper, so that the line *EP* represents the vertical projection of this plane. The dip of the plane is the angle δ as shown, and *EP* is the dip vector as defined above. The epicenter is used as the pole to pro-

ject onto the equatorial plane. The map produced is shown in the lower section of the diagram. The point P projects into the point P', the dip vector EP into the line $O'P'$, and the tral point. This is exactly the projection shown in Figure 15; the vectors are considered as free and are translated to act from a single point. Focal depths are indicated by the symbols de-

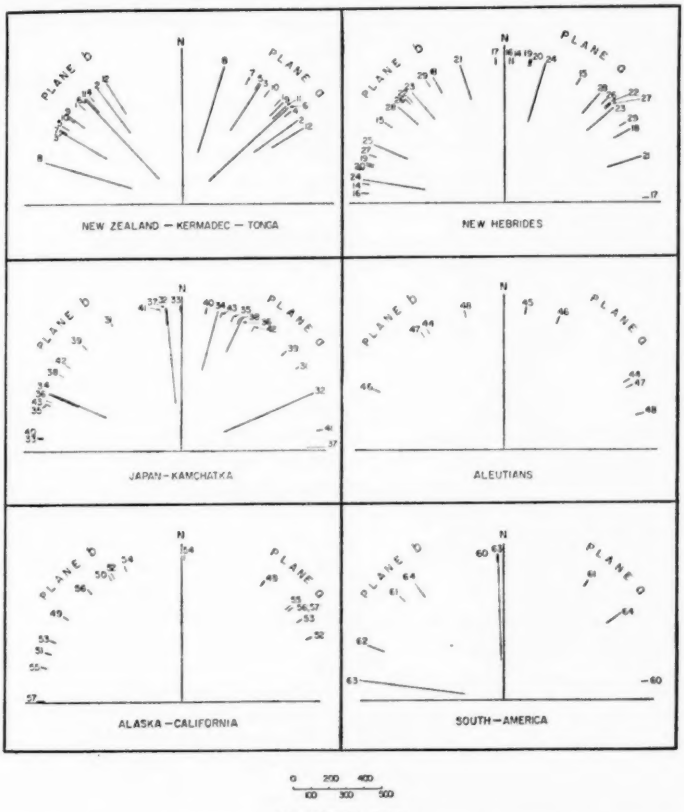

FIGURE 14.—DIAGRAMS SHOWING STRIKE DIRECTIONS OF THE FAULTS DETERMINED BY THE SEISMIC METHOD

plane through EP perpendicular to the paper becomes the line $Q'R'$. The projected length of the dip vector is equal to cot δ, but the dip vectors will be represented by the projection P' of their points of emergence.

This projection is used to plot the dip vectors listed in Table 1. The results are shown in Figure 16, arranged by geographic areas. The map for the New Zealand–Kermadec–Tonga sector is discussed as an example. The dip vector for each of the planes is plotted at an appropriate azimuth and at a distance = cot δ from a central point. This is exactly the projection shown in Figure 15; the vectors are considered as free and are translated to act from a single point. Focal depths are indicated by the symbols defined in the legend; open symbols refer to planes a, closed symbols to planes b.

The solid symbols can be enclosed between a pair of parallel lines striking N. 33° E. It was demonstrated in Figure 15 that a straight line on the map represents a plane through the origin. These parallel lines then represent a pair of planes through the origin, both striking N. 33° E., one dipping at about 88° SE., the other dipping at about 87° NW. With the exception of earthquake 8, the dip vectors for planes b lie within 3° of a vertical plane striking N. 33° E.

Similarly, because the open symbols lie between a second pair of parallel lines, the dip vectors for planes *a* lie with 1° of a vertical plane striking N. 50° W.

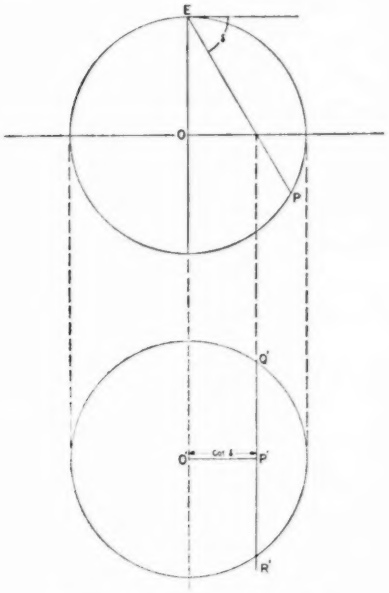

FIGURE 15.—PROJECTION USED IN DRAWING DIP VECTORS

Does this remarkable arrangement occur in other areas? In the New Hebrides the solid symbols tend to lie within 6° of a vertical plane striking N. 18° E., whereas the open symbols tend to lie within 7° of a vertical plane striking N. 57° W. One apparent exception is provided by earthquake 17, but, since there is no significance to the designations *a* or *b*, interchanging open and closed symbols would be justified. Again the diagram for the Japan–Kuriles–Kamchatka sector shows a pair of favored directions. If open and closed symbols for earthquake 37 are interchanged there remains only one exception—earthquake 32. Again in the Aleutians the phenomenon seems to be repeated, although the number of earthquakes is too small to be certain.

In the sector from Alaska to California the open symbols apparently define a favored direction, but the closed symbols seem to be random. South America also is anomalous in that no pattern is apparent in the dip vectors.

Is there any significance to the directions defined in the diagrams of Figure 16? The mean of the two directions shown in the New Hebrides (Fig. 16) is N. 20° W., a close approximation to the direction of the feature, but the mean direction shows no similar significance in other areas.

The dips of the fault planes appear to have some favored directions, whereas the strikes do not. How are these conflicting facts to be reconciled? It must be inferred that there are one or two favored directions for strike, and that when a fault plane develops a strike that does not adhere to one of these directions such a plane tends to have a very steep dip.

Directions of the Null Vectors

The conclusions of the last section are open to question because of the ambiguity between planes *a* and *b*. Since there is no certain connection between the planes of any one system their arrangement in a particular pattern could be a matter of accident. One line in each solution avoids this criticism. This has been shown in Figures 9 and 10 as the line joining the points of intersection of the two circles. This line is uniquely defined; it has been defined as a vector, the null vector, pointing from the epicenter to the other point of intersection of the circles. Its trend and plunge are listed for each of the earthquakes in Table 1.

This quantity is certainly a vector in the same sense that the dip of a plane is a vector, for it has a direction and an amount. It is the line common to both the planes *a* and *b* and is therefore perpendicular to the motion vector, whichever plane represents the fault. In the language of mechanics it is the direction of the moment-vector of the couple and as such is the one line in space which undergoes no motion during the earthquake; hence the name null vector.

The points of emergence of the null vectors are plotted in Figure 17 for each of the geographical areas by the use once again of the special projection described in Figure 15. Whereas in Figure 14 the strikes are constrained to lie within a single quadrant and in Figure 16 the dips are constrained to lie within an opposite pair of quadrants, here the symbols representing the points of emergence of the null vectors may lie anywhere in the diagram. Any systematic arrangement has a high significance.

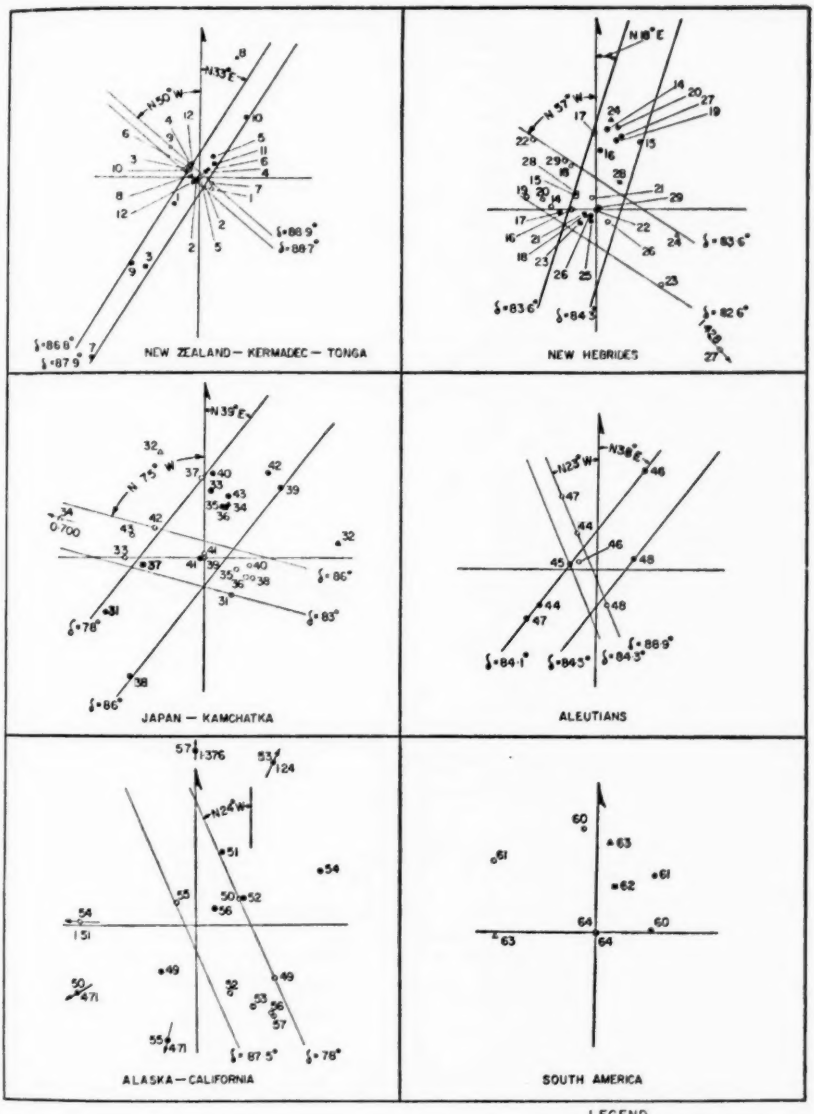

FIGURE 16.—DIAGRAMS SHOWING POINTS OF EMERGENCE OF THE DIP VECTORS FOR PACIFIC EARTHQUAKES

There is no doubt that such systematic arrangements do exist. In the diagram for the New Zealand–Kermadec–Tonga sector all the symbols except that for earthquake 9 lie between the parallel planes shown. This means that all the null vectors but one lie within 5° of a plane striking N. 27° E. and dipping 88° NW. Similarly in the New Hebrides, with only three

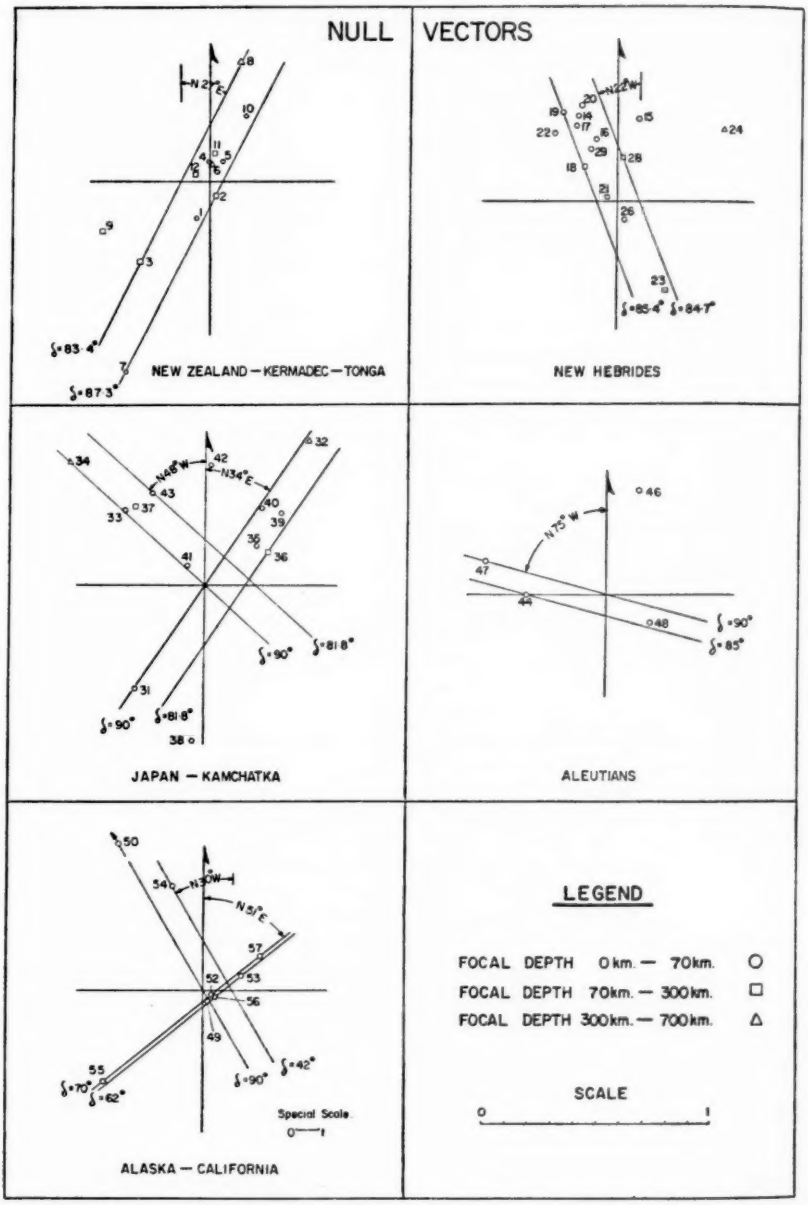

FIGURE 17.—DIAGRAMS SHOWING POINTS OF EMERGENCE OF THE NULL VECTORS FOR PACIFIC EARTHQUAKES

exceptions, the null vectors lie within 5° of a vertical plane striking N. 22° W.

These directions, N. 27° E. for the New Zealand–Kermadec–Tonga sector and N. 22° W. for the New Hebrides arc, are remarkably close to the mean directions of the associated geographical features. In proof of this the reader is referred to Figure 18, which has been adapted

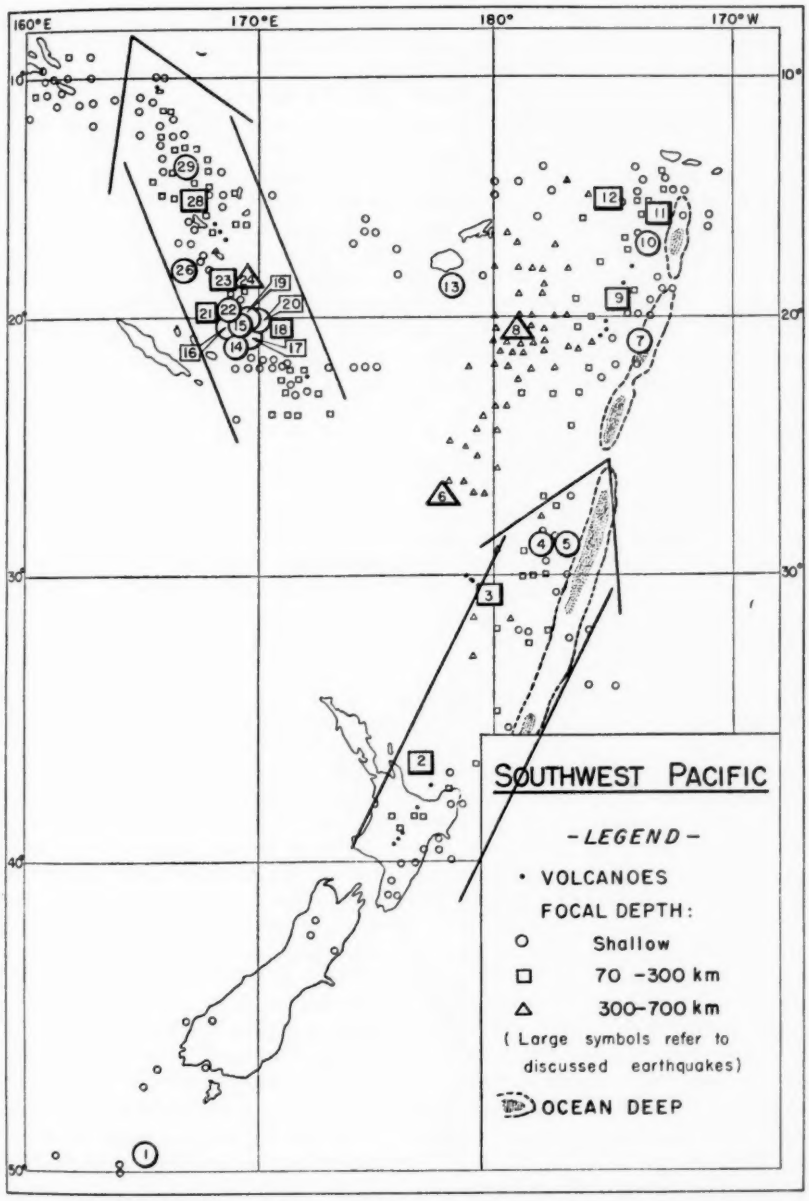

FIGURE 18.—MAP OF THE SOUTHWEST PACIFIC, SHOWING EARTHQUAKE EPICENTERS

from Figures 14 and 15 of Gutenberg and Richter (1949, p. 46, 49). It appears that the null vector is very closely associated with what might be called the tectonic direction, in this case the direction of the island arcs.

In 4 earthquakes out of 28 the null vectors do not lie within the lines as drawn. This is not a serious number of exceptions. It is stated in the Introduction that in basing the project on questionnaires instead of on personal examina-

tion of original records some accuracy was sacrificed in order to obtain a large number of solutions rapidly. The fact that the null vectors for earthquakes occurring over a 6 year period and studied by two investigators so closely define the direction of the associated geographic feature surely cannot be a matter of accident.

The null vectors may have a still greater significance. In the diagram for the New Hebrides the symbols for earthquakes numbered 14 to 22, the epicenters of which lie within about 1° of each other, tend to be clustered northwest of the origin. Again, in the diagram for the New Zealand–Kermadec–Tonga sector, earthquakes 4, 5, and 6 from the Kermadecs are closely grouped, and the symbols for shocks 8, 10, 11, and 12 progress systematically from north to south. It seems possible that not only do the null vectors for an entire feature define a plane, but also that the null vectors for a particular part of the feature define a unique direction. Substantiation of this point must await the accumulation of more data.

There does not appear to be any relationship between the points of emergence of the null vectors and the focal depths of the earthquakes.

This preliminary discussion is limited to the earthquakes of the southwest Pacific because: (1) more solutions are available for this area than for other parts of the Pacific, and the area itself is sufficiently limited that a reasonable density of data is provided; (2) the pattern of the arcs in the southwest Pacific is very clear so that the connection between null vectors and arcuate feature can be established beyond reasonable doubt.

In the north Pacific the tectonic pattern is very confused. No two students would agree exactly on tectonic directions. For example in the northwest Pacific are a number of arcuate features and a very complicated pattern of earthquake foci. This is shown in Figure 19, which has been adapted from Figures 17 and 18 of Gutenberg and Richter (1949, p. 55, 56). Rather than attempt to associate a particular epicenter with a particular feature we shall use the null vectors to define tectonic directions and then examine the directions so defined.

The null-vector diagram for the area from Japan to Kamchatka suggests that there are two tectonic directions in the area, one striking N. 34° E., the other N. 48° W. There are two inconsistent solutions, 42 and 38. These might well define a northerly tectonic direction, although this cannot be established with so few data. Are these tectonic directions reasonable?

The equivalent areas are covered in Figure 19. A line drawn through the point 40° N., 140° E., and striking N. 38° E., is a good approximation to the band of islands, volcanoes, and normal-focus earthquakes stretching through Japan, the Kuriles, and Kamchatka. The line is, of course, only an approximation to a number of separate systems; the Japan arc and the Kurile arc, for example, appear as scallops on the general line. On the continental side of this line the foci become increasingly deep with distance from the line, as if the line corresponded to the outcrop of a plane, or system of planes, dipping toward the continent.

A second line, drawn through the point 30° N., 140° E., and striking N. 30° W., appears necessary to account for a number of deep-focus earthquakes. There does not seem to be an accompanying trend of normal-focus earthquakes associated with this direction. Another trend does seem to exist, however, for normal-focus earthquakes. This would be defined by a line running along the 141st meridian.

In summary, it appears that three directions might be defined by earthquakes in this area, one N. 38° E., another N. 30° W., and a third due north. The first two correspond reasonably well to the directions N. 34° E. and N. 48° W. defined by the null vectors; we recall that a northerly direction was also suggested by the null vectors. In the northwest Pacific the null vectors have had some success in defining the tectonic directions.

There is, however, an essential difference between the results found in the southwest Pacific and those suggested here. In the southwest Pacific the null vectors of the New Hebrides earthquakes lay parallel to a plane having the strike of the New Hebrides arc, whereas the New Zealand–Kermadec–Tonga shocks had null vectors associated with the plane through that feature. In the northwest Pacific this close relationship does not obtain. The null vectors of earthquakes 33 and 34, for example, which lie in the Sakhalin Islands and so are associated geographically with the northerly trend, are associated with the northwesterly trend. Similarly the null vectors for Kurile earthquake

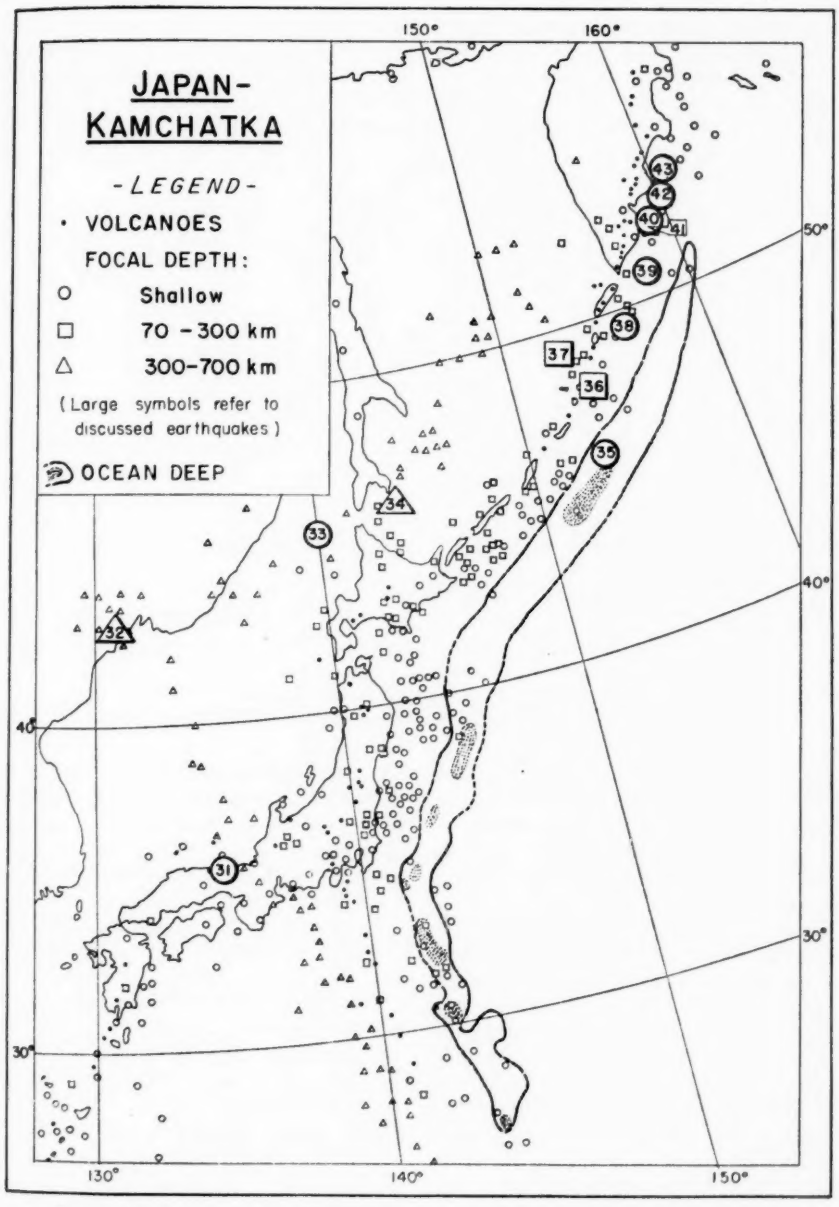

FIGURE 19.—MAP OF THE NORTHWEST PACIFIC, SHOWING EARTHQUAKE EPICENTERS

number 37 and the Kamchatka earthquakes numbers 41 and 43 are associated with the northwesterly direction, whereas the null vector of the Vladivostok earthquake number 32 is associated with the northwesterly system. If these trends are maintained when more data are available it will be necessary to conclude that the association of epicenters with particu-

lar arcs is more complicated than many authors have supposed.

In the Aleutians the data are too meager to be conclusive; a direction N. 75° W. accounts for three of the four observations, and this direction as shown in Figure 20 is a good approximation to that of the western Aleutians. Again, however, two of the earthquakes, numbers 47 and 48, which define the direction, are associated with the eastern rather than with the western Aleutians.

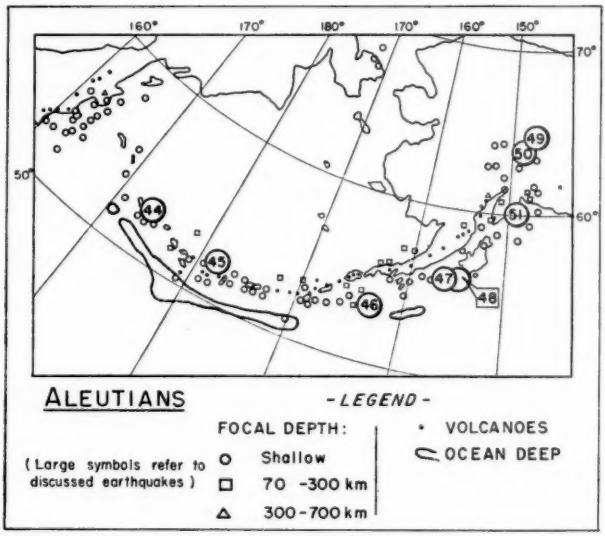

FIGURE 20.—MAP OF THE ALEUTIANS, SHOWING EARTHQUAKE EPICENTERS

In the null-vector diagram for the northeastern Pacific, from Alaska to California, a different scale has been used, so that the linear arrangement is not so good as it appears. The diagram appears to define two tectonic directions, N. 51° E. and N. 30° W.; the latter direction is not well defined, and the plane associated with the former direction is not vertical as usual but dips 66° SE. Earthquake number 57, which is known to have a fault striking N. 50° E. (Buwalda and St. Amand, 1955, p. 43) is associated with the N. 51° E. trend.

The equivalent area is covered in Figure 21, adapted from Figures 7 and 8 of Gutenberg and Richter (1949, p. 31, 35). The map appears to define two directions. A line through the length of Vancouver Island passes through several epicenters and, continued to the north, passes along a line of sea mounts. This line has a direction N. 55° W. An equivalent northwesterly direction is evident again further south, in California and off the California coast, where the San Andreas fault system and a line of sea mounts off the coast define a direction varying between N. 40° W. and N. 50° W. A second direction would appear to be defined by a line along the length of the Queen Charlotte Islands, continued to the north through a line of earthquake epicenters lying inland from Sitka, and to the south through a line of sea mounts. This line has a direction about N. 15° W.

The direction defined by the null vector, N. 30° W., seems to be a mean of these two directions. Perhaps when more earthquakes have been analyzed it will be possible to define the direction more accurately.

The second direction defined by the null vectors, N. 51° E., finds considerable support in California. It has already been pointed out that the Kern County earthquake of July 21, 1952, resulted from a fault striking N. 50° E. There is some evidence in Figure 21 that this direction has a general importance, but more specific evidence is given by Benioff (1955, p. 204) for transverse motion parallel to the Gar-

lock fault in a direction about N. 55° E. A recent paper by Menard (1955) describes fracture zones in the northeastern Pacific which trend about latitude 28° S. could define a northwesterly trend at least as well as a northerly one.

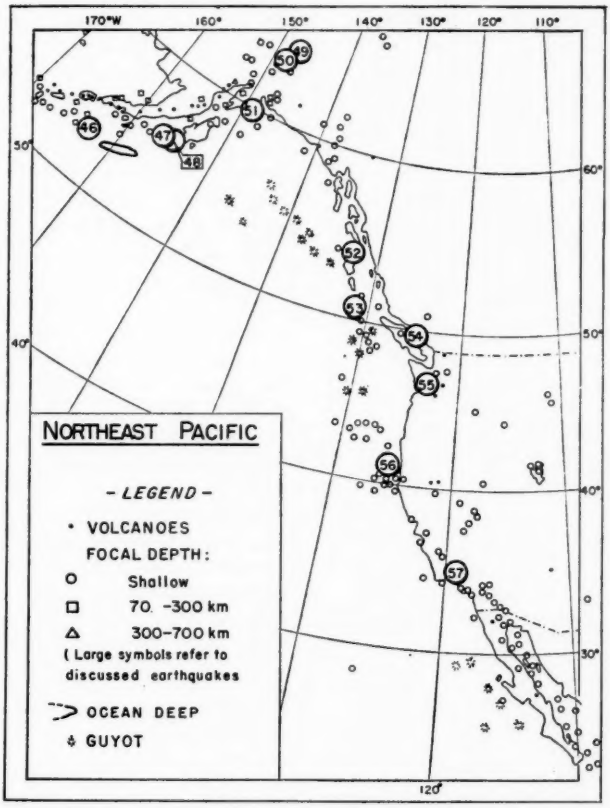

FIGURE 21.—MAP OF THE NORTHEAST PACIFIC, SHOWING EARTHQUAKE EPICENTERS

north of east. The correlation of direction is reasonably satisfactory, but too much stress should not be placed on this correlation until more earthquake solutions have been obtained.

The data for South America are so limited that the null vectors have been simply plotted on the map shown in Figure 22. Except for earthquake 63 these directions approximately parallel the mountain ranges. This supports the idea that the null vectors have tectonic significance. In earthquake 63, the null vector suggests that the earthquake is tectonically associated with the northern zone; this is a possible interpretation. The group of earthquakes at

To summarize: in the southwest Pacific the null vectors are nearly parallel to vertical planes having the strike of the associated features; elsewhere in the Pacific the data are yet too meager to establish a similar conclusion independently, but there has been no serious conflict with the postulate that the null vectors define tectonically significant directions.

Areas of Anomalous Mechanism

Before beginning a discussion of the results one additional piece of evidence must be presented. It frequently happens that after first-

motion data have been collected and plotted no definite pattern can be seen. This usually occurs in the case of the smaller earthquakes with magnitudes less than about 6.7 Even

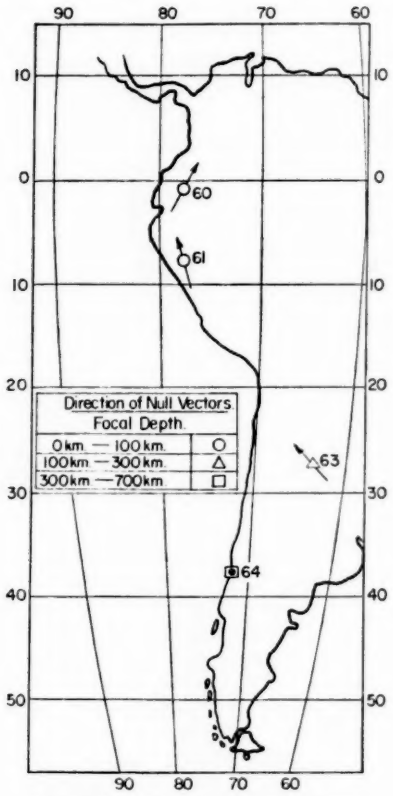

FIGURE 22.—NULL-VECTOR DIRECTIONS IN SOUTH AMERICAN EARTHQUAKES

when solutions are obtained about 20 per cent of the data are inconsistent. This usually does not obscure the solution because the inconsistent observations lie among large bodies of consistent data in such a way that it would be impossible to satisfy them. But there have been some instances in which large bodies of data, sufficiently self-consistent that they cannot be questioned, have been so arranged that no solution has been possible. In these instances it seemed clear that some mechanism other than failure under a couple was active.

Two such earthquakes occurred in South America on April 25 and May 30, 1949 (Hodgson and Storey, 1954 p. 69). Both had the same epicenter—20° S., 69.5° W. It may be significant that this point is approximately at the intersection of the northward-trending band of earthquakes and of the northwestward-trending band (Gutenberg and Richter, 1949, p. 41, Fig. 11).

Five earthquakes occurring in the North Pacific between July 1 and November 10, 1953, and lying within 1° of 50° N., 156° E. appear to be due to an anomalous mechanism (Hodgson, 1956b). This point is at about the tip of the Kamchatka peninsula and does not appear to have any tectonic significance.

The final group of anomalous earthquakes occurred in the Solomon Islands between May 1951, and November 1953 (Hodgson, 1956a). The epicenters were stretched along the length of the islands over a range of about 12°. Only one solution has been obtained for a Solomon Islands earthquake, this suggests that the whole area may be anomalous.

An examination of these unusual cases has been begun. Until a suitable mechanism has been discovered it would be unwise to speculate on their significance.

DISCUSSION AND CONCLUSIONS

The following points argue for the acceptance of the techniques and results of the work described.

(1) Satisfactory agreement was found between the seismic solutions and observed or inferred displacement in five examples. The seismic solution agreed with the strike but not with the observed displacement of the observed or inferred fault in two other examples. Three solutions, for a closely allied group of earthquakes in Nevada, gave a strike direction which differed slightly from that observed on the surface, but which agreed exactly with geodetic data for one of them. No instances of complete nonagreement between seismic results and geological observations exist.

(2) When the solutions of the several investigators have been compiled by regions it is found that the null vectors tend to lie parallel to planes that are usually nearly vertical. In the southwest Pacific the directions of the planes parallel tectonic features; in other parts of the Pacific this cannot be so definitely established, but there are no strong exceptions to the hypothesis that the null vectors

define tectonically significant directions. This property of the null vectors seems to insist at least on the self-consistency of the method and to argue strongly for the acceptance of the results.

If we accept the results we are led to the following conclusions.

(1) In most areas faulting in large earthquakes is almost purely strike-slip on steeply dipping planes. The Hindu-Kush and the Pacific Coast of North America appear to provide exceptions to this rule; in addition, in certain minor areas failure under a couple does not seem to be the causative mechanism. Because of the ambiguity between the two planes obtained in most solutions it is not possible to say whether the faults in any particular area are sinistral or dextral.

(2) The strikes of the faults in any particular area appear to be completely random. Some evidence suggests, however, that the dip vectors tend to lie parallel to steeply dipping planes. From this it is inferred that in a particular area there may, in fact, be one or two preferred directions for strike, and that when the strike of a fault does not adhere to one of these directions such a fault develops a very steep dip. Because of the ambiguity between the two planes in the solution this conclusion must not be regarded as established.

(3) The consistency of the null-vector directions has already been adduced as evidence of the dependability of the fault-plane techniques. It seems probable that, once the method has been generally accepted, the null vectors may aid in defining tectonically significant directions in areas where these cannot otherwise be established, and in assigning earthquakes to particular tectonic systems.

(4) In two particular examples the seismic solutions demand that faulting at depth must be quite different from faulting at the surface, although with the same strike direction. The Nevada earthquakes, on the other hand, suggest that even the strike of surface features may differ from the strike of the true displacement. It is too early to draw any conclusion from this fact, but probably when more data have accumulated the seismic results may improve our understanding of the relation between faulting on the surface and faulting at depth.

The seismic results indicate that such an understanding is urgently needed. Field geologists have not found strike-slip faulting in the proportion indicated in this paper. In discussing this problem with geologists one is always brought up against the fact that, whereas the seismologist is dealing with present conditions usually at a depth of at least several kilometers, the field geologist is dealing with observations at the surface, many of them conditioned by circumstances which obtained millions of years ago. It would be a denial of geologic principle to suggest that the mechanism of faulting has changed during these millions of years; if strike-slip faulting is occurring at depth now it must have been occurring at depth then. The explanation must lie in the different depths involved rather than in the different times. Could the observed surface effects, including large-scale orogeny be the result of strike-slip faulting at depth?

On an elementary basis there is some logic to the suggestion. It is always difficult to envisage what happens when a fault displacement occurs at great depth within the earth. For gravity faulting at depth there must be a void, or at least an attenuation, behind the movement, and a compaction ahead of it. How could this occur under the pressures at depth? The problem is less severe for horizontal displacement because two sections of a sphere can be rotated relative to each other without creating any change in volume.

The following remarks were made by Prof. C. A. Cotton during the discussion following his reading of a paper on tectonic relief in New Zealand (Cotton, 1953).

"As for the great problem of the cause of these movements, and of their relation to isostasy, it would be dangerous to try to open such a problem now. But I do think that whereas vertical movement (and possibly some kind of gravity movement) is responsible for the fault scarps in the Great Basin of North America, in the coast ranges of California and New Zealand, and probably in many other parts of the Pacific rim, compressional faulting has definitely been the cause. But whether to think of compression or transcurrent movement on some very deep-seated vertical fault as the prime cause, I do not know".

Transcurrent movement on very deep-seated vertical faults is exactly the mechanism suggested by the studies reported in this paper. Clearly there is some body of geologic opinion receptive to the findings. A recent paper by Moody and Hill (1956) reviews much of this opinion and suggests that strike-slip faulting controls many of the larger features of the earth.

If the horizontal displacement in Pacific earthquake zones is so much larger than the vertical displacement, then, since the accumu-

lated vertical displacement is of the order of miles, the accumulated horizontal displacement should be of the order of tens of miles. Displacements of this magnitude are very difficult to establish. It can be done only where it is possible to study a fault in great detail. Two such areas are New Zealand and California. In New Zealand Wellman (1955) finds that the Alpine fault has undergone a horizontal displacement of 300 miles since the Jurassic. In California Hill and Dibblee (1953, p. 449) find evidence that the horizontal displacement on the San Andreas fault may have accumulated to more than 300 miles since the Cretaceous. These displacements might be expected from the seismic evidence.

The findings of this paper appear to be incompatible with the theories of the various tectonophysicists who have sought to explain the mechanism of the deep-focus earthquakes associated with island arcs. As has been pointed out elsewhere (Hodgson, 1955b, p. 39), these authorities disagree as to whether the displacement at a particular depth is that of thrust or of gravity faulting, but none has suggested any appreciable amount of strike-slip faulting. The adjustments of the various theories to satisfy the findings of the fault-plane project is beyond the scope of the present paper and may be left to the individuals concerned. It is hoped that this paper will convince them that the adjustment is necessary.

References Cited

Adkins, J. D., 1940, The Alaskan earthquake of July 22, 1937: Seismol. Soc. America Bull., v. 30, p. 353–376

Anderson, E. M., 1942, The dynamics of faulting and dyke formation with application to Britain: Edinburgh and London, Oliver and Boyd, 191 p.

Båth, M., 1954, The density ratio at the boundary of the earth's core: Tellus, v. 6, p. 408–414

Benioff, H., 1955, Relation of the White Wolf fault to the regional tectonic pattern, p. 203–204 *in* Oakeshott, Gordon B., *Editor*, Earthquakes in Kern County, California during 1952: Calif. Div. Mines Bull. 171, 283 p.

Benioff, H., Gutenberg, B., and Richter, C. F., 1954, Progress report, Seismological Laboratory, California Institute of Technology, 1953: Am. Geophys. Union Trans., v. 35, p. 979–987

Billings, M. P., 1947, Structural geology: New York, Prentice Hall, 473 p.

Buwalda, J. P., and St. Amand, P., 1955, Geological effects of the Arvin-Tehachapi earthquake, p. 41–56 *in* Oakeshott, Gordon B., *Editor*, Earthquakes in Kern County, California during 1952: Calif. Div. Mines Bull. 171, 283 p.

Byerly, P., 1926, The Montana earthquake of June 28, 1925, G.M.C.T.: Seismol. Soc. America Bull., v. 16, p. 209–265

—— 1928, The nature of the first motion in the Chilean earthquake of November 11, 1922: Am. Jour. Sci., 5th ser., v. 16, p. 232–236

—— 1930, Love waves and the nature of the motion at the origin of the Chilean earthquake of November 11, 1922: Am. Jour. Sci., 5th ser., v. 19, p. 274–282

—— 1934, The Texas earthquake of August 16, 1931: Seismol. Soc. America Bull., 24, p. 81–99

—— 1938, The earthquake of July 6, 1934: amplitudes and first motion: Seismol. Soc. America Bull., v. 28, p. 1–13

—— 1955, Nature of faulting as deduced from seismograms, p. 75–85 *in* Poldervaart, Arie, *Editor*, Crust of the earth: Geol. Soc. America Special Paper 62, 762 p.

Cotton, C. A., 1953, Tectonic relief: with illustrations from New Zealand: Geog. Jour., v. 69, pt 2, p. 211–222

DeBremaecker, J. C., 1956, Remark on Byerly's fault-plane method: Seismol. Soc. America Bull., v. 46, 215–216

Gutenberg, B., 1955a, The first motion in longitudinal and transverse waves of the main shock and the direction of slip, p. 165–170 *in* Oakeshott, Gordon B., *Editor*, Earthquakes in Kern County, California during 1952: Calif. Div. Mines Bull. 171, 283 p.

—— 1955b, Wave velocities in the earth's crust, p. 19–34 *in* Poldervaart, Arie, *Editor*, Crust of the earth: Geol. Soc. America Special Paper 62, 762 p.

Gutenberg, B., and Richter, C. F., 1934, On seismic waves (first paper): Gerlands Beitr. zur Geophysik, v. 43, p. 56–133

—— 1949, Seismicity of the earth and associated phenomena: Princeton, N. J., Princeton University Press, 273 p.

Hill, M. L., and Dibblee, T. W., Jr., 1953, San Andreas, Garlock, and Big Pine faults, California: Geol. Soc. America Bull., v. 64, p. 443–458

Hodgson, J. H., 1953, A seismic survey in the Canadian Shield. I: Refraction studies based on rockbursts: Pubs. Dominion Observatory, Ottawa, v. 16, p. 109–164

—— 1955a, Fault-plane solution for the Tango, Japan, earthquake of March 7, 1927: Seismol. Soc. America Bull. v. 45, p. 37–41

—— 1955b, Direction of faulting in Pacific earthquakes: Geofisica Pura e Applicata, v. 32, p. 31–42

—— 1956a, Direction of faulting in some of the larger earthquakes of the southwest Pacific, 1950–1954: Pubs. Dominion Observatory, Ottawa, v. 18, p. 169–216

—— 1956b, Direction of faulting in some of the larger earthquakes of the north Pacific, 1950–1953: Pubs. Dominion Observatory, Ottawa, v. 18, p. 217–252

Hodgson, J. H., and Allen, J. F. J., 1954a, Tables of extended distances for PKP and PcP:

Pubs. Dominion Observatory, Ottawa, v. 16, p. 327–348
—— 1954b, Tables of extended distances for PP and pP: Pubs. Dominion Observatory, Ottawa, v. 16, p. 349–362
Hodgson, J. H., and Bremner, P. C., 1953, Direction of faulting in the Ancash, Peru, earthquake of November 10, 1946, from teleseismic evidence: Seismol. Soc. America Bull., v. 43, p. 121–125
Hodgson, J. H., and Cock, J. I., 1956a, Direction of faulting in the Greek earthquakes of August 9–13, 1953: Annales Géologiques des Pays Helléniques, v. 8, p. 29–47; *also in* Pubs. Dominion Observatory, v. 18, p. 149–167
—— 1956b, Direction of faulting in the deep focus Spanish earthquake of March 29, 1954: Tellus, v. 8, p. 321–328
Hodgson, J. H., and Milne, W. G., 1951, Direction of faulting in certain earthquakes of the North Pacific: Seismol. Soc. America Bull., v. 41, p. 221–242
Hodgson, J. H., and Storey, R. S., 1953, Tables extending Byerly's fault-plane techniques to earthquakes of any focal depth: Seismol. Soc. America Bull., v. 43, p. 49–61
—— 1954, Direction of faulting in some of the larger earthquakes of 1949: Seismol. Soc. America Bull., v. 44, p. 57–83
Hodgson, J. H., Allen, J. F. J., and Cock, J. I., 1956a, Tables of extended distances for PPP, pPP, pPKP and P at very short distances: Pubs. Dominion Observatory, Ottawa, v. 18, p. 83–100
—— 1956b, Tables of extended distances for S, SS and sS: Pubs. Dominion Observatory, Ottawa, v. 18, p. 101–116
Honda, H., and Masatuka, A., 1952, On the mechanisms of the earthquakes and the stresses producing them in Japan and its vicinity: Sci. Repts. of the Tohoku Univ., ser. 5, v. 4, p. 42–60
Ingram, R. E., S.J., and Hodgson, J. H., 1956, Phase change of PP and pP on reflection at a free surface: Seismol. Soc. America Bull., v. 46, p. 203–213
Koning, L. P. G., 1941, On the mechanism of deep-focus earthquakes: Gerlands Beitr. zur Geophysik, v. 58, p. 159–197
Lehmann, I., 1955, The times of P and S in northeastern America: Annali di Geofisica, v. 8, p. 351–370
Menard, H. W., 1955, Deformation of the northeastern Pacific basin and the west coast of North America: Geol. Soc. America Bull., v. 66, p. 1149–1198
Moody, J. D., and Hill, M. J., 1956, Wrench-fault tectonics: Geol. Soc. America Bull., v. 67, p. 1207–1246
Nakano, H., 1923, Notes on the nature of the forces which give rise to the earthquake motions: Central Meteorol. Observatory of Japan, Seismol. Bull., v. 1, p. 92–120
Ramirez, J. E., S.J., and Semanate, A. D., O.P., 1951, The earthquake of Pelileo, Ecuador, August 5, 1949: Earthquake Notes, v. 22, p. 16
Reid, H. F., 1933, The Mechanics of Earthquakes, p. 87–103 *in* Macelwane, J. B., *Editor*, Seismology, Physics of the Earth, v. 9: National Research Council, Washington, 223 p.
Ritsema, A. R., 1955, The fault plane technique and the mechanism in the focus of the Hindu Kush earthquakes: Indian Jour. of Meteorology and Geophysics, v. 6, p. 1
Romney, C., 1956, Seismic evidence for the direction of faulting in the Fairview Peak earthquake (Abstract): Geol. Soc. America Bull., v. 67, p. 1782
Scheidegger, A. E., 1955, The physics of orogenesis in the light of new seismological evidence: Royal Soc. of Canada Trans., Sec. IV, v. 49, p. 65–93
—— in press, The geometrical representation of the fault plane solutions of earthquakes: Seismol. Soc. America Bull.
—— in press, A review of the Russian fault plane work: Pubs. Dominion Observatory, Ottawa
Silgado F., E., 1951, The Ancash, Peru, earthquake of November 10, 1946: Seismol. Soc. America Bull., v. 41, p. 83–100
Wellman, H. W., 1955, New Zealand tectonics: Geologische Rundschau, v. 43, p. 248–257
Wilson, J. Tuzo, 1953, On grabens, rifts, major wrench faults and straight chains of islands (Abstract): Am. Geophys. Union Trans., v. 34, p. 350

DOMINION OBSERVATORY, DEPARTMENT OF MINES AND TECHNICAL SURVEYS, OTTAWA, ONTARIO
MANUSCRIPT RECEIVED BY THE SECRETARY OF THE SOCIETY, SEPTEMBER 21, 1956
PUBLISHED BY PERMISSION OF THE DEPUTY MINISTER, DEPT. OF MINES AND TECHNICAL SURVEYS, OTTAWA, CANADA
CONTRIBUTIONS FROM THE DOMINION OBSERVATORY, V. 3, NO. 1

Short Notes

BULLETIN OF THE GEOLOGICAL SOCIETY OF AMERICA
VOL. 68, PP. 645-652, 4 FIGS. MAY 1957

NATURE OF THE FAULTING IN LARGE EARTHQUAKES

BY DONALD B. MCINTYRE AND JOHN M. CHRISTIE

Contribution to discussion of paper by John H. Hodgson

Doctor Hodgson and his collaborators have extended Byerly's technique for inferring, from analysis of first motions in an earthquake, the attitude of the active fault and the direction of movement on it. This highly ingenious method promises to give invaluable information concerning the present tectonic activity of the earth. In the analysis of a single earthquake two possible solutions are obtained, but the line of intersection of the two planes is a direction which is unambiguously determined; it occurred to the writers that, if the data for certain limited areas were analyzed with the aid of a stereographic or equal-area projection, it might be possible to ascertain the orientation of the actual fault plane for each individual solution.

Hodgson summarized the results of the 75 analyses so far completed. He has emphasized the predominance of strike-slip faulting and has considered the relationship between fault orientation and the trend of the associated physiographic feature. His conclusions were summarized as follows:

> "Within any particular area the strike direction of the faults is random. The dip directions may have some consistent orientation, although this is not clear. In any solution the intersection of the two planes defines a unique line, here called the *null vector*. . . . For any area the null vectors tend to lie parallel to a vertical plane having the direction of the associated geographical feature. The correlation is too definite to be accidental and must be regarded as a confirmation of the method. The physical significance of the null vector is not understood."

It seems clear that the intersection of Hodgson's two planes is the *B* kinematic axis of the fault movement; it is not a vector. The fact of great importance in Hodgson's method is that in every case he can determine unambiguously the orientation of the *B* axis.

It may appear that to call this direction a *B* kinematic axis instead of a null vector is arbitrarily to change the nomenclature without adding to the understanding. However, in the writers' view, the difference in terms has considerable meaning; the physical significance of the "null vector" can be clearly appreciated only if this meaning is understood. Although the concept of axes in structural geology is familiar to many geologists, it is reviewed so that the importance of Hodgson's results may be more widely appreciated.

Reference Axes in Structural Geology

The idea of using reference axes in structural geology had to await a real appreciation that geological structures are three-dimensional, and it was not until about 1900 that a definite start was made. With the magnificent exposures of folded rocks that exist in the Alps, it is not surprising that Swiss geologists initiated the work. Indeed, portions of the following discussion are nearly direct transcriptions from Wegmann's writings (Wegmann, 1929; Clark and McIntyre, 1951).

When one thinks of a fold, in general one thinks of a long structure; there is, therefore, a privileged direction parallel to which the structure has the highest degree of continuity or, in other words, undergoes least change. This is the only direction parallel to which it is possible to lay a long line on the folded surface, and this direction came to be called the "fold axis". The crest line of an anticline is, of course, parallel to the fold axis, but there is a considerable advantage in treating the latter as a *penetrative* direction, with orientation only and not

position, comparable to a crystallographic axis or the north direction.

In two dimensions we can describe a circle as the locus of a point moving at a constant distance from a fixed point; so in three dimensions we can describe a cylinder as the locus of a line moving at a constant distance from a fixed parallel line. Now, if the moving line is not constrained to remain at a constant distance from the fixed parallel line, or even to return to its former position, a surface will be generated which will be the ideal of a type of folded surface commonly found in nature. It is therefore clear that the orientation of the generator (the moving line) is a very important direction in the structure; the fold axis can then be defined as the nearest approximation (for we are dealing with real folds) to the line, which, moved parallel to itself in space, generates the fold. The orientation of the fold axis (often referred to as "the axis" for brevity) is defined by two angles: (1) trend, the strike of the vertical plane containing the axis, and (2) plunge, the vertical angle between the axis and the horizontal.

Any structures which can reasonably closely be described in terms of a rectilinear generator, and which are therefore homogeneous with respect to the axis, are said to be *cylindroidal*. An area can be tested for this homogeneity by plotting the normals to the bedding (or foliation in metamorphic terrain) on a standard stereographic projection. The more nearly cylindroidal the structure, the more closely will the normals to the bedding lie on a great circle, the pole of which defines the trend and the plunge of the fold axis; such a diagram is called a π diagram since it is the poles (π) of the bedding planes that are plotted. Alternatively, the great circles representing the bedding plane may be plotted on the projection, in which case, if the structures are homogeneous with respect to the fold axis (*i.e.*, if they are cylindroidal), the intersections of the great circles will give a concentration, the center of which defines the fold axis. In practice an equal-area (Lambert) projection is used, and the points of intersection are contoured; such a diagram is called a β diagram, and the maximum is called a β maximum. Cylindroidal structures possess a penetrative plane of symmetry normal to the direction of the fold axis. By analogy with crystals possessing this order of symmetry (a single mirror plane) the structures are said to be monoclinic.

In the Swiss Alps the homogeneity of the complex structures with respect to the fold axis is very striking when first perceived, for it appears as the only element of uniformity in an otherwise chaotic picture. Indeed, for the Swiss geologists working on the scale of the big recumbent folds (nappes), the fold axis was the unique and only axis. A group of Austrian geologists, notably Schmidt and Sander, initiating the study of petrofabrics, developed techniques suitable for structural analysis of hand specimens and thin sections. On this much smaller scale, the orientation of the bedding may be constant (although monoclinic symmetry may be defined by orientation of mineral grains, etc.)—that is, the field may be homogeneous with respect to the principal fabric plane as well as with respect to the fold axis. Making use of the increased homogeneity on the smaller scale, Bruno Sander adopted three orthogonal reference axes—*a*, *b*, and *c*; Sander's nomenclature is now generally accepted.

b is normal to the plane of symmetry;
a is normal to *b* in the principal fabric plane, which is thus the *ab* plane;
c is normal to *ab*, and the plane of symmetry is *ac*.

If, over a large area, such as the outcrop of an alpine nappe, there is a plane of symmetry of constant orientation on all scales of observation, the area is homogeneous with respect to both *b* and the fold axis, and these are mutually parallel. However, the uniformity does not extend to *a* and *c*, for the orientations of these within the plane of symmetry change from point to point around the fold. The peculiar status of the *b* axis, of constant orientation normal to the penetrative mirror plane, and thus parallel to the fold axis, has led tectonicians to dignify *b* by calling it the principal fabric axis, *B*; it is analogous to the *b* axis in a monoclinic crystal. Thus, when we write $b = B$ we imply that in the field considered the structures are cylindroidal.

The fabric of a body is defined by the spatial arrangement of *all* structural elements which it

contains. Now, in a deformed rock we have no *a priori* guarantee that all the visible fabric elements were active during the deformation—*e.g.*, planes defined by color banding may have been purely passive like lines drawn on the side of a deck of cards before the deck is flexed. Thus, the observed symmetry of the fabric need not agree with the symmetry of the movements operative during deformation, and considerable caution must be exercised in drawing kinematic conclusions from the symmetry and orientation of the fabric. It is vital to separate the descriptive geometry of the structure from its kinematic interpretation (Weiss, 1955).

If we know the symmetry of movement (as in the case of a controlled experiment or of certain seismological observations), we require a set of kinematic axes to facilitate description of the movement. Let us suppose that the movement is one of "simple shear"—*i.e.*, planar slip on a single set of planes, as can be illustrated with a deck of cards. The symmetry of the movement is monoclinic for there is a single plane of symmetry, and we can define our orthogonal kinematic reference axes as follows:

b is normal to the plane of deformation;
a is normal to *b* in the slip plane and is equal to the direction of slip;
c is normal to the slip plane (*ab*), and the plane of deformation is *ac*.

Where folding is by flexural slip on *ab*, the orientations of *a* and *c* vary within the plane of deformation, whereas the orientation of *b* is normal to that plane and is constant. With fabric axes in an analogous case we dignified *b* as *B*, so here *b* can be called the principal kinematic axis and written *B*. When an earthquake originates by a single monoclinic movement on a planar fault, *a*, *b*, and *c* all have equivalent status—*i.e.*, are equally uniform in orientation throughout the field. By a natural extension of the nomenclature outlined above, we can designate the kinematic axes as *A*, *B*, and *C* in such cases. The null vector is the intersection of the fault plane and the auxiliary plane. Since the latter is normal to the motion direction in the fault, it follows that the null vector is the *B* kinematic axis. We therefore propose the following definitions:[1]

A = motion direction in the fault plane;
B = normal to *A* in the fault plane (equal to null vector);
C = normal to the fault plane (*AB*).

The physical significance of the null vector is thus defined.

Representation of Planes and Lines

The problem of defining the orientation of planes and lines in space is a basic one in solid geometry. What is difficult to keep in mind is that strike and dip (or trend and plunge) are the two necessary parts of one definition. When taken together they constitute the whole, but when separated they each have a value much less than a half. For this reason the term attitude has real value as well as convenience as a synonym for strike and dip (or trend and plunge). The writers consider Hodgson's separate analysis of direction of strike and of direction of dip to be a defect in procedure.

The problem of comparing the orientations of planes (without consideration of their locations) was solved by crystallographers long before rigorous study of structural geology had begun. Their solution was the use of the stereographic projection, where the plane (crystal face) and the direction normal to it are considered to pass through the center of the fundamental sphere. The intersection of the face-normal with the sphere is then joined to the south pole of the sphere, and the point where this line meets the equatorial plane is the stereographic projection of the face-normal and is usually referred to as the pole of the face. The plane itself can be projected as a great circle, and this is necessary for some constructions. For various reasons structural geologists have adopted the convention of using lower hemisphere projections; the face-normal is drawn from the center to meet the lower hemisphere, and this point is then joined to the north pole of the sphere. Bucher (1944) and Phillips (1954) have given excellent introductions to the procedure.

The great advantage of this method of pro-

[1] These kinematic axes are not to be confused with other axes, such as those of the strain ellipsoid.

jection is that the attitude (strike and dip) of the plane can be represented as a single point on the diagram. Although the strike and dip can each be read off the projection, their fused unity, the attitude, can be held in the mind without effort. The importance of this is that attitudes in limited fields are seldom (probably never) random, and strike and dip are not independent variables. For example, if the structure is cylindroidal the strike and dip will change in such a way that the poles will lie on a great circle on the projection (a π diagram); in such a case the great circle represents in stereographic projection the relationship between strike and dip, but one can, if one wishes, prepare a Cartesian graph showing this.

As a glance at a stereonet shows, the stereographic projection suffers from the defect that equal areas on the fundamental sphere do not project as equal areas; hence, this projection is not used for statistical studies. If the problem is the detection of patterns of preferred orientation of planes, the Lambert equal-area projection is used. In this equal areas on the fundamental sphere do project as equal areas on the projection. It is therefore possible to prepare contoured diagrams representing the pattern of preferred orientation (Ingerson, 1938, p. 245-252; Fairbairn, 1949, p. 285–291).

Hodgson states that the strike direction of the planes is random. To us it seems that, in the New Zealand-Kermadec-Tonga sector, there are two very high concentrations of strike directions given by the data, but even if the strike directions can be shown to be random this could be of very little significance. In a cylindroidal structure the strike directions can vary through 180°, yet the poles of the individual planes may define a great circle. If the attitudes (strikes and dips) of a number of planes are known, the existence of a preferred orientation must be looked for in a π diagram in stereographic or, better, equal-area projection. The writers' objections to the separate treatment of strike and of dip obtain with equal force to the separate treatment of trend and of plunge when discussing the orientation of lines. The lines may lie within a plane, and if so will define a great circle in stereographic projection. If the plane containing the lines is not vertical, then the trends of the lines need show no preferred direction, although the lines themselves may be far from random in their orientation.

The symbol used on a geological map to represent a linear structure, such as a fold axis, is an arrow parallel to the trend and pointing in the direction of the plunge, together with a figure giving the amount of plunge. At casual glance this might appear closely comparable to the representation of a vector. However, there is a fundamental fallacy in referring to such a linear structure as a vector. A vector is an entity with orientation, sense, and magnitude; a force of given amount acting in a given sense along a line of given orientation would constitute a vector. But the fold axis is only a direction; it is a line of given orientation—along which a force might or might not act—but the axis as such possesses orientation only, and neither sense nor magnitude. In a two-dimensional problem the orientation of a vector can be represented by an arrow together with a figure giving the magnitude. On the other hand, to represent on paper a vector contained in three-dimensional space, a line (for trend), an arrowhead (for sense of plunge), and a figure (for plunge) are required *for the orientation alone*; a second figure is needed to specify the magnitude, and a second arrow to specify the sense of the vector.

Following this line of argument, the writers conclude that Hodgson's "displacement vectors" are lines with orientation only. He writes, "The dip of a plane has both a direction and an amount and may therefore be regarded as a vector quantity", but the "amount" is only part of the definition of the direction. And again, with reference to the null vector, "It is certainly a vector . . . for it has a direction and amount", but the "null vector" can have no sense, since it is normal to the symmetry plane, or magnitude, since it is normal to the direction of slip in the plane of slip. The writers conclude that (1) dip is part of the description of the orientation of a plane, and it does not become a vector when taken out of its context in that definition; and (2) the "null vector" is a kinematic axis (B), although superficially it may *appear* to be a vector when its plunge, which is part of the definition of its orientation, is mistaken for a magnitude.

Preferred Orientations of the B *Kinematic Axes*

Hodgson has written: "For any area the null vectors tend to lie parallel to a vertical plane having the direction of the associated geographic feature." The writers have plotted Hodgson's data on equal-area projections. A synoptic diagram (Fig. 1) shows a very high concentration of steeply plunging B axes, and, as Hodgson points out, this implies that the majority of the faults analyzed had strike-slip movement. In some areas (*e.g.*, the Kurile Islands and Kamchatka, and also the New Hebrides) there is a strong maximum, but in only one area do the present data definitely justify the claim that the B axes define a plane; this is the New Zealand-Kermadec-Tonga-Fiji arc, and the nearly vertical plane contains the physiographic feature. The writers believe that further discussion of other areas must await the accumulation of more data.

Significance of the B *Kinematic Axes Defining a Plane*

To illustrate the utility of equal-area projection as a tool for analyzing structural data in three dimensions, let us consider the following data:

(1) The fault movements giving rise to the earthquakes have monoclinic symmetry, and their orientations can be described in terms of three kinematic axes, A, B, and C, as defined above.
(2) In any one region the B axes define a plane. This plane is stated to be vertical, but, to illustrate the principles more clearly, the more general case of a steeply dipping plane will be discussed.
(3) The plane of the B's is parallel to the physiographic feature.

Since A, B, and C are mutually perpendicular, the simplest working hypothesis to account for the restriction of the various B's in a plane is to suppose that either A or C has a preferred orientation normal to this plane. On kinematic grounds it seems unlikely either that A and C would have random orientation, or that within a single area the A axis in some earthquakes would be in the plane defined by the B's, while in others it would be at right angles to this plane. Accordingly, we shall proceed on the assumption that either A or C was normal to the plane of the B's and try to discover the implications in each of the two cases.

(1) If A is normal to the plane of the B axes, this plane will contain also the C axes; hence, the steep faults (those with nearly horizontal C axes) will have a strike perpendicular to the trend of the associated physiographic feature, and, since A is nearly horizontal, they will be strike-slip. On the other hand, the gently dipping faults (those with nearly vertical C axes) will have a strike nearly parallel to the trend of the feature and will be dip-slip. Oblique-slip faults could also occur, and these could have a variety of attitudes, but in all the C axes would lie on the great circle normal to A. If we plotted the great circles representing the fault planes, we would have a β diagram with β maximum (*i.e.*, a concentration of great-circle intersections) coinciding with A. This situation could be symbolized as $\beta = A$, and it is a most unlikely one to occur. The reason for this is as follows: If we consider two intersecting planes, it would be possible from a purely kinematic point of view to imagine slip parallel to the line of intersection—*i.e.*, $\beta = A$. But since we must suppose that the fault planes are shear planes produced by the forces which give rise to the movements, this would not be a plausible dynamic arrangement. If the faults intersect, or if they would intersect if their surfaces were extended, then β, the line common to them, would have to coincide with the B kinematic axis.

(2) If C is normal to the plane of the B axes, this plane will include also the A axes. Hence, since on the π diagram there would be a single maximum in the preferred orientation of the C axes (the normals to the fault planes), the faults will all be steep, and they will have strikes parallel to the trend of the associated physiographic feature. Whether they are strike-slip, dip-slip, oblique-slip, or vary in the orientation of the slip will depend on whether the B axes (and hence the A axes which are each 90° from their respective B's in the plane normal to C) are concentrated with some particular orientation in the plane normal to C, or not. If we plot the great circles representing the fault planes, we would have a β diagram

with a β maximum, if there is one, in the AB plane. If there is a β maximum, C would have to spread from its maximum in the plane normal to β—*i.e.*, the strike of the faults would vary somewhat. The position of the β maximum might coincide with A or with B, but it is difficult to imagine a kinematic-dynamic arrangement other than $\beta = B$. Since the orientations of the B axes (Hodgson's null vectors) have been determined unambiguously, this could be tested if only we could decide which planes were the fault planes and which were the auxiliary planes—*i.e.*, if we could distinguish between A and C in each case. However, one might hope to discover, in some regions at least, one set of planes giving $\beta = B$

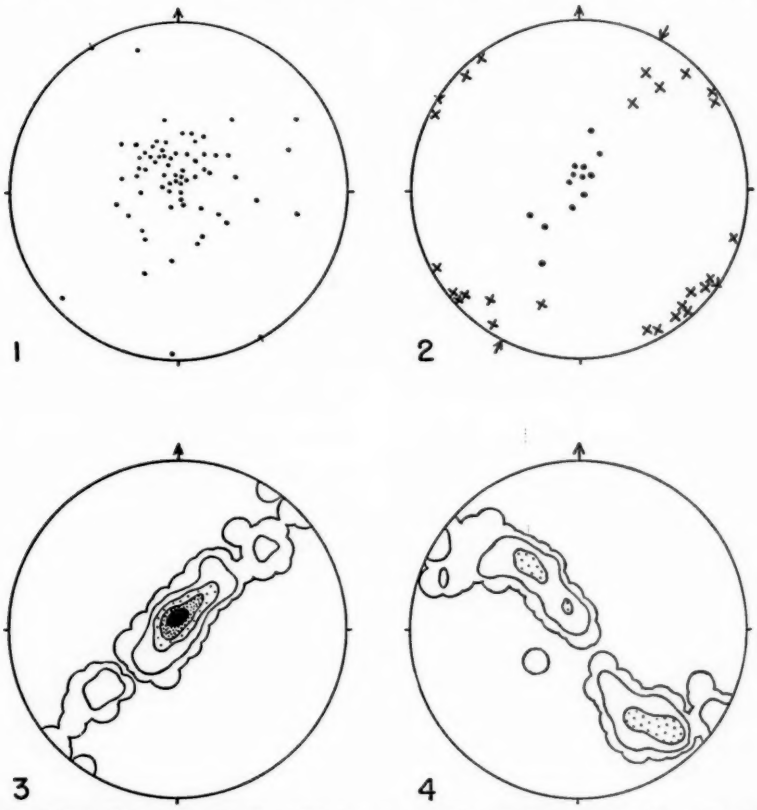

FIGURE 1.—*B* AXES ("NULL VECTORS") OF MOVEMENTS IN EARTHQUAKES IN WHICH BOTH PLANES ARE DEFINED BY THE FIRST-MOTION DATA (HODGSON, TABLE 1)

The majority of the B axes plunge steeply, indicating the prevalence of strike-slip movement in the analyzed earthquakes.

FIGURE 2.—DATA FOR THE NEW ZEALAND-KERMADEC-TONGA-FIJI AREA (HODGSON, TABLE 1, NOS. 1–13)

B axes are represented by dots. The two groups of crosses represent the *a* planes (with northeasterly strike) and the *b* planes (with southeasterly strike). The arrows show the mean trend of the physiographic feature.

FIGURE 3.—NEW ZEALAND-KERMADEC-TONGA-FIJI AREA

Contoured β diagram for the *a* planes. Contours: 1⅓, 4, 12, 20, 28% per 1% area.

FIGURE 4.—NEW ZEALAND-KERMADEC-TONGA-FIJI AREA

Contoured β diagram for the *b* planes. Contours: 1⅓, 4, 12% per 1% area.

All diagrams are oriented geographically with north at the top; the lower hemisphere of an equal-area projection is used.

and another giving $\beta \neq B$; the probability that the first set are the faults would be very high.

Analysis of the New Zealand, Kermadec, Tonga, Fiji Data

It has been pointed out that the New Zealand-Fiji arc is the only area in which the present data definitely justify the claim that the B axes define a plane. It remains for the future to tell whether this is due solely to the present deficiency of data in the other regions, or whether this arc is indeed an unusual tectonic area. The data for the 13 analyzed earthquakes from New Zealand, Kermadec, Tonga, and Fiji are shown on Figure 2,[2] on which the poles of the planes constitute two groups; these correspond to Hodgson's "a" and "b" planes. In agreement with the theoretical discussion of the previous section, the normals to one set (a planes) are perpendicular to the plane of the B axes, and the normals to the other set (b planes) lie close to that plane. It seems reasonable to assume that either the a planes or the b planes are the faults.

The contoured β diagram for the a planes is given in Figure 3; in it there is a strong β maximum (nearly 30 per cent per 1 per cent area) which coincides almost exactly with the B maximum. Figure 4 is the contoured β diagram for the b planes; in it there are two widely separated and rather diffuse maxima (about 12 per cent per 1 per cent area) neither of which coincides with B. We conclude therefore that the a planes, with strikes parallel to the great physiographic feature, are the faults. The normals to the b planes are therefore the A axes, and, although they vary somewhat in orientation, the faulting is clearly strike-slip in character.

[2] In using a single plane of projection for a sector of the globe of the magnitude of the New Zealand-Fiji arc we face a real difficulty since the orientation of the horizontal plane varies with latitude and longitude. A great circle defined by directions such as B axes measured at various localities along the arc might be due to the curvature of the globe. However, the data used for figure 2 show no obvious correlation between geographical position and location of B axes on the great correlation between geographical position and location of B axes on the great circle of the projection. In this light the preferred orientation shown on figure 1 increases in interest.

If our conclusion is accepted, the faults in this section of the circum-Pacific dip more steeply than the zone defined by earthquake foci (Benioff, 1955, Fig. 8). However, in our interpretation of Hodgson's data that zone cannot represent an imbricate zone. Perhaps it is a dipping geological boundary (for example, the boundary between the sial and the sima) cut by steep strike-slip faults with strikes approximately parallel to the strike of this boundary.

Conclusions

To resolve the ambiguity in the interpretation of the first-motion data in the manner outlined above, it is necessary that the following conditions be fulfilled:

(1) There must be sufficient data to test the preferred orientation.
(2) The B kinematic axes must define a plane.
(3) There must be a maximum of B axes in this plane.
(4) The C axes must spread sufficiently for the fault planes to define a β maximum.
(5) It must be possible to show that $\beta = B$ for one set of planes and not for the other set. If there is a B maximum which does not spread into a plane then both the faults and the auxiliary planes will give β maxima coincident with B, and the ambiguity cannot be resolved.

It must be emphasized, however, that the B kinematic axis is unambiguously determined for each earthquake; this is a major contribution to the understanding of the processes of earth deformation.

References Cited

Benioff, Hugo, 1955, Seismic evidence for crustal structure and tectonic activity, p. 61–74 *in* Poldervaart, Arie, 1955, Crust of the earth: Geol. Soc. America Sp. Paper 62, 762 p.

Bucher, W. H., 1944, The stereographic projection, a handy tool for the practical geologist: Jour. Geology, vol. 52, p. 191–212.

Clark, R. H., and McIntyre, D. B., 1951, The use of the terms pitch and plunge: Am. Jour. Sci., v. 249, p. 591–599.

Fairbairn, H. W., 1949, Structural petrology of deformed rocks: Addison-Wesley Press, Inc., Cambridge, Mass., 344 p.

Ingerson, Earl, 1938, Laboratory technique of petrofabric analysis, Pt 2: *in* Knopf, E. B., and

Ingerson, Earl: Structural petrology: Geol. Soc. America Mem. 6, 262 p.

Phillips, F. Coles, 1954, The use of the stereographic projection in structural geology: E. Arnold, London, 86 p.

Wegmann, C. E., 1929, Beispiele tektonischer Analysen des Grundgebirges in Finnland: Bull. Comm. géol. Finlande 87, no. 8, p. 98–127

Weiss, L. E., 1955, Fabric analysis of a triclinic tectonite and its bearing on the geometry of flow in rocks: Am. Jour. Sci., v. 253, p. 225–236.

Department of Geology, Pomona College, Claremont, California

Manuscript Received by the Secretary of the Society, February 5, 1957

BULLETIN OF THE GEOLOGICAL SOCIETY OF AMERICA
VOL. 68, PP. 653-654 MAY 1957

ORIGIN OF PORPHYROBLASTS

BY GEORGE J. NEUERBURG

Hypotheses concerning the mechanism of the growth of porphyroblasts have occasionally gained the attention of petrologists. Oddly enough, except for an offhand implication (Turner and Verhoogen, 1951, p. 400), the problem of *why* porphyroblasts have formed seems to have elicited no published comment. Porphyroblasts in slaty rocks of the Santa Monica slate, Santa Monica Mountains, southern California, exhibit certain features that encourage a few remarks on this problem.

The Santa Monica slate (Triassic?) (Hoots, 1931; Neuerburg, 1951, PhD. thesis, Univ. Calif. Los Angeles), originally subgraywacke to graywacke siltstones and mudstones, has been intruded and metamorphosed by a thick sill-like body of medium-grained biotite-hornblende quartz diorite. The metamorphism is of low grade, and relics of clastic texture persist to within a few hundred yards of the intrusive contact. The metamorphism is progressive, and consists of a gradual change from very slightly recrystallized rocks of clastic texture to medium-grained schists and gneisses adjacent to the quartz diorite intrusive. Clays, fragments of mafic volcanic rocks, and angular grains of feldspars and quartz were progressively recrystallized and coarsened in grain to a mixture of feldspar, quartz, biotite, and muscovite. Parallel to the intrusive contact and superimposed on several intermediate units or zones of metamorphic intensity is a band, about 1300 yards wide, in which abundant porphyroblasts of andalusite, chloritoid, and cordierite occur. The porphyroblastic texture is coextensive with the outer limit of occurrence of these minerals. Toward the intrusive, the porphyroblastic texture extends into the metamorphic zones from which all relics of clastic texture have disappeared; the porphyroblasts occur to within about 500 yards of the intrusive contact. Although the porphyroblast minerals continue into the higher-grade metamorphic rocks, they decrease drastically in abundance and occur only sporadically; the porphyroblastic texture disappears largely because of the coarsening of the other minerals of the rock to a grain size commensurate with that of the porphyroblasts.

Investigations of the origin and growth of large crystals from melts, as in igneous porphyries, have shown that formation of such large crystals is contingent upon the formation of few crystal nuclei in a system cooling sufficiently slowly so that further crystal growth is concentrated upon these few nuclei. It seems logical that a similar physical-chemical situation should control the appearance and growth of porphyroblasts in a recrystallizing solid. Calculations of the rates of temperature change relative to distance and time in an ideal mathematical model of the intrusive-metamorphic system of the Santa Monica Mountains were made according to the procedures discussed by Lovering (1935). Values were obtained of dT/dt having a magnitude of 10^{-3}°C/year at the maximum for the distances embracing the porphyroblast zone, which serves to document the intuitive belief of very slow temperature changes during metamorphism.

Among the metamorphic minerals of the Santa Monica slate, only the porphyroblast minerals have a crystal structure foreign to the structures of the minerals of the unmetamorphosed sediments. All other metamorphic minerals have analogous structures—and thus many nuclei for their growth—in the original minerals of the sediments. Thus, it would seem that only the porphyroblast minerals were nucleated during metamorphism. On this basis, the writer suggests that, owing to the slow change of temperature during metamorphism, a few nuclei—or "seed" crystals—of andalusite, chloritoid, and cordierite sufficed to gather the necessary components into a relatively few large crystals, analogous, from a physical-chemical viewpoint, to the formation of phenocrysts from a cooling magma.

This hypothesis provides a satisfactory explanation for the appearance of porphyroblasts in the Santa Monica slate. Obvious exceptions to general application of this hypothesis, such

as pyrite porphyroblasts in metamorphosed mudstones and feldspar porphyroblasts in sandstones, are easily found. However, it probably applies to other occurrences and types of porphyroblasts in like and in different geologic situations; this needs further testing.

References Cited

Hoots, H. W., 1931, Geology of the eastern part of the Santa Monica Mountains, Los Angeles County, California: U. S. Geol. Survey Prof. Paper 165-C, p. 83–134

Lovering, T. S., 1935, Theory of heat conduction applied to geological problems: Geol. Soc. America Bull., v. 46, p. 69–94

Turner, F. J., and Verhoogen, Jean, 1951, Igneous and metamorphic petrology: 1st ed., New York, McGraw-Hill Book Co., 602 p.

U. S. Geological Survey, Denver, Colo.

Manuscript Received by the Secretary of the Society January 9, 1957

Publication Authorized by the Director, U.S. Geological Survey

BULLETIN OF THE GEOLOGICAL SOCIETY OF AMERICA
VOL. 68, PP. 655-656, 1 FIG. MAY 1957

OCCURRENCE OF 1350 MILLION-YEAR-OLD GRANITIC ROCKS IN WESTERN UNITED STATES

BY L. T. ALDRICH, G. W. WETHERILL, AND G. L. DAVIS

Values for K-A and Rb-Sr ages of micas from 11 granites and pegmatites in Arizona, New Mexico, Colorado, Wyoming are close to 1350 million years. The ages are given in Table 1. The location of the samples of Table 1 are shown in Figure 1. The sample numbers correspond to the numbered locations on the map.

Four other locations are also shown on the map. The age of the sample from each of these locations is indicated by letter with (A) 2500 m.y., (B) 1600 m.y., and (C) 1100 m.y. The map shows the location of all the Precambrian rocks measured at this laboratory from these States.

The micas analyzed include biotite, muscovite, and lepidolite. The analytical procedures have been described (Aldrich, Davis, Tilton, and Wetherill, 1956), and the analytical errors are such that they affect the ages given by less than 5 per cent. That micas usually give reliable absolute K-A ages has been demonstrated by Wetherill, Wasserburg, Aldrich, Tilton, and Hayden (1956). That reliable Rb-Sr ages of micas are obtained has also been shown (Aldrich, Wetherill, Davis, Tilton, 1956). When the K-A and Rb-Sr ages of a mica agree, it is believed that this is the time of formation of the mica. Even from this short list it is apparent that these two ages commonly agree.

The agreement of the ages in Table 1 shows

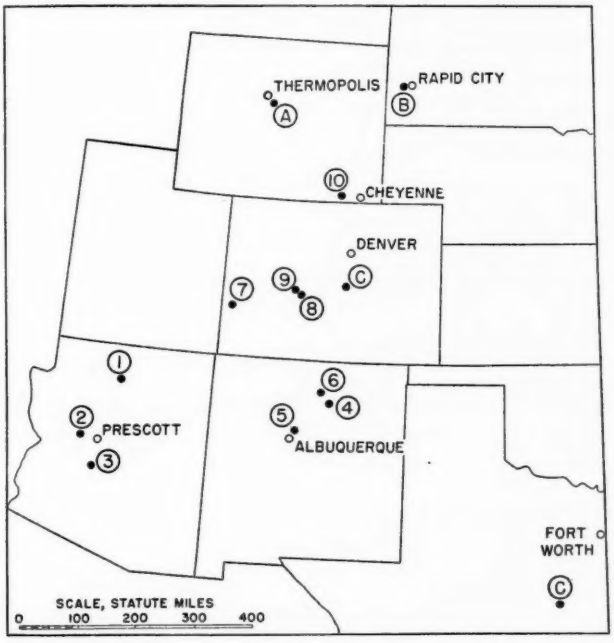

FIGURE 1.—LOCATION OF SAMPLES OF TABLE 1

TABLE 1.—K-A AND Rb-Sr AGES OF ROCKS FROM WESTERN UNITED STATES

K-A ages are calculated from decay constants of K^{40} of $\lambda_e = 0.557 \times 10^{-10}$ yr^{-1}, $\lambda_\beta = 4.72 \times 10^{-10}$ yr^{-1} or a total half-life of K^{40} of 1.31×10^9 years. Rb-Sr ages are calculated using a half-life for Rb^{87} of 50×10^9 years.

Sample location	Ages in millions of years	
	K-A	Rb-Sr
1. Gneiss, Zoroaster Creek, Grand Canyon, Arizona	1390	1370
2a. Lawler Peak granite, Bagdad, Arizona	1410	1390
2b. Pegmatite in Lawler Peak granite	1410	1500
3. Pegmatite, Wickenberg, Arizona	1160	1300
4. Pidlite Mine, Mora County, New Mexico	1330	1490
5. Granite, Sandia Mountains, Albuquerque, New Mexico	1350	1340
6. Harding Mine, Dixon, New Mexico	1300	1300
7. Uncompahgre Granite, Mesa County, Colorado	1320	1320
8. Granite, Doyleville, Colorado	1320	1310
9. Brown Derby Pegmatite, Ohio City, Colorado	1330	1420
10. Granite, Sherman, Wyoming	1420	1410

that the mica in all these rocks was formed close to 1350 million years ago and therefore that there was widespread crystallization of granitic rocks at this time. It is suggested that this crystallization accompanied a period of regional rock formation comparable to the periods of igneous intrusion and metamorphism in the Grenville subprovince and in the Appalachians. It is evident that these mica ages have been preserved in spite of subsequent geologic events such as the Laramide orogeny.

References Cited

Aldrich, L. T., Davis, G. L., Tilton, G. R., and Wetherill, G. W., 1956, Radioactive ages of minerals from the Brown Derby mine and the Quartz Creek granite near Gunnison, Colorado: Jour. Geophys. Res., v. 61, p. 215–232

Aldrich, L. T., Wetherill, G. W., Tilton, G. R., and Davis, G. L., 1956, Half-life of Rb^{87}: Phys. Rev., v. 103, p. 1045–1047

Wetherill, G. W., Wasserburg, G. J., Aldrich, L. T., Tilton, G. R., and Hayden, R. J., 1956, Decay constants of K^{40} as determined by radiogenic argon content of potassium minerals: Phys. Rev., v. 103, p. 987–989

CARNEGIE INST. OF WASHINGTON, WASHINGTON, D.C.

MANUSCRIPT RECEIVED BY THE SECRETARY OF THE SOCIETY, JANUARY 21, 1957